OPTICAL SURFACE ANALYSIS CODE (OSAC) VERSION 7.0

USER'S MANUAL

SECOND EDITION
AUGUST 11, 1993

NASA
GODDARD SPACE FLIGHT CENTER

TABLE OF CONTENTS

4. CONVENTIONS

5. PROGRAM DESCRIPTIONS

FIGURES

TABLES

PREFACE

During the past few years several new features have been added to the Optical Surface Analysis Code (OSAC). In this users manual the updates have been incorporated in the main body of the document. Figures and tables of the original manual were also moved from the end of the manual to their appropriate sections in the manual. Version 3.0 of the software package was originally developed for Goddard Space Flight Center by the Perkin-Elmer Corporation under NASA Contract NAS5-25802. This version was released in March, 1982. All four updates were developed and programmed by Paul Glenn of Bauer Associates, Inc.

The first update (Version 4.0, NASA Contract Order Number S-92505-D) was released in February, 1988. This update included the implementation of: (1) large amplitude scattering theory, (2) reflectivity and polarization generalization, and (3) obscuration surfaces. Version 5.0 was released in June, 1988 (NASA Contract Order Number S-80971-D). The new features added were: (1) Point light source at finite distance, (2) OPD file conversion, and (3) wavefront tolerancing. Version 6.0 was released in July, 1989 (NASA Contract Order Number S-16917-E). This update included the addition of: (1) toroidal surfaces and (2) new autocovariance function models. The last update added into the manual (Version 7.0) was delivered in September, 1989. The features incorporated into the program were: (1) Mixed (conventional/x-ray) systems, (2) increased pixel array size, and (3) additional Legendre polynomials.

My intention in upgrading the manual was to change the original manual as little as possible, just to place the new features in their appropriate locations in the manual. If any typographical errors and inconsistencies are found in the document, I would appreciate, if you could report them to the address shown below.

Several people have participated in putting together this manual. I would like to particularly than Dave Naves of Project Engineering, Inc. for preparing the first draft of this manual including the figures. I would also like to thank Mark Wilson of GSFC for writing the Appendices and Sandra Laase of McDonnell Douglas for preparing the final document.

Timo T. Saha
Code 717.4
NASA/Goddard Space Flight Center
Greenbelt, MD 20771

1. INTRODUCTION

This report is the Users Manual for the Optical Surface Analysis Code (OSAC) designated Version 7.0, a software package originally developed for Goddard Space Flight Center by the Perkin-Elmer under NASA Contract NA35-25802. This report incorporates four revisions to OSAC documented in reports by Bauer Associates, Inc., from 1988 and 1989 into a single coherent Users Manual.

This Users Manual has five sections: 1 — introduction, 2 — the hardware and software configuration, 3 — provides an overview of each of the twelve software modules, and 4 — describes the conventions, quantities and concepts that a user should be familiar with before trying to understand in detail how to use the various OSAC modules. Section 5 provides detailed information about each of the twelve modules. This includes how to run each module, what analytical methods or theory were used as foundation for the module, and what the input and output files mean. Many tables and figures are used to provide specific information and examples for each module. Each module in the OSAC program is designed to be run interactively.

2. CONFIGURATION

The target machine is a Digital Equipment Corp. MicroVAX II running VAX/VMS. Version 5.x of VAX/VMS is **REQUIRED**. The source was written in USASI full FORTRAN 77, allowing for greater portability across different hardware platforms. The program is designed to be run interactively using a DEC VT100-compatible terminal (**REQUIRED**). OSAC is run by executing a VAX/VMS DCL Command Procedure which executes another series of command procedures. Appendix A describes the installation procedure and resource requirements and Appendix B explains how to run the program. Appendix C describes the utility programs developed at GSFC and, finally, Appendix D describes the various screens that are displayed during an interactive session.

Certain OSAC routines require use of numerical algorithms (see Section 2.2.4) implemented in the CMLIB software package distributed by NIST. The method of implementation in OSAC is such that other libraries such as IMSL™ can be used instead of CMLIB. A sufficient number of routines from CMLIB are included as part of OSAC so that the program can be self-contained.

GSFC has developed a number of post-processing programs that help analyze OSAC-generated results. Such programs include encircled energy calculations, point spread function plots, etc. Appendix C lists these programs and provides information on their usage.

2.1 Software Configuration Control

Software configuration control assures that the details of the data processing as performed at any given time is as intended, and is documented, without ambiguity. This requires restriction of access to all source material. Such restrictions will also apply to the delivered product, regardless of what computer it is installed on. This necessary configuration control is accomplished during development (and will be maintained after delivery) by adhering to the following control elements:

(1) Software users will be granted access only to officially released versions of the software.

(2) Each release of software will state on each printed page of output, the mainline procedure name which produced the printout, and the release identification. The release identification format should be MM.N, where MM is a two-digit release number, and N is a one-digit revision number. Software updates which correct errors, represent cosmetic changes, and do not appreciably impact the user's documentation normally result in an incrementing of the revision number.

An experimental version of OSAC will be designated by replacing the decimal point in the release identification with an 'X'. Release 05X3, for example, means the release 05.3 is the

base release to which modifications are being made during normal program development which will subsequently yield the next official software release.

The software mechanism which automates the "self-identification" element described here is the set of subroutines PROGID, INCLIN, and PRHDR. Their definition appears in their comment blocks. Their usage as exemplified in the mainline procedure listings is simple and clear. Each mainline procedure must call PROGID once as the first executable statement in order to capture the program name and release identification. Prior to any printing, INCLIN will be called to specify the number of print lines that are needed. If the current page does not have sufficient space, then PRHDR will automatically be called to advance the next page and print the standard OSAC "self-identification" header block.

(3) Each new release before being made available to the users, will be accompanied by the following:

(a) Documentation indicating what is different from the previous release.
(b) Updated version of user's manual for the software.
(c) Results from test and checkouts of the new release. (The specification, execution and interpretation of the tests are the responsibility of performance certification, not configuration control).
(d) Magnetic tape of all source software comprising the new release for archival purposes. The complete version, and not just the revised portions, should be saved as one unit.

2.2 Programming Standards

Orderly program development, especially by a group effort, dictates that proper attention be paid to software guidelines. The programming standards outlined below are not extensive, but should serve as the cornerstone of good software engineering discipline. They should help produce uniform source code which is easy to follow, check out and maintain.

(1) The mainline procedures should conform to USASI full FORTRAN IV. This should enhance program transportability.
(2) In the source code, each subprogram has a "comment block" of uniform format as demonstrated in the source listings. This includes the sections on purpose, calling sequence, input/output, author and date. Self-documenting subprograms are a pleasure to work with.
(3) The software is modularized to the extent that each sub-program performs a single function. If a subroutine, for example, reads into memory optical system data, and prints out the values, then it is performing two functions and should really be two subroutines. The derived benefit is independent building blocks that offer greater flexibility.

2.3 Non-delivered Subroutines

OSAC uses certain subroutines which are not to be delivered to GSFC. The one non-delivered subroutine used by all the OSAC modules is ZTIME, which returns date or time of day in character format. The use of ZTIME is clear from the program listings. All other non-delivered subroutines are taken directly from the IMSL subroutine library, to which GSFC has access. Complete documentation for the IMSL routines can be found in the IMSL reference manuals. The specific routines used by the various modules are as follows:

The IMSL routine LINV3P is used in double precision (R*8) by the OSAC modules NABRAT, DRAT, and FPLOOK. It is also used in single precision (R*4) by the OSAC module COGEN.

The IMSL routines DCADRE, MMBSJ0, and MMBSJ1 are used in double precision (R*8) by the OSAC module DEDRIQ. The IMSL routine FFT2C is used in single precision (R*4) by the OSAC module PSF.

3. OVERVIEW

The purpose of OSAC is to provide a comprehensive analysis of optical system performance, taking into account the effects of optical surface misalignments, low spatial frequency surface deformations (discrete polynomial deformations), high spatial frequency deformations (surface roughness), and diffraction. OSAC can analyze both conventional systems (i.e., near normal incidence systems used in the infra-red, visible, and near ultra-violet spectra) and X-ray systems (i.e., near grazing incidence systems used in the far ultra-violet and X-ray spectra). OSAC is composed of a set of twelve compatible programs which are executed in a user defined sequence. The general purpose of each of these modules is discussed below.

3.1 GEOSAC

GEOSAC reads a user input data file containing all the parameters necessary to define an optical system, and performs all the necessary geometric calculations for subsequent geometrical ray tracing by NABRAT or DRAT. This includes such calculations as finding the distances between the foci of the various conical optical elements, and finding the location of the geometrical (Gaussian) focal plane of the system. GEOSAC outputs a condensed geometry file that is used by NABRAT or DRAT, as well as every other OSAC module except FPLOOK and COGEN. GEOSAC is described in detail in Section 5.1.

3.2 NABRAT

NABRAT traces an input bundle of collimated rays through an optical system that must consist of exactly two (conic) elements. Fold flats are not allowed by NABRAT, but only by DRAT. The elements are also not allowed to have polynomial deformations, which again must be analyzed by DRAT. The purpose of NABRAT, then, is to analyze a non-aberrated, two-element system in order to verify that the system parameters given to GEOSAC are reasonable, and to get a basic feel for the system performance. NABRAT traces the entire optical system in one run, and outputs three files containing ray intersection information — one for each of the surfaces, and one for the focal plane. NABRAT is described in detail in Section 5.2.

3.3 DRAT

DRAT traces a bundle of rays through a single element of an optical system. The element may be a conic, toroidal, obscuration, or fold flat. Surfaces traced by DRAT may have polynomial deformations. If the surface is the first surface in the system, the input ray bundle is collimated or emerging from a point source. If not, the input ray information is taken from the output of a previous DRAT run. DRAT outputs a ray intersection information file for the surface being traced. If the surface is the last surface in the system, then DRAT outputs two such files — one for the surface, and one for the system focal plane. Thus, DRAT must be run N times for an N-element optical system, and it outputs N+1 ray intersection information files. If the user wishes to look at system performance only in terms of the effects of finite field angles, surface

misalignments, and polynomial deformations, and ignore the effects of surface roughness and diffraction, then one run of GEOSAC and N+1 runs of DRAT are all that is required. DRAT is described in detail in Section 5.3.

3.4 SUSEQ

If the user wishes to include the effects of scatter in the performance analysis, then both SUSEQ and DEDRIQ must be run. The purpose of SUSEQ is to provide a mapping from scatter angles at the optical surfaces to ray displacements at the focal plane. Thus, when an angular scatter distribution at a surface is later defined by DEDRIQ, it is combined with the scale factors given by SUSEQ, described in detail in Section 5.4, to give a focal plane energy distribution. The scale factors are calculated for each ray intersection with each optical surface. If the system is an X-ray system, then an additional set of scale factors is calculated, again for each ray intersection with each surface. These additional scale factors relate scatter angle at a given ray-surface intersection to a change in grazing angle of the ray at each succeeding surface. This information is important for X-ray systems, where the reflectivity of a surface can be a rapidly varying function of grazing angle. The output of SUSEQ is a single file containing all the scale factors.

3.5 DEDRIQ

The purpose of DEDRIQ, described in detail in Section 5.5, is to allow the user to specify high spatial frequency deformations (roughness) on the optical surfaces and see the effect on system performance. The input to DEDRIQ is a user-created file that contains all the parameters needed to specify the roughness characteristics of various areas on the surfaces. Roughness can be specified via a surface height autocovariance function, a roughness power spectral density function, or a one- or two- dimensional grating profile. Part of the output of DEDRIQ is a pixel array type of focal plane file that tells how much diffusely scattered energy is contained in each pixel. The remaining output is a focal plane ray intersection information file which is identical to the one produced by NABRAT or the final running of DRAT, except that the intensity of each ray has been attenuated by the amount of diffuse scatter calculated by DEDRIQ.

3.6 OPD

If the user wishes to include the effects of diffraction in the performance analysis, then both OPD and PSF must be run. The purpose of OPD, described in detail in Section 5.6, is to provide an Optical Path Difference (OPD) map of the pupil plane of the system so that a Point Spread Function can be calculated later by PSF. The input to OPD is a focal plane ray intersection information file, produced by NABRAT, DRAT, or DEDRIQ. The output is a file that gives the OPD at each entrance pupil location defined by the intersection of a ray in the original collimated bundle of rays. Also included in the output file is the effective focal length from the entrance pupil to the system focal plane.

3.7 PSF

The purpose of PSF, described in detail in Section 5.7, is to use the OPD and ray intensity information produced by OPD to calculate a pupil function, and then to Fourier transform that pupil function in order to calculate the energy distribution or Point Spread Function (PSF) in the focal plane due to diffraction. The output of PSF is a pixel array type of focal plane file (similar in type and format as diffuse energy files produced by DEDRIQ) that indicate how much diffracted energy is in each pixel.

3.8 FPLOOK

The purposes of FPLOOK are (1) to combine specular ray files and focal plane pixel array files into a single focal plane pixel array file, and (2) to show the user the energy contained in a user-specified set of pixels. FPLOOK, described in detail in Section 5.8, takes as input (1) the files created by NABRAT, DRAT, DEDRIQ, or PSF (or even a previous run of FPLOOK), and (2) a user-created file telling how to combine these files and which (if any) pixel energies to display.

3.9 COGEN

The purpose of COGEN, described in detail in Section 5.9, is to fit a set of polynomials to a set of actual mirror deformation data so that the resulting polynomial coefficients can later be used by DRAT in ray-tracing the deformed system. As detailed in Section 4.7, the polynomials are Zernike polynomials for a conventional system, and Legendre-Fourier polynomials for an X-ray system.

3.10 ZERGEN

The purpose of ZERGEN, described in Section 5.10, is to provide annular Zernike polynomials for OPD conversion and Wavefront Tolerancing. The Zernike polynomials are normalized over unit annulus with any desired inner obscuration. The Zernike polynomials are used by COGEN, DRAT, and OPDCNV routines of the OSAC program.

3.11 OPD CNV

The OPDCNV, described in Section 5.11, has the capability to convert the Optical Path Difference file of OPD routine to the same format as the surface deformation data (DEFDAT, or DFD) file.Therefore, the wavefront errors can be directly fit to a set of annular Zernike polynomials using ZERGEN routine.

3.12 WAVEFRONT TOLERANCING (WFSNSI, WFSNS2, and OPDGEN)

The purpose of WFSNS1, WFSNS2, and OPDGEN routines, described in Section 5.12, is to analyze the sensitivities of wavefront errors to various constructional changes within the optical system. OSAC can also use the derived sensitivities to calculate the wavefront from a specific set of constructional changes, without having to perform a new ray trace.

4. CONVENTIONS

4.1 Standard Coordinate System

OSAC employs a standard coordinate system with respect to which each optical surface and the focal plane are defined. The standard coordinate system is illustrated in Figure 4.1. It is defined with the optical axis aligned along the positive z axis. The ray direction cosines and the ray surface intersection coordinates listed in the OSAC-created ray intersection information files are always defined with respect to the standard coordinate system. There is, however, one instance where the standard coordinate system is redefined. This is after reflection by a flat surface. In this case, the optical system is effectively folded to realign the new optical axis with the standard coordinate system's positive z axis. In other words, the intersection coordinates at the flat surface are defined with respect to the old coordinate system, but the direction cosines of the reflected ray are redefined as if the direction of the optical axis were unchanged. Thus, if the flat surface had no deformations, the direction cosines of the ray would be unchanged, as depicted in Figure 4.2.

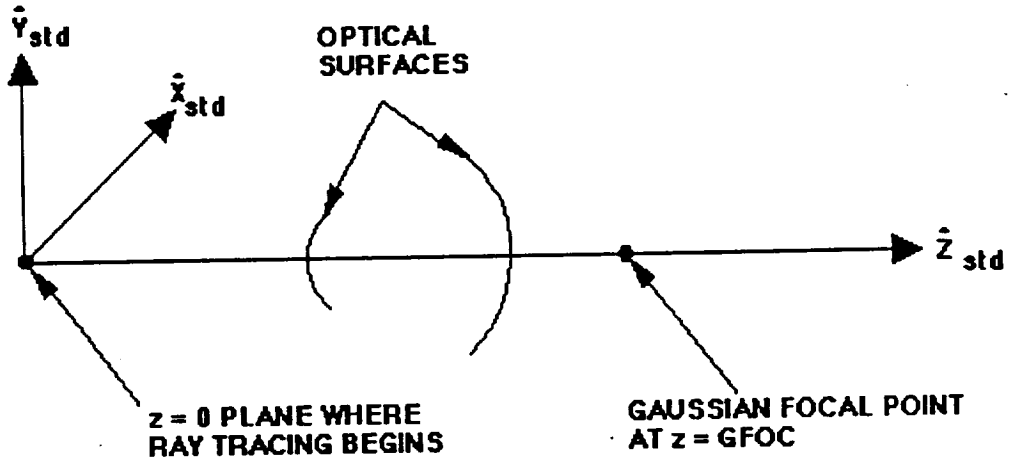

Figure 4.1 Standard Coordinate System (STD)

4.2 Input Ray Bundle

The input bundle of rays to be traced is a group of collimated rays that lie within an annulus with inner and outer radii R1 and R2. The center of the annulus where ray tracing begins lies at the coordinates (XAP, YAP, 0) in the standard coordinate system. The initial direction of propagation is along the positive z-axis for on-axis radiation. For off-axis radiation, the direction vector is rotated first about the y-axis by the angle AZBU, and then about the x-axis by the angle ELBU. A bundle of off-axis input rays is pictured in Figure 4.3.

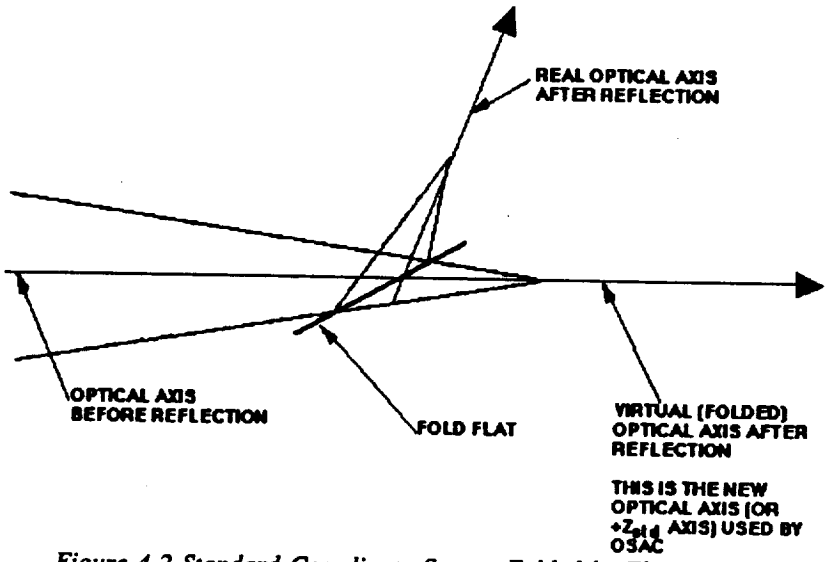

Figure 4.2 Standard Coordinate System Folded by Flat Surface

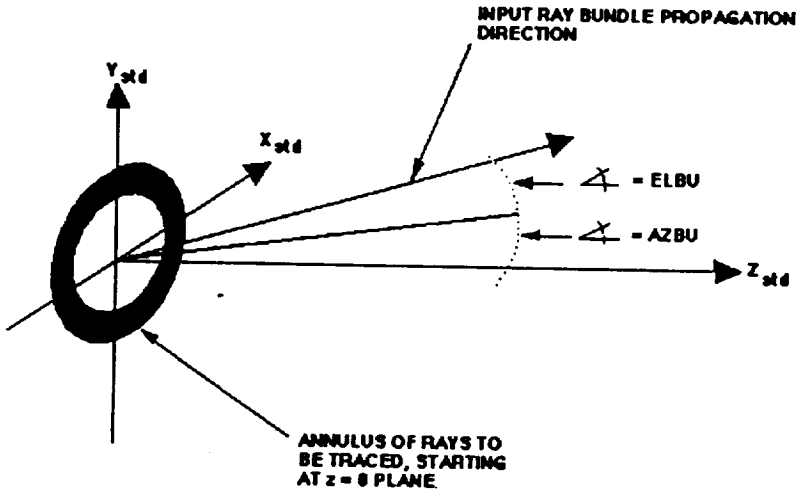

Figure 4.3 Off-Axis Input Rays

A point source that lies at a finite distance from the origin of the standard coordinate system is also allowed. Figure 4.4 illustrates the point source at finite distance. The (positive) distance PTSRC is the distance along the z-axis from the plane containing the point source, to the plane containing the entrance pupil (z_{STD}=0). The unchanged system parameters which specify the azimuthal and elevational angles of the incoming ray bundle now define the angles of the ray connecting the point source with the center of the pupil.

The annulus of rays consists of concentric rings of rays. There are MING rings with M2 rays per ring. If the inner radius, R1, is zero, then the center "ring" has only one ray, but each of

the other rings has M2 rays. The rings are unequally spaced in order to divide the annulus into equal area sections. Therefore, if Rl is non-zero, then the area between each consecutive pair of rings is equal. If Rl is zero, however, the area between the center and the first non-zero ring is (1 + 1/M2) times the area between successive pairs of rings. Both of these situations are depicted in Figure 4.5.

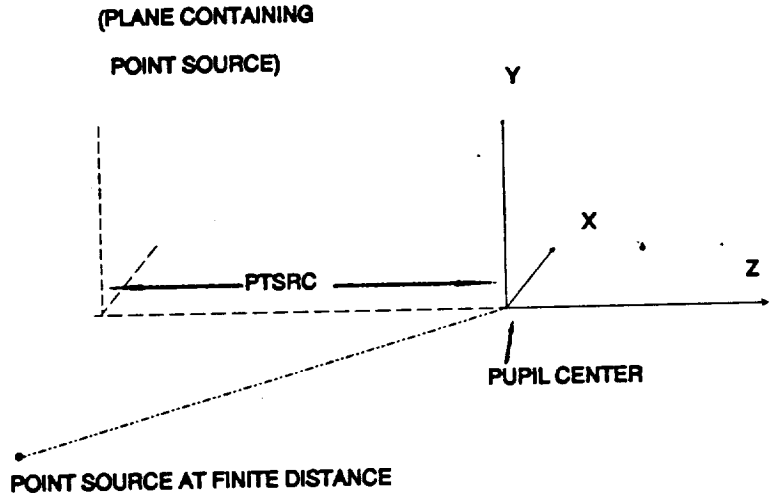

Figure 4.4 Point Source at Finite Distance

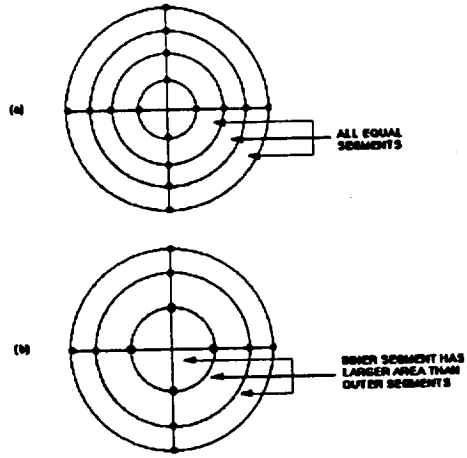

Figure 4.5 Configuration of Input Rays in Annulus, (a) Inner Radius ≠ 0 and (b) Inner Radius = 0

Upon entering the optical system, each ray is assigned an intensity or "weight" of unity. This weight is subsequently attenuated by reflections and scattering by the mirror surfaces. See Section 4.4 for an explanation of mirror reflectivity and Sections 5.4-5.5 for an explanation of OSAC's scatter analysis.

4.3 Body Centered Coordinate Systems

There is one body centered coordinate system (BCS) defined for each optical element in the system. The location of the BCS origin with respect to the standard coordinate system (STD) is specified by the user with the surface definition parameters in the GEOSAC input file. (These parameters are detailed further in the GEOSAC program description, Section 5.1.) The x-, y-, and z-axis of the BCS are nominally defined to lie parallel to the corresponding STD axes (with the exception of flat surfaces, which are described below). Angular misalignments of the surface are introduced by rotating the BCS about its origin by azimuth and elevation angles AZMIS and ELMIS. The BCS is first rotated about the BCS y-axis by the angle AZMIS, and then this coordinate system is rotated about the old, unrotated BCS x-axis by the angle ELMIS.

Flat surfaces, described in Section 4.6.3, where the normal to the fold flat is already assigned azimuth and elevation angles AZF and ELF, the orientation of the final, misaligned BC is found by rotating the BCS by the angles (AZI + AZMIS) and (ELF + ELMIS) , respectively. The angles AZMIS and ELMIS are specified along with the BCS origin location in the GEOSAC input file. A misaligned BCS is pictured in Figure 4.6.

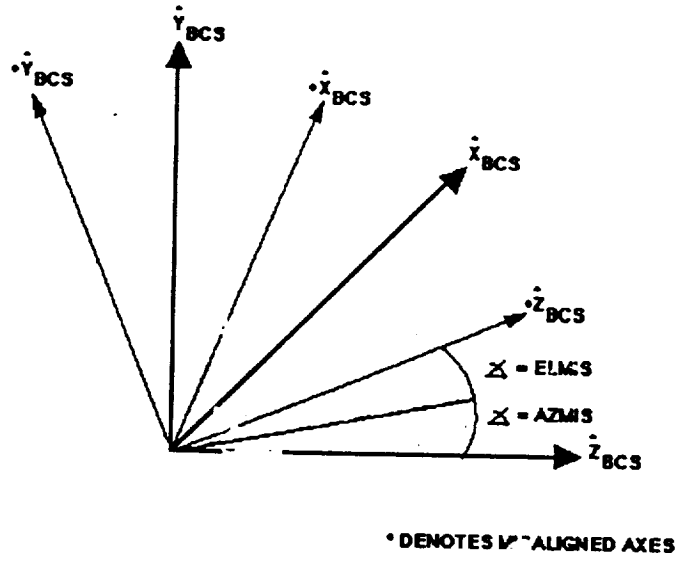

Figure 4.6 Misaligned Body Centered Coordinate System (BCS)

4.4 Mirror Reflectivity and Polarization

The surface reflectivity of all the optical surfaces is obtained from the user-defined complex dielectric constant. All surfaces are given the same reflectivity versus grazing angle. (The grazing angle is the complement of the more commonly used angle of incidence, and is, therefore, near zero for x-ray systems, and near $\pi/2$ for conventional systems.) The Fresnel reflectivity equations are used in the form

$$R^{+}=\frac{Y^2\sin(\theta)-\sqrt{Y^2-\cos^2(\theta)}}{Y^2\sin(\theta)+\sqrt{Y^2-\cos^2(\theta)}} \qquad (4\text{-}1)$$

and

$$R^{-}=\frac{\sin(\theta)-\sqrt{Y^2-\cos^2(\theta)}}{\sin(\theta)+\sqrt{Y^2-\cos^2(\theta)}} \qquad (4\text{-}2)$$

where θ is the grazing angle, and $Y^2 = \epsilon_1 + i\epsilon_2$ is the user-defined complex dielectric constant.

There are three characteristics in the area of reflectivity and polarization which must be noted:

(1) Arbitrary incoming polarization states are allowed — either random polarization, or arbitrary discrete elliptical polarization.
(2) The complex surface dielectric constant, and therefore the reflectivity, must be specified separately for each surface.
(3) Reflectivity is calculated correctly for systems with more than one surface and with non-negligible differences between reflectivities for S and P polarization.

Overall, the operation of the ray trace programs GEOSAC, NABRAT, and DRAT is unaffected if the user wishes to use random polarization. The complex surface dielectric constant must be specified separately for each surface in the geometry input file (GI file). If the user wishes to use a discrete elliptical input polarization, including circular and linear, then the appropriate parameters must be defined within the GI file. Section 5.1.2 and Tables 5.1 - 5.8 define the GI file completely.

PSI is the orientation angle of the incoming polarization ellipse, and E is the ratio of the minor axis amplitude to the major axis amplitude (positive for left-handed polarization, negative for right-handed). Figure 4.7 graphically shows these parameters.

The polarization information consists of the x and y components of the complex amplitudes for each of the two incoming polarization states. The first polarization state (the "cosine" state, with complex amplitude vector "C") is the one which was originally oriented along the major axis of the polarization ellipse for discrete polarization, or along the x direction for random

polarization. The second polarization state (the "sine" state, with complex amplitude vector "S") is the one which was originally oriented along the minor axis of the polarization ellipse for discrete polarization, or along the y direction for random polarization. The two polarization states are given a phase difference of $\pi/2$ radians as they enter the system. Phase differences caused by reflection are kept track of via the new records in the RAY file. (Phase changes inherently due to the propagation along a given optical path length are ignored.)

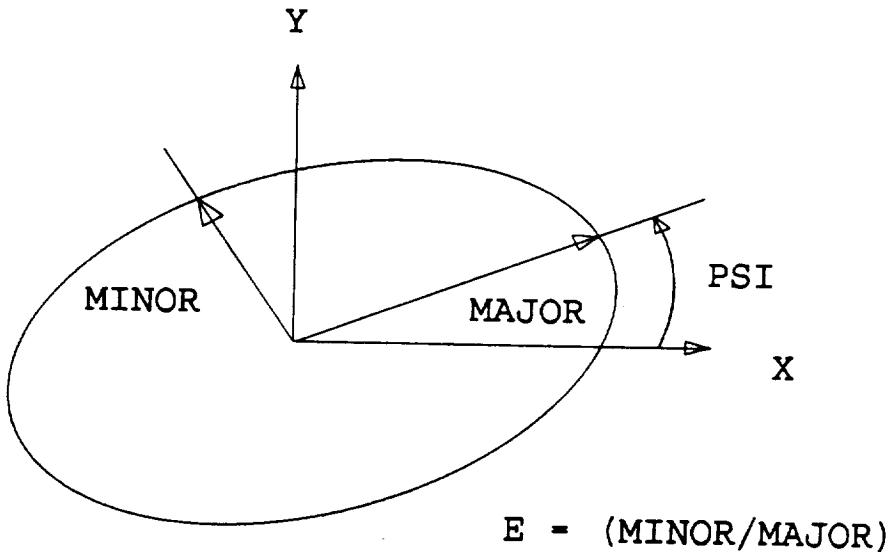

Figure 4.7

Electric Polarization Ellipse, Looking into the Incoming Wavefront from the Optical System. (The angle PSI defines the orientation of the major axis, while the parameter E defines the ratio of the minor axis amplitude to the major axis amplitude. A positive value of E is used for left-handed polarization, and a negative value for right-handed.)

The interested user may examine the RAY file according to the format in Table 5.12(b) to determine the complex vectors C and S. The user may then verify the ray weight according to the OSAC formulae

$$W = |C|^2 + |S|^2 \text{ (random polarization)} \qquad (4\text{-}3)$$

and

$$W = |C|^2 + |S|^2 + Im\ (C \cdot S*)\ (\textit{discrete polarization}) \qquad (4\text{-}4)$$

where C and S are the complex amplitude vectors described above.

Again, the total ray weight derived according to Equation (4-3) or (4-4) is still shown in the output listings from NABRAT and DRAT. It is only the detailed (and usually irrelevant to the user) polarization information which has been added to the RAY file.

4.5 Surface Definition Equations

All mirror surfaces (except flats and toroids) are conics, with the conic constants defined according to the following equations:

For conventional systems:

$$Z = \frac{K - \sqrt{K^2 + P*(\rho_0^2 - \rho^2)}}{P} \qquad (4\text{-}5)$$

for $P \neq 0$

$$Z = \frac{\rho^2 - \rho_0^2}{2K} \qquad (4\text{-}6)$$

for $P = 0$
For X-ray Systems:

$$\rho = \sqrt{\rho_0^2 + 2Kz - Pz^2} \qquad (4\text{-}7)$$

where (ρ , z) are the conventional cylindrical coordinates of the surface with respect to the body centered coordinate system (BCS). In this coordinate system, $Z = 0$ when $\rho=\rho_0$. For conventional surfaces, ρ_0 is usually zero, and, therefore, the BCS origin is usually located at the intersection of the surface with the optical axis. In general, though, the BCS origin for conventional surfaces is located on the plane where $\rho=\rho_0$. For x-ray surfaces, the BCS origin is always located at the axial midpoint of the surface. Again, at that point, $\rho=\rho_0$.

4.6 Surface Types

OSAC allows for six types of surfaces. The six surface types are: (1) on-axis (near normal incidence) conic surfaces for conventional systems, (2) off-axis conic surfaces for conventional systems, (3) flat surfaces for conventional systems, (4) on-axis (near cylindrical or grazing incidence) conic surfaces for x-ray systems, (5) toroidal surfaces, and (6) obscuration surfaces. Each of these types is discussed below along with its corresponding body centered coordinate system (BCS) and defining parameters.

4.6.1 Conventional On-Axis Surfaces

Conventional on-axis surfaces are defined by their inner and outer radii R1S and R2S, and by the conic constants in the defining equation

$$Z = \frac{K - \sqrt{K^2 + P*(\rho_0^2 - \rho^2)}}{P} \qquad (4\text{-}8)$$

The BCS origin is located by definition at whatever plane $\rho=\rho_0$. Since ρ_0 for conventional on-axis surfaces is usually defined to be zero, the BCS origin is usually located at the intersection of the surface with the optical axis. The surface is defined for ρ values ranging from R1S to R2S. A conventional on-axis surface is pictured in Figure 4.8.

4.6.2 Conventional Off-Axis Surfaces

Conventional off-axis surfaces are defined as a section of a parent on-axis conic surface. The parent conic and the corresponding BCS are defined in the same way as for conventional on-axis surfaces. The off-axis segment is that portion of the parent conic enclosed by a cylinder whose radius is R2S, and whose axis lies in the Y_{BCS} - Z_{BCS} plane, is elevated to the boresight angle B, and intersects the parent conic at y = YE. A conventional off-axis surface is shown in Figure 4.9.

4.6.3 Flat Surfaces

Flat surfaces (fold flats) are allowed in conventional systems, and are defined as a circular disk of radius R2S. The BCS origin is defined to coincide with the center of the disk. A unit normal is defined to point into the reflecting surface. The azimuth and elevation angles of the (nonmisaligned) normal with respect to the standard coordinate system are AZF and ELF. The intersection of the fold flat plane with the optical axis occurs at z = ZFOLD. The orientation of the body centered coordinate system (BCS) is found by rotating the STD coordinate system by azimuth and elevation angles AZF and ELF. The sense of rotation through these angles is the same as for the azimuth and elevation surface misalignment angles, described fully in Section 4.3. A flat surface is pictured in Figure 4.10.

4.6.4 X-Ray Surfaces

X-ray surfaces are defined by their length L, and by the conic constants in the defining equation

$$\rho = \sqrt{\rho_0^2 + 2Kz - Pz^2} \qquad (4\text{-}9)$$

The BCS origin is located at the axial midpoint of the surface. Thus the surface is defined for z values ranging from -L/2 to +L/2. An x-ray surface is pictured in Figure 4.11.

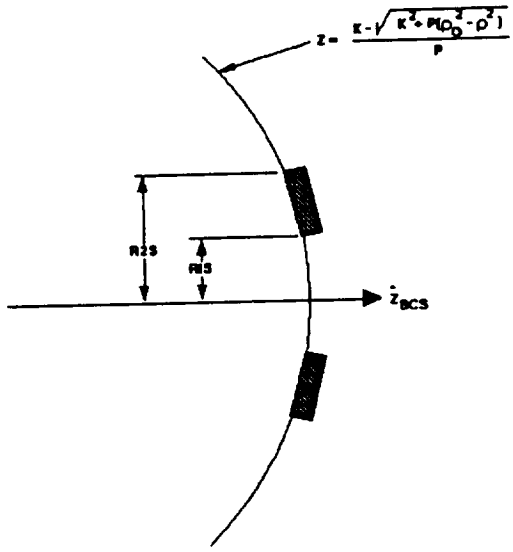

Figure 4.8 Conventional On-Axis Surface

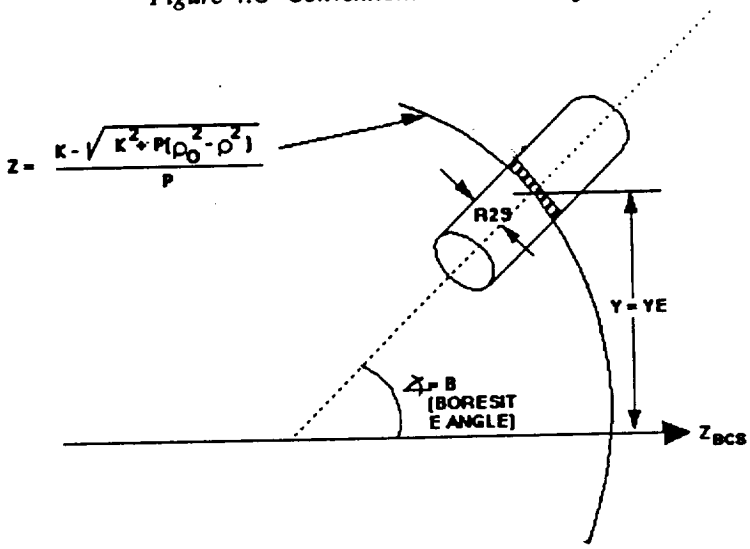

Figure 4.9 Conventional Off-Axis Surface

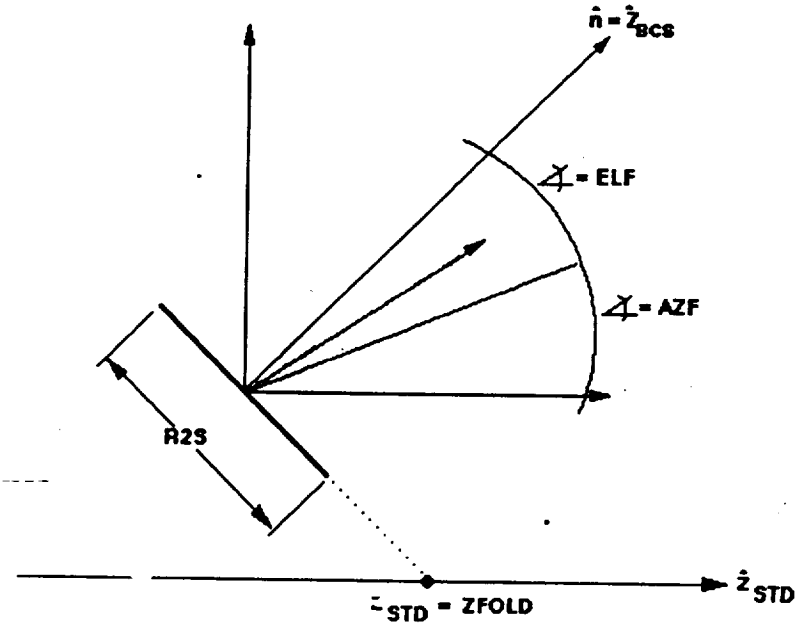

Figure 4.10 Flat Surface

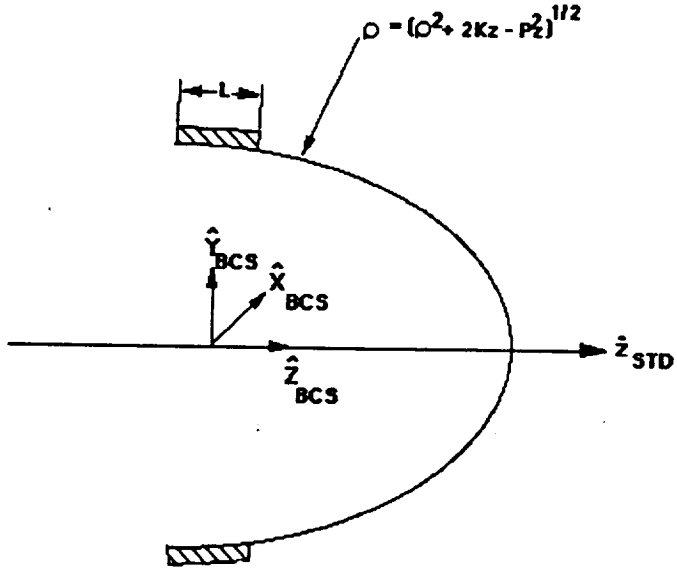

Figure 4.11 X-Ray Surface

4.6.5 Toroidal Surfaces

The configuration of a toroidal surface is shown in Figure 4.12. As shown the toroid consists of a conic curve in the y-z plane which is rotated about a line parallel to the y axis, displaced

by a distance RTOR along the z axis. The conic curve may have a positive or negative vertex radius, and the distance RTOR may be positive or negative. (In the figure, the conic curve vertex radius and the distance RTOR are both shown as positive.) In OSAC, the user is able to specify the vertex radius or the toroidal radius (or both) as infinite, simply by using values greater than or equal to 10^{15}.

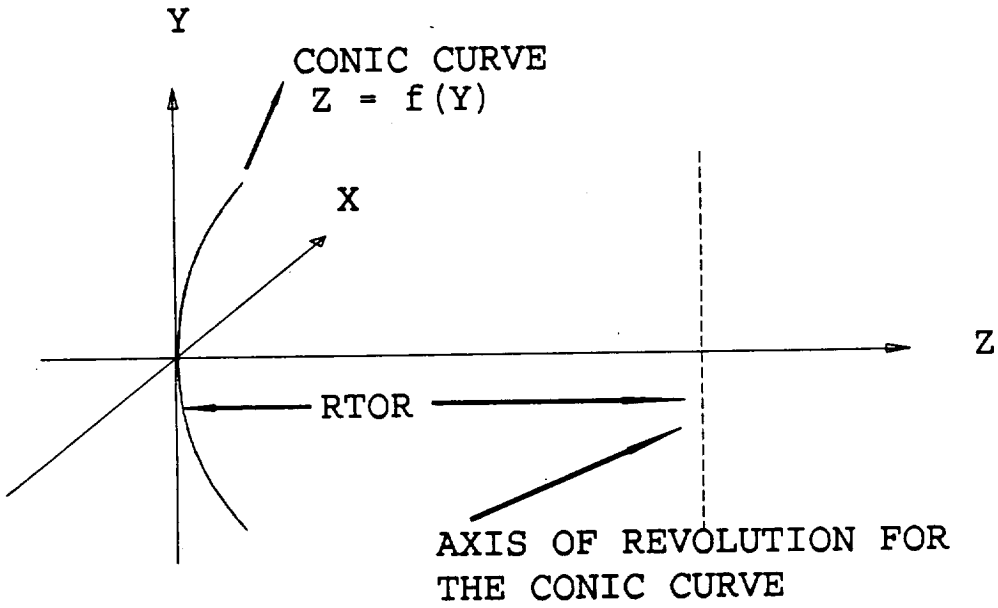

Figure 4.12

Toroidal Surface Configuration, Showing the Conic Curve in the y-z Plane which is Rotated about a Line Parallel to the y Axis, Displaced by a Distance RTOR Along the z Axis. The Conic Curve may have a Positive or Negative Vertex Radius, and the Distance RTOR may be Positive or Negative. (In this figure, the conic curve vertex radius and the distance RTOR are both shown as positive

The defining conic curve in the y-z plane is defined in the same way as conventional on-axis OSAC surfaces, with the exception that the $z_{BCS}=0$ radius, PO, is defined to be zero. (The BCS is the body-centered coordinate system. PO is thus the radius of the surface at the BCS origin. Thus, the defining conic function z=f(y) is as follows:

$$z = f(y) = (K / P)\,(1 - (1 - P\,y^2 / K^2)^{1/2}) \qquad (4\text{-}10)$$

where K is the vertex radius and P is 1-eccentricity^2. When P is zero, the defining conic

function degenerates to its paraboloidal form,

$$z = f(y) = y^2 / (2K) \qquad (P=0) \qquad (4\text{-}11)$$

This completes the technical definition of the toroidal surface. The reader is referred to G. H. Spencer and M. V. R. K. Murty, General Ray-Tracing Procedure, Journal of the Optical Society of America 52, 672 (1962), for related discussions of toroidal surfaces. In the sections below we discuss the topics of alignment, deformations, focusing calculations, and convexity, and then discuss the operation of the OSAC using a toroidal surface.

4.6.5.1 Toroidal Alignment

Because of the inherent non-symmetry of the toroidal surfaces, they have been given an additional rotational degree of freedom in their positioning. Recall that all other OSAC surfaces can be rotated arbitrarily in elevation and then azimuth, and then translated arbitrarily in x, y, and z. The toroidal surfaces can additionally be rotated about the +z axis before giving them the usual elevational, azimuthal, and translational changes.

4.6.5.2 Toroidal Deformations

In order to make a toroidal surface arbitrarily aspheric, the user can apply Zernike polynomials, discussed in Section 4.7, in exactly the same way as for a conventional on-axis surface. (As in the conventional on-axis case, positive deformations are in the positive z direction.) Because of the z rotation capability for toroidal surfaces, the user should keep in mind that the Zernike polynomials are applied *before* the z rotation rather than after it. In other words, the Zernike polynomials are fixed with the local x-y-z coordinate system of the toroid. Both annular and full circle Zernike polynomials are allowed. Note that Zernike polynomial amplitudes comparable to or even greater than the nominal sags can be applied.

4.6.5.3 Toroidal Focusing Calculations

The focusing properties of toroidal surfaces need to be discussed because of the possibly different radii in the two directions. The GEOSAC program reports on the conic information for all surfaces, giving vertex locations, focus locations, etc., in both the body centered coordinate system and the standard (overall) coordinate system. GEOSAC now behaves exactly the same for toroidal surfaces, using the conic information of the curve in the y-z plane only. Thus, any modified focusing properties due to a different radius in the x-z plane are ignored. The user may fully intend to take advantage of such modified focusing properties, and is perfectly able to set up the system to do so. He must simply be aware that, as far as focusing calculations are concerned, GEOSAC treats the surface as if it were a full conic surface with the same conic constants as the defining conic curve in the y-z plane.

4.6.5.4 Toroidal Convexity

Just as there is possible confusion about the focusing properties of this asymmetric surface, so there is possible confusion over the convexity or concavity of it. We have followed the same convention as in the GEOSAC focusing calculations previously discussed. Thus, the convexity or concavity of the surface at any location can be determined by the following intuitive process: From the point and side of the surface in question, move to the surface's origin without crossing through the surface. Consider only the conic curve which is contained in the y-z plane at the origin. The surface at the original point will then be judged to be convex or concave according to the convexity or concavity at the origin, referring at the origin only to the conic curve in the y-z plane.

4.6.5.5 Program Usage

OSAC is run in exactly the same way for a toroidal surface as for any other surface. The only restriction is that, since the toroid is not a conventional full conic surface, NABRAT cannot be used to perform the geometric ray trace for a system with a toroid — only DRAT can be used.

4.6.6 Obscuration Surfaces

There are two types of obscuration surfaces which are included in OSAC:

(1) a rectangular, or
(2) an annular (including a full circle) obscuration

Either type of obscuration can be defined as either opaque or transmitting. Figure 4.13 shows the two types of obscuration surfaces in both the opaque and the transmitting mode, and shows the definition of the dimensional and rotational parameters.

As with any other type of surface in OSAC, the obscurations can be arbitrarily displaced and tilted. If rays are interrupted by the obscuration, they are flagged as failed in the RAY file. Otherwise, they are passed through with no change in intensity or polarization state.

Multiple obscuration surfaces can be placed in very close proximity, in order to simulate various odd shapes of obscuration, such as multiple slits, sections of an annulus, etc.

4.7 Low Spatial Frequency Deformations

Through the module DRAT, OSAC is capable of analyzing the effect of low spatial frequency deformations on the optical surfaces. These deformations are modelled as a sum of discrete polynomials. For conventional on-axis, conventional off-axis, and flat surfaces the polynomials are Zernike polynomials. Thus, for conventional on-axis surfaces, the surface definition equation discussed in Section 4.6.1 is modified to become

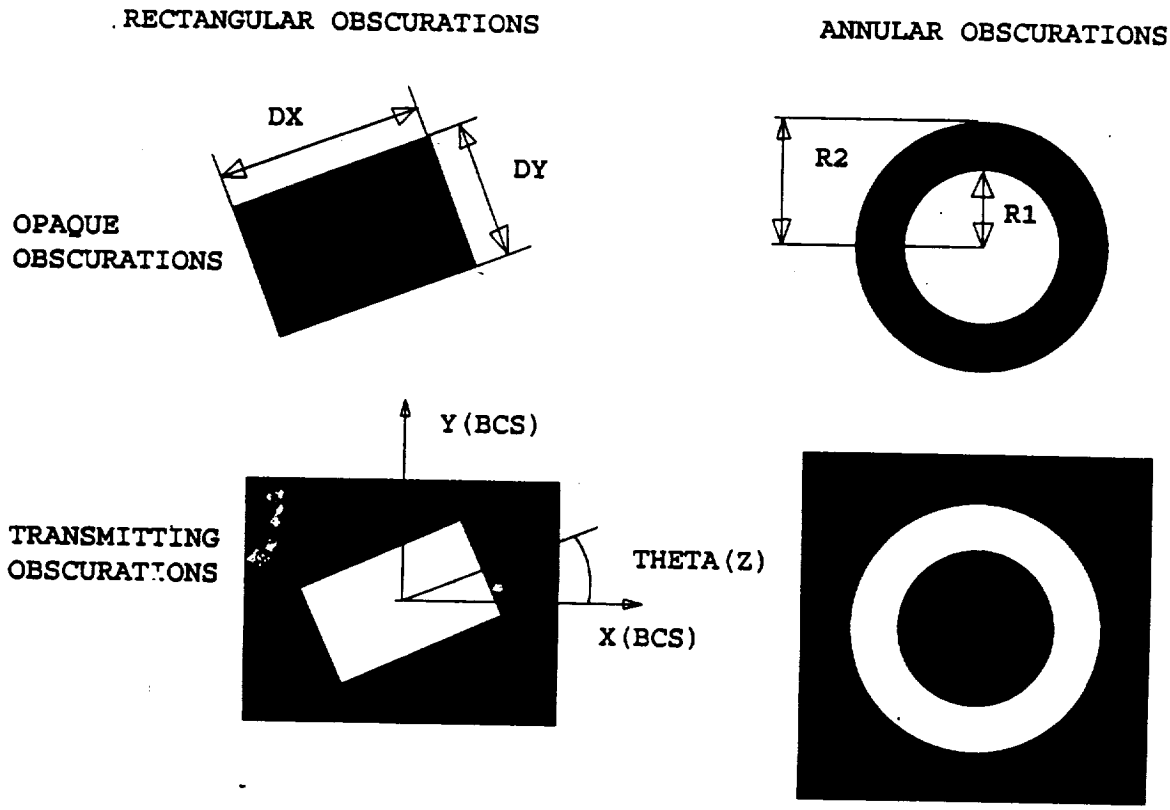

Figure 4.13

Annular and Rectangular Obscurations, shown with their Defining Dimensional and Rotational Parameters. Both the Annular and the Rectangular Obscurations can be either Opaque or Transmitting.

$$Z(\rho,\theta)=\frac{K-\sqrt{(K^2+P(\rho_0^2-\rho^2)}}{P}+\sum_{l=0}^{\infty} d_l[\sqrt{l+1}R_l^0(\frac{\rho}{R2S})]+$$
$$\sum_{l=0,m=1}^{\infty} e_{ml}[\sqrt{2(l+1)}R_l^m(\frac{\rho}{R2S})\cos(m\theta)]+\sum_{l=0,m=1}^{\infty} f_{ml}[\sqrt{2(l+1)}R_l^m(\frac{\rho}{R2S})\sin(m\theta)] \quad (4\text{-}12)$$

where R2S is the outer radius of the element, $R_l^m(r)$ are the radial polynomials of Zernike, and d_l, e_{ml} and f_{ml} are the coefficients defined by the user. The terms within the brackets are defined for the purposes of OSAC to be the "Zernike polynomials." The first several Zernike polynomials (in the OSAC-defined order), along with the defining normalization relations of the radial polynomials, are listed in Table 4.1. For conventional off-axis surfaces, the deformation sag defined above is applied along the direction of the boresight angle B, defined in Section 4.6.2. For flat surfaces, the deformation sag is applied normal to the flat's body-centered coordinate system. Figure 4.14 illustrates deformations applied to each of these three types of

surfaces.

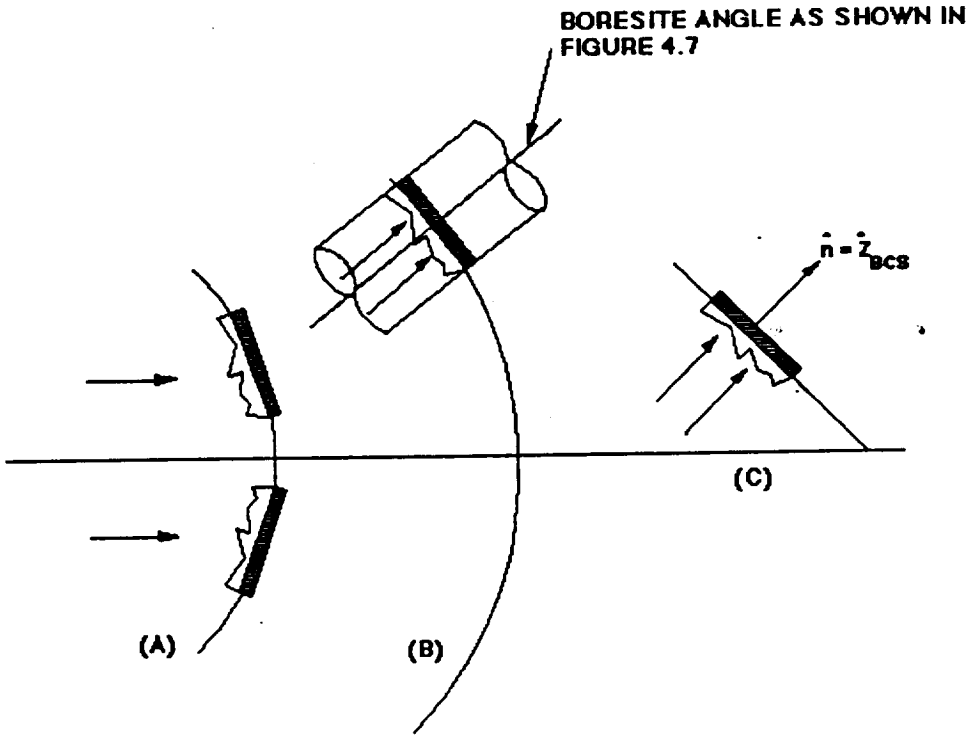

Figure 4.14 Polynomial Deformations Applied to Conventional Surfaces

For x-ray surfaces, the deformation polynomials are Legendre-Fourier polynomials. Thus, the surface definition equation discussed in Section 4.5 is modified to become

$$\rho(z,\theta) = \sqrt{\rho_0^2+2Kz-Pz^2} + \sum_{l=0}^{\infty} d_l P_l(\frac{2z}{L}) + \sum_{m=1,l=0}^{\infty} e_{ml} P_l(\frac{2z}{L})\cos(m\theta) + \sum_{m=1,l=0}^{\infty} f_{ml} P_l(\frac{2z}{L})\sin(m\theta) \quad (4\text{-}13)$$

where $P_l(2z/L)$ is the l^{th} Legendre polynomial, and d_l, e_{ml} and f_{ml} are the user-defined coefficients. L is the axial length of the x-ray surface, so that the argument of the Legendre polynomials goes between -1 and +1. The first several Legendre polynomials, along with the defining normalization relations, are listed in Table 4.2. Figure 4.15 illustrates deformations applied to an x-ray surface. It should be noted that the Zernike and the Legendre-Fourier polynomials described above were chosen because of their convenient orthogonality relations, which are listed in Tables 4.1 and 4.2. These orthogonality relations allow for simple

Table 4.1
Zernike Polynomial Conventions

$$R_n^m(r) = \sum_{s=0}^{(n-m)/2} \frac{(-1)^s(n-s)!}{s![(n+m)/2-s]![(n-m)/2-s]!} r^{(n-2s)}$$

- Explicit Expression for the Radial Polynomials of Zernike -

$Z_1 = R_0^0(r)$	$= 1$
$Z_2 = 2\,R_1^1(r)\cos\theta$	$= 2r\cos\theta$
$Z_3 = 2\,R_1^1(r)\sin\theta$	$= 2r\sin\theta$
$Z_4 = \sqrt{3}\,R_2^0(r)$	$= \sqrt{3}(2r^2-1)$
$Z_5 = \sqrt{6}\,R_2^2(r)\cos2\theta$	$= \sqrt{6}r^2\cos2\theta$
$Z_6 = \sqrt{6}\,R_2^2(r)\sin2\theta$	$= \sqrt{6}r^2\sin2\theta$
$Z_7 = \sqrt{8}\,R_3^1(r)\cos\theta$	$= \sqrt{8}(3r^3-2r)\cos\theta$
$Z_9 = \sqrt{8}\,R_3^3(r)\cos3\theta$	$= \sqrt{8}r^3\cos3\theta$

- Specific Zernike Polynomials in OSAC-defined Order -

$$\int_0^1 dr r \int_0^{2\pi} d\theta Z_n(r,\theta)Z_{n'}(r,\theta) = \delta_{nn'}\pi$$

- Orthogonality Relations for Zernike Polynomials -

expressions for the mean square surface deformation in terms of the polynomial coefficients. They also allow for simple expressions for the polynomial coefficients in terms of actual surface deformation data. These expressions can be derived from the relations listed in Tables 4.1 and 4.2, and are summarized below.

Table 4.2
Legendre-Fourier Polynomial Conventions

$P_0(x) = 1$

$P_1(x) = x$

$P_2(x) = (3x^2 - 1)/2$

$P_3(x) = (5x^3 - 3x)/2$

- Specific Legendre Polynomial -

$$P_n(x) = 2^{\frac{1}{n}} \sum_{m=0}^{[n/2]} (-1)^m \binom{n}{m} \binom{2n-2m}{n} x^{(n-2m)}$$

[] denotes largest integer less than or equal to argument

(a/b) denotes 'combinations' = a!/b! (a-b)!

- Explicit Expression for Legendre Polynomials -

$$\int_{-1}^{1} P_{n'}(x)dx = \delta_{nn'} \left(\frac{2}{2n+1}\right)$$

- Orthogonality Relation for Legendre Polynomials -

For a conventional surface with Zernike polynomial deformations, the mean square roughness σ^2 is defined by

$$\sigma^2 = \sum_{l=0,m=1}^{\infty} (d_l^2 + e_{ml}^2 + f_{ml}^2) \qquad (4\text{-}18)$$

where d_l, e_{ml}, and f_{ml} are the polynomial coefficients. If the user has at his disposal actual surface deformation data over the surface as a function $\Delta(r = \rho/2RS, \theta)$, then the polynomial coefficients can be written as

$$d_l = \frac{1}{\pi}\int_0^1 r dr \int_0^{2\pi} d\theta(\sqrt{l+1}\,R_l^0(r))\ \Delta(r,\theta)$$

$$e_{ml} = \frac{1}{\pi}\int_0^1 r dr \int_0^{2\pi} d\theta\sqrt{2(l+1)}\,R_l^m(r)\cos(m\theta)\Delta(r,\theta) \qquad (4\text{-}19)$$

$$f_{ml} = \frac{1}{\pi}\int_0^1 r dr \int_0^{2\pi} d\theta\sqrt{2(l+1)}\,R_l^m(r)\sin(m\theta)\Delta(r,\theta)$$

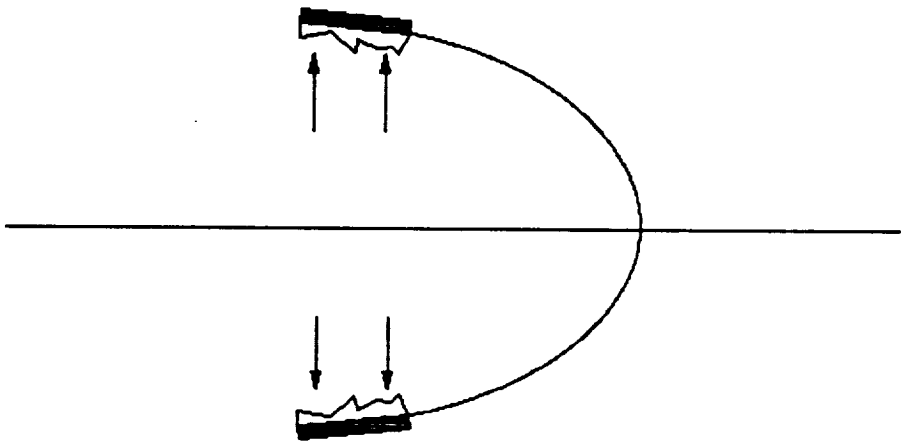

Figure 4.15 Polynomial Deformations Applied to X-Ray Surfaces

For an X .. surface with Legendre-Fourier polynomial deformations, σ^2 is given by

$$\sigma^2 = \sum_{l=0}^{\infty}\left(\frac{1}{2(2l+1)}(2d_l^2+e_{ml}^2+f_{ml}^2)\right) \qquad (4\text{-}20)$$

where d_l, e_{ml}, and f_{ml} are again the polynomial coefficients. If the user has at his disposal actual surface deformation data over the surface as a function $\Delta(s=2z/L,\ \theta)$ then the polynomial coefficients can be written as

$$d_l = \frac{1}{\pi}\int_{-1}^{1} ds \int_{0}^{2\pi} d\theta(\sqrt{2l+1}\,P_l^0(s))\ \Delta(s,\theta)$$

$$e_{ml} = \frac{1}{\pi}\int_{-1}^{1} ds \int_{0}^{2\pi} d\theta\sqrt{2(2l+1)}\,P_l^m(s)\cos(m\theta)\Delta(s,\theta) \qquad (4\text{-}21)$$

$$f_{ml} = \frac{1}{\pi}\int_{-1}^{1} ds \int_{0}^{2\pi} d\theta\sqrt{2(2l+1)}\,P_l^m(s)\sin(m\theta)\Delta(s,\theta)$$

Despite the choice of using Zernike and Legendre-Fourier polynomials, there is one case where the orthogonality relations break down, and the above relations no longer strictly hold. That case is when the Zernike polynomials are used on a conventional surface with a non-zero central obscuration. In that case, the user would have to use a different procedure (e.g., a least squares fitting scheme) to relate the deformation function $\Delta(r, \theta)$ to the coefficients of the polynomials which are no longer orthogonal over the aperture. (Note that COGEN, the polynomial fitting module, uses just such a method). Also, the above expression for σ^2 would give the mean square deformation for an unobscured aperture with the same polynomial coefficients, rather than for the real, obscured aperture.

4.8 High Spatial Frequency Deformations

Through the modules SUSEQ and DEDRIQ, OSAC is capable of analyzing the effect of high spatial frequency deformations (roughness) on the optical surfaces. This is accomplished by the user's specifying the roughness characteristics in various regions on the optical surfaces. Using this characterization, DEDRIQ calculates an angular scatter profile for each ray-surface intersection previously calculated by NABRAT or DRAT. The angular scatter profile is then multiplied by the appropriate scale factors calculated by SUSEQ to arrive at a focal plane distribution of diffusely scattered energy. The user has basically three options for specifying the roughness in a region on an optical surface. First, he may specify a surface height autocovariance function from a list of analytic functions. The autocovariance function of the surface height z(x, y) is defined by

$$ACV(X_0, Y_0) = \langle z(x,y) * z(x-x_0, y-y_0) \rangle \qquad (4\text{-}22)$$

where the $\langle\ \rangle$ notation denotes expectation value, or ensemble average. The ACV is assumed to be radially symmetric, i.e., $ACV(x_0,y_0) = ACV(\sqrt{x_{02} + y_{02}})$. The reason for using an autocovariance function for a roughness descriptor is that it can be Fourier transformed to yield the scattering profile. That theory is briefly reviewed in the DEDRIQ program description, Section 5.5. The second option for specifying roughness is to define a surface roughness power spectral density (PSD). This method is useful because the PSD is the Fourier transform of the autocovariance function, and is therefore proportional to the scatter profile. Again, that theory is reviewed in Section 5.5. The third option for specifying roughness is to define a periodic

grating profile on the surface. The grating may be periodic in either one direction, or in two orthogonal directions. The orientation of the grating relative to the surface is arbitrary. Figures 4.16 and 4.17 illustrates a grating and defines the relevant orientation, amplitude, and spatial wavelength parameters.

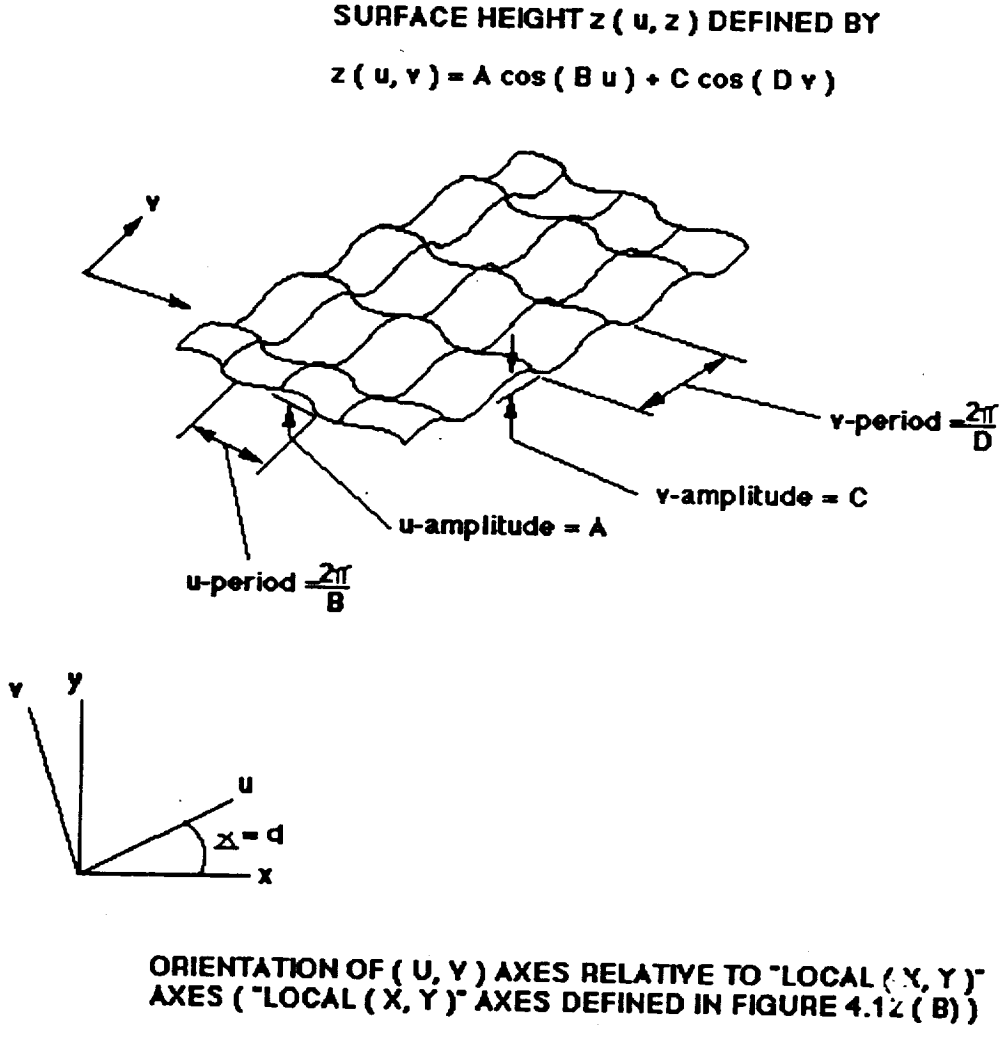

Figure 4.16 Grating Orientation — Defining Parameters

As mentioned above, the user is free to specify the surface roughness over various regions. This is done by allowing the user first to define a menu of surface roughness models, and then to define the regions on the surfaces where each model will apply. The regions are bounded by user-specified X and Y values on conventional surfaces, and by user-specified z and θ values on

x-ray surfaces. The user may have one region overlap, or even be contained in, another region by defining the regions in a particular order, since any region definition takes precedence over any previous definition at the same coordinates. Overlapping scatter regions are illustrated in Figure 4.18.

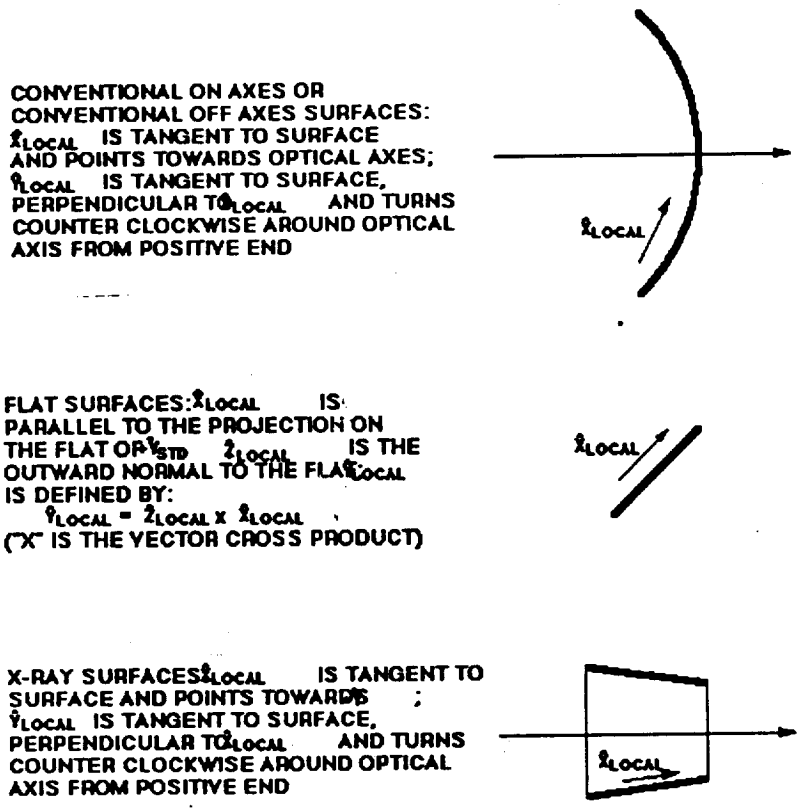

Figure 4.17 Grating Orientation — Definition of "Local (X, Y)" Axes

4.9 Pupil OPD Map

Through the modules OPD and PSF, OSAC is capable of modelling the effects on system performance of diffraction. This is done by calculating an intensity point spread function (PSF) from an optical path difference (OPD) map at a pseudo-pupil. (The theory of using an OPD map to obtain a PSF is briefly reviewed in the PSF program description, Section 5.7.) The term pseudo-pupil has been coined, because the pupil location is not defined by the user. Instead, the

module OPD uses a convenient location of its own choice at which to calculate the OPD map. That location is at the surface where the rays hitting the focal plane appear to intersect their predecessor rays in the input collimated bundle. This location is acceptable, since it is well known that for the purposes of calculating the PSF at a given input ray field angle any apparent pupil location will work as well as any other, as long as it is not contained in the caustic region. This pseudo-pupil location is particularly convenient, since the distance from that surface to the focal plane is the effective focal length of the system, a useful parameter both for the user and for the PSF module. Figure 4.19 illustrates an optical system, the pseudo-pupil surface and the OPD function.

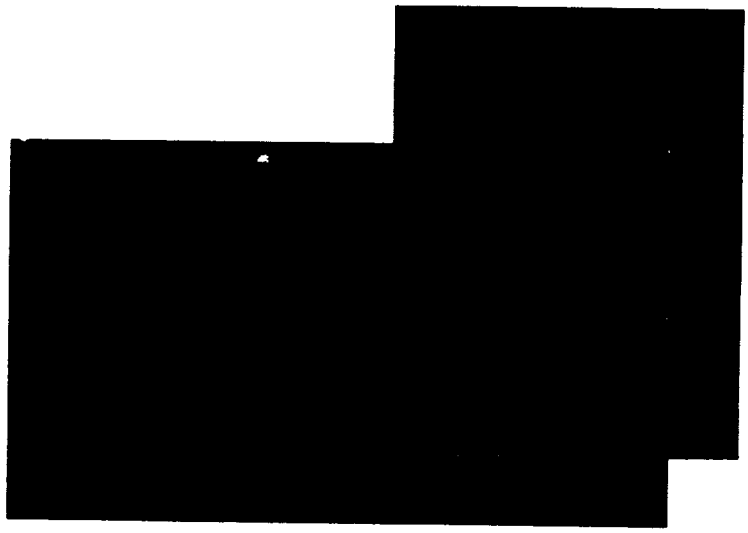

Figure 4.19 Roughness Definition Regions. Regions are Assumed to Have Been Defined in the Order 1, 2, 3. Note that the Coordinate Plane in this Figure Corresponds to the (x,y) Plane for Conventional Surfaces and to an Unrolled (z,θ) Plane for X-Ray Surfaces.

4.10 Storage Limitations, Maximum Parameter Values

Because of the limitation on the total memory requirement of any OSAC module (see Section 2.1), several arrays have been given fairly conservative lengths. This imposes maximum allowed values for many of the user input variables. These maximum values are not called out individually in the rest of this report, but are instead listed collectively in Table 4.3 for

reference. Table 4.3 also lists the programs where the maximum values are imposed. Any user who changes these maximum values should be aware that COMMON blocks may have to be changed in several subroutines.

Table 4.3
Parameter Maximum Values

Parameter Name	*Description*	*Maximum Value*	*Program Where Maximum Value Imposed*
NS	Number of Optical Surfaces Allowed in System	21	OSACBL (/PARX/COMMON Block)
NAREA	Number of roughness Regions Allowed on a Surface	5	DEDBLK (/LIMITS/COMMON Block)
NDEFN	Number of Roughness Definitions Allowed in User Menu	5	DEDBLK (/LIMITS/COMMON Block)
NTABG	Number of Entries in G(v) Look-up Tables	800	DEDBLK (/LIMITS/COMMON Block)
NTABF	Numer of Entries in Taylor Improvement Look-up Tables	100	DEDBLK (/LIMITS/COMMON Block)
NTABR	Number of Entries in Reflectivity Look-up Tables	800	DEDBLK (/LIMITS/COMMON Block)
NSEGS	Number of Segments Allowed in User-Defined Power Spectral Density Roughness Definition	5	PCHK1
NGRID	Number of Pixels in One Direction Allowed in Scatter or Diffraction Analysis	1001	DED (/LIMITS/COMMON Block) and PSFBLK (/LIMITS/COMMON Block)
NR	Number of Rings of Rays Allowed in Diffraction Analysis	50	PAFBLK (/LIMIT/COMMON Block)
NTHETA	Number of Spokes of Rays Allowed in Diffraction Analysis	20	PSFBLK (/LIMIT/COMMON Block)
MFFT	Log (Base 2) of Number of Entries Allowed in the FFT Arrays in Diffraction Analysis	9	PSFBLK (LIMIT/COMMON Block)

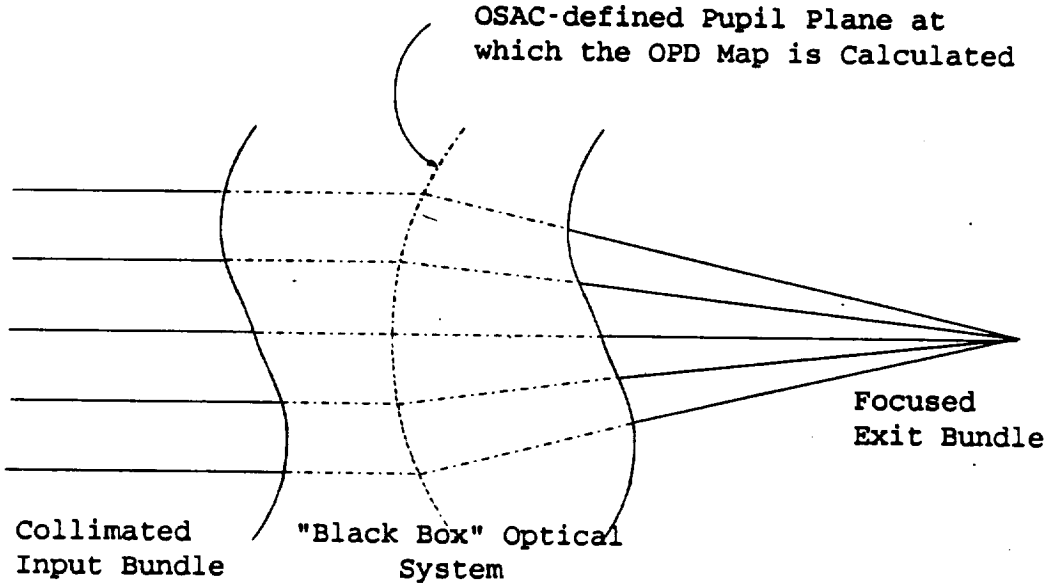

Figure 4.19 Pupil Plane and OPD Map

5. PROGRAM DESCRIPTIONS

The purpose of this section is to provide detailed information on how to use the various OSAC modules. This is done by listing the format and meanings of the various quantities in the input and output files, by explaining the analytical foundation of the modules, and by showing concrete examples of program runs.

Each subsection below details the use of one of the OSAC modules. For each module, all of the required input and output files are described, and the corresponding FORTRAN file numbers and OSAC file name conventions are listed. Any complicated or unusual analytical methods in the module are described. The printer output of each module is described in detail. The standard OSAC printer page headers are not described individually below. However, each header contains the name of the module and the version number, the date and time of the program run, an identification line for the module being run, and sometimes an identification line and date and time of running from another module required for input.

For reference, Figure 5.1 shows the input/output file structure that links all the OSAC modules except OPD convertion and wavefront tolerancing modules. The use of these modules is illustrated in Sections 5.11 and 5.12.

Several optical systems have been used for documentation purposes. They are DOCON, an on-axis conventional system; DOCOF, an off-axis subsection of DOCON with a fold flat added; and DOCXR, a Wolter Type 1 X-ray telescope system. Some information is provided about the geometrical ray trace of each of these systems. DOCXR is then used to illustrate the scatter analysis, and DOCON is used to illustrate the diffraction analysis. TOR1 system is used to demonstrate the use of toroidal surfaces.

5.1 GEOSAC

5.1.1 Introduction

GEOSAC reads a user input data file containing all the parameters necessary to define an optical system, and performs all the necessary geometric calculations for subsequent geometrical ray tracing by NABRAT or DRAT. No particularly unusual or complex analytical methods are used by GEOSAC. The subroutine structure of GEOSAC is shown in Figure 5.2.

5.1.2 Inputs and Outputs

The only input to GEOSAC is a user-created geometry file, called the GI file. The GI file contains all the information needed to define the optical system and the configuration of the ray bundle that is to be traced through it. (Since information about scatter and diffraction is provided by the modules SUSEQ, DEDRIQ, OPD, and PSF, and since a basic geometrical ray trace can be performed without using these other modules, the GI file contains no information

trace can be performed without using these other modules, the GI file contains no information for scatter or diffraction analysis).

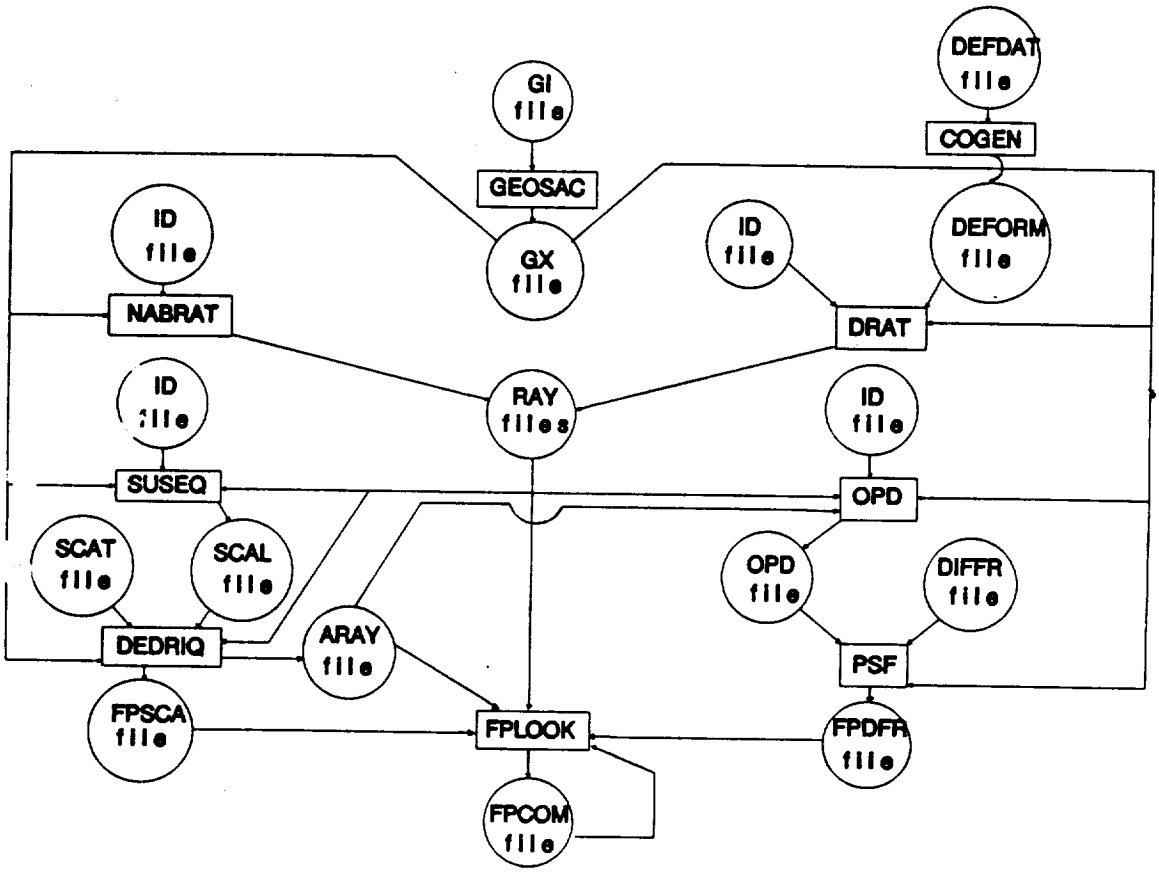

Figure 5.1 OSAC Input/Output File Structure

The GI file is a card image file that consists of an identifier line, then a series of lines with one parameter defined in each line and finally, a terminator line. The parameter lines may appear in any order, and specify some or all of the parameters for defining the optical system and the configuration of the traced ray bundle. Any parameters not specified take on an assumed default value. Each parameter line consists of three numbers. The first tells whether the parameter relates to general surface information, or to particular surface information. The second is the data item number, and tells GEOSAC how to interpret the parameter. The third is the parameter itself. The terminator line is just another parameter line, but with a -1 for the first value. Table 5.1 shows the format of the GI file records. Table 5.2 gives the parameter default value, value range, and description for the case when the parameter relates to general system information.

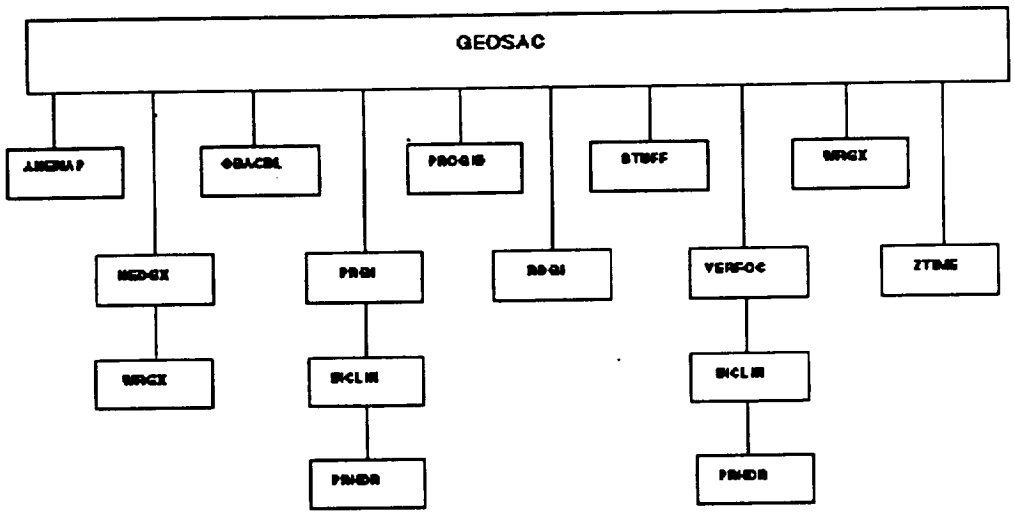

Figure 5.2 GEOSAC Subroutine Structure External Reference Tree

Table 5.1 GI File Format	
Header Record:	GID = 64 charcter comment line (16A4)
Data Records:	ITY = System/Surface specifier, ITN = Parameter number, VAL = Parameter value (6x, 213, d23.15) (Refer to Tables 5.2 through 5.8)
Terminator Record:	As above, but with ITY = -1

Table 5.2
GI File Data Record Interpretation
(ITY = 0 i.e., General System Information)

ITN	VAL (Default)	Units	Value Range	Description
1	0	mm*		XAP — X location of center of aperture
2	0	mm*		YAP — Y location of center of aperture
3	0	mm*		ZOFF — Z offset of focal plane, wrt either GFOC or STD
4	0			NS = No. of surfaces in system (exclude focal plane)
5	0			PSI — orientation angle of the major axis of the incoming polarization ellipse (valid only if discrete polarization flag is set — see ITN=24)
6	0			E — minor axis to major axis amplitude ratio for the incoming polarization ellipse (valid only if discrete polarization flag is set — see ITN=24)
7	0	deg	±180	AZBU — Azimuth angle of incoming bundle
8	0	deg	±90	ELBU — Elevation angle of incoming bundle
9	0	mm*	≥0	R1 — Inner radius of aperture annulus
10	0	mm*	>0	R2 — Outer radius of aperture annulus
11	0			MING — Number of rings
12	2			M2 — Number of points in outermost ring
13	$1.E+^{30}$	mm*	1.E-6 to 1.E+30	PTSRC=distance from the plane
23	0		0 or 1	0 — Zoff wrt GFOC; 1 — Zoff wrt STD
24	0		0 or 1	Discrete polarization switch.

*Length units are usually mm, but are arbitrary, user can use any units as long as the same units are used in all OSAC modules.

Tables 5.3 through 5.8 provide the same information for the cases when the parameter relates to specific surface information for conventional on-axis, conventional off-axis, flat, X-ray, toroidal, and obscuration surfaces respectively.

Table 5.3
GI File Data Record Interpretation
(ITY = Surface Number: Conventional, On-Axis Surface)

ITN	VAL (Default)	Units	Value Range	Description
1	0	mm*		X_o — X coordinate at surface center
2	0	mm*		Y_o — Y coordinate at surface center
3	0	mm*		Z_o — Z coordinate at surface center
4	0			P — Conic Constant = 1 - Eccentricity^2
5	0	mm*		K — Factor of surface = Vertex radius when $\rho_o = 0$
6	0	mm*	≥0	ρ_o — Center radius of surface (0 when BCS is at vertex)
7	0	deg	±180	AZMIS — Azimuth misalignment of surface
8	0	deg	±90	ELMIS — Elevation misalignment of surface
9	0	mm*	≥0	R1S — Inner radius of surface
10	0	mm*	>0	R2S — Outer radius of conventional surface
14	-1		±100	EPS1 — Real part of the dielectric constant
15	0		±100	EPS2 — Imaginary part of the dielectric constant
21	0		0 or 1	Convexity switch: 0 — concave; 1 — convex
22	0		0 or 1	Deformation switch: 0 — none; 1 — some
23	0		0 or 1	Flat switch: 0 — on-axis surfaces
24	0		0 or 1	Off-axis switch: 0 — on-axis surfaces

See units in Table 5.2

Table 5.4
GI File Data Record Interpretation
(ITN = Surface Number; Conventional, Off-Axis Surface)

ITN	VAL	Units	Value	Description
1	0	mm*		X_o — X coordinate at surface center
2	0	mm*		Y_o — Y coordinate at surface center
3	0	mm*		Z_o — Z coordinate at surface center
4	0			P — Conic Constant = 1 - Eccentricity^2
5	0	mm*		K — Factor of surface = Vertex radius when $\rho_o = 0$
6	0	mm*		ρ_o — Center radius of surface (0 when BCS is at vertex)
7	0	deg	±180	AZMIS — Azimuth misalignment of surface
8	0	deg	±90	ELMIS — Elevation misalignment of surface
9	0	mm*		YE — Epicenter offset
10	0	mm*	>0	R2S — Outer radius of surface
11	0	deg	±90	B — Boresight angle
14	-1		±100	EPS1 — Real part of the dielectric constant
15	0		±100	EPS2 — Imaginary part of the dielectric constant
21	0		0 or 1	Convexity switch: 0 — concave; 1 — convex
22	0		0 or 1	Deformation switch: 0 — none; 1 — some
23	0		0 or 1	Flat switch: 0 — off-axis surfaces
24	0		0 or 1	Off-axis switch: 0 — on-axis surfaces

See units in Table 5.2

Table 5.5
GI File Data Record Interpretation
(ITY = Surface Number; Flat Surface)

ITN	VAL	Unit	Value	Description
1	0	mm*		X_c — X coordinate at surface center
2	0	mm*		Y_c — Y coordinate at surface center
3	0	mm*		Z_c — Z coordinate at surface center
4	0			N.A. for flat surface
5	0			N.A. for flat surface
6	0			N.A. for flat surface
7	0	deg	±180	AZMIS — Azimuth angle of normal to fold plane wrt STD
8	0	deg	±90	ELMIS — Elevation deviation of actual from fold plane
9	0			N.A. for flat surface
10	0	mm*	0	R2S — Radius of mirror
11	0	deg	±90	AZF — Azimuth angle of normal to fold plane wrt STD
12	0	deg	±90	ELF — Elevation angle of normal to fold plane wrt STD
13	0	mm*		ZFOLD — Z coordinate of the intersection of the STD Z axis with the fold plane
14	-1		±100	EPS1 — Real part of the dielectric constant
15	0		±100	EPS2 — Imaginary part of the dielectric constant
21	0		0 or 1	Convexity switch: 0 for flat surface
22	0		0 or 1	Deformation switch: 0 — none; 1 — some
23	0		0 or 1	Flat switch: 1 for flat surface
24	0		0 or 1	Off-axis switch: 0 for flat surface

See units in Table 5.2

Table 5.6
GI File Data Record Interpretation
(ITY = Surface Number;X-ray System)

ITN	VALUE (Default)	Units	Value Range	Description
1	0	mm*		X_o — X cordinate at surface center
2	0	mm*		Y_o — Y coordinate at surface center
3	0	mm*		Z_o — Z coordinate at surface center
4	0			P — Conic Constant = 1 - Eccentricity^2
5	0	mm*		K — Factor of surface = 1/2 linear coefficient in surface equation
6	0	mm*	>0	ρ_o — Center radius of surface
7	0	deg	±180	AZMIS — Azimuth misalignment of surface
8	0	deg	±90	ELMIS — Elevation misalignment of surface
9	0			Not used
10	0	mm*	>0	L — Length of surface
14	-1		±100	EPS1 — Real part of the dielectric constant
15	0		±100	EPS2 — Imaginary part of the dielectric constant
21	0		0 or 1	Convexity switch: 0 — concave; 1 — convex
22	0		0 or 1	Deformation switch: 0 — none; 1 — some
29	0		0 or 1	X-Ray switch: 0 for conventional, 1 for X-Ray

See units in Table 5.2

Table 5.7 shows the GI file parameters used in defining a toroidal surface. A user familiar with conventional on-axis surfaces will find the changes very simple — only the z_{BCS}=0 radius, PO, has been eliminated in favor of the toroidal radius, RTOR. The rotation angle ZROT8 about the +z axis has been added, as has a flag to show that the surface is toroidal. Otherwise, the specification is the same.

Table 5.7
GI File Data Record Interpretation
(ITY = Surface Number; Toroidal Surface)

ITN	VAL (Default)	Units	Value Range	Description
1	0.	mm*	±1000.	X_0 - x coordinate of center of toroid
2	0.	mm*	±1000.	Y_0 - y coordinate of center of toroid
3	0	mm*	0 to 1.D6	Z_0 - z coordinate of center of toroid
4	0.			P = 1-eccentricity^2 of toroid
5	0.	mm*	±1.D30	K = vertex radius of toroid
6	0.	mm*	±1.D30	RTOR = toroidal radius of toroid
7	0.	deg	±180	AZMIS — azimuthal misalignment
8	0.	deg	±90	ELMIS — elevational misalignment
9	0.			R1 — inner radius of toroid
10	0.			R2 — outer radius of toroid
11	0.	deg	±180	ZROT8 — rotation angle about the z-axis
14	-1		±100	EPS1 - Real part of the dielectric constant EPS2 - Imaginary part of the dielectric constant
15	0.		±100	
21	0.		0 or 1	Convexity switch: 1 for convex
22	0		0 or 1	Deformation switch: 1 for deformed
28	0		0 or 1	Toroidal surface switch: 1 for toroid

See units in Table 5.2

Table 5.8
GI File Data Record Interpretation
(ITY = Surface Number; Obscuration Surface)

ITN	VAL (Default)	Units	Value Range	Description
1	0.	mm*	±1000.	X_0 - x coordinate of center of obscuration
2	0.	mm*	±1000.	Y_0 - y coordinate of center of obscuration
3	0	mm*	0 to 1.D6	Z_0 - z coordinate of center of obscuration
7	0.	deg	±180	AZMIS - azimuthal misalignment
8	0.	deg	±90	ELMIS - elevational misalignment
9	0.	mm*		R1 or DX - inner radius for annular obscuration, or x-width for rectangular obscuration
10	0.	mm*		R2 or DY — outer radius for annular obscuration, or y-width for rectangular obscuration
13	0.	deg		ZROTθ - θ_z, or z-rotation angle for rectangular obscuration
25	0		0 or 1	Annular obscuration switch: 1 for annular obscuration
26	0		0 or 1	Rectangular obscuration switch: 1 for rectangular obscuration
27	0		0 or 1	Opacity switch: If either an annular or a rectangular obscuration is selected, then 1=opaque and 0=transmitting

*See units in Table 5.2

If the user wishes to use an obscuration, he must define the appropriate parameters in the geometry input file (GI file) as listed in Table 5.8. Apart from the standard position and misalignment parameters that are common to all types of OSAC surfaces, the only parameters that need to be defined are the dimensional and rotational parameters shown in Figure 4.13 and listed in Table 5.8.

The output of GEOSAC consists of terminal and printer output, and a condensed geometry file called the GX file.

The GX file is simply a reformatted version of the GI file, with default values used for all the parameters not explicitly specified by the user in the GI file. Tables 5.9(a) and 5.9(b) show the format of a GX file. However, the GX file will not be detailed here, since it is intended to be used by the rest of the OSAC modules, rather than by the user. The names, types, formats, and file numbers of all GEOSAC files are summarized in Table 5.10.

Table 5.9(a)
GX File Formats (Records Group)

Header Record Group (8 Cards)

Card 1	GID Card		
	GID	=	64 character comments
	GDATE	=	current date, and
	GTIME	=	current time
	Format (16A4, 2AB)		
Card 2	PARX Card (see Table 5.9b.)		
Cards 3-8	GEN Cards	=	General system parameters GEN (1 to 20) and the corresponding switches LSWO (1 to 10). Format (1P5(4D20.12/), 5X, 5L2, 5X, 5L2). (Note: GEN (I) equals VAL (0, I) as specified by the user in the GI file, and LSWO (I) corresponds to VAL (0, 20 + I).)

Data Record Group for Each Surface (6 Cards Each)

Surface geometry parameters for surface #KURF: SURF (1 to 20, KURF) and the corresponding switches LSW (1 to 10, KURF). Format (1P5(4D20.12/), 5X, 5L2, 5X, 5L2). (Note: SURF (I, KURF) equals VAL (KURF, I) as specified by the user in the GI file, except as redefined or rearranged for flat, off-axis, or obscuration surfaces by the routine STUFF. LSW (I, KURF) corresponds to VAL (KURF, 20 + I).)

Table 5.9(b) PARX Card Format

Item #	Name	Precision	Format	Description
1	NS	I*4	I5	Number of optical surfaces
2	KURF	I*4	I5	Surface # (0 in GX file, -1 in ARAY file, -2 in OPD file, -3 in SCAL file, or NS+1 in focal plane RAY file
3	MING	I*4	I5	Number of rings
4	M2	I*4	I5	Number of spokes
5	RZER	R*4	1PE 15.6	Initial non-zero radius of annular aperture
6	DR	R*4	1PE 15.6	Delta (r^2) between rings
7	H2	R*4	1PE 15.6	Not needed, dummied to -1
8	GFOC	R*8	1PD 15.8	System focus wrt STD

Table 5.10
Files Used by GEOSAC

Input/ Output	File Name	File Type	Format	Logical Record Length	Block Size	File Number
Input	name1	GI	FB	80	800	9
Output	name1	GX	FB	80	800	12
Output	terminal			80		6
Output	printer			132		8

As is the case with all the OSAC modules, information from GEOSAC is output to both the terminal and the printer. As is also the case with all the OSAC modules, no information is presented in GEOSAC's terminal output that is not also presented in the printer output. Therefore, the format of the terminal output will not be examined here. What follows then, are examples of the printer output for the three separate optical systems. The associated GI and GX files are also shown.

Figures 5.3, 5.4, and 5.5 show the GI and GX files and the printer output for DOCON, a conventional on-axis Cassegrain system. The first element is a parabola, and the second a hyperbola. The input system geometry section in the printer output therefore shows information in turn about the system in general, then about the parabola, and finally about the hyperbola. The first item to understand in each of these three parameter lists is the line of switches at the end. Switches 1-10 correspond to parameters 21-30 as specified in the GI file. These are logical switches, with a false value (F) corresponding to zero, and a true (T) value corresponding to one in the GI file. These switches tell how the remaining parameters are to be interpreted. For example, the only two switches used in the general information section are 3 and 4. Referring to Table 5.2, it is found that both these flags being false means that discrete polarization is not assumed, and that the system focal plane location is to be defined relative to the geometric focus found by GEOSAC, rather than relative to the standard coordinate system origin. Thus, again referring to Table 5.2, the third parameter in the general information section, ZOFF, is to be interpreted as the offset of the focal plane from the geometrical focus, rather than from the standard coordinate system origin. The remaining parameters in the general information section relate either to the location, size and orientation of the input ray bundle. If the meaning of any of these parameters is unclear, the user should refer to Section 4. By reading these parameters, the user can find, for example, that the input beam is elevated to an angle of 0.1°.

```
+ +ID LINE FROM FILE 'DOCON GI' (ON-AXIS CASSEGRAIN)+ +
      0  4  2
      0  8  0.1
      0  9  97.1
      0 10  500.
      0 11  5
      0 12  10
      1  1  .002
      1  2  .003
      1  3  3275.
      1  5 -5473.68
      1  9  97.
      1 10  500.
      2  3  25.
      2  4  .4235
      2  5  902.78
      2  7  .004
      2  8  .005
      2 10  97.
     -1  0  0
```

Figure 5.3 GI File for DOCON System

```
+ +ID LINE FROM FILE 'DOCON GI' (ON-AXIS CASSEGRAIN)+ +          16-07-91 08:57:31
  2   0   5   10  9.710000E+01  6.014290E+04  -1.000000E+00 3.77526957D+03
0.000000000000D+00 0.000000000000D+00 0.000000000000D+00 2.000000000000D+00
0.000000000000D+00 0.000000000000D+00 0.000000000000D+00 1.000000000000D-01
9.710000000000D+01 5.000000000000D+02 5.000000000000D+00 1.000000000000D+01
1.000000000000D+30 0.000000000000D+00 0.000000000000D+00 0.000000000000D+00
0.000000000000D+00 0.000000000000D+00 0.000000000000D+00 0.000000000000D+00
   F F F F F     F F F F F
2.000000000000D-03 3.000000000000D-03 3.275000000000D+03 0.000000000000D+00
-5.473680000000D+03 0.000000000000D+00 0.000000000000D+00 0.000000000000D+00
9.700000000000D+01 5.000000000000D+02 0.000000000000D+00 0.000000000000D+00
0.000000000000D+00 -1.000000000000D+00 0.000000000000D+00 0.000000000000D+00
0.000000000000D+00 0.000000000000D+00 0.000000000000D+00 0.000000000000D+00
   F F F F F     F F F F F
0.000000000000D+00 0.000000000000D+00 2.500000000000D+01 4.235000000000D-01
9.027800000000D+02 0.000000000000D+00 4.000000000000D-03 5.000000000000D-03
0.000000000000D+00 9.700000000000D+01 0.000000000000D+00 0.000000000000D+00
0.000000000000D+00 -1.000000000000D+00 0.000000000000D+00 0.000000000000D+00
0.000000000000D+00 0.000000000000D+00 0.000000000000D+00 0.000000000000D+00
   F F F F F     F F F F F
```

Figure 5.4 GX File for DOCON System

```
*** OPTICAL SURFACE ANALYSIS PROGRAM (GEOSAC ) RELEASE (06.0) VAX      PAGE  1
+ +ID LINE FROM FILE 'DOCON GI' (ON-AXIS CASSEGRAIN)+ +          16-07-91 08:57:31
-------------------------------------------------------------------

INPUT SYSTEM GEOMETRY :
-----------------------

 GENERAL INFORMATION:
  XAP   =  0.00000000000000D+00  X OF CENTER OF ANNULAR APERTURE
  YAP   =  0.00000000000000D+00  Y OF CENTER OF ANNULAR APERTURE
  ZOFF  =  0.00000000000000D+00  Z OFFSET OF FOCAL PLANE.
  NS    =                    2  NUMBER OF SURFACES.
  AZBU  =  0.00000000000000D+00  AZIMUTH  OF INCOMING BUNDLE (DEG.)
  ELBU  =  1.00000000000000D-01  ELEVATION OF INCOMING BUNDLE (DEG.)
  R1    =  9.71000000000000D+01  INNER RADIUS OF APERTURE ANNULUS.
  R2    =  5.00000000000000D+02  OUTER RADIUS OF APERTURE ANNULUS.
  MING  =                    5  NUMBER OF RINGS.
  M2    =                   10  NO. OF POINTS PER RING.
  PTSRC =  1.00000000000000D+30  DISTANCE TO POINT SOURCE
  LSW0  =           FFFFFFFFFF  SYSTEM SWITCHES.
 SURFACE NUMBER  1
  X0    =  2.00000000000000D-03  X COORD. AT CENTER.
  Y0    =  3.00000000000000D-03  Y COORD. AT CENTER.
  Z0    =  3.27500000000000D+03  Z COORD. AT CENTER.
  P     =  0.00000000000000D+00  CONIC CONSTANT = 1 - ECCEN. ** 2
  K     = -5.47368000000000D+03  VERTEX RADIUS OF CURVATURE.
  P0    =  0.00000000000000D+00  CENTER RADIUS OF SURFACE.
  AZMIS =  0.00000000000000D+00  AZIMUTH  MISALIGNMENT (DEG.)
  ELMIS =  0.00000000000000D+00  ELEVATION MISALIGNMENT (DEG.)
  R1S   =  9.70000000000000D+01  INNER RADIUS OF CONV. SURFACE.
  R2S   =  5.00000000000000D+02  OUTER RADIUS OF CONV. SURFACE.
  EP1   = -1.00000000000000D+00  REAL  PART OF DIELECTRIC CONST.
  EP2   =  0.00000000000000D+00  IMAG. PART OF DIELECTRIC CONST.
  LSW   =           FFFFFFFFFF  SURFACE SWITCHES.
 SURFACE NUMBER  2
  X0    =  0.00000000000000D+00  X COORD. AT CENTER.
  Y0    =  0.00000000000000D+00  Y COORD. AT CENTER.
  Z0    =  2.50000000000000D+01  Z COORD. AT CENTER.
  P     =  4.23500000000000D-01  CONIC CONSTANT = 1 - ECCEN. ** 2
  K     =  9.02780000000000D+02  VERTEX RADIUS OF CURVATURE.
  P0    =  0.00000000000000D+00  CENTER RADIUS OF SURFACE.
 AZMIS =  4.00000000000000D-03  AZIMUTH  MISALIGNMENT (DEG.)
  ELMIS =  5.00000000000000D-03  ELEVATION MISALIGNMENT (DEG.)
  R1S   =  0.00000000000000D+00  INNER RADIUS OF CONV. SURFACE.
  R2S   =  9.70000000000000D+01  OUTER RADIUS OF CONV. SURFACE.
  EP1   = -1.00000000000000D+00  REAL  PART OF DIELECTRIC CONST.
  EP2   =  0.00000000000000D+00  IMAG. PART OF DIELECTRIC CONST.
  LSW   =           FFFFFFFFFF  SURFACE SWITCHES.
```

Figure 5.5 GEOSAC Printout for DOCON System

SURFACE NUMBER = 1

IN BODY CENTERED COORDINATE SYSTEM:

GEOMETRIC CENTER = -1.00000000000000D+06
RADIUS OF CURVATURE = -5.47368000000000D+03
LEFT VERTEX = -1.00000000000000D+30
RIGHT VERTEX = 0.00000000000000D+00
LEFT GEOM FOCUS = -1.00000000000000D+30
RIGHT GEOM FOCUS = -2.73684000000000D+03
ECCENTRICITY = 1.00000000000000D+00

IN STANDARD COORDINATE SYSTEM:

GEOMETRIC CENTER = -9.96725000000000D+05
LEFT VERTEX = -1.00000000000000D+30
RIGHT VERTEX = 3.27500000000000D+03
LEFT GEOM FOCUS = -1.00000000000000D+30
RIGHT GEOM FOCUS = 5.38160000000000D+02
CONFOCAL DELTA = 0.00000000000000D+00

SURFACE NUMBER = 2

IN BODY CENTERED COORDINATE SYSTEM:

GEOMETRIC CENTER = 2.13171192443920D+03
RADIUS OF CURVATURE = 9.02780000000000D+02
LEFT VERTEX = 0.00000000000000D+00
RIGHT VERTEX = 4.26342384887839D+03
LEFT GEOM FOCUS = 5.13154283312059D+02
RIGHT GEOM FOCUS = 3.75026956556634D+03
ECCENTRICITY = 7.59275970909129D-01

IN STANDARD COORDINATE SYSTEM:

GEOMETRIC CENTER = 2.15671192443920D+03
LEFT VERTEX = 2.50000000000000D+01
RIGHT VERTEX = 4.28842384887839D+03
LEFT GEOM FOCUS = 5.38154283312059D+02
RIGHT GEOM FOCUS = 3.77526956556634D+03
CONFOCAL DELTA = -5.71668794489710D-03

GENERAL SYSTEM FOCUS = 3.77526956556634D+03

Figure 5.5 GEOSAC Printout for DOCON System (continued)

Referring to Table 5.3, it is found that the only switches used in the surface information sections are 1 through 4. A true value for these switches would indicate surface convexness, presence of polynomial deformations, surface flatness, and off-axis configuration, respectively. Thus, surfaces 1 and 2 are concave conventional on-axis surfaces with no deformations. The remaining parameters give the location, orientation, and defining constants of the surfaces. If the meaning of any of these parameters is unclear, the user should refer to Sections 4.3, 4.5 and 4.6.

Following the input system geometry information in the printout is a list of calculated parameters for each conic (non-flat) surface. Most of these parameters are output in both the body centered coordinate system and the standard coordinate system. (For a full explanation of the two coordinate systems, the user should refer to Sections 4.1 and 4.3). The first parameter in these two lists is the geometric center. This is the z-coordinate of the center of the conic surface. For spherical or ellipsoidal surfaces, the term 'geometric center' is self-explanatory. For hyperboloidal surfaces, the center is the point midway between the axial intercepts of the two halves of the hyperbola. For paraboloidal surfaces, the geometric center is undefined, and is set to 1.0×10^{60}. The next parameter (body centered coordinate system only) is the radius of curvature. This parameter is the radius of curvature of the surface at the axial intercept. The general formula for the axial radius of curvature is

$$Radius = K - P*Z_{\rho=0}. \tag{5-1}$$

Thus, if the surface is a parabola (i.e., if P=0), or if the axial intercept corresponds to the origin of the body centered coordinate system (i.e., if $\rho_0 = 0$, as is often the case for conventional surfaces), then the axial radius of curvature is simply the conic K constant. The next parameters are the left and right vertex positions, and the left and right focus positions. These parameters are self-explanatory for spherical, ellipsoidal, and hyperboloidal surfaces. For paraboloidal surfaces, only one (either left or right) of each of these parameters is defined. The other is set to $+1.0 \times 10^{60}$, with the sign and the left or right choice being determined by whether the open end of the parabola points left or right. The next parameter (body centered coordinate system only) is the eccentricity, which is defined as

$$Eccentricity = \sqrt{1 - P}. \tag{5-2}$$

The next parameter (standard coordinate system only) is the confocal delta, which is the mismatch between the geometric focus of the preceding surface and the current surface. This parameter would be zero for a perfectly confocal system. The confocal delta is undefined for the first surface, which has no preceding focal point to match. For the first surface, then, the confocal delta is to be interpreted as the reciprocal of the distance from the geometrical center to either one of the axial vertices. This number is set equal to 1.0×10^{-60} if the first surface is a parabola, which has no real geometrical center. The final parameter in the printout is the geometrical (Gaussian) focal plane location of the system as calculated by GEOSAC.

Figures 5.6, 5.7, and 5.8 show the GI and GX files and the printer output for DOCOF, an off-axis system with a fold flat for the third element. By looking at the input system geometry section, the user can find, for example, that this system is an off-axis section of the parent on-axis system already discussed. If the meaning of any of the rest of the surface definitions is unclear, the user should refer to Sections 4.6.2 and 4.6.3. Figures 5.9, 5.10, and 5.11 show the GI and GX files and the printer output for DOCXR, a Wolter Type I X-ray system. Again, if any of the X-ray surface definition parameters are unclear, the user should refer to Section 4.6.4.

```
++ID LINE FROM FILE 'DOCOF GI' (OFF-AXIS SYSTEM)
    0  2  400
    0  3  3775
    0  4  3
    0 10  100.
    0 11  5
    0 12  10
    0 23  1
    1  3  3275.
    1  5 -5473.68
    1  9  400.
    1 10  100.
    1 24  1
    2  3  25.
    2  4  .4235
    2  5  902.78
    2  9 -75.
    2 10  25.
    2 11  7.93
    2 24  1
    3  3  3525.
    3 10  25.
    3 11  45.
    3 12  60.
    3 13  3525.
    3 23  1
   -1  0  0
```

Figure 5.6 GI File for DOCOF System

```
++ID LINE FROM FILE 'DOCOF GI' (OFF-AXIS SYSTEM)          16-07-91 08:59:50

3   0   5   10  5.179698E+01  2.439024E+03  -1.000000E+00 3.77500000D+03
0.000000000000D+00 4.000000000000D+02 0.000000000000D+00 3.000000000000D+00
0.000000000000D+00 0.000000000000D+00 0.000000000000D+00 0.000000000000D+00
0.000000000000D+00 1.000000000000D+02 5.000000000000D+00 1.000000000000D+01
1.000000000000D+30 0.000000000000D+00 0.000000000000D+00 0.000000000000D+00
0.000000000000D+00 0.000000000000D+00 0.000000000000D+00 0.000000000000D+00
  F F T F F    F F F F F
0.000000000000D+00 0.000000000000D+00 3.260384604142D+03 0.000000000000D+00
-5.473680000000D+03 4.000000000000D+02 0.000000000000D+00 0.000000000000D+00
0.000000000000D+00 1.000000000000D+02 0.000000000000D+00 0.000000000000D+00
0.000000000000D+00 -1.000000000000D+00 0.000000000000D+00 0.000000000000D+00
0.000000000000D+00 0.000000000000D+00 0.000000000000D+00 0.000000000000D+00
  F F F T F    F F F F F
0.000000000000D+00 0.000000000000D+00 2.811765675379D+01 4.235000000000D-01
9.014596723648D+02 -7.500000000000D+01 0.000000000000D+00 0.000000000000D+00
7.930000000000D+00 2.500000000000D+01 7.930000000000D+00 0.000000000000D+00
0.000000000000D+00 -1.000000000000D+00 0.000000000000D+00 0.000000000000D+00
0.000000000000D+00 0.000000000000D+00 0.000000000000D+00 0.000000000000D+00
  F F F T F    F F F F F
0.000000000000D+00 0.000000000000D+00 3.525000000000D+03 4.500000000000D+01
6.000000000000D+01 3.525000000000D+03 0.000000000000D+00 0.000000000000D+00
0.000000000000D+00 2.500000000000D+01 4.500000000000D+01 6.000000000000D+01
3.525000000000D+03 -1.000000000000D+00 0.000000000000D+00 0.000000000000D+00
0.000000000000D+00 0.000000000000D+00 0.000000000000D+00 0.000000000000D+00
  F F T F F    F F F F F
```

Figure 5.7 GX File for DOCOF System

```
*** OPTICAL SURFACE ANALYSIS PROGRAM (GEOSAC ) RELEASE (06.0) VAX     PAGE  1
++ID LINE FROM FILE 'DOCOF GI' (OFF-AXIS SYSTEM)          16-07-91 08:59:50
-------------------------------------------------------------------------

INPUT SYSTEM GEOMETRY :
-----------------------

GENERAL INFORMATION:
 XAP   =  0.00000000000000D+00  X OF CENTER OF ANNULAR APERTURE
 YAP   =  4.00000000000000D+02  Y OF CENTER OF ANNULAR APERTURE
 ZOFF  =  3.77500000000000D+03  Z OFFSET OF FOCAL PLANE.
 NS    =                    3  NUMBER OF SURFACES.
 AZBU  =  0.00000000000000D+00  AZIMUTH   OF INCOMING BUNDLE (DEG.)
 ELBU  =  0.00000000000000D+00  ELEVATION OF INCOMING BUNDLE (DEG.)
 R1    =  0.00000000000000D+00  INNER RADIUS OF APERTURE ANNULUS.
 R2    =  1.00000000000000D+02  OUTER RADIUS OF APERTURE ANNULUS.
 MING  =                    5  NUMBER OF RINGS.
 M2    =                   10  NO. OF POINTS PER RING.
 PTSRC =  1.00000000000000D+30  DISTANCE TO POINT SOURCE
 LSW0  =           FFTFFFFFFF  SYSTEM SWITCHES.
```

Figure 5.8 GEOSAC Printout for DOCOF System

```
SURFACE NUMBER  1
 X0   = 0.00000000000000D+00 X COORD. AT CENTER.
 Y0   = 0.00000000000000D+00 Y COORD. AT CENTER.
 Z0   = 3.27500000000000D+03 Z COORD. AT CENTER.
 P    = 0.00000000000000D+00 CONIC CONSTANT = 1 - ECCEN. ** 2
 K    = -5.47368000000000D+03 VERTEX RADIUS OF CURVATURE.
 P0   = 0.00000000000000D+00 CENTER RADIUS OF SURFACE.
 AZMIS = 0.00000000000000D+00 AZIMUTH  MISALIGNMENT (DEG.)
 ELMIS = 0.00000000000000D+00 ELEVATION MISALIGNMENT (DEG.)
 YE   = 4.00000000000000D+02 EPICENTER OF OFFSET
 R2S  = 1.00000000000000D+02 OUTER RADIUS OF CONV. SURFACE.
 B    = 0.00000000000000D+00 BORESIGHT ANGLE (DEG.)
 EP1  = -1.00000000000000D+00 REAL  PART OF DIELECTRIC CONST.
 EP2  = 0.00000000000000D+00 IMAG. PART OF DIELECTRIC CONST.
 LSW  =          FFFTFFFFFF SURFACE SWITCHES.

 SURFACE NUMBER  2
 X0   = 0.00000000000000D+00 X COORD. AT CENTER.
 Y0   = 0.00000000000000D+00 Y COORD. AT CENTER.
 Z0   = 2.50000000000000D+01 Z COORD. AT CENTER.
 P    = 4.23500000000000D-01 CONIC CONSTANT = 1 - ECCEN. ** 2
 K    = 9.02780000000000D+02 VERTEX RADIUS OF CURVATURE.
 P0   = 0.00000000000000D+00 CENTER RADIUS OF SURFACE.
 AZMIS = 0.00000000000000D+00 AZIMUTH  MISALIGNMENT (DEG.)
 ELMIS = 0.00000000000000D+00 ELEVATION MISALIGNMENT (DEG.)
 YE   = -7.50000000000000D+01 EPICENTER OF OFFSET
 R2S  = 2.50000000000000D+01 OUTER RADIUS OF CONV. SURFACE.
 B    = 7.93000000000000D+00 BORESIGHT ANGLE (DEG.)
 EP1  = -1.00000000000000D+00 REAL  PART OF DIELECTRIC CONST.
 EP2  = 0.00000000000000D+00 IMAG. PART OF DIELECTRIC CONST.
 LSW  =          FFFTFFFFFF SURFACE SWITCHES.

*** OPTICAL SURFACE ANALYSIS PROGRAM (GEOSAC  ) RELEASE (06.0) VAX     PAGE  2
++ID LINE FROM FILE 'DOCOF GI' (OFF-AXIS SYSTEM)          16-07-91 08:59:50
-------------------------------------------------------------------------------
SURFACE NUMBER  3
 X0   = 0.00000000000000D+00 X COORD. AT CENTER.
 Y0   = 0.00000000000000D+00 Y COORD. AT CENTER.
 Z0   = 3.52500000000000D+03 Z COORD. AT CENTER.
 AZMIS = 0.00000000000000D+00 AZIMUTH  MISALIGNMENT (DEG.)
 ELMIS = 0.00000000000000D+00 ELEVATION MISALIGNMENT (DEG.)
 R2S  = 2.50000000000000D+01 RADIUS OF MIRROR
 AZF  = 4.50000000000000D+01 AZIMUTH ANGLE OF NORMAL (DEG.)
 ELF  = 6.00000000000000D+01 ELEVATION ANGLE OF NORMAL (DEG.)
 ZFOLD = 3.52500000000000D+03 Z COORD. OF FOLD PLANE
 EP1  = -1.00000000000000D+00 REAL  PART OF DIELECTRIC CONST.
 EP2  = 0.00000000000000D+00 IMAG. PART OF DIELECTRIC CONST.
 LSW  =          FFTFFFFFFF SURFACE SWITCHES.

 SURFACE NUMBER =  1
```

Figure 5.8 GEOSAC Printout for DOCOF System (continued)

```
 IN BODY CENTERED COORDINATE SYSTEM:

   GEOMETRIC CENTER    = -1.00000000000000D+06
   RADIUS OF CURVATURE = -5.47368000000000D+03
   LEFT VERTEX         = -1.00000000000000D+30
   RIGHT VERTEX        =  0.00000000000000D+00
   LEFT GEOM FOCUS     = -1.00000000000000D+30
   RIGHT GEOM FOCUS    = -2.73684000000000D+03
   ECCENTRICITY        =  1.00000000000000D+00

 IN STANDARD COORDINATE SYSTEM:

   GEOMETRIC CENTER    = -9.96725000000000D+05
   LEFT VERTEX         = -1.00000000000000D+30
   RIGHT VERTEX        =  3.27500000000000D+03
   LEFT GEOM FOCUS     = -1.00000000000000D+30
   RIGHT GEOM FOCUS    =  5.38160000000000D+02
   CONFOCAL DELTA      =  0.00000000000000D+00

*** OPTICAL SURFACE ANALYSIS PROGRAM (GEOSAC ) RELEASE (06.0) VAX     PAGE  3
++ID LINE FROM FILE 'DOCOF GI' (OFF-AXIS SYSTEM)          16 07-91 08:59:50
-------------------------------------------------------------------------

SURFACE NUMBER =  2

 IN BODY CENTERED COORDINATE SYSTEM:

   GEOMETRIC CENTER    =  2.13171192443920D+03
   RADIUS OF CURVATURE =  9.02780000000000D+02
   LEFT VERTEX         =  0.00000000000000D+00
   RIGHT VERTEX        =  4.26342384887839D+03
   LEFT GEOM FOCUS     =  5.13154283312059D+02
   RIGHT GEOM FOCUS    =  3.75026956556634D+03
   ECCENTRICITY        =  7.59275970909129D-01

 IN STANDARD COORDINATE SYSTEM:

   GEOMETRIC CENTER    =  2.15671192443920D+03
   LEFT VERTEX         =  2.50000000000000D+01
   RIGHT VERTEX        =  4.28842384887839D+03
   LEFT GEOM FOCUS     =  5.38154283312059D+02
   RIGHT GEOM FOCUS    =  3.77526956556634D+03
   CONFOCAL DELTA      = -5.71668794489710D-03

GENERAL SYSTEM FOCUS   =  3.77500000000000D+03
```

Figure 5.8 GEOSAC Printout for DOCOF System (continued)

```
++ID LINE FROM FILE 'DOCXR GI' (X-RAY SYSTEM)
    0  4  2
    0  9  210.097
    0 10  213.632
    0 11  5
    0 12  10
    0 21  1
    1  3  205.
    1  5 -1.83679707708
    1  6  211.872184922
    1 10  410
    1 14  .9994116
    1 15 -4.724786E-04
    1 22  1
    2  3  635.
    2  4 -6.1226566367E-04
    2  5 -5.37987854918
    2  6  204.348599807
    2 10  410.
    2 14  .9994116
    2 15 -4.724786E-04
   -1  0  0
```

Figure 5.9 GI File for DOCXR System

```
+++LINE FROM FILE 'DOCXR GI' (X-RAY SYSTEM)          16-07-91 09:01:54

  2   0   5   10  2.100970E+02  3.744705E+02  -1.000000E+00 6.42000000D+03
0.000000000000D+00  0.000000000000D+00  0.000000000000D+00  2.000000000000D+00
0.000000000000D+00  0.000000000000D+00  0.000000000000D+00  0.000000000000D+00
2.100970000000D+02  2.136320000000D+02  5.000000000000D+00  1.000000000000D+01
1.000000000000D+30  0.000000000000D+00  0.000000000000D+00  0.000000000000D+00
0.000000000000D+00  0.000000000000D+00  0.000000000000D+00  0.000000000000D+00
   T F F F F     F F F F F
0.000000000000D+00  0.000000000000D+00  2.050000000000D+02  0.000000000000D+00
-1.836797077080D+00  2.118721849220D+02  0.000000000000D+00  0.000000000000D+00
0.000000000000D+00  4.100000000000D+02  0.000000000000D+00  0.000000000000D+00
0.000000000000D+00  9.994116000000D-01 -4.724786000000D-04  0.000000000000D+00
0.000000000000D+00  0.000000000000D+00  0.000000000000D+00  0.000000000000D+00
   F T F F F     F F F F F
0.000000000000D+00  0.000000000000D+00  6.350000000000D+02 -6.122656636700D-04
-5.379878549180D+00  2.043485998070D+02  0.000000000000D+00  0.000000000000D+00
0.000000000000D+00  4.100000000000D+02  0.000000000000D+00  0.000000000000D+00
0.000000000000D+00  9.994116000000D-01 -4.724786000000D-04  0.000000000000D+00
0.000000000000D+00  0.000000000000D+00  0.000000000000D+00  0.000000000000D+00
   F F F F F     F F F F F GENERAL SYSTEM FOCUS    =  6.42000000001219D+03
```

Figure 5.10 GX File for DOCXR System

```
*** OPTICAL SURFACE ANALYSIS PROGRAM (GEOSAC ) RELEASE (06.0) VAX     PAGE  1
++ID LINE FROM FILE 'DOCXR GI' (X-RAY SYSTEM)              16-07-91 09:01:54
-----------------------------------------------------------------------------

INPUT SYSTEM GEOMETRY :
-----------------------

GENERAL INFORMATION:
 XAP   =  0.00000000000000D+00  X OF CENTER OF ANNULAR APERTURE
 YAP   =  0.00000000000000D+00  Y OF CENTER OF ANNULAR APERTURE
 ZOFF  =  0.00000000000000D+00  Z OFFSET OF FOCAL PLANE.
 NS    =                   2  NUMBER OF SURFACES.
 AZBU  =  0.00000000000000D+00  AZIMUTH   OF INCOMING BUNDLE (DEG.)
 ELBU  =  0.00000000000000D+00  ELEVATION OF INCOMING BUNDLE (DEG.)
 R1    =  2.10097000000000D+02  INNER RADIUS OF APERTURE ANNULUS.
 R2    =  2.13632000000000D+02  OUTER RADIUS OF APERTURE ANNULUS.
 MING  =                   5  NUMBER OF RINGS.
 M2    =                  10  NO. OF POINTS PER RING.
 PTSRC =  1.00000000000000D+30  DISTANCE TO POINT SOURCE
 LSW0  =           TFFFFFFFFF  SYSTEM SWITCHES.

SURFACE NUMBER   1

 X0    =  0.00000000000000D+00  X COORD. AT CENTER.
 Y0    =  0.00000000000000D+00  Y COORD. AT CENTER.
 Z0    =  2.05000000000000D+02  Z COORD. AT CENTER.
 P     =  0.00000000000000D+00  CONIC CONSTANT = 1 - ECCEN. ** 2
 K     = -1.83679707708000D+00  FACTOR OF SURFACE.
 P0    =  2.11872184922000D+02  CENTER RADIUS OF SURFACE.
 AZMIS =  0.00000000000000D+00  AZIMUTH   MISALIGNMENT (DEG.)
 ELMIS =  0.00000000000000D+00  ELEVATION MISALIGNMENT (DEG.)
 L     =  4.10000000000000D+02  LENGTH OF SURFACE.
 EP1   =  9.99411600000000D-01  REAL  PART OF DIELECTRIC CONST.
 EP2   = -4.72478600000000D-04  IMAG. PART OF DIELECTRIC CONST.
 LSW   =           FTFFFFFFFF  SURFACE SWITCHES.

SURFACE NUMBER   2

 X0    =  0.00000000000000D+00  X COORD. AT CENTER.
 Y0    =  0.00000000000000D+00  Y COORD. AT CENTER.
 Z0    =  6.35000000000000D+02  Z COORD. AT CENTER.
 P     = -6.12265663670000D-04  CONIC CONSTANT = 1 - ECCEN. ** 2
 K     = -5.37987854918000D+00  FACTOR OF SURFACE.
 P0    =  2.0[illegible]348599[illegible]/000D+02  CENTER RADIUS OF SURFACE.
 AZMIS =  0.000000[illegible]000000D+00  AZIMUTH   MISALIGNMENT (DEG.)
 ELMI[illegible] =  0.00000000000000D+00  ELEVATION MISALIGNMENT (DEG.)
 L     =  4.10000000000000D+02  LENGTH OF SURFACE.
 EP1   =  9.99411600000000D-01  REAL  PA[illegible]T OF DIELECTRIC CONST.
 EP2   = -4.72478600000000D-04  IMAG. PART OF DIELECTRIC CONST.
 LSW   =           FFFFFFFFFF  SURFACE SWITCHES.
```

Figure 5.11 GEOSAC Printout for DOCXR System

SURFACE NUMBER = 1

IN BODY CENTERED COORDINATE SYSTEM:

GEOMETRIC CENTER = -1.00000000000000D+06
RADIUS OF CURVATURE = -1.83679707708000D+00
LEFT VERTEX = -1.00000000000000D+30
RIGHT VERTEX = 1.22195922739012D+04
LEFT GEOM FOCUS = -1.00000000000000D+30
RIGHT GEOM FOCUS = 1.22186738753627D+04
ECCENTRICITY = 1.00000000000000D+00

IN STANDARD COORDINATE SYSTEM:

GEOMETRIC CENTER = -9.99795000000000D+05
LEFT VERTEX = -1.00000000000000D+30
RIGHT VERTEX = 1.24245922739012D+04
LEFT GEOM FOCUS = -1.00000000000000D+30
RIGHT GEOM FOCUS = 1.24236738753627D+04
CONFOCAL DELTA = 0.00000000000000D+00

SURFACE NUMBER = 2

IN BODY CENTERED COORDINATE SYSTEM:

GEOMETRIC CENTER = 8.78683693763310D+03
RADIUS OF CURVATURE = -1.83735929490738D+00
LEFT VERTEX = 5.78591853908367D+03
RIGHT VERTEX = 1.17877553361825D+04
LEFT GEOM FOCUS = 5.78500000001219D+03
RIGHT GEOM FOCUS = 1.17886738752540D+04
ECCENTRICITY = 1.00030608598752D+00

IN STANDARD COORDINATE SYSTEM:

GEOMETRIC CENTER = 9.42183693763310D+03
LEFT VERTEX = 6.42091853908367D+03
RIGHT VERTEX = 1.24227553361825D+04
LEFT GEOM FOCUS = 6.42000000001219D+03
RIGHT GEOM FOCUS = 1.24236738752540D+04
CONFOCAL DELTA = -1.08660742625943D-07

Figure 5.11 GEOSAC Printout for DOCXR System (continued)

Figure 5.12 shows a GI file for an example system consisting of a single toroid. Note that the toroid is rotated and translated in all six possible degrees of freedom. Figure 5.12 also shows a DEFORM file used to add Zernike deformations. The GI file parameters have been chosen to

give nominal radii of 100 (for the conic curve) and 180 (for the toroidal radius). The DEFORM file parameters have been chosen to give effective radii of curvature (i.e., after the Zernike additions) of 110 and 190. Thus, the toroid should give approximate line foci at distances of 110/2=55 and 190/2=95 back from the surface. The GI file shown corresponds to the first of these line foci.

```
TOR1.GI - TOROID TEST AT FIRST LINE FOCUS
     0  1  1.000000000000000D+01
     0  2  1.500000000000000D+01
     0  3 -3.500000000000000D+01
     0  4  1.000000000000000D+00
     0  9  0.000000000000000D+00
     0 10  4.000000000000000D+00
     0 11  2.000000000000000D+00
     0 12  1.600000000000000D+01
     0 23  1.000000000000000D+00
     1  1  1.000000000000000D+01
     1  2  1.500000000000000D+01
     1  3  2.000000000000000D+01
     1  4  1.000000000000000D+00
     1  5 -1.000000000000000D+02
     1  6 -1.800000000000000D+02
     1  7  2.000000000000000D-01
     1  8  3.000000000000000D-01
     1 10  5.000000000000000D+00
     1 11  2.250000000000000D+01
     1 22  1.000000000000000D+00
     1 28  .000000000000000D+00
    -1  0  0.000000000000000D+00

TOR1.DFR - FULL CIRCLE ZERNIKES FOR TOR1.GI                    5  0.000000
  3.75470E-03   0.00000E+00   0.00000E+00   2.16770E-03  -1.57350E-03
```

Figure 5.12

GI File (TOR1.GI) and DEFORM File (TOR1.DFR) for Toroidal Test Case. As Shown, the System Consists of a Single Displaced, Rotated, Concave Toroid.

As an example of how to use the obscuration parameters, Figure 5.13 shows the same GI file as discussed in Section 4.6, except that a rotated, opaque, rectangular obscuration has been inserted in between the two original surfaces. Figure 5.14 shows the results of running GEOSAC.

The reflectivity parameters of GI file is also shown Figure 5.13. Note that elliptical, 45-degree left-handed polarization has been specified by setting PSI=45.

```
GI = LYMAN, POLARIZATION, AND OBSCURATION
     0  4  3.000000000000000D+00
     0  5  4.500000000000000D+01
     0  6  5.000000000000000D-01
     0  9  1.520010000000000D+01
     0 10  3.999990000000000D+01
     0 11  4.000000000000000D+01
     0 12  2.000000000000000D+01
     0 21  1.000000000000000D+00
     0 24  1.000000000000000D+00
     1  3  7.287921763260000D+01
     1  4  0.000000000000000D+00
     1  5 -4.695988940570000D+00
     1  6  3.025756103850000D+01
     1 10  1.457584352650000D+02
     1 14  7.332000000000000D-01
     1 15  2.094700000000000D+00
     1 21  0.000000000000000D+00
     2  3  1.473077188000000D+02
     2  9  1.000000000000000D+02
     2 10  8.000000000000000D+00
     2 13  3.000000000000000D+01
     2 26  1.000000000000000D+00
     2 27  1.000000000000000D+00
     3  3  1.574036527610000D+02
     3  4 -1.180919040930000D-02
     3  5 -5.503251158770000D-01
     3  6  3.244089874670000D+00
     3 10  1.709330055230000D+01
     3 14  7.332000000000000D-01
     3 15  2.094700000000000D+00
     3 21  1.000000000000000D+00
    -1  0  0.000000000000000D+00
```

Figure 5.13

GI File with a Rotated, Opaque, Rectangular Obscuration Inserted in Between the Two Original Surfaces.

Figure 5.14 shows the GEOSAC listing with the display of the polarization parameters and the dielectric constant as a surface parameter and E=+0.5.

```
*** OPTICAL SURFACE ANALYSIS PROGRAM (GEOSAC ) RELEASE (06.0) VAX     PAGE  1
GI = LYMAN, POLARIZATION, AND OBSCURATION                  8-01-92 13:47:46
-----------------------------------------------------------------------------

INPUT SYSTEM GEOMETRY :
-----------------------

GENERAL INFORMATION:
 XAP   =  0.00000000000000D+00  X OF CENTER OF ANNULAR APERTURE
 YAP   =  0.00000000000000D+00  Y OF CENTER OF ANNULAR APERTURE
 ZOFF  =  0.00000000000000D+00  Z OFFSET OF FOCAL PLANE.
 NS    =                   3  NUMBER OF SURFACES.
 AZBU  =  0.00000000000000D+00  AZIMUTH   OF INCOMING BUNDLE (DEG.)
 ELBU  =  0.00000000000000D+00  ELEVATION OF INCOMING BUNDLE (DEG.)
 R1    =  1.52001000000000D+01  INNER RADIUS OF APERTURE ANNULUS.
 R2    =  3.99999000000000D+01  OUTER RADIUS OF APERTURE ANNULUS.
 MING  =                  40  NUMBER OF RINGS.
 M2    =                  20  NO. OF POINTS PER RING.
 PTSRC =  1.00000000000000D+30  DISTANCE TO POINT SOURCE
 LSW0  =          TFFFFFFFFF  SYSTEM SWITCHES.

 SURFACE NUMBER   1

 X0    =  0.00000000000000D+00  X COORD. AT CENTER.
 Y0    =  0.00000000000000D+00  Y COORD. AT CENTER.
 Z0    =  7.28792176326000D+01  Z COORD. AT CENTER.
 P     =  0.00000000000000D+00  CONIC CONSTANT = 1 - ECCEN. ** 2
 K     = -4.69598894057000D+00  FACTOR OF SURFACE.
 P0    =  3.02575610385000D+01  CENTER RADIUS OF SURFACE.
 AZMIS =  0.00000000000000D+00  AZIMUTH   MISALIGNMENT (DEG.)
 ELMIS =  0.00000000000000D+00  ELEVATION MISALIGNMENT (DEG.)
 L     =  1.45758435265000D+02  LENGTH OF SURFACE.
 EP1   =  7.33200000000000D-01  REAL  PART OF DIELECTRIC CONST.
 EP2   =  2.09470000000000D+00  IMAG. PART OF DIELECTRIC CONST.
 LSW   =          FFFFFFFFFF  SURFACE SWITCHES.
```

Figure 5.14 GEOSAC Output of GI File Shown in Figure 5.13.

```
SURFACE NUMBER  2

X0   =  0.00000000000000D+00  X COORD. AT CENTER.
Y0   =  0.00000000000000D+00  Y COORD. AT CENTER.
Z0   =  1.47307718800000D+02  Z COORD. AT CENTER.
AZNOR =  0.00000000000000D+00  AZIMUTH ANGLE OF NORMAL (DEG.)
ELNOR =  0.00000000000000D+00  ELEVATION ANGLE OF NORMAL (DEG.)
DIM1  =  1.00000000000000D+02  INNER RADIUS OR X-WIDTH OF OBSC
DIM2  =  8.00000000000000D+00  OUTER RADIUS OR Y-WIDTH OF OBSC
ZROT8 =  3.00000000000000D+01  ANGLE ABOUT Z FOR RECT OBSC (DEG.)
LSW   =          FFFFFTTFFF  SURFACE SWITCHES.

SURFACE NUMBER  3

X0   =  0.00000000000000D+00  X COORD. AT CENTER.
Y0   =  0.00000000000000D+00  Y COORD. AT CENTER.
Z0   =  1.57403652761000D+02  Z COORD. AT CENTER.
P    = -1.18091904093000D-02  CONIC CONSTANT = 1 - ECCEN. ** 2
K    = -5.50325115877000D-01  FACTOR OF SURFACE.
P0   =  3.24408987467000D+00  CENTER RADIUS OF SURFACE.
AZMIS =  0.00000000000000D+00  AZIMUTH  MISALIGNMENT (DEG.)
ELMIS =  0.00000000000000D+00  ELEVATION MISALIGNMENT (DEG.)
L    =  1.70933005523000D+01  LENGTH OF SURFACE.
EP1  =  7.33200000000000D-01  REAL  PART OF DIELECTRIC CONST.
EP2  =  2.09470000000000D+0C  IMAG. PART OF DIELECTRIC CONST.
LSW  =          TFFFFFFFFF  SURFACE SWITCHES.
```

Figure 5.14 GEOSAC Output of GI File Shown in Figure 5.13 (continued).

SURFACE NUMBER = 1

IN BODY CENTERED COORDINATE SYSTEM:

GEOMETRIC CENTER = -1.00000000000000D+06
RADIUS OF CURVATURE = -4.69598894057000D+00
LEFT VERTEX = -1.00000000000000D+30
RIGHT VERTEX = 9.74789348510931D+01
LEFT GEOM FOCUS = -1.00000000000000D+30
RIGHT GEOM FOCUS = 9.51309403808081D+01
ECCENTRICITY = 1.00000000000000D+00

IN STANDARD COORDINATE SYSTEM:

GEOMETRIC CENTER = -9.99927120782367D+0[illegible]
LEFT VERTEX = -1.00000000000000D+30
RIGHT VERTEX = 1.70358152483695D+02
LEFT GEOM FOCUS = -1.00000000000000D+30
RIGHT GEOM FOCUS = 1.68010158013[illegible]08D+02
CONFOCAL DELTA = 0.00000000000000D+00

SURFACE NUMBER = 3

IN BODY CENTERED COORDINATE SYSTEM:

GEOMETRIC CENTER = 4.66014262454102D+01
RADIUS OF CURVATURE = -4.22583017461180D-01
LEFT VERTEX = 1.08171766216269D+01
RIGHT VERTEX = 8.23856758691936D+01
LEFT GEOM FOCUS = 1.06065052520139D+01
RIGHT GEOM FOCUS = 8.25963472388065D+01
ECCENTRICITY = 1.00588726525854D+00

IN STANDARD COORDINATE SYSTEM:

GEOMETRIC CENTER = 2.04005079[illegible]6410D+02
LEFT VERTEX = 1.68220829382[illegible]+02
RIGHT VERTEX = 2.39789328630194D+02
LEFT GEOM FOCUS = 1.68010158013014D+02
RIGHT GEOM FOCUS = 2.39999999999807D+02
CONFOCAL DELTA = -3.92958554[illegible]6D-10

GENERAL SYSTEM FOCUS = 2.39999999999807D+02

Figure 5.14 GEOSAC Output of GI File Shown in Figure 5.13 (continued).

5.1.3 Point Source at Finite Distance

OSAC allows for a point source located infinitely far from the optical system, at z = minus infinity and also a point source located at any distance from the system. For simplicity, we took the approach of always using a finite source distance, but to allow the distance to be so large that it could effectively (i.e., within computer accuracy) be considered infinitely far away if so desired.

The system parameter, PTSRC (the distance to the *plane* containing the point source), is to be inserted in the geometry input (GI) file. Table 5.2 defines how this parameter is to be specified. If PTSRC is not specified, then the default value of 1.0E+30 places the point source effectively at minus infinity.

Figure 5.15 shows a geometry input (GI) file defining a two surface, confocal, ellipsoidal system. (The system is called the ELLIP3 system, and is used for other demonstrations in this report.)

```
ELLIP3.GI - 2 CONFOCAL ELLIPSES, .33 OBSC., SURFACE 1 DEFORM
      0  1  9.651005033000000D+00
      0  2  1.947664044000000D+01
      0  4  2.000000000000000D+00
      0  7  2.000000000000000D+00
      0  8  3.000000000000000D+00
      0  9  4.951000000000000D+00
      0 10  1.499900000000000D+01
      0 11  1.100000000000000D+01
      0 12  1.100000000000000D+01
      0 13  1.896042393000000D+02
      1  1  1.000000000000000D+01
      1  2  2.000000000000000D+01
      1  3  1.000000000000000D+01
      1  4  8.888888888888889D-01
      1  5 -1.333333333333333D+02
      1  7  2.000000000000000D+00
      1  8  3.000000000000000D+00
      1  9  5.000000000000000D+00
      1 10  1.600000000000000D+01
      1 22  1.000000000000000D+00
      2  1  6.510050330000000D+00
      2  2  1.476640438000000D+01
      2  3  1.197880330000000D+00
      2  4 -9.320415225000000D+01
      2  5  7.922352940000000D+02
      2 10  3.000000000000000D+01
     -1  0  0.000000000000000D+00
```

Figure 5.15
GI File (ELLIP3.GI) Used to Demonstrate a Finite Distance Point Source. The System Consists of Two Concave, Confocal Ellipses.

Figure 5.16 shows the corresponding printout from running GEOSAC. As shown, the first ellipse has its foci at z-coordinates of -190 and -90, while the second ellipse has its foci at (approximately) -90 and +75. Thus, the system focus is approximately at z=+75. Note that the second surface appears to be slightly non-confocal (see the "CONFOCAL DELTA" parameters in Figure 5.16). The reason for this is that there are deliberate tilts and decenters on the first surface for more complete program demonstration. The second surface was therefore displaced to make it truly confocal, even though the GEOSAC listing, which ignores misalignments, implies that it is slightly non-confocal. Figure 5.17, which shows the corresponding printout from running NABRAT, shows that the system brings the beam to a negligibly small focus at the Gaussian focal plane approximately at z=+75.

```
*** OPTICAL SURFACE ANALYSIS PROGRAM (GEOSAC ) RELEASE (06.0) VAX      PAGE  1
ELLIP3.GI - 2 CONFOCAL ELLIPSES, .33 OBSC., SURFACE 1 DEFORM  9-01-92 08:35:58
-------------------------------------------------------------------------------

INPUT SYSTEM GEOMETRY :
-----------------------

GENERAL INFORMATION:
 XAP   =  9.65100503300000D+00  X OF CENTER OF ANNULAR APERTURE
 YAP   =  1.94766404400000D+01  Y OF CENTER OF ANNULAR APERTURE
 ZOFF  =  0.00000000000000D+00  Z OFFSET OF FOCAL PLANE.
 NS    =                   2  NUMBER OF SURFACES.
 AZBU  =  2.00000000000000D+00  AZIMUTH   OF INCOMING BUNDLE (DEG.)
 ELBU  =  3.00000000000000D+00  ELEVATION OF INCOMING BUNDLE (DEG.)
 R1    =  4.95100000000000D+00  INNER RADIUS OF APERTURE ANNULUS.
 R2    =  1.49990000000000D+01  OUTER RADIUS OF APERTURE ANNULUS.
 MING  =                  11  NUMBER OF RINGS.
 M2    =                  11  NO. OF POINTS PER RING.
 PTSRC =  1.89604239300000D+02  DISTANCE TO POINT SOURCE
 LSW0  =          FFFFFFFFFF  SYSTEM SWITCHES.

SURFACE NUMBER  1
 X0    =  1.00000000000000D+01  X COORD. AT CENTER.
 Y0    =  2.00000000000000D+01  Y COORD. AT CENTER.
 Z0    =  1.00000000000000D+01  Z COORD. AT CENTER.
 P     =  8.88888888888889D-01  CONIC CONSTANT = 1 - ECCEN. ** 2
 K     = -1.33333333333333D+02  VERTEX RADIUS OF CURVATURE.
 P0    =  0.00000000000000D+00  CENTER RADIUS OF SURFACE.
 AZMIS =  2.00000000000000D+00  AZIMUTH   MISALIGNMENT (DEG.)
 ELMIS =  3.00000000000000D+00  ELEVATION MISALIGNMENT (DEG.)
 R1S   =  5.00[illegible]D+00  INNER RADIUS OF CONV. SURFACE.
 R2S   =  1.60000000000[illegible]D+01  OUTER RADIUS OF CONV. SURFACE.
 EP1   =  [illegible].00000000000000D+00  REAL  PART OF DIELECTRIC CONST.
 EP2   =  0.00000000000000D+00  IMAG. PART OF DIELECTRIC CONST.
 LSW   =          FTFFFFFFFF  SURFACE SWITCHES.
```

Figure 5.16

GEOSAC Output From Running the GI File (ELLIP3.GI) in Figure 5.15. As Shown, the System Consists of Two Displaced, Concave, Confocal Ellipses.

```
SURFACE NUMBER  2
 X0   =  6.51005033000000D+00  X COORD. AT CENTER.
 Y0   =  1.47664043800000D+01  Y COORD. AT CENTER.
 Z0   =  1.19788033000000D+00  Z COORD. AT CENTER.
 P    = -9.32041522500000D+01  CONIC CONSTANT = 1 - ECCEN. ** 2
 K    =  7.92235294000000D+02  VERTEX RADIUS OF CURVATURE.
 P0   =  0.00000000000000D+00  CENTER RADIUS OF SURFACE.
 AZMIS =  0.00000000000000D+00  AZIMUTH  MISALIGNMENT (DEG.)
 ELMIS =  0.00000000000000D+00  ELEVATION MISALIGNMENT (DEG.)
 R1S  =  0.00000000000000D+00  INNER RADIUS OF CONV. SURFACE.
 R2S  =  3.00000000000000D+01  OUTER RADIUS OF CONV. SURFACE.
 EP1  = -1.00000000000000D+00  REAL  PART OF DIELECTRIC CONST.
 EP2  =  0.00000000000000D+00  IMAG. PART OF DIELECTRIC CONST.
 LSW  =          FFFFFFFFFF  SURFACE SWITCHES.

SURFACE NUMBER =   1

  IN BODY CENTERED COORDINATE SYSTEM:
   GEOMETRIC CENTER    = -1.50000000000000D+02
   RADIUS OF CURVATURE = -1.33333333333333D+02
   LEFT VERTEX         = -3.00000000000000D+02
   RIGHT VERTEX        =  0.00000000000000D+00
   LEFT GEOM FOCUS     = -2.00000000000000D+02
   RIGHT GEOM FOCUS    = -1.00000000000000D+02
   ECCENTRICITY        =  3.33333333333333D-01

  IN STANDARD COORDINATE SYSTEM:
   GEOMETRIC CENTER    = -1.40000000000000D+02
   LEFT VERTEX         = -2.90000000000000D+02
   RIGHT VERTEX        =  1.00000000000000D+01
   LEFT GEOM FOCUS     = -1.90000000000000D+02
   RIGHT GEOM FOCUS    = -9.00000000000000D+01
   CONFOCAL DELTA      = -3.95760699999943D-01

 SURFACE NUMBER =   2

  IN BODY CENTERED COORDINATE SYSTEM:
   GEOMETRIC CENTER    = -8.49999999865886D+00
   RADIUS OF CURVATURE =  7.92235294000000D+02
   LEFT VERTEX         = -1.69999999973177D+01
   RIGHT VERTEX        =  0.00000000000000D+00
   LEFT GEOM FOCUS     = -9.09999999860207D+01
   RIGHT GEOM FOCUS    =  7.39999999887030D+01
   ECCENTRICITY        =  9.70588235298574D+00

  IN STANDARD COORDINATE SYSTEM:
   GEOMETRIC CENTER    = -7.30211966865886D+00
```

Figure 5.16

GEOSAC Output From Running the GI File (ELLIP3.GI) in Figure 5.15. As Shown, the System Consists of Two Displaced, Concave, Confocal Ellipses (continued).

```
LEFT VERTEX          = -1.58021196673177D+01
RIGHT VERTEX         =  1.19788033000000D+00
LEFT GEOM FOCUS      = -8.98021196560207D+01
RIGHT GEOM FOCUS     =  7.51978803187030D+01
CONFOCAL DELTA       =  1.97880343979302D-01

GENERAL SYSTEM FOCUS    =  7.51978803187030D+01
```

Figure 5.16

GEOSAC Output From Running the GI File (ELLIP3.GI) in Figure 5.15. As Shown, the System Consists of Two Displaced, Concave, Confocal Ellipses (continued).

```
*** OPTICAL SURFACE ANALYSIS PROGRAM (NABRAT ) RELEASE (06.0) VAX      PAGE  1
 ELLIP3.GI - 2 CONFOCAL ELLIPSES, .33 OBSC., SURFACE 1 DEFORM  9-01-92 08:36:14
ELLIP3.GI - 2 CONFOCAL ELLIPSES, .33 OBSC., SURFACE 1 DEFORM  9-01-92 08:35:58
```

RAY SUMMARY REPORT

SURFACE NUM	STARTED NUM	STARTED WEIGHT	FAILED NUM	FAILED WEIGHT	SUCCEEDED NUM	SUCCEEDED WEIGHT
1	121	121.00000	0	0.00000	121	121.00000
2	121	121.00000	0	0.00000	121	121.00000

RAY FOCUS REPORT

FOCAL PLANE INTERSECTIONS FOR GFOC = 7.519788030000D+01, ZOFF = 0.000000D+00

MINIMUM X	MINIMUM Y	MAXIMUM X	MAXIMUM Y
6.51385341E+00	1.47659605E+01	6.51390444E+00	1.47659959E+01

PLANAR OPTIMAL FOCUS

SUM WEIGHTS	X LOCATION	Y LOCATION	Z SPOT PLANE	SIZE
1.21000D+02	6.51387D+00	1.47660D+01	0.00000D+00	1.33314D-05

GLOBAL OPTIMAL FOCUS

SUM WEIGHTS	X LOCATION	Y LOCATION	Z SPOT PLANE	SIZE
1.21000D+02	6.51387D+00	1.47660D+01	3.51984D-05	1.23346D-05

Figure 5.17

NABRAT Output from running the GI file (ELLIP3.GI) in Figure 5.15. As shown, the system comes to an essentially perfect focus at the second ellipse's back focus.

The reader may notice that the ELLIP3 system is physically unrealizable, since the second surface would physically obscure the first surface. This, however, does not detract from the current examples. The reader may also notice that, according to the GI file and the GEOSAC printout, the ELLIP3 system is supposed to have deformations on the first surface. There is in fact a deformation file, which is used by the DRAT program. The use of the deformed first surface is covered later, in Section 5.

The confocal delta for the first surface is properly defined as the distance from the plane containing the point source, to the nearer focal point of the first surface.

5.2 NABRAT

5.2.1 Introduction

NABRAT traces an input bundle of collimated rays through an optical system that must consist of exactly two (conic) elements with no polynomial deformations. The only unusual analytical method used by NABRAT is in finding the position in space that minimizes the RMS spot size. This method is detailed in Section 5.2.3. The subroutine structure of NABRAT is shown in Figure 5.18

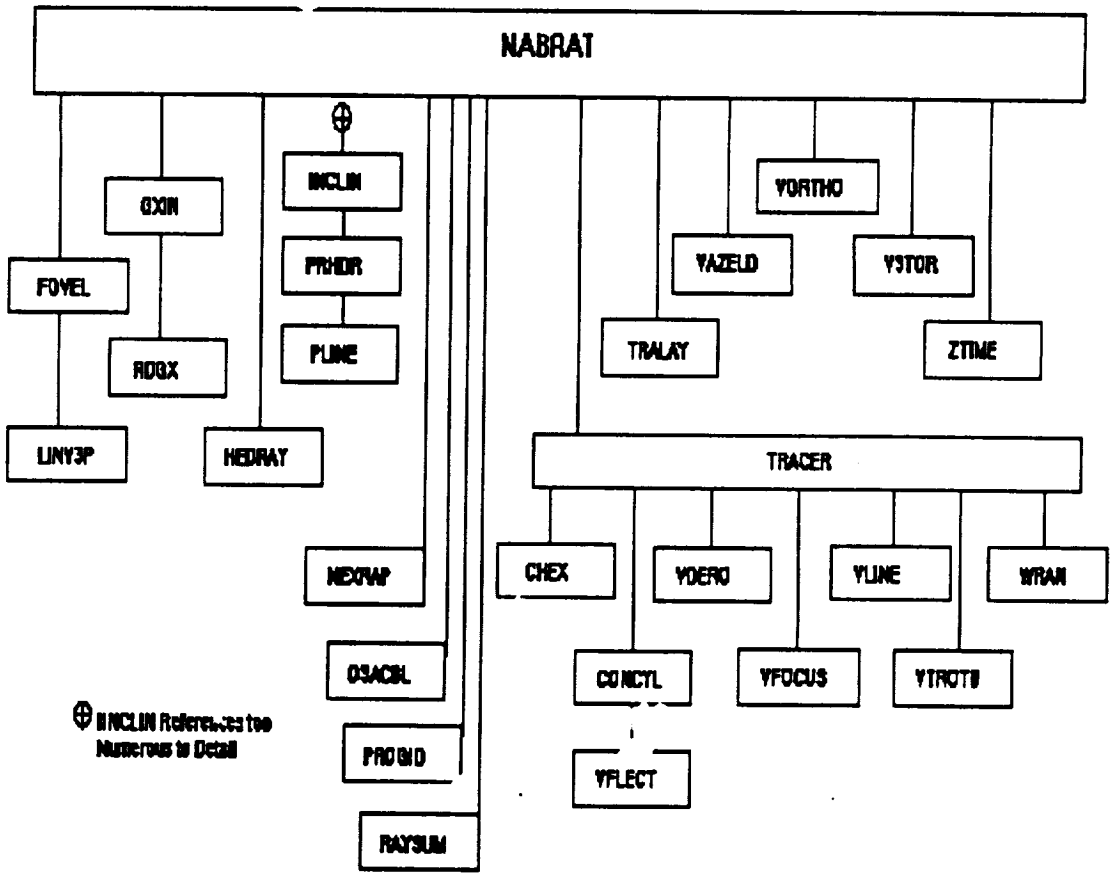

Figure 5.18 NABRAT External Reference Tree

5.2.2 Inputs and Outputs

The inputs to NABRAT are a GX file created by GEOSAC, and a user-created file consisting of a single identifier line (ID file) that is to be printed in the headers of the printer output. The output of NABRAT consists of terminal and printer output, as well as three ray intersection information (RAY) file containing intersection information at the first surface, second surface, and focal plane, respectively. The file numbers of all NABRAT files are summarized in Table 5.11.

Table 5.11 Files Used by NABRAT

Input/ Output	File Name	File Type	Format	Logical Record Length	Block Size	File Number
Input	name1	GX	FB	80	800	11
Input	name2	ID	FB	80	800	5
Output	name1	RAY001	FB	80	800	24
Output	name1	RAY002	FB	80	800	26
Output	name1	RAY003	FB	80	800	28
Output	terminal			80		6
Output	printer			132		8

Tables 5.12 (a), (b) and (c) show the format of a RAY file. The file consists of a header, followed by several parameters for every ray-surface intersection, followed by a trailer. Note that the final, focal plane RAY file has additional information at the end. These numbers are the matrix elements used to find the global optimal focus information, and are therefore of little use to the user.

Table 5.12(a)
RAY File Format (Record Groups)

Header Record Group (3 Cards)	
Card 1	64-character user ray file comments RDATE = current date, and RTIME = current time appended by program Format (16A4, 2A8)
Card 2	64-character geometry comments with GDATE and GTIME. Same format as above.
Card 3	PARX record (See Table 5.9(b))
Data Record Group for Each Ray (1 or 4 Cards) (See Table 5.12 (b))	
Trailer Record Group (2 or 5 Cards) (See Table 5.12 (c))	

Figure 5.19 shows the input ID file for NABRAT for analyzing DOCON, the conventional on-axis system described in the GEOSAC program description. The GX file input is the same file created previously by GEOSAC.

Figures 5.20 thru 5.22 show the output RAY files.

Table 5.12(b) RAY File Format (Data Record Group Format)

Card #	Item #	Name	Precision	Format	Description
1	1	JRAY	I*4	I10	Ray #
	2	JING	I*4	I10	Ring #
	3	J2	I*4	I10	Spoke #
	4	KODE	I*4	I10	Ray Status Code
	5	IN10	I*4	I10	1.0E8 * Ray Weight
	6	DUM	3 * R*4	3F10.6	Not needed, dummied to 0
The remaining cards are omitted whenever KODE.GT.4, *i.e.*, when the ray fails					
2	7	P	3 * R*8	1P3D25.17	Position of ray at intersection
3	8	L	3 * R*8	1P3F20.17	Direction cosines of ray after reflection
	9	IOP	I*4	I5	Integer portion of path length
	10	FOP	R*8	1PF15.12	Fractional portion of path length
4	11	Q3	6*R*4	1P3F1[illegible].9, 4X, 1P312.9	Second derivative matrix of surface
5	1,2,3,4	C (1)	CMP*16	1P2F15.9	x component of complex amplitude
6	1,2	S (1)	CMP*16	1P2F15.9	y component of complex amplitude

Table 5.12(c) RAY File Format (Trailer Record Group Format)

Card	Item #	Name	Precision	Format	Description
1	1	NRAY	I*4	I10	Minus # of rays started
	2	NAIL	I*4	I10	Total # of ray failures
	3	LEFT	I*4	I10	# of active rays
	4	JAIL	I*4	I10	# of rays which failed at current surface
	5	JEFT	I*4	I10	# of rays which were active leaving preceding surface
2	6	WF	R*8	1PD20.12	Total weight of failed rays
	7	WS	R*8	1PD20.12	Total weight of active rays
The remaining cards are printed only when the RAY file is for the focal plane, rather than for an optical surface.					
3-5	8	AQ	R*8	1P2(4D20.12/), 1PD20.12, 1P3D13.6	Coefficients of quadratic focus function for FOVEL routine
	9	P	R*8	(part of above format)	Coordinates of global optimal focus

+++ID LINE FROM 'DOCON.N ID' ++++

Figure 5.19 NABRAT ID File for DOCON System

```
++ID LINE FROM FILE 'DOCON GI' (ON-AXIS CASSEGRAIN)++          16-07-91 08:57:31

  2    1    5   10  9.710000E+01   6.014290E+04  -1.000000E+00 3.77526957D+03
       1         1         1         2 100000000  0.000000  0.000000  0.000000
 9.709999999999996D+01 5.71445079970746384D+00 3.27413580605056950D+03
0.35466954083395583-0.00340891363270135-9.993707915289123113774 1.407928509053
0.000000000 0.000000000 0.000000000     0.000000000 0.000000000 0.000000000
  -0.002220894    7.071067456   -0.000176109    0.000261683
   0.000176109    0.000261683   -0.002220894   -7.071067456
       2         2         1         2 100000000  0.000000  0.000000  0.000000
 2.63763738978654914D+02 5.70486237704486432D+00 3.26864205012134335D+03
0.96151215336065576-0.00333217974275079-9.953666825623505303769-3.529714458002
0.000000000 0.000000000 0.000000000     0.000000000 0.000000000 0.000000000
  -0.016377521    7.071048794   -0.000480041    0.000708232
   0.000480041    0.000708232   -0.016377521   -7.071048794
       3         3         1         2 100000000  0.000000  0.000000  0.000000

          to

      50        5        10         2 100000000  0.000000  0.000000  0.000000
 4.04508505277643451D+02 -2.88216003468109321D+02 3.25246527868161070D+03
1.46579843430423944 1.06186408671963840-9.834829922846978493752-0.427066713962
0.000000000 0.000000000 0.000000000     0.000000000 0.000000000 0.000000000
  -0.017983270    7.070608135   -0.056252366   -0.054889624
   0.056252366   -0.054889624   -0.017983270   -7.070608135
      -50        10        40        10        50
 1.000000000000D+01 4.000000000000D+01
```

Figure 5.20 NABRAT RAY File for DOCON System, Surface 1

```
++ID LINE FROM FILE 'DOCON GI' (ON-AXIS CASSEGRAIN)++          16-07-91 08:57:31

  2   2   5   10   9.710000E+01   6.014290E+04  -1.000000E+00 3.77526957D+03
      1       1       1       2 100000000  0.000000  0.000000  0.000000
-1.82025434405159130D+01 4.60621801688856802D+00 2.51961358297220084D+01
0.04987900231096049-0.10368296895520081 9.99933807444658262 7025 1.260105100848
0.000000000 0.000000000 0.000000000    0.000000000 0.000000000 0.000000000
 -7.071066669  -0.003660937   0.001343000  -0.000977716
 -0.001343000  -0.000977716  -7.071066669   0.003660937
      2       2       1       2 100000000  0.000000  0.000000  0.000000
-4.94359225354388201D+01 4.61944960936848348D+00 2.63688560559520506D+01
0.13316497268775175-0.10374812651056192 9.99857506929335435 7026 0.126314683729
0.000000000 0.000000000 0.000000000    0.000000000 0.000000000 0.000000000
 -7.071009572  -0.028340284   0.003664149  -0.002652315
 -0.003664149  -0.002652315  -7.071009572   0.028340284
to
     50       5       10       2 100000000  0.000000  0.000000  0.000000
-7.5749223653501555 D+01 5.96957030712561627D+00 3.01579186573708720D+01
0.20346554114305063-0.25079544881038482 9.99478381038946539 7028 3.813751915761
0.000000000 0.000000000 0.000000000    0.000000000 0.000000000 0.000000000
 -7.070371708  -0.034212078   0.004545916   0.093020335
 -0.004545916   0.093020335  -7.070371708   0.034212078
    -50      12       38       2       40
2.000000000000D+00 3.800000000000D+01
```

Figure 5.21 NABRAT RAY File for DOCON System, Surface 2

```
++ID LINE FROM FILE 'DOCON GI' (ON-AXIS CASSEGRAIN)++          16-07-91 08:57:31

  2   3   5   10   9.710000E+01   6.014290E+04  -1.000000E+00 3.77526957D+03
      1       1       1       2 100000000  0.000000  0.000000  0.000000
 5.03686921597652049D-01 -3.42782305896077713D+01  0.00000000000000000D+00
0.04987900231096049-0.10368296895520081 9.99933807444658262 10775 4.476880555530
0.000000000 0.000000000 0.000000000    0.000000000 0.000000000 0.000000000
 -7.071066669  -0.003660937   0.001343000  -0.000977716
 -0.001343000  -0.000977716  -7.071066669   0.003660937
      2       2       1       2 100000000  0.000000  0.000000  0.000000
 4.93418167779458017D-01 -3.42802358808452006D+01  0.00000000000000000D+00
0.13316497268775175-0.10374812651056192 9.99857506929335435 10775 4.476139163270
0.000000000 0.000000000 0.000000000    0.000000000 0.000000000 0.000000000
 -7.071009572  -0.028340284   0.003664149  -0.002652315
 -0.003664149  -0.002652315  -7.071009572   0.028340284
to
    -50      12       38       0       38
0.000000000000D+00 3.800000000000D+01
3.79942400474D+01  5.498525844480D-05  3.799025544802D+01 -5.1.1513035778D-03
4.087144016797D-01  1.550394723876D-02  1.926606504320D+01 -1.302492007308D+03
-1.400595430398D+01  4.466558570474D+04 5.072417D-01-3.429397D+01 8.436306D-01
```

Figure 5.22 NABRAT RAY File for DOCON System, Focal Plane

Figure 5.23 shows the resultant printout. The first section shows, for each surface, the number of rays started, failed, and succeeded, and the total corresponding ray weights. For a further explanation of ray weights, refer back to Section 4.2 and 4.4. Next is shown some rough information about the focal plane and the spot of rays, The parameter ZOFF can have a different value here than that specified by the user in the original GI file, although the same information is present. Specifically, if the user has set system parameter 23 in the GI file equal to zero (ZOFF relative to geometrical focus), then GFOC here is the geometrical focus calculated by GEOSAC, and ZOFF is the same as defined by the user, and tells the displacement of the focal plane from the geometrical focus.

```
*** OPTICAL SURFACE ANALYSIS PROGRAM (NABRAT ) RELEASE (06.0) VAX      PAGE  1
 + +ID LINE FROM FILE 'DOCON GI' (ON-AXIS CASSEGRAIN)+ +        16-07-91 09:09:55
+ +ID LINE FROM FILE 'DOCON GI' (ON-AXIS CASSEGRAIN)+ +         16-07-91 08:57:31
-------------------------------------------------------------

                    RAY SUMMARY REPORT
                    -----------------

SURFACE        STARTED          FAILED          SUCCEEDED
 NUM       NUM      WEIGHT    NUM      WEIGHT    NUM      WEIGHT

  1        50        50.00000  10        10.00000 40        40.00000
  2        40        40.00000   2         2.00000 38        38.00000

                    RAY FOCUS REPORT
                    ---------------

FOCAL PLANE INTERSECTIONS FOR GFOC =  3.775269570000D+03, ZOFF =   0.000000D+00
        MINIMUM                  MAXIMUM
     X           Y            X           Y
4.80959377E-01 -3.43107017E+01 5.29791866E-01 -3.42748055E+01

                  PLANAR OPTIMAL FOCUS
                  --------------------

   SUM          X           Y           Z          SPOT
  WEIGHTS     LOCATION    LOCATION    PLANE        SIZE
3.80000D+01 5.07128D-01 -3.42849D+01 0.00000D+00 1.59354D-02
                  GLOBAL OPTIMAL FOCUS
                  --------------------

   SUM          X           Y           Z          SPOT
  WEIGHTS     LOCATION    LOCATION    PLANE        SIZE
3.80000D+01 5.07242D-01 -3.42940D+01 8.43631D-01 6.77700D-03
```

Figure 5.23 NABRAT Printout for DOCON System

If, on the other hand, the user has set system parameter 23 equal to one (ZOFF relative to the standard coordinate system), then GFOC here is the ZOFF originally defined by user, and ZOFF here is zero. The minimum and maximum x and y values shown next are those of all the ray-focal plane intersection coordinates. The parameters shown next relate to the focal plane (planar optimal focus). The x and y locations are those of the image centroid. The z plane parameter is the ZOFF value displayed above.

The spot size is defined by

$$RMS = \sqrt{\frac{\sum_{allrays} [(X_i - X_c)^2 + (Y_i - Y_c)^2] W_i}{\sum_{allrays} W_i}} \qquad (5\text{-}2)$$

where (X_i, Y_i) are the focal plane intersection coordinates, W_i is the ray weight, and (X_c, Y_c) are the image centroid coordinates, defined by

$$X_c = \frac{\sum_{allrays} (X_i W_i)}{\sum_{allrays} (W_i)}$$

and (5-3)

$$Y_c = \frac{\sum_{allrays} (Y_i W_i)}{\sum_{allrays} (W_i)}$$

The global optimal focus parameters convey the same kind of information as the planar optimal focus information, except the z plane is selected by the program to minimize the spot size. The 'z plane' parameter is the displacement of this plane from the location defined by GFOC above. The procedure by which NABRAT finds this focal plane location and the resulting spot size is detailed below.

5.2.3 Finding the Focus of a Bundle of Rays

This section describes the mathematical analysis performed for VFOCUS, a FORTRAN program which finds a focus in three dimensional Euclidean space. The Focus of a bundle of rays is defined as that point F which minimizes the sum of the weighted squares of the perpendicular distances from the point to the various rays in the bundle.

The bundle is a set $\{R_i\}$ of at least two rays, not all of which are parallel. Consider now, R as any ray selected from $\{R_i\}$. As our attention is directed to just this ray, the subscript i will, for the moment, be omitted from R as well as the vectors P, L, and T, and the quantities t, and d.

It is assumed that some point P on R and the direction cosine vector L of R are given. Let S be any point in space and let T be the foot of the perpendicular dropped from S to R as shown in Figure 5.24.

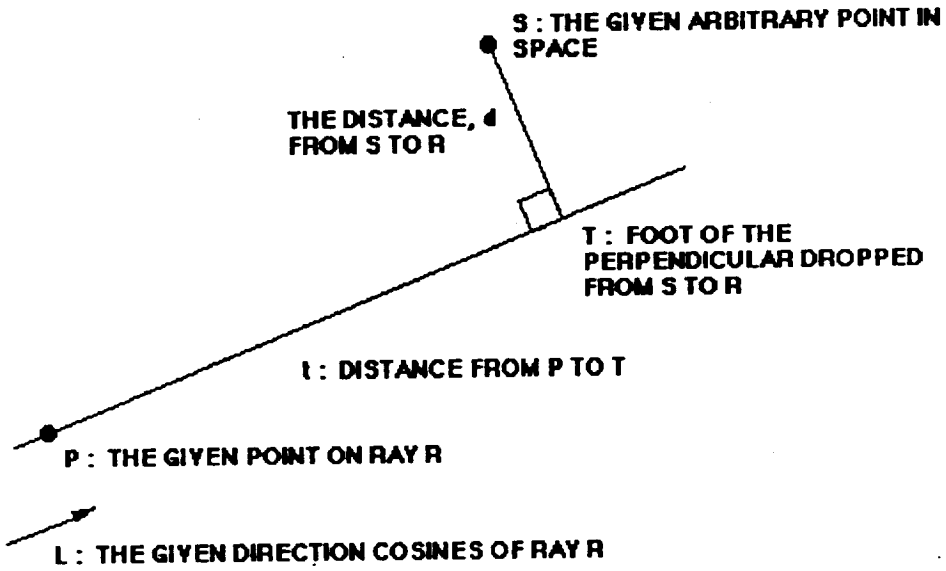

Figure 5.24 Geometry for FOVEL Routine

T may be calculated as follows:

Any point Q on R is of the form

$$Q = P + t\,L \tag{5-4}$$

where t is the distance along the line from P to Q. Hence, for some particular t,

$$T = P + t\,L \tag{5-5}$$

We also know that the difference vector from S to T is perpendicular to R.

$$\textit{Hence, } (T - S) \cdot L = 0 \tag{5-6}$$

Substituting formula (5-5) for T into (5-6), we have

$$(P - S + t\,L) \cdot L = 0 \quad i.e.,$$
$$(P - S) \cdot L + t\,L \cdot L = 0 \tag{5-7}$$

As L is a unit vector, L • L = 1 so

$$t = (S - P) \cdot L \tag{5-8}$$

Substituting for t in (5-5),

$$T = P + [(S - P) \cdot L]\,L \tag{5-9}$$

Then, d, the perpendicular distance from S to R, is the distance from S to T.

$$i.e.,\ d = |T - S| = |\ (P-S) - ((P - S) \cdot L)\,L| \tag{5-10}$$

Let Q = P - S.

$$Then\ d = |Q - (Q \cdot L)\,L| \tag{5-11}$$

Let V = Q - (Q•L) L. Then d = |V|

In order to use matrix algebra, it is assumed that all vectors are column vectors, i.e., 3 x 1 arrays.

$$V = Q - L(L^T Q) = AQ \tag{5-12}$$

where A is the 3 x 3 array ($I - LL^T$)

$$d^2 = V^T V = (AQ)^T AQ = Q^T A^T AQ \tag{5-13}$$

Now A has the remarkable property that it is both symmetric and indempotent i.e., that

$$A = A^T = AA = A^T A \tag{5-14}$$

Thus, $d^2 = Q^T AQ$,

$$d^2 = (P - S)^T A(P - S)$$
$$d^2 = S^T AS - (S^T AP + P^T AS) + P^T AP \tag{5-15}$$

Now, $S^T AP$ is a scalar, and therefore is equal to its transpose.

$$S^TAP = P^TA^TS = P^TAS \quad so \qquad (5\text{-}16)$$
$$d^2 = S^TAS - 2B^TS + C$$

where, $B^T = P^TA$ and $C = P^TAP$

The index i, which is the index in $\{R_i\}$ of the various rays in the bundle, will now be reintroduced.

We now know the following:

S is the location of an arbitrary point in space,

$\{P_i | P_i$ is a point on the line $R_i\}$
$\{L_i | L_i$ is the direction cosine vector of $R_i\}$
$\{W_i | W_i$ is the weight of R_i, $W_i > 0\}$

For each R_i, we compute A_i using (11), and B_i, and C_i, and d_i^2 using (5-15) we would then calculate:

$$\phi(s) = \sum W_i\, d_i^2 = \sum W_i[(S^TA_iS) - 2D_i^TS + C_i] \qquad (5\text{-}17)$$

$$\phi(S) = \sum W_i(S^TA_iS) - 2\sum W_iB_i^TS + \sum W_iC_i \qquad (5\text{-}18)$$

$$\phi(s) = S^TAS - 2B^TS + C \qquad (5\text{-}19)$$

where

$$A = \sum W_iA_i$$
$$B^T = \sum W_iB_i^T \qquad (5\text{-}20)$$
$$C = \sum W_iC_i$$

Note that ϕ is a quadratic form in S. Consider now the question, "of all points S in space, which one minimizes ϕ?"

The answer to the question is F, the Focus, also called the global optimal focus, to distinguish it from the planar optimal focus. That is, the focus is the solution to the equations

$$\left.\frac{\partial \phi}{\partial S}\right|_{S=F} = 0 \tag{5-21}$$

$$\frac{\partial (S^T A S)}{\partial S} = AS + A^T S = 2AS \tag{5-22}$$

$$\frac{\partial C}{\partial S} = 0 \tag{5-23}$$

$$\frac{\partial (B^T S)}{\partial S} = B \tag{5-24}$$

Thus, when evaluated at S=F,

$$\begin{aligned} &2AF - 2B - 0 = 0 \\ &AF = D \\ &F = A^{-1}B \end{aligned} \tag{5-25}$$

Now that we have a formula for the focus, we can evaluate ϕ(F) and the RMS spot size. Substituting (24) into (16)

$$\begin{aligned} \phi(F) &= (A^{-1}B)^T A(A^{-1}B) - 2B^T(A^{-1}B) + C \\ \phi(F) &= B^T A^{-1} A A^{-1} B - 2B^T A^{-1} B + C \\ \phi(F) &= C - B^T A^{-1} B = C - B^T F \end{aligned} \tag{5-26}$$

The RMS spot size may be evaluated as:

$$SIZE = \sqrt{\frac{\phi(F)}{W}} \tag{5-27}$$

where

$$W = \sum W_i \tag{5-28}$$

5.3 DRAT

5.3.1 Introduction

DRAT traces a bundle of rays through a single element of an optical system. The element may be conic, toroidal, or flat, and may have polynomial deformations. The only unusual analytical method used by DRAT is in finding the position in space that minimizes the RMS spot size. This method was detailed in the NABRAT program description, Section 5.2.3. The subroutine structure of DRAT is shown in Figure 5.25.

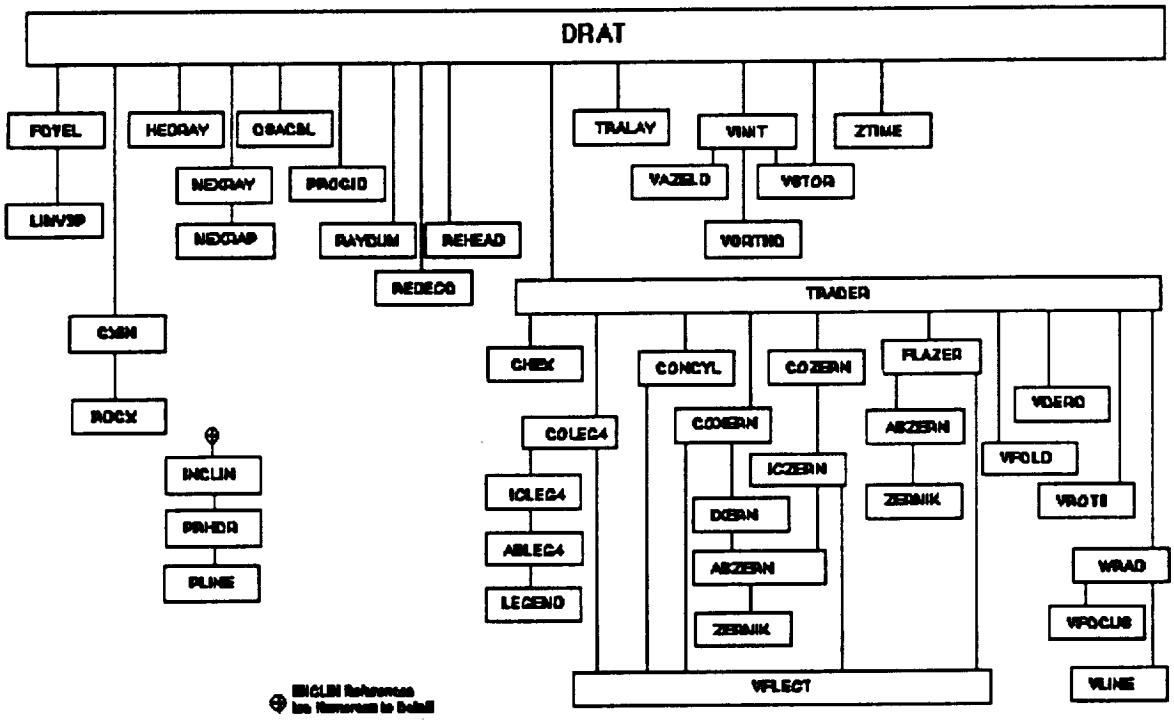

Figure 5.25 DRAT External Reference Tree

5.3.2 Inputs and Outputs

The inputs to DRAT consist of (1) a GX file created by GEOSAC, (2) a one line ID file, (3) a file (DEFORM file) containing polynomial deformation coefficients (only if the surface is defined in the original GI file to have polynomial deformations), and (4) a RAY file from a previous DRAT run (only if the surface is not the first surface in the system). The output

consists of terminal and printer output and a RAY file, and (only if the surface is the last surface in the system) an additional RAY file for the focal plane. The names, types, formats, and file numbers of all DRAT files are summarized in Table 5.13.

Table 5.13 Files Used by DRAT

Input/ Output	File Name	File Type	Format	Logical Record Length	Block Size	File Number
Input	name1	GX	FB	80	800	11
Input	name2	ID	FB	80	800	5
Input	name1	RAY00i[1,2]	FB	80	800	23
Input	name3	DEFORM[3]	FB	80	800	13
Output	name1	RAY00j[4]	FB	80	800	24
Output	name1	RAY00k[5,6]	FB	80	800	26
Output	terminal			80		6
Output	printer			132		8

1 "i" = surface # of previous surface

2 input RAY file required only if current surface #.GT.1

3 input DEFORM file required only if system is deformed

4 "j" = "i" + 1 = surface # of current surface

5 "k" = "i" + 2

6 output focal plane RAY file produced only if current surface is the last surface in the system

Table 5.14 shows the format of a DRAT ID file. It contains a 64 character identifier, just as does a NABRAT ID file. However, following the identifier is an integer that specifies the optical surface number.

Table 5.14
ID File Format Used by DRAT

Card 1	RID	=	64-character user comments, KURF = surface #
	Format (16A4, 1X, I5)		

Table 5.15 shows the format of a DEFORM file. The first line is a 64 character identifier line

with one or two numbers at the end to tell the program how many deformation coefficients are to follow. For a conventional system, the single number is the number of deformation coefficients. For an X-ray system, the two numbers I and J are the Legendre and Fourier index limits respectively, making the total number of deformation coefficients I(1 + 2J). (See Section 4.7 for a discussion of the polynomials and their coefficients). For a conventional system, the expected ordering of the coefficients is the same as the ordering defined in Table 4.1. For an X-ray system, the expected ordering is as follows: first, all the d_l coefficients in increasing order; then all the e_{ml} coefficients increasing first in the l (Legendre) and then in the m (Fourier) index; and then all the f_{ml} coefficients, ordered in the same way as the e_{ml} coefficients. Figures 5.26(a) and 5.26(b) show the ID files used in analyzing the on-axis system defined in the DOCON GI file, and Figures 5.27 and 5.28 show the printer outputs of the required two runs of DRAT. (Note that two runs of DRAT were required for this two-element undeformed system, as opposed to a single NABRAT run). The information output is substantially the same as that in the NABRAT output.

Table 5.15
DEFORM File Format
(UPDATED SPECIFICATION FOR CARD #1, ITEM #3)

Card	Item #	Name	Precision	Format	Description
	1	DFID	R*4	16A4	User Comments
	2	I	I*4	1X,I5	Total # of Legendre Terms for an X-ray System, or Total # of Deformation Coefficients for a conventional System
1					
	3	J --or--	I*4	I5	Azimuthal Index Limit (highest degree of Fourier terms) for an X-ray System
	3	OBSC	R*8	F9.6	Linear Obscuration Ratio for a Conventional System
2 - End	1 - NDFC NDFC=Total # of Coeff's	DEFC	R*4	5E15.5	Deformation Coefficients, Packed Five to a Card

```
(a) +++ID LINE FROM 'DOCON.1 ID'+++  1
(b) +++ID LINE FROM 'DOCON.2 ID'+++  2
(c) +++ID LINE FROM 'DOCON.1 ID'+++  1
(d) +++ID LINE FROM 'DOCON.2 ID'+++  2
(e) +++ID LINE FROM 'DOCON.3 ID'+++  3
(f) +++ID LINE FROM 'DOCON.1 ID'+++  1
(g) +++ID LINE FROM 'DOCON.2 ID'+++  2
```

64 character User Comments — Integer Surface Number

Figure 5.26

DRAT ID Files (a) DOCON System, Surface 1, (b) DOCON System, Surface 2, (c) DOCOF System, Surface 1, (d) DOCOF System, Surface 1, (e) DOCOF System, Surface 3, (f) DOCXR System, Surface 1, (g) DOCXR System, Surface 2

```
*** OPTICAL SURFACE ANALYSIS PROGRAM (DRAT   ) RELEASE (06.0) VAX      PAGE  1
 ++ID LINE FROM FILE 'DOCON GI' (ON-AXIS CASSEGRAIN)++          16-07-91 09:15:28
++ID LINE FROM FILE 'DOCON GI' (ON-AXIS CASSEGRAIN)++           16-07-91 08:57:31
```

RAY SUMMARY REPORT

PREVIOUS SURFACES

STARTED		FAILED		SUCCEEDED	
NUM	WEIGHT	NUM	WEIGHT	NUM	WEIGHT
50	50.00000	0	0.00000	50	50.00000

CURRENT SURFACE (# 1)

STARTED		FAILED		SUCCEEDED	
NUM	WEIGHT	NUM	WEIGHT	NUM	WEIGHT
50	50.00000	10	10.00000	40	40.00000

Figure 5.27 DRAT Printout for DOCON System, Surface 1

```
*** OPTICAL SURFACE ANALYSIS PROGRAM (DRAT    ) RELEASE (06.0) VAX      PAGE  1
 + +ID LINE FROM FILE 'DOCON GI' (ON-AXIS CASSEGRAIN)+ +        16-07-91 09:15:38
+ +ID LINE FROM FILE 'DOCON GI' (ON-AXIS CASSEGRAIN)+ +         16-07-91 08:57:31
-------------------------------------------------------------

                    RAY SUMMARY REPORT
                    ------------------

                     PREVIOUS SURFACES
       STARTED              FAILED             SUCCEEDED
     NUM      WEIGHT     NUM      WEIGHT     NUM      WEIGHT
      50    50.00000     10    10.00000      40    40.00000
                  CURRENT SURFACE (#  2)
       STARTED              FAILED             SUCCEEDED
     NUM      WEIGHT     NUM      WEIGHT     NUM      WEIGHT
      40    40.00000      2     2.00000      38    38.00000
FOCAL PLANE HITS: GFOC =  3.775269570000D+03 ZOFF =   0.000000D+00
        MINIMUM                  MAXIMUM
    X            Y           X            Y
4.80959377E-01 -3.43107017E+01  5.29791866E-01 -3.42748055E+01

                    PLANAR OPTIMAL FOCUS
                    --------------------

   SUM          X           Y           Z          SPOT
  WEIGHTS     LOCATION    LOCATION    PLANE        SIZE
 3.80000D+01 5.07128D-01 -3.42849D+01 0.00000D+00 1.59354D-02

                    GLOBAL OPTIMAL FOCUS
                    --------------------

   SUM          X           Y           Z          SPOT
  WEIGHTS     LOCATION    LOCATION    PLANE        SIZE
 3.80000D+01 5.07242D-01 -3.42940D+01 8.43631D-01 6.77700D-03
```

Figure 5.28 DRAT Printout for DOCON System, Surface 2

Perhaps the only item that is not self-explanatory after understanding the NABRAT output is the term 'previous surfaces'. This refers to summary information for all preceding surfaces. The 'number started' is the number of rays in the input collimated bundle, and the number 'failed' and 'succeeded' are for all rays entering the current surface, regardless of where they may have previously failed or succeeded.

Figures 5.26(c), (d) and (e) show the ID files, and Figure 5.29, 5.30 and 5.31 show the printer outputs of the three runs of DRAT required to analyze the three-element off-axis system defined in the DOCOF GI file. (Note that this system could not have been analyzed by NABRAT, since it contains a third, flat element). The same types of information are displayed here as for the on-axis case.

Figure 5.32 shows the DRAT output for toroidal surface of Figure 5.12. To demonstrate that the line foci exist as predicted, Figures 5.33 and 5.34 show plots of the ray distributions at the two locations. Although the scale factors are unequal in the x and y directions, thereby skewing the angles, it is clear that the two line foci exist as predicted. (The first line focus corresponds

to the GEOSAC and DRAT outputs in Figures 5.33 and 5.34.).

```
*** OPTICAL SURFACE ANALYSIS PROGRAM (DRAT    ) RELEASE (06.0) VAX      PAGE  1
 + +ID LINE FROM FILE 'DOCOF GI' (OFF-AXIS SYSTEM)          16-07-91 09:17:45
 + +ID LINE FROM FILE 'DOCOF GI' (OFF-AXIS SYSTEM)          16-07-91 08:59:50
-------------------------------------------------------------------------------

                    RAY SUMMARY REPORT
                    ------------------

                    PREVIOUS SURFACES

      STARTED              FAILED              SUCCEEDED
  NUM       WEIGHT     NUM       WEIGHT     NUM       WEIGHT

   41     41.00000      0      0.00000      41     41.00000

                  CURRENT SURFACE (#   1)

      STARTED              FAILED              SUCCEEDED
  NUM       WEIGHT     NUM       WEIGHT     NUM       WEIGHT

   41     41.00000      0      0.00000      41     41.00000
```

Figure 5.29 DRAT Printout for DOCOF System, Surface 1

```
*** OPTICAL SURFACE ANALYSIS PROGRAM (DRAT) RELEASE (06.0) VAX       GE  1
 + +ID LINE FROM FILE 'DOCOF GI' (OFF-AXIS SYSTEM)          16-07-91 09:17:5^
 + +ID LINE FROM FILE 'DOCOF GI' (OFF-AXIS SYSTEM)          16-07-91 08:59:5u
-------------------------------------------------------------------------------

                    RAY SUMMARY REPORT
                    ------------------

                    PREVIOUS SURFACES
      STARTED              FAILED              SUCCEEDED
  NUM       WEIGHT     NUM       WEIGHT     NUM       WEIGHT
   41     41.00000      0      0.00000      41     41.00000
                  CURRENT SURFACE (#   2)
      STARTED              FAILED              SUCCEEDED
  NUM       WEIGHT     NUM       WEIGHT     NUM       WEIGHT
   41     41.00000      0      0.00000      41     41.00000
```

Figure 5.30 DRAT Printout for DOCOF System, Surface 2

```
*** OPTICAL SURFACE ANALYSIS PROGRAM (DRAT    ) RELEASE (06.0) VAX      PAGE  1
 + +ID LINE FROM FILE 'DOCOF GI' (OFF-AXIS SYSTEM)          16-07-91 09:18:02
 + +ID LINE FROM FILE 'DOCOF GI' (OFF-AXIS SYSTEM)          16-07-91 08:59:50
-------------------------------------------------------------------------------

                        RAY SUMMARY REPORT
                        ------------------

                        PREVIOUS SURFACES
          STARTED                 FAILED                SUCCEEDED
      NUM         WEIGHT      NUM         WEIGHT      NUM         WEIGHT
       41      41.00000        0        0.00000       41      41.00000

                      CURRENT SURFACE (#   3)
          STARTED                 FAILED                SUCCEEDED
      NUM         WEIGHT      NUM         WEIGHT      NUM         WEIGHT
       41      41.00000        0        0.00000       41      41.00000

 FOCAL PLANE HITS: GFOC =  3.7750000000000D+03 ZOFF =    0.000000D+00
          MINIMUM                    MAXIMUM
      X             Y             X             Y
-1.61859749E-04  5.16372114E-04  1.61859749E-04  7.64513036E-04

                      PLANAR OPTIMAL FOCUS
                      --------------------

    SUM          X            Y            Z           SPOT
  WEIGHTS     LOCATION     LOCATION     PLANE          SIZE
4.10000D+01 -2.05168D-14  6.46531D-04  0.00000D+00  1.15853D-04

                      GLOBAL OPTIMAL FOCUS
                      --------------------

    SUM          X            Y            Z           SPOT
  WEIGHTS     LOCATION     LOCATION     PLANE          SIZE
4.10000D+01 -2.05142D-14  6.10112D-05 -2.92731D-02  1.28502D-05
```

Figure 5.31 DRAT Printout for DOCOF System, Surface 3

```
*** OPTICAL SURFACE ANALYSIS PROGRAM (DRAT  ) RELEASE (06.0) VAX     PAGE  1
 TOR1.GI - TOROID TEST AT FIRST LINE FOCUS                 7-01-92 10:05:50
TOR1.GI - TOROID TEST AT FIRST LINE FOCUS                  7-01-92 10:01:40
-------------------------------------------------------------------------

                SUMMARY OF DEFORMATION COEFFICIENTS
                -----------------------------------

 TOR1.DFR - FULL CIRCLE ZERNIKES FOR TOR1.GI
TOTAL NUMBER OF COEFFICIENTS   =          5
LINEAR OBSCURATION RATIO       =    0.000000
INDEX OF LARGEST CONTRIBUTION  =          1
LARGEST CONTRIBUTION           = 3.7547000E-03
ROOT SUM SQUARE                = 4.6122226E-03
SUM OF THE WEIGHTED SQUARES    = 2.1272598E-05

THE DEFORMATION COEFFICIENTS:

 3.75470E-03   0.00000E+00   0.00000E+00   2.16770E-03  -1.57350E-03

                    RAY SUMMARY REPORT
                    ------------------
                     PREVIOUS SURFACES

      STARTED              FAILED             SUCCEEDED
    NUM       WEIGHT     NUM       WEIGHT     NUM       WEIGHT
     17     17.00000      0       0.00000     17     17.00000

                  CURRENT SURFACE (#   1)
      STARTED              FAILED             SUCCEEDED
    NUM       WEIGHT     NUM       WEIGHT     NUM       WEIGHT
     17     17.00000      0       0.00000     17     17.00000

FOCAL PLANE HITS: GFOC = -3.500000000000D+01 ZOFF =   0.000000D+00

        MINIMUM                    MAXIMUM
    X            Y            X            Y
8.06015214E+00  1.37795060E+01  1.11722084E+01  1.50686035E+01

                    PLANAR OPTIMAL FOCUS
                    --------------------

   SUM          X           Y           Z          SPOT
  WEIGHTS     LOCATION    LOCATION    PLANE        SIZE
1.70000D+01  9.61558D+00  1.44232D+01  0.00000D+00  1.15434D+00

                    GLOBAL OPTIMAL FOCUS
                    --------------------

   SUM          X           Y           Z          SPOT
  WEIGHTS     LOCATION    LOCATION    PLANE        SIZE
1.70000D+01  9.54593D+00  1.43187D+01 -9.99947D+00  1.00020D+00
```

Figure 5.32
DRAT Output Corresponding to the GI File (TOR1.GI) and DEFORM File (TOR1.DFR) in Figure 5.12

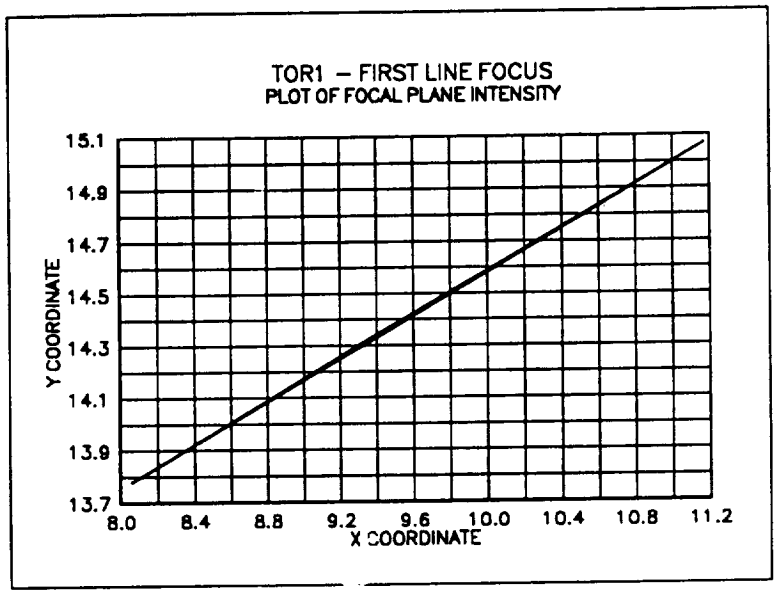

Figure 5.33

Focal Plane Plot at the First Toroidal Line Focus. (This is the focal plane location corresponding to the GEOSAC and DRAT outputs in Figures 5.12 and 5.32.)Note that the x and y scales are unequal, giving an unimportant skewing of the polar angle.

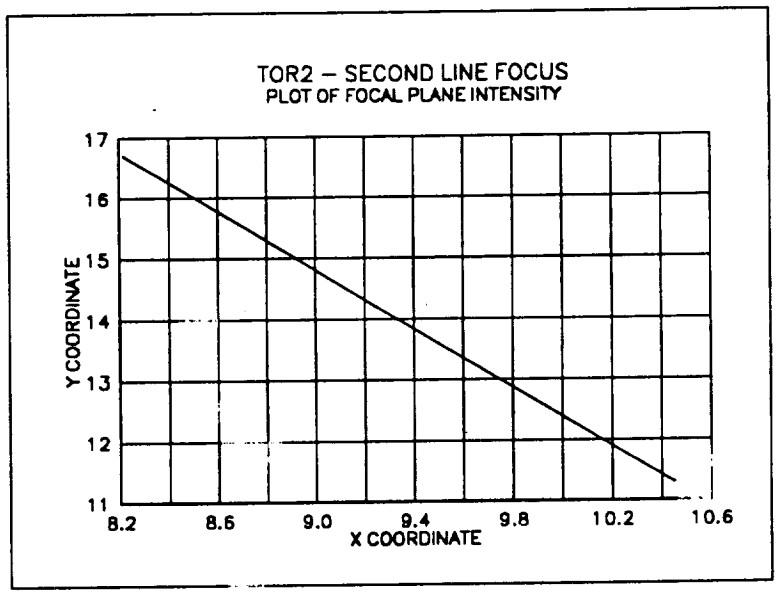

Figure 5.34

Focal Plane Plot at the Second Toroidal Line Focus. (the x and y scales are unequal, giving an unimportant skewing of the polar angle.)

Figures 5.26 (f) and (g) show the ID files, Figure 5.35 shows the DEFORM file, and Figures 5.36 and 5.37 show the printer outputs of the two runs of DRAT required to analyze the X-ray system defined in the DOCXR GI file. (Note that this system should also not be analyzed by NABRAT, since the first element has polynomial deformations. In this case, though, NABRAT could actually be used — it would ignore the polynomial deformations and analyze the correspondin$_g$ undeformed system). Note in this example the surface by surface reduction in ray weight due to the choice of surface dielectric constant in the GI file.

```
+ID LINE FROM FILE 'DOCXR.1'  DEFORM + +                    2   3
  0.001        0.002        0.003        0.004        0.005
  0.002        0.003        0.004        0.005        0.001
  0.003        0.004        0.005        0.001
```

Figure 5.35 DEFORM File for DOCXR System, Surface 1

```
*** OPTICAL SURFACE ANALYSIS PROGRAM (DRAT    ) RELEASE (06.0) VAX      PAGE   1
 + +ID LINE FROM FILE 'DOCXR GI' (X-RAY SYSTEM)              16-07-91 09:20:23
+ +ID LINE FROM FILE 'DOCXR GI' (X-RAY SYSTEM)               16-07-91 09:01:54
---------- ----------------------------------------------------

                SUMMARY OF DEFORMATION COEFFICIENTS
                -----------------------------------

+ +ID LINE FROM FILE 'DOCXR.1'  DEFORM + +
TOTAL NUMBER OF COEFFICIENTS   =          14
NUMBER OF LEGENDRE TERMS       =          2
AZIMUTHAL INDEX LIMIT          =          3
INDEX OF LARGEST CONTRIBUTION  =          5
LARGEST CONTRIBUTION           = 3.5355339E-04
ROOT SUM SQUARE                = 7.8951462E-04
SUM OF THE WEIGHTED SQUARES    = 6.2333334E-07

THE DEFORMATION COEFFICIENTS:
  1.00000E-04  2.00000E-04  3.00000E-04  4.00000E-04  5.00000E-04
  2.00000E-04  3.00000E-04  4.00000E-04  5.00000E-04  1.00000E-04
  3.00000E-04  4.00000E-04  5.00000E-04  1.00000E-04

                    RAY SUMMARY REPORT
                    ------------------

                    PREVIOUS SURFACES

     STARTED              FAILED              SUCCEEDED
  NUM       WEIGHT     NUM       WEIGHT     NUM       WEIGHT
   50     50.00000      0       0.00000     50     50.00000

                  CURRENT SURFACE (#   1)

     STARTED              FAILED              SUCCEEDED
  NUM       WEIGHT     NUM       WEIGHT     NUM       WEIGHT
   50     50.00000      0       0.00000     50     32.27201
```

Figure 5.36 DRAT Printout for DOCXR System, Surface 1

```
*** OPTICAL SURFACE ANALYSIS PROGRAM (DRAT    ) RELEASE (06.0) VAX      PAGE  1
 + +ID LINE FROM FILE 'DOCXR GI' (X-RAY SYSTEM)          16-07-91 09:20:34
 + +ID LINE FROM FILE 'DOCXR GI' (X-RAY SYSTEM)          16-07-91 09:01:54
-------------------------------------------------------------------------

                RAY SUMMARY REPORT
                ------------------
                PREVIOUS SURFACES

        STARTED              FAILED              SUCCEEDED
    NUM       WEIGHT     NUM       WEIGHT     NUM       WEIGHT

     50     50.00000      0       0.00000     50     32.27201

                CURRENT SURFACE (#   2)
        STARTED              FAILED              SUCCEEDED
    NUM       WEIGHT     NUM       WEIGHT     NUM       WEIGHT

     50     32.27201      0       0.00000     50     20.47280

FOCAL PLANE HITS: GFOC =  6.420000000000D+03 ZOFF =   0.000000D+00
        MINIMUM                    MAXIMUM
    X             Y            X             Y
-7.15237644E-02 -3.63960281E-02  1.40953194E-02  2.46789753E-02

                    PLANAR OPTIMAL FOCUS
                    --------------------

   SUM            X             Y             Z            SPOT
  WEIGHTS      LOCATION      LOCATION      PLANE          SIZE
2.04728D+01  -1.17120D-02  -2.92833D-03  0.00000D+00   3.05947D-02

                    GLOBAL OPTIMAL FOCUS
                    --------------------

   SUM            X             Y             Z            SPOT
  WEIGHTS      LOCATION      LOCATION      PLANE          SIZE
2.04728D+01  -1.17120D-02  -2.92833D-03  -3.33358D-01   2.82424D-02
```

Figure 5.37 DRAT Printout for DOCXR System, Surface 2

There is additional printer output for a deformed surface. This output consists of the identifier line from the DEFORM file, followed by several summary parameters concerning the deformation coefficients.

The 'total number of coefficients' is self-explanatory. The 'number of Legendre terms' and 'azimuthal index limit' are self-explanatory for an X-ray surface with Legendre-Fourier deformations, and are set to zero for a conventional surface with Zernike deformations. The 'index of largest contribution' is the number of the term in the DEFORM file itself that contributes most heavily to the mean square roughness σ^2. (The weighting of the squares of the coefficients to give σ^2 is discussed in Section 4.7). The 'largest contribution' is the square root of the contribution to σ^2 of the largest contributing term indexed above. The root sum square'

is the square root of σ^2 as defined by the weighted sum of squares of coefficients in Section 4.7. The 'sum of the weighted squares' is just σ^2. Referring to Table 4.2, the coefficients listed next in the output can be easily seen to imply the following polynomial deformations:

$$\rho(z,\theta) = (\rho^2 + 2Kz - Pz^2)^{1/2} +$$

$$+ 1. \times 10^{-3} \times P_0 (2z/L)$$
$$+ 2. \times 10^{-3} \times P_1 (2z/L)$$
$$+ 3. \times 10^{-3} \times P_0 (2z/L) \cos\theta$$
$$+ 4. \times 10^{-3} \times P_1 (2z/L) \cos\theta$$
$$+ 5. \times 10^{-3} \times P_0 (2z/L) \cos 2\theta$$
$$+ 2. \times 10^{-3} \times P_1 (2z/L) \cos 2\theta$$
$$+ 3. \times 10^{-3} \times P_0 (2z/L) \cos 3\theta$$
$$+ 4. \times 10^{-3} \times P_1 (2z/L) \cos 3\theta$$
$$+ 5. \times 10^{-3} \times P_0 (2z/L) \sin\theta$$
$$+ 1. \times 10^{-3} \times P_1 (2z/L) \sin\theta$$
$$+ 3. \times 10^{-3} \times P_0 (2z/L) \sin 2\theta$$
$$+ 4. \times 10^{-3} \times P_1 (2z/L) \sin 2\theta$$
$$+ 5. \times 10^{-3} \times P_0 (2z/L) \sin 3\theta$$
$$+ 1. \times 10^{-3} \times P_1 (2z/L) \sin 3\theta$$

None of the RAY file outputs are being dealt with here because the format corresponds exactly with that of the NABRAT RAY files already discussed.

5.4 SUSEQ

5.4.1 Introduction

The purpose of SUSEQ is to provide information about the path of a scattered ray through an optical system, relative to the path of a specular (non-scattered) ray previously traced by DRAT. (NABRAT does not provide enough specular ray trace information for SUSEQ to be run). The output from SUSEQ is provided in the form of a series of scale factors, which are the ratios of (resultant focal plane displacement) to (scattering angle away from the specular ray). These scale factors are evaluated for each successful ray, at each surface in the system, for each of two orthogonal scatter angle directions. The scatter angle directions are referred to as sagittal and tangential, and are illustrated in Figure 5.38. For X-ray systems, where mirror reflectivity is a strong function of the grazing incidence angle, additional scale factors are calculated. They are the ratios of (change in the sine of the grazing angle at a later surface) to (scattering angle away from the specular ray at an earlier, originating surface). These factors are evaluated for each successful ray, for each pair of surfaces in the system, for sagittal and tangential scatter directions.

Characterizing the behavior of a scattered ray with these scale factors is equivalent to assuming that focal plane displacement or sine-of-grazing-angle terms which are quadratic or higher in the

scattering angle can be ignored. The merit of this assumption can be examined by considering the hypothetical optical system whose object point is the intersection point of the scattered ray with its originating scattering surface; whose optical elements are the remaining intervening elements in the original system; and whose image point is the system focal plane for the focal plane scale factors, or a subsequent surface for the sine-of-grazing-angle scale factors. This system is not a focussing system. Nevertheless, the departure of the scattered ray from the specular ray (both in angle and in position) is linear in scatter angle to the extent that Gaussian optics applies to this hypothetical system. It is assumed that the original system being analyzed is well-corrected enough that Gaussian optics approximates its true behavior. It is also assumed that scatter angles to be considered are on the order of or less than the field of view of the original system. Therefore, Gaussian optics approximates the behavior of both the original system and this hypothetical system. Therefore, the behavior of a scattered ray can be closely approximated with linear scale factors.

The design of SUSEQ uses one other simplifying assumption, that deformation terms on the surfaces can be ignored when calculating the scale factors. This is equivalent to assuming that the deformation terms affect image aberrations rather than the first order Gaussian imaging properties of the system. Since this assumption is implicit in calling the terms "deformation terms", the terms can be ignored with the same legitimacy that allows the system to be characterized by linear scale factors. The following section details the novel methods used by SUSEQ. Since such detailed knowledge is not necessary for understanding the usage and output of SUSEQ, the user may wish to proceed to Section 5.4.3 on input and output. The subroutine structure of SUSEQ is shown in Figure 5.39.

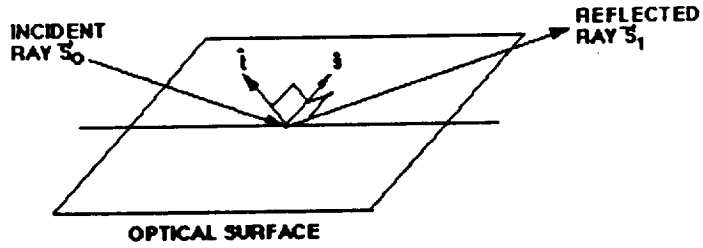

Figure 5.38 Scatter Angle Geometry

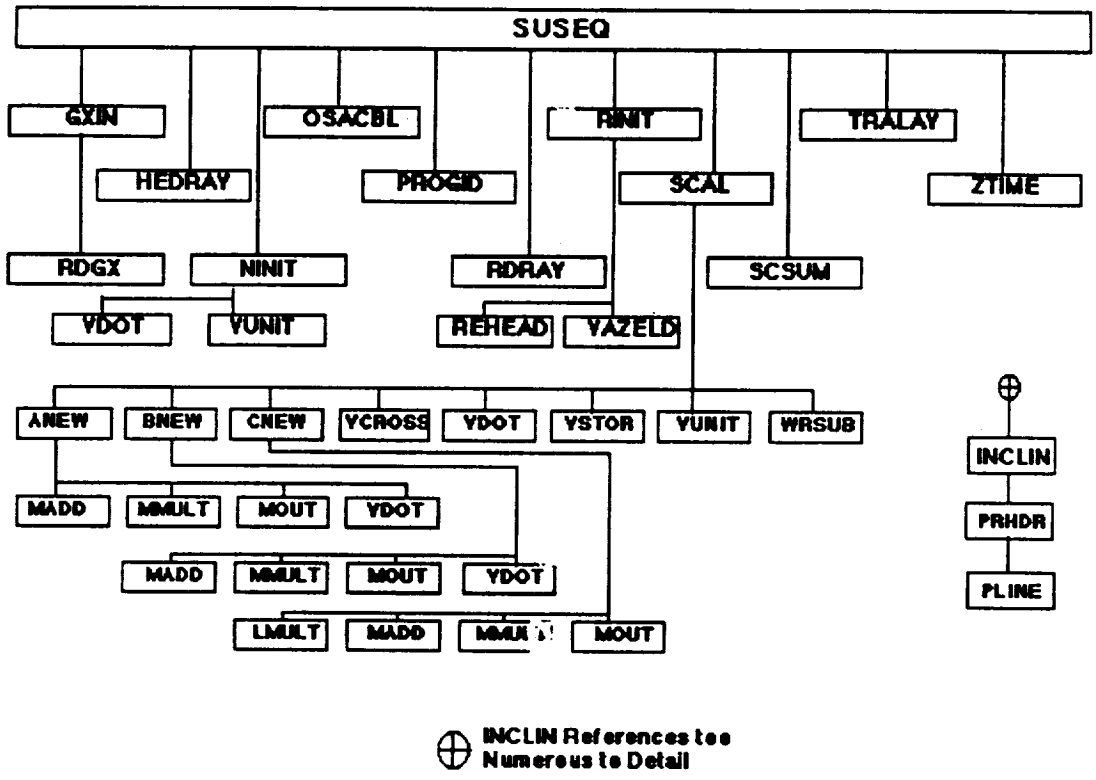

Figure 5.39 SUSEQ External Reference Tree

5.4.2 Method

SUSEQ uses a matrix analysis to evaluate the departure of the scattered ray from the specular ray as the specular ray intersects each subsequent surface, including the focal plane. SUSEQ evaluates at each surface the departure in position, the departure in direction, and (for X-ray systems only) the departure in the sine of the grazing angle. The original scattering direction is defined by a direction vector. This vector is left as a free variable until the very end of the analysis. At any subsequent surface, the departure in position is defined by a matrix $\bar{A}$ which, when operating on the original scattering direction vector, gives the departure in position of the ray-surface intersection. The departure in direction is defined by a matrix $\bar{B}$ which, when operating on the original scattering direction vector, gives the departure in direction of the ray after reflection by the surface. For X-ray systems, the departure in sine-of-grazing-angle is defined by a vector $\bar{C}$ which, when dot-multiplied by the original scattering direction vector $\bar{C}$ gives the departure in the sine of the grazing angle at the ray-surface intersection. $\bar{A}$ and $\bar{B}$ are evaluated at a surface in terms of the intersection parameters and in terms of the value of $\bar{A}$ and

$\vec{B}$ at the previous surface. At the originating scattering surface, $\vec{A}$ and $\vec{B}$ are defined to be the Zero and the Identity matrices respectively. $\vec{C}$ is evaluated in terms of the intersection parameters and in terms of the new values of $\vec{A}$ and $\vec{B}$. Figure 5.40 defines the situation and all relevant parameters.

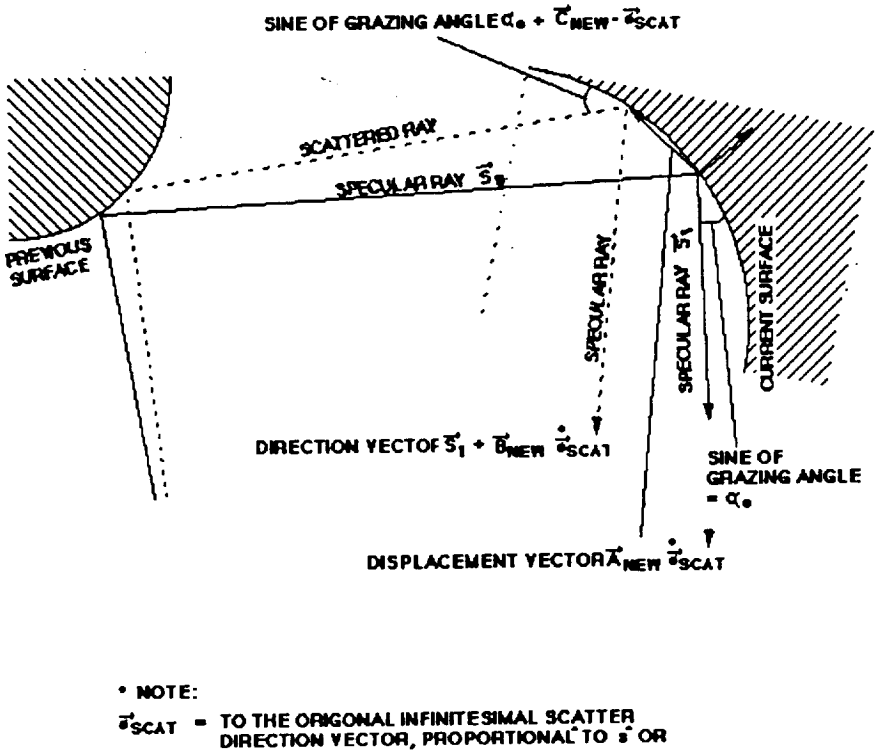

* NOTE:
$\vec{e}_{SCAT}$ = TO THE ORIGONAL INFINITESIMAL SCATTER DIRECTION VECTOR, PROPORTIONAL TO $\vec{s}$ OR

Figure 5.40 Geometry for SUSEQ Module

Explicit expressions

In terms of the intersection parameters and the old values of $\vec{A}$ and $\vec{B}$ the expression for the new value of $\vec{A}$ is found to be

$$\vec{A}_{new} = \left(\vec{I} - \left(\frac{1}{\vec{s}_0 \cdot \hat{n}_0}\right) \vec{s}_0 \circ \hat{n}_0\right) \left(\vec{A}_{old} + l\vec{B}_{old}\right) \qquad (5\text{-}29)$$

where $\vec{I}$ is the identity matrix, $\vec{s}_0$ is the unit direction vector of the Specular incident ray, $\hat{n}_o$ is the unit normal into the surface at the specular intersection point, l is the path length from

the old to the new surface, and the signs " · " and " o " refer to the vector inner and outer products respectively. (The inner product is a scalar defined by:

$$(a \cdot b)_{ij} = \sum_{i=1}^{3} a_i b_i \qquad (5\text{-}30)$$

The outer product is a matrix defined by:

$$(a \circ b)_{ij} = a_i b_j \qquad (5\text{-}31)$$

In terms of the intersection parameters and the old value of $\vec{B}$ and the new value of $\vec{A}$, the expression for the new value of $\vec{A}$ is found to be:

$$\vec{B}_{new} = \vec{M}_0 \vec{B}_{old} - 2(\hat{n}_0 \circ \vec{s}_0 + (\hat{n}_0 \cdot \vec{s}_0)\vec{M}_0)\vec{Q}_3 \vec{A}_{new} , \qquad (5\text{-}31)$$

where $\vec{M}_o$ and $\vec{Q}_3$ are matrices described below.

$\vec{M}_o$ is a mirror reflection matrix defined at the specular intersection point. $\vec{M}_o$ operating on the specular incident ray direction vector would give the specular ray reflected direction vector. $\vec{M}_o$ is given by is given by

$$\vec{M}_0 = (\vec{I} - 2\hat{n}_0 \circ \hat{n}_0) \qquad (5\text{-}32)$$

$\vec{Q}_3$ is related to the curvature of the reflecting surface and is proportional to the symmetric second derivative matrix of the scalar function F, which is the scalar surface defining function that is zero when evaluated on the surface. For OSAC surface,

$$F = x^2 + y^2 - \rho^2 - 2Kz + Pz^2 , \qquad (5\text{-}33)$$

in a surface-centered coordinate system. The proportionality constant is $\pm 1/\| \vec{\nabla}F \|$, where $\vec{\nabla}F$ is evaluated at the specular intersection point. If the OSAC surface is convex, the minus sign is used. If the surface is concave, the plus sign is used. This particular normalization constant is the same one that would be multiplied by $\vec{\nabla}F$ at the specular intersection point to give the into-the-surface unit normal vector. That is, $\vec{n}_o = \pm \vec{\Delta}F / \| \vec{\Delta}F \|$. $\vec{Q}_3$ is evaluated and transformed to the standard coordinate system by NABRAT or DRAT for later use by SUSEQ.

In terms of the intersection parameters and the new values of $\vec{A}$ and $\vec{B}$, the expression for the new value of $\vec{C}$ is found to be

$$\vec{C}' = -\vec{s}_1'(-\vec{I}n_0 \circ n_0)\vec{Q}_3\vec{A}_{new} - \hat{n}_o\vec{B}_{new} \quad (5\text{-}34)$$

where $\vec{s}_1$ is the unit direction vector of the specular reflected ray, and the symbol " ' " means transpose. The transpose of a column vector is a row vector. Only a row vector can appear on the left-hand side of a matrix multiplication expression.

To summarize, for each originating scattering surface, SUSEQ defines two orthogonal scatter direction unit vectors, $\hat{s}$ and $\hat{t}$. The focal plane scale factors are given by $(\vec{A} \cdot \hat{s})$ and $(\vec{A} \cdot \hat{t})$, where $\vec{A}$ is evaluated at the focal plane through the process described above. The sine-of-grazing angle derivative scale factors are given by $(\vec{C} \cdot \hat{s})$ and $(\vec{C} \cdot \hat{t})$ where $\vec{C}$ is evaluated in turn at each subsequent surface through the process described above.

5.4.3 Inputs and Outputs

The input to SUSEQ consists of a GX file created by GEOSAC, all the RAY files created by DRAT, and a one line user-created ID file with a 64-character identifier. Thus there are no user-defined parameters required to run SUSEQ. SUSEQ simply operates on the ray surface intersection information in the RAY files and with the system definition information in the GX file to produce the required scattering scale factors. The output consists of terminal and printer output, as well as a single file containing all the calculated scale factors (SCAL file). Table 5.16 summarizes the names, types, formats, and file numbers of all SUSEQ files.

Table 5.16 Files Used by SUSEQ

Input/ Output	File Name	File Type	Format	Logical Record Length	Block Size	File Number
Input	name1	GX	FB	80	800	1
Input	name2	ID	FB	80	800	5
Input	name1	RAY001	FB	80	800	9
Input	name	RAY002	FB	80	800	10
etc.[1]						
Output	name1	SCAL	FB	80	800	2
Output	terminal			80		6
Output	printer			132		8

[1] The total # of input RAY files is one greater than the # of surfaces in the system.

Figure 5.41 shows the ID file input, and Figure 5.42 shows the printer output from analyzing the X-ray system defined in the DOCXR GI file. The first several lines summarize some basic system definition quantities.

```
+++ID LINE FROM 'DOCXR.S ID'+++
```

Figure 5.41 SUSEQ ID File for DOCXR System

```
*** OPTICAL SURFACE ANALYSIS PROGRAM (SUSEQ  ) RELEASE (06.0) VAX     PAGE  1
 +++ID LINE FROM FILE 'DOCXR GI' (X-RAY SYSTEM)          16-07-91 09:32:28
+++ID LINE FROM FILE 'DOCXR GI' (X-RAY SYSTEM)           16-07-91 09:01:54
-------------------------------------------------------------------

                SCALE FACTOR RUN SUMMARY REPORT
                -------------------------------

      NUMBER OF SURFACES          :  2
      NUMBER OF RINGS OF RAYS     :   5
      NUMBER OF RAYS PER RING     :  10
      TOTAL NUMBER OF RAYS TRACED :  50

      NUMBER OF SUCCESSFUL RAYS   :  50
      NUMBER OF FAILED RAYS       :   0

AVERAGE SCALE FACTORS FOR 1-ARC-SEC SAGITTAL AND TANGENTIAL SCATTERING ANGLES

-------------------------------------------------------------------

 SURFACE      SAGITTAL      TANGENTIAL    SAGITTAL      TANGENTIAL
 NUMBER       (DISTANCE)    (DISTANCE)    (ANGLE)       (ANGLE)

   1        2.911E-02     2.913E-02     1.000E+00     1.000E+00
   2        2.812E-02     2.813E-02     9.660E-01     9.659E-01
```

Figure 5.42 SUSEQ Printout for DOCXR System

The final numbers displayed show the average values of the sagittal and the tangential scale factors, surface by surface. These average values are presented in terms of both distance and angle. The angle refers to the object space field angle that corresponds to a focal plane displacement. Thus some knowledge of the plate scale of the system is required. This is done by setting the angle scale factors equal to one for the first surface, and scaling the following surfaces' average values accordingly. This makes sense, since a ray scattered by one arc-second at the first surface should suffer a focal plane displacement equal to that of an unscattered ray that entered the system at a field angle of one arc-second. Note that the average scale factors listed here are for scatter angles of one arc second, while the scale factors in the SCAL file refer to scatter angles in radians.

Table 5.17 shows the format of a SCAL scale factor file, and Figure 5.43 shows the SCAL file produced by this run of SUSEQ. The SCAL file will not be detailed here, since it is intended to be used by DEDRIQ, rather than by the user.

```
 + +ID LINE FROM FILE 'DOCXR GI' (X-RAY SYSTEM)          16-07-91 09:32:28
 + +ID LINE FROM FILE 'DOCXR GI' (X-RAY SYSTEM)          16-07-91 09:01:54

  2  -3   5  10  2.100970E+02  3.744705E+02 -1.000000E+00 6.42000000D+03
      1       1       1       2 41272276
-1.09274E-01 6.00381E+03 6.00753E+03 1.08371E-01 8.73653E-03
-2.08884E-04 5.99318E+03 -5.99685E+03 -1.42617E-04 8.76973E-03
      2       2       1       2 41103253
-9.78756E-02 6.00380E+03 6.00782E+03 9.09368E-02 8.69966E-03
-1.68810E-03 5.89343E+03 -5.89708E+03 -1.63343E-03 8.88063E-03
      3       3       1       2 40934673
to
     49       4      10       2 40779722
3.52885E+03 4.85711E+03 4.86014E+03 -3.53106E+03 8.63345E-03
3.35184E+03 4.61341E+03 -4.61631E+03 3.35394E+03 9.08826E-03
     50       5      10       2 40611994
3.52889E+03 4.85710E+03 4.86015E+03 -3.53110E+03 8.59796E-03
3.29863E+03 4.54018E+03 -4.54306E+03 3.30072E+03 9.19689E-03
    -50       0      50       0      50
0.000000000000D+00 0.000000000000D+00
```

Figure 5.43 SCAL File for DOCXR System

Table 5.17
SCAL File Format

Header Record Group (3 Cards)	
	Same format as for a RAY file (see Tables 5.10(a) and 5.7(b), except KURF = surface # = -3.
Data Record Group for Each Ray (1 or 4 Cards)	
Card 1	Same format as Card 1 of focal plane RAY file Data Record Group (see Table 5.10(b)).
	(The remaining cards are omitted whenever KODE .GT. 4, *i.e.*, when the ray fails.)
	For each optical surface
	Card 1: (x,y) components of sagittal scale factor and tangential scale factor, and sine of grazing angle at ray-surface intersection. Format (1P5E13.5)
	For each optical surface between current surface and focal plane (but only if X-ray system)
	Cards 1,...: Sagittal and tangential copmonents of (change in sine or grazing angle) scale factor, packed three pairs (*i.e.*, three intervening surfaces) per card. Format 1P6E13.5
Trailer Record Group (2 or 5 Cards)	
	Same format as Cards 1 and 2 of focal plane RAY file Trailer Record Group (see Table 5.10(c)).

5.5 DEDRIQ

5.5.1 Introduction

The purpose of DEDRIQ is to determine an angular scatter profile at each ray-surface intersection point, multiply that profile by the appropriate scale factors found by SUSEQ, and thereby arrive at a distribution of energy at the focal plane. Information about this distribution is provided in the form of a pixel array focal plane file (FPSCA file) and an attenuated specular ray file (ARAY file) that duplicates the focal plane RAY file already produced by NABRAT or DRAT, but shows the attenuation in ray intensity due to the diffuse scatter at the various surfaces. The angular scatter profile at each ray-surface intersection is defined in terms of a surface roughness characterization that the user has specified for each section of each surface, and in terms of the user-specified wavelength of the incoming rays. (See Section 4.8 for a further discussion of how the user specifies surface roughness characteristics over different areas of the surfaces.) The subroutine structure of DEDRIQ is shown in Figure 5.44.

5.5.2 Method

DEDRIQ uses an adaptation of the scalar scattering theory contained in Beckmann's and Spizzichino's book, *The Scattering of Electromagnetic Waves from Rough Surfaces*, in order to define the angular scattering profile at a ray-surface intersection in terms of the roughness characteristics at that point on the surface. Using the scale factors found by SUSEQ, DEDRIQ relates focal plane pixel position to scatter angle at each ray-surface intersection. The energy contained in each pixel is thus found as a sum of contributions from each ray-surface intersection found by NABRAT or DRAT.

Two qualitatively different surface roughness descriptions are treated by Beckmann's analysis and by DEDRIQ: a statistical description that uses surface height autocovariance functions or power spectral densities, and a periodic description that treats the surface as a one-dimensional or two-dimensional grating. Each method is outlined separately below.

Sections 5.5.2.1 and 5.5.2.2 describe the implementation of the approximated scatter theory (wavelength of the radiation $\prec \prec$ surface roughness) and large amplitude scatter theory (no limitation in the wavelength), respectively. Section 5.5.2.2 reviews the scatter theory of periodic surface errors.

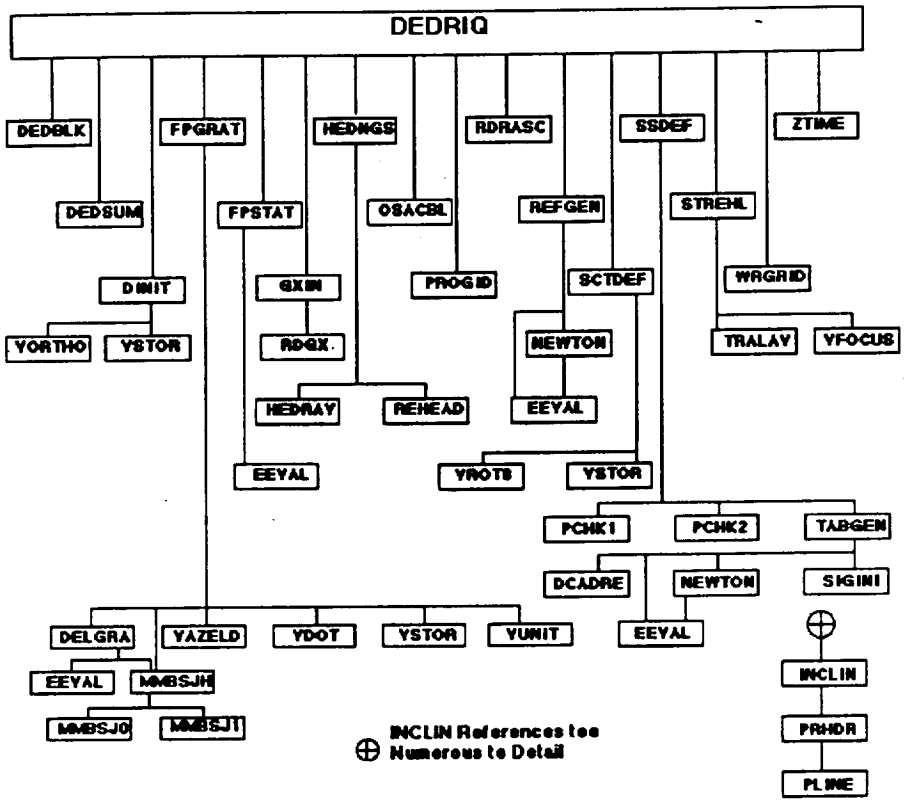

Figure 5.44 DEDRIQ External Reference Tree

5.5.2.1 Statistical Surface Roughness Description

The statistical scalar theory developed by Beckmann can be phrased in terms of the well known Bi-directional Reflectance Distribution Function (BRDF), defined by

$$BRDF(\theta_1,\theta_2,\theta_3) = \frac{dP}{P_{IN} d\Omega \cos\theta_2} \qquad (5\text{-}35)$$

where dP is the power scattered into an elemental solid angle $d\Omega$, P_{IN} is the total incident power, and the incidence angle θ_1 and the scatter angles θ_2 and θ_3 are defined in Figure 5.45.

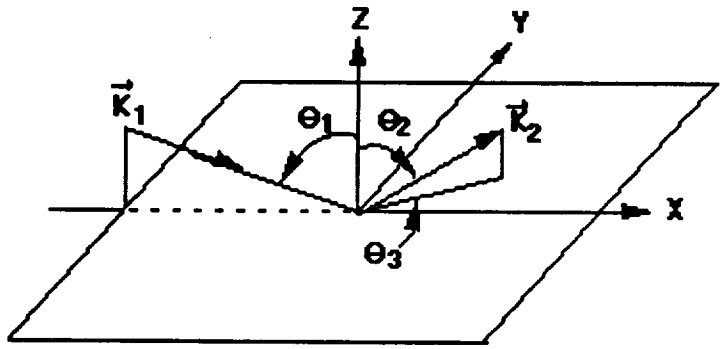

$$\vec{k}_1 - \vec{k}_2 = \vec{v}$$

$$\vec{v} = 2\pi/\lambda\{[\sin\theta_1 - \sin\theta_2\cos\theta_3]\,\hat{e}_x - \sin\theta_2\sin\theta_3\hat{e}_y - (\cos\theta_1 + \cos\theta_2)\,\hat{e}_z\}$$

$$= v_x\hat{e}_x + v_y\hat{e}_y + v_z\hat{e}_z$$

$\hat{e}_x\,\hat{e}_y\,\hat{e}_z$ are unit triad vectors

Figure 5.45 Geometry for DEDRIQ Module

Also defined there is the vector $\vec{v}=\vec{K}_1$, where $\vec{k}_1$ and $\vec{k}_2$, are the reflected and incident wave vectors, respectively. Beckmann essentially shows that the BRDF can be approximated as

$$BRDF \approx \frac{\langle R^2\rangle F^2}{\lambda^2\cos\theta_1\cos\theta_2} \iint_{surface} d^2\vec{r}\; e^{i\vec{v}\cdot\vec{r}} \left[X_2(v_z;-v_z) - |X(v_z)|^2\right] \qquad (5\text{-}36)$$

where

$$F = \frac{1 + \cos\theta_1 \cos\theta_2 - \sin\theta_1 \sin\theta_2 \cos\theta_3}{\cos\theta_1 + \cos\theta_2} \tag{5-37}$$

X and X_2 are the characteristic functions defined by

$$X(v_z) = \langle e^{iv_z z(\vec{r})} \rangle \tag{5-38}$$

and

$$X_2(v_z; -v_z) = \langle e^{iv_z(z(\vec{r}) - z(\vec{r}'))} \rangle \tag{5-39}$$

and $<R^2>$ is the average reflectance of the surface. (Throughout, the $< >$ notation denotes expectation value over the surface.) If it is assumed that the surface height obeys Gaussian probability distribution, then X and X_2 can be written as

$$X(v_z) = e^{-\frac{1}{2}\sigma^2 v_z^2} \tag{5-40}$$

and

$$X_2(v_z; -v_z) = e^{-v_z^2(\sigma^2 - g(\vec{r}))} \tag{5-41}$$

where g(r) is the surface height autocovariance function, and σ^2 is the mean surface roughness. If it is further assumed that $v_z^2\sigma^2 << 1$, then X and X_2 can be written as the first two terms of their respective Taylor series, yielding after some algebra

$$BRDF \approx \frac{\langle R^2 \rangle k^4}{4\pi^2} \frac{(1 + \cos\theta_1 \cos\theta_2 - \sin\theta_1 \sin\theta_2 \cos\theta_3)^2}{\cos\theta_1 \cos\theta_2} G(v) \tag{5-42}$$

where $G(\vec{v})$ is the Fourier Transform of $g(\vec{r})$

$$G(\vec{v}) = \int\int d^2\vec{r}\, e^{i\vec{v}\cdot\vec{r}}\, g(\vec{r}) \,. \tag{5-43}$$

If g(r) is radially symmetric, as assumed by DEDRIQ, then $G(\vec{v})$ can be written as a Hankel transform, so that

Note: v, the argument of G(v), is expressed in units of radian/distance. The normalization of

$$G(v) = 2\pi \int_0^\infty dr\ r\ g(r) J_o(vr) \qquad (5\text{-}44)$$

Note: v, the argument of G(v), is expressed in units of radian/distance. The normalization of G(v) is such that

$$\iint d^2\vec{v}\ G(v) = 4\pi^2\ g(0) = 4\pi^2\sigma^2\ . \qquad (5\text{-}45)$$

A more conventional power spectral density function can be defined, with the normalization

$$\iint d^2\vec{f} PSD(f) = g(0) = \sigma^2 \qquad (5\text{-}46)$$

where f, the argument of PSD(f) is in units of cycles/distance. The relation between G(v) and PSD(f) is then

$$PSD(f) = G(2\pi f) \qquad (5\text{-}47)$$

The user input for defining the scatter, then, is either g(r) as an analytical function, or G(v) as a piecewise-defined power function. See Section 5.5.3 for a list and discussion of available definitions for g(r) and G(v).

The above expression for the BRDF can now be combined with the relation

$$\Delta P = (\Delta\Omega)(P_{IN})(BRDF)\cos\theta_2 \qquad (5\text{-}48)$$

to yield

$$\Delta P \approx \frac{(\Delta\Omega)P_{IN}k^4}{4\pi^2\cos\theta_1} \langle R^2\rangle\ (1+\cos\theta_1\cos\theta_2-\sin\theta_1\sin\theta_2\cos\theta_3)^2\ G(v)\ , \qquad (5\text{-}49)$$

where ΔP is now the energy scattered into a pixel that subtends a solid angle $\Delta\Omega$ when viewed from the scattering surface through the rest of the optical system. The pixel appears to be located at angular position (θ_2, θ_3). The incoming ray is located at angular position θ_1, has a wavenumber $k = 2\pi/\lambda$, and has an intensity (or ray weight) of $W = P_{IN}$.

The method used by DEDRIQ in evaluating the above equation is to break it into separate terms using a different method to evaluate each term. This philosophy was chosen to minimize the program execution time, which could otherwise become prohibitive for an optical system with several surfaces, many rays, and a focal plane array with many pixels. The terms are defined as follows:

$$Term_1 = \frac{(\Delta\Omega)k^4}{4\pi^2\cos\theta_1} \tag{5-50}$$

$$Term_2 = P_{IN}\langle R^2\rangle \tag{5-51}$$

($<R^2>$ now assumed to mean the product of $<R^2>$ at the current surface times $<R^2>$ at each subsequent surface.)

$$Term_3 = (\ 1+\cos\theta_1\cos\theta_2-\sin\theta_1\sin\theta_2\cos\theta_3\ )^2 \tag{5-52}$$

$$Term_4 = G\ (v) \tag{5-53}$$

The basic calculation loop is represented by the following diagram:

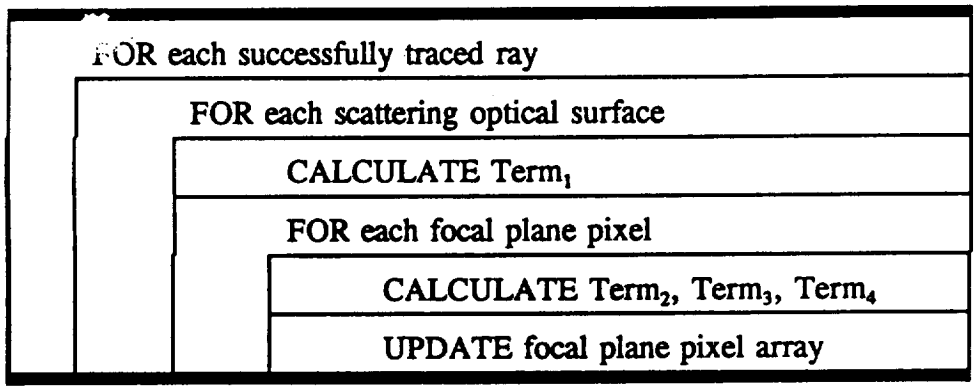

Thus $Term_1$, which is constant with respect to scattering angle is calculated only once per ray per surface. It is easily calculated in terms of the system wavelength and in terms of the SUSEQ scale factors at the given ray-surface intersection. If the system is a conventional (non-x-ray) system, or if the default values of the surface dielectric constant (implying perfect reflectance regardless of incidence angle) are used, then $Term_2$ is evaluated simply as the specular ray weight at the focal plane. Otherwise, grazing angles are calculated at all subsequent surfaces for the pixel in question, and the corresponding reflectivities are found in a look-up table. $Term_3$ is calculated separately for the pixel in question. The argument of $Term_4$ is calculated for the pixel in question, and then $Term_4$ itself is found in a look-up table. This use of look-up tables rather than repeated calculations saves on execution time. Another time saver is the fact that $Term_3$ as well as the arguments of $Term_2$ and $Term_4$ are calculated as linear or quadratic functions of the pixel row and column numbers, so that very few multiplication operations are required in the software.

There is one case when additional calculations beyond those described above are required. That is when the condition $v_z^2\sigma^2 << 1$ used early in the derivation breaks down, which can happen for shallow grazing angles or very short wavelengths. In particular, when $v_z^2\sigma^2$ (using $\theta_2 = \theta_1$ and $\theta_3 = 0$) is too large, the assumption that X and X_2 can be written as the first two terms of their Taylor series is questionable. In this case, the integral

$$\iint d^2\vec{r}\; e^{i\vec{V}\cdot\vec{r}} \left(e^{-v_z^2(\sigma^2 - g(r))} - e^{-v_z^2\sigma^2} \right) \tag{5-54}$$

which had before been approximated by

$$\iint d^2\vec{r}\; e^{i\vec{V}\cdot\vec{r}}\, g(r) v_z^2 \tag{5-55}$$

is now approximated by the more complicated expression

$$\iint d^2\vec{r}\; e^{i\vec{V}\cdot\vec{r}}\; C \left(1 - \frac{e^{-v_z^2\sigma^2}}{\sigma^2} \right) g(r) \tag{5-56}$$

where the constant C is chosen so that the approximation inside the integral is exact at the maximum of the function (r*g(r)). This criterion was chosen so that the integrand could be most accurate at the point where it contributed most to the entire integral.

Evaluation of the constant C thus requires knowing both the maximum of the function (r*g(r)), and the mean square roughness σ^2. These quantities are evaluated for each autocovariance function roughness definition prior to any scatter calculations. (Note: If the roughness is specified by a power spectral density function rather than by an autocovariance function, then (r*g(r)) cannot be analytically maximized, and this entire approximation scheme is bypassed. If $v_z^2\sigma^2$ is found to be too large, and if the roughness was specified with a power spectral density function, then a diagnostic error message is printed, and the original Taylor series approximation is used.) (r*g(r)) is maximized and σ^2 is calculated separately for each term in a given autocovariance function definition. Thus the original $Term_3$ described above is replaced by a more complicated expression (evaluated using an "auxiliary look-up table that has one term for each term in the autocovariance function definition. And, the original $Term_4$ is now replaced by a sum of similar terms, again one for each term in the autocovariance definition, each for it in its own look up table. The calculations, therefore, take more time when $v_z^2\sigma^2$ is too large. Figure 5.46 illustrates the accuracy of this approximation scheme compared to the original Taylor series approximation.

The final calculation of DEDRIQ is to calculate the attenuation of the specular ray due to the loss of the scattered energy. The attenuation factor at the ray-surface intersection is referred to here as the "Strehl factor," and is calculated as

$$STREHL = e^{-v_z^2\sigma^2}, \tag{5-57}$$

where v_z^2 is calculated at the specular ray, and is given by $v_z^2 = 4k^2\cos^2\theta_1$.

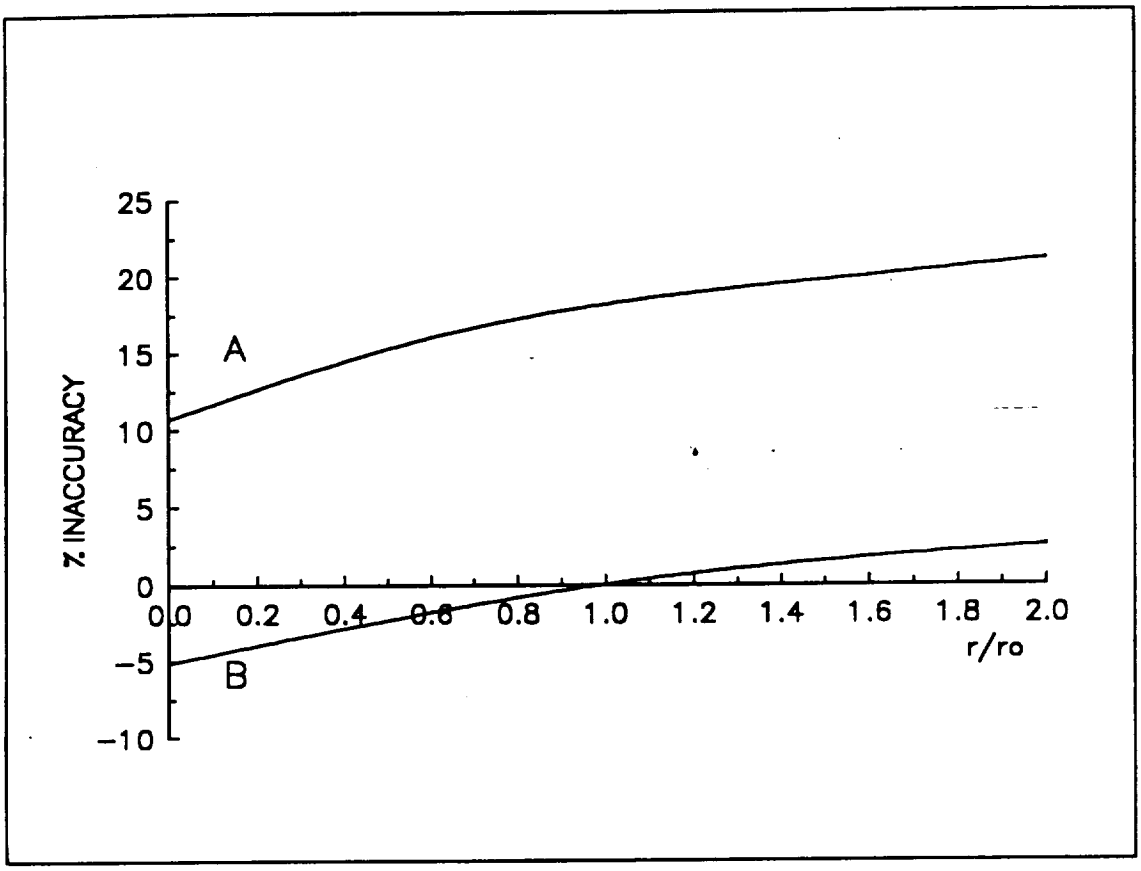

Graph showing the accuracies of the Taylor series approximation and of the improved algorithm, using
$g(r) = \sigma^2 \exp(-r/r_0)$, and $v_z^2\sigma^2 = .20$.
For both curves, the x axis is (r/r_0), and represents the argument of the integrand for both the Taylor series apprximation and the improvement algorithm. (Note that $r*g(r)$ Is maximized at $(r/r_0) = 1.0$, at which point in the integral, the improvement algorithm is exact.)
Curve A shows the % inaccuracy in approximating the function $r(\exp(-v_z^2(\sigma^2-g(r))-\exp(-v_z^2))$ with the function $r(v_z^2 g(r))$ ("Taylor series approxitation").
Curve B shows the % inaccuracy in using the improved approximation $rC((1-\exp(-v_z^2\sigma^2))/\sigma^2)g(r)$, with the constant C chosen to give no error at $r=r_0$, where $r*g(r)$ is maximized ("improved algorithm).

Figure 5.46 Accuracy of DEDRIQ Taylor Series Improvement Algorithm.

5.5.2.2 Periodic Surface Roughness Description

The scalar theory developed by Beckmann for periodic surface profiles expresses the reflected field amplitude directly in terms of the surface profile and the incidence and reflection angles. Figure 4.16 shows a sinusoidal grating periodic in two directions. For a profile defined by

$$z(x,y) = A_x \cos\left(\frac{2\pi x}{L_x}\right) + A_y \cos\left(\frac{2\pi y}{L_y}\right) , \tag{5-58}$$

Beckmann shows that the field amplitude is

$$E = W_x W_y F_3 \frac{1}{4\pi^2} \int_0^{2\pi} dx' e^{ix'P_x} e^{iv_z A_x \cos x'} \int_0^{2\pi} dy' e^{iy'P_y} e^{iv_z A_y \cos y'} \tag{5-59}$$

where

$$W_{xy} = e^{iP_{xy}\pi} \frac{\sin(2n_{xy}P_{xy}\pi)}{2n_{xy}\sin(P_{xy}\pi)} \tag{5-60}$$

and

$$P_{xy} = \frac{L_{xy}}{2\pi} v_{xy} . \tag{5-61}$$

The quantities v_x, v_y, and v_z are the same as defined in Figure 5.45 The quantities $(2n_x)$ and $(2n_y)$ are the number of identical surface elements in the x- and y- directions, and will eventually be allowed to tend to infinity. F_3 is related to the F factor in the previous section by the expression $F_3 = F/\cos\theta_1$. The above expression for E, when squared, yields the lobe intensity structure produced by the grating. At the peaks of the lobes, Beckmann shows that

$$|E^2| \propto |W_x^2 W_y^2| \; F_3^2 [J_{Px}(s_x) J_{Py}(s_y)]^2 , \tag{5-62}$$

where P_x and P_y are the orders of the corresponding J Bessel functions, and s_x and s_y are defined by $s_{x,y} = kA_{x,y}(\cos\theta_1 + \cos\theta_2)$. Note that the lobe peaks correspond to the values of P_x and P_y that maximize $W_{x,y}$, i.e., P_x and P_y integers. Thus the field at the lobe peaks can be written in terms of Bessel functions of integer order. (The proportionality sign in the above equation will now be used to make calculations easier.)

To summarize so far, the intensity profile of the reflected beam is proportional to a simple function of the scatter angles and the surface profile. By solving for P_x and P_y being

integers, the angular positions of the corresponding lobes can be found. What is needed now is an expression for the energy within a lobe. This can be found by letting n_x and n_y tend to infinity. In that case, the terms W_x and W_y are peaked arbitrarily sharply around the lobe, and the total energy

$$P_{TOT} = \int d\Omega \, |E^2(\theta_2,\theta_3)| \tag{5-63}$$

can be simplified to yield

$$P_{TOT} \propto F_3^2(\theta_1;\theta_{20},\theta_{30}) \; (J_{Pxo}(s_{xo})J_{Pyo}(s_{yo}))^2 \cdot \int d\Omega \, |W_x^2 W_y^2| \; , \tag{5-64}$$

where the subscripted zero denotes values of the variables at the lobe peak, and the integration is over solid angle in the neighborhood of the lobe. Extending the integration limits to infinity and noting that

$$d\Omega \propto \frac{1}{\cos\theta_2} d_{Px} d_{Py} \; , \tag{5-65}$$

this becomes

$$P_{TOT} \propto F_3^2(\theta_1;\theta_{20},\theta_{30}) \; (J_{Pxo}(s_{xo})J_{Pyo}(s_{yo})^2 \frac{1}{\cos\theta_{20}} \cdot \int_{-\infty}^{\infty} d_{Px} \frac{\sin^2(2n_x P_x \pi)}{4n_x^2 \sin^2(P_x \pi)} \int_{-\infty}^{\infty} d_{Py} \frac{\sin^2(2n_y P_y \pi)}{4n_y^2 \sin^2(P_x \pi)} \; , \tag{5-66}$$

or, since the integrals are constants,

$$P_{TOT} \propto \frac{F_3^2(\theta_1;\theta_{20},\theta_{30})(J_{Pxo}(s_{xo})J_{Pyo}(s_{yo}))^2}{\cos\theta_{20}} . \tag{5-67}$$

Now the actual proportionality constant can be found by noting that, for $A_x = A_y = 0$, the energy in the specular lobe must equal the energy in the incident ray, P_{IN}. This yields the result

$$P_{TOT} = P_{IN} \frac{\cos\theta_1}{\cos\theta_{20}} [F_3(\theta_1;\theta_{20},\theta_{30}) J_{Pxo}(s_{xo}) J_{Pyo}(s_{yo})]^2 \tag{5-68}$$

(All the above equations must be modified to account for the rotation of the grating coordinate system relative to the direction of the incident ray. These tedious modifications will not be dealt with here, but have been done for DEDRIQ.)

The method for modelling a periodic surface, then, is to solve the equations

$$Px(\text{rotated}) = \text{integer} \quad ; \quad Py(\text{rotated}) = \text{integer}$$

to find the angular position of the lobes. (The "rotated" subscript above refers to the orientation of the grating coordinate system relative to the incident ray.) Then, for each lobe position, the energy is P_{TOT} defined above. This energy, attenuated by (possibly variable) reflectivities at subsequent surfaces, is then added to the proper focal plane pixel. All these calculations are performed for every ray-surface intersection where a periodic roughness profile has been specified by the user.

Just as in the statistical roughness case, DEDRIQ must in the end calculate a specular ray attenuation factor. For a grating surface, this is simply P_{TOT}/P_{IN} for the specular lobe. In other words,

$$SPECHL = (J_o(s_{xo})J_o(s_{yo}))^2 . \qquad (5\text{-}69)$$

5.5.2.3 Large Amplitude Scattering Theory

In this section we define in detail the theoretical approach chosen for analyzing high amplitude scatter (i.e., where the projected surface errors are comparable to or greater than the wavelength). We discuss both the mathematical theory and the numerical approach used to solve the equations. We also briefly mention alternative theories which were considered before choosing the Beckmann theory.

5.5.2.3.1 Brief Review of Candidate Theories

We reviewed the following candidate theoretical approaches: (1) an Optical Transfer Function (OTF) approach; (2) a geometrical slope theory; and (3) the full Beckmann scattering theory. (All of the theories were considered in scalar rather than vector form. This is because OSAC is intended to analyze images within angles that are very, very small compared to a radian. In that region, the scalar theories and the vector theories give the same result.)

We rejected the OTF approach, because we found that it was incompatible with the OSAC architecture, whereby different parts of the mirror surfaces can be given different statistical errors. The OTF approach calculates an effective image degradation as a product of effects from each of the surface error spatial frequency ranges. In this approach, there is no correlation between various types of errors. In particular, there is no convenient way to

specify different types of mid frequency surface errors on different zones of a mirror, which is one of the fundamental capabilities of OSAC. (Actually, the approach we chose has much in common with the OTF approach, in that it characterizes surfaces in terms of the Fourier transform of the scatter they induce. However, we kept the fundamental OSAC features of calculating ray-by-ray, and separating the specular ray from the scattered halo.)

We also rejected the geometrical slope theory, because we found that it was accurate only at such high surface error amplitudes that we could implement no satisfactory bridging between the slope theory and the small amplitude Beckmann scattering theory currently being used.

We chose the full Beckmann theory, since we found no insurmountable problems in its implementation.

5.5.2.3.2 Analytical Definition of the Beckmann Approach

In this section, we define the analytical approach used in the large amplitude scatter implementation.

5.5.2.3.2.1 Scatter from a Single Surface

In the full Beckmann scattering theory, as shown in Section 5.5.2.1, the scattering profile is defined in terms of a two dimensional Fourier transform of a function which depends on the surface autocovariance function.

$$BRDF \approx (\langle R^2 \rangle F^2 / (\lambda^2 \cos\theta_1 \cos\theta_2)) \; x$$
$$\iint_{surface} d^2r \; e^{iv.r} \; [\exp\{-v_z^2(\sigma^2 - g(r))\} - \exp\{-v_z^2\sigma^2\}] \qquad (5\text{-}70)$$

where BRDF = Bi-directional Reflectance Distribution Function of the scatter (i.e., specular ray not included)

$\langle R_2 \rangle$ = average reflectance

F = $(1 + \cos\theta_1 \cos\theta_2 - \sin\theta_2 - \sin\theta_2 \cos\theta_3) / (\cos\theta_1 + \cos\theta_2)$

θ_1 = incidence angle (positive, measured from the normal)

θ_2 = scatter elevation angle (positive, from the normal)

θ_3 = scatter azimuth angle

v = $k_{incident} \; K_{scattered}$

$k_{incident}$ = $(2\pi/\text{lambda})$ x (incident direction unit vector)

$k_{scattered}$ = $(2\pi/\text{lambda})$ x (scattered unit vector)

(x,y,z) = surface coordinate system (see Figure 5.45) with r_2 = (x,y)

σ^2 = mean square surface error

g(r) = surface autocovariance function for shift r, normalized to be σ^2 at the origin

The three terms in Equation (5-72) can easily be thought of as three physical processes: (1) scatter of the incident specular ray; (2) reflection of the incident scatter halo; and (3) scatter of the incident scatter halo. It is the third process, scatter of scatter, that was not accounted for in the small amplitude implementation. The Fourier transform approach makes it simple to define the scatter recursively in terms of the scatter at the previous surface, without having to use the convolution operation that would be present if we were not working in the Fourier transform domain. (As alluded to in Section 5.5.2.3.1, this approach has much in common with the OTF approach, in that it characterizes surfaces in terms of the Fourier transform of the scatter they induce. Again, however, we kept the fundamental OSAC features of calculating ray-by-ray, and separating the specular ray from the scattered halo as shown in Equation (5-72).)

5.5.2.4 Large Amplitude Scattering Implementation

In implementing the large amplitude scattering theory, we used the recursive approach summarized in Equation (5-72), whereby we first calculate the Fourier transform of the scatter at each successive surface, and finally use Fast Fourier Transform (FFT) techniques to transform the function at the final surface to get the resulting focal plane distribution. Because the surface autocovariance functions can have a tremendous dynamic range of important spatial frequencies, we used new, innovative techniques to perform the FFT's. Below we discuss several aspects of the modified FFT technique and of Fourier transform techniques in general. We also discuss the operational considerations for running the modified OSAC code, including a description of how the program transitions between the small and the large amplitude theories.

5.5.2.4.1 Modified FFT Techniques

The general idea of the Fourier transform approach is to derive the transform of the scatter via Equations (5-70) and (5-72), and then perform a final Fast Fourier Transform (FFT) to get the focal plane distribution.

It is straightforward but tedious to derive the transform of the scatter in terms of a usable coordinate system. The results involve scale factors which are already defined by the OSAC module SUSEQ. Once the scatter transform is so written, however, the problem remains that the function has a tremendous range of spatial frequencies of interest. This is caused by two factors. First, at least for X-ray systems, the grazing angle causes the surface errors to be foreshortened in the tangential direction. Thus, the spatial frequency range is automatically expanded by the inverse of the sine of the grazing angle. This factor can be as high as perhaps 100. The second factor is that the user often wishes to define a set of surface errors which may themselves cover a spatial frequency range of a factor of 100 or more. Put together, these factors imply that important spatial frequencies can exist on the surface over a dynamic range of 10,000 or more. Trying to transform such a function directly using the limited resolution of FFT routines can lead to large inaccuracies.

(As discussed later, even though we refer to the function in Equation 1 as a Fourier transform, a slight approximation is required to make the integral a true Fourier transform.) In the small amplitude implementation of this theory, (see Section 5.5.2.1) when the projected rms surface error is much smaller than a wavelength (i.e., when $v_z^2\sigma^2$ is much smaller than unity), Equation (5-70) can be approximated as

$$BRDF \approx (<R^2> F^2 / (\lambda^2 \cos\theta_1 \cos\theta_2)) \iint_{surface} d^2\vec{r}\, e^{i\vec{v}\cdot\vec{r}}\, v_z^2\sigma^2 g(r) \qquad (5\text{-}71)$$

In the small amplitude implementation of Section 5.5.2.1, the Fourier transform implied in Equation (5-71) was known analytically, and was evaluated via a table lookup to determine the scatter quickly over the focal plane.

Simply put, the current large amplitude theory involves using Equation 5-70 rather than Equation (5-71) to determine the scatter from a single surface. In the following section we define how subsequent scattering surfaces are handled.

5.5.2.3.2.2 Scatter from Subsequent Surfaces

There is one more important approximation used in the small amplitude implementation of Section 5.5.2.1 which had to be changed. In the small amplitude implementation, it is assumed that the scatter halo from one surface would not rescatter at a later surface to give any appreciable amount of scatter. In other words, only single surface scatter is considered. (This is reasonable, since in the small amplitude limit, the scattered energy from any one surface is small, and two surface scatter would involve the square of this small proportion of scatter.)

To evaluate multiple surface scatter correctly, we worked in the Fourier transform domain of the scatter. In particular, we noted that the Fourier transform of the BRDF after a given surface could be easily written in terms of the Fourier transform of the BRDF incident on the surface, as follows:

$$FT(BRDF)_i = W_{i-1} FT(BRDF)_{0i} + [<R^2> Strehl] \times [FT(BRDF)_{i-1}] + [FT(BRDF)_{i-1}] \times [FT(BRDF)_{0i}] \qquad (5\text{-}72)$$

where $FT(BRDF)_i$ = Fourier transform of the BRDF after this surface
W_{i-1} = weight (or intensity) of the incident specular ray
$FT(BRDF)_{0i}$ = Fourier transform of the BRDF that would arise from this surface alone (see Equation 5-70)
Strehl = conventional Strehl ratio = $\exp\{-v_z^2\sigma^2\}$
$FT(BRDF)_{i-1}$ = Fourier transform of the BRDF incident on this surface

We solved the problem by applying a series of Gaussian-like filters to the function, thus windowing it over different regions. The different regions are dominated by different spatial frequencies. Therefore, we transformed each region separately using the optimum sample size for that region. We then summed and interpolated the results onto the focal plane pixel array specified by the user.

The form of a set of M filters as used in the software is given below:

$$F_1 = H_1 \tag{5-73}$$

$$F_2 = (1 - H_1)\, H_2 \tag{5-74}$$

$$F_3 = (1 - H_1)\ \ (1 - H_2)\, H_3 \tag{5-75}$$

...

$$F_{M-1} = (1-H_1)(1-H_2)\cdots(1-H_{M-2})H_{M-1} \tag{5-76}$$

$$F_M = (1-H_1)(1-H_2)\cdots(1-H_{M-2})(1-H_{M-1}) \tag{5-77}$$

where $H_1 = \exp(-r^2 / r_i^2)$

It can be shown that the sum of filters is unity - in other words, the function multiplied by the sum of the filters gives the original functions.)

The set of radii $\{r_i\}$ determine the exact nature of the filters. We used a set of $\{r_i\}$ which increased by a constant ratio for each succeeding radius. The user may refer to the software listings to learn about the selection of the optimum first radius r_1, the ratio between succeeding r_i's, and the optimum FFT sampling interval, all of which we determined empirically.

5.5.2.4.2 Imposed Limitations

As can be seen by examining Equation (5-70), there is one approximation that is required to allow the definition of scatter in terms of a Fourier transform -- the scatter angles must be small in comparison with the grazing angle. However, this is true in any real system of interest. For example, assuming a very small grazing angle of 0.5 degrees for an X-ray system, we could analyze scatter angles equal to one percent of the grazing angle, giving an image diameter of 36 arc seconds, which is already very large compared to most scatter patterns of interest for such a system.

Another limitation imposed by the chosen approach is that the surface autocovariance function, g(r), must be known and must be transformable using Fast Fourier Transform (FFT) techniques. This eliminates autocovariance functions which diverge at the origin. Some such autocovariance functions are allowed in OSAC. They have analytically reasonable transforms. However, there are enough problems with numerically finding their transform so that we do not use the full large amplitude scattering theory to analyze errors defined with divergent autocovariance functions. However, such errors are still analyzed with the "non-Taylor" approach used in the previous version. This approach allowed the analysis of projected errors up to a reasonable fraction of a wave with improved accuracy, but did not give good results for projected errors comparable to or larger than a wave.

The previous "non-Taylor" approach discussed in Section 5.5.2.1 is not used for errors defined with piecewise power law falloff power spectral density functions. Such errors are also not analyzed with the new large amplitude theory.

Finally, errors defined as gratings are not implemented in the large amplitude theory. However, such errors were already dealt with in a general way so that large amplitudes were allowed.

This version of OSAC does not use the full large amplitude theory for any ray where any intervening surface uses the power spectral density or grating definition. For example, assume the first mirror in a two mirror system uses a grating error and the second mirror uses a non divergent autocovariance function. If the non divergent autocovariance function were the only error defined, the full large amplitude scatter theory could be used. However, since the ray strikes a grating error on the first surface, it is not considered for the full large amplitude theory.

5.5.2.4.3 Transition from Small to Large Amplitude Theory

In Section 5.5.2.4.2 we discussed general limitations on when the large amplitude theory can be used. These considerations define the general method OSAC uses to choose the appropriate theory. The only additional piece of information used is value of the single parameter

$$\nu_z^2\sigma^2 = (2\ \pi\ \sigma\ (\cos\theta_1 + \cos\theta_2)\ /\ \lambda)^2 \qquad (5\text{-}78)$$

or, using the approximation that the scatter angle is much smaller than the grazing angle (which implies that $\theta_2 \approx \theta_1$),

$$\nu_z^2\sigma^2 \approx (4\ \pi\ \sigma\ \cos\theta_1\ /\ \lambda)^2 \qquad (5\text{-}79)$$

This single parameter is used to define the transition from the Taylor approach to the non-Taylor approach. In particular, when $v_z^2\sigma^2$ became greater than 0.01, the non-Taylor approach is used to increase the accuracy.

OSAC uses the full large amplitude theory when $v_z^2\sigma^2$ becomes greater than 0.20, but only when allowed by the limitations which we discussed in Section 5.5.2.4.2. Figure 5.47 summarizes the decision process used by OSAC to select the appropriate scattering theory.

For each traced ray:

Does the ray

(1) not strike any surface with errors defined by a divergent autocovariance function, grating, or piecewise log-log power spectral density

and (2) give rise to a value of $v_z^2\sigma^2 > 0.20$ on at least one surface

YES
(both conditions satisfied)

Use the full large amplitude theory for all of the surfaces along the ray's path

NO
(at least one condition not satisfied)

For each surface intersected by the ray:

CASES:

(a) [(1) the errors are defined as any autocovariance function, AND
(2) $v_z^2\sigma^2 > 0.01$]:
Use the non-Taylor theory.

(b) [the errors are defined as a grating]:
Use the grating theory.

(c) [OTHERWISE]:
Use the Taylor theory.

Required Parameter Value at Each Surface:
$v_z^2\sigma^2 \approx (4\ \pi\ \sigma\ \cos\theta_1\ /\ \text{lambda})^2$

Available Theories
(1) "grating" (the original grating theory)
(2) "Taylor" (the original small amplitude statistical theory)
(2) "non-Taylor" (the original way of extending the small amplitude statistical theory to slightly higher values of $v^2_z\sigma^2$)
(3) "Large Amplitude" (the full large amplitude statistical theory, usable for arbitrary values of $v^2_z\sigma^2$)

Figure 5.47 Dynamic decision process used by OSAC to select the approriate scattering theory

5.5.2.4.4 Operational Considerations

The implementation of the full large amplitude scattering theory requires no changes in operator input or procedures. After running GEOSAC and DRAT to ray trace the system, the user must still run SUSEQ to define the necessary scale factors, and then DEDRIQ to calculate the actual scatter distribution. In this section we discuss some general factors to keep in mind when analyzing scatter.

5.5.2.4.4.1 Surface Error Amplitude

There are two pieces of information which the user should be able to derive which make the running and interpretation of the program much more reliable. The first useful piece of information is a typical value of the quantity $v_z^2\sigma^2$ as defined in Equation (5-70). This parameter alone determines which scattering theory the program will use, as discussed in Section 5.5.2.4.3. $v_z^2\sigma^2$ is proportional to the square of the surface error, and inversely proportional to the square of the wavelength. A value of $v_z^2\sigma^2 = 0.223$, e.g., corresponds to the classical diffraction limit defined by a Strehl ratio of 0.80. If $v_z^2\sigma^2$ is never larger than 0.20, the full large amplitude theory will not be used, and the results of SUSEQ and DEDRIQ are reliable and are essentially the same as in the small amplitude theory discussed in Section 5.5.2.1. If $v_z^2\sigma^2$ is larger than 0.20, however, the small amplitude theory quickly becomes very inaccurate, and the full large amplitude theory provides the only believable results. There is no inherent limit to how large $v_z^2\sigma^2$ can be made in the full large amplitude implementation. (See Section 5.5.2.4.3, however, for a discussion of limitations on when the full large amplitude theory can be used.)

5.5.2.4.4.2 Size of the Scatter Pattern

The second useful piece of information is a typical distance in the focal plane over which the scatter shows noticeable variation. For errors with period L on a primary mirror being illuminated at normal incidence, the grating equation can be used to show that light is scattered (diffracted) by a focal plane distance of

$$D_{fp} = EFL\ \lambda\ /\ L \qquad (5\text{-}80)$$

where D_{fp} = scatter distance, and
EFL = Effective Focal Length

If the primary mirror is illuminated at an angle of incidence θ_1 as shown in Figure 5-45, then Equation (5-80) holds only for the scatter out of the plane containing the incident and reflected ray, which we call sagittal scatter. The scatter in the tangential plane is broadened by a factor of $(1 / \cos\theta_1)$. Thus the scatter pattern will be very noticeably lengthened in one direction if one is analyzing an extreme ultraviolet or X-ray system.

For errors on a secondary mirror, the pattern discussed above is shrunk by the magnification factor of the secondary mirror. Thus, primary mirror scatter often dominates.

A handy rule of thumb to keep in mind is that, when specifying a surface with an autocovariance function with correlation length R_c, a typical spatial period is on the order of (5 R_c). (The correlation length is the distance at which the autocovariance function drops to 1/e of its maximum value, and is easily expressed in terms of the OSAC defining parameters for at least the exponential and Gaussian autocovariance functions.)

A final rule to keep in mind is that the scatter pattern dimensions discussed above apply only in the smooth surface limit (i.e., when the quantity $v_z^2\sigma^2$ is small). When $v_z^2\sigma^2$ becomes larger, it can be semi-rigorously shown (for at least some autocovariance functions of interest) that the scatter pattern expands by a factor on the order of $v_z^2\sigma^2$ for large $v_z^2\sigma^2$.

These rules are intended to give the user an idea of what size of focal plane and what size of pixels to specify. This is a very important choice, since pixels that are too small will not show a useful portion of the image, while pixels that are too large will give inaccurate results since the scatter in reality varies considerably within a pixel.

5.5.2.4.4.3 Computer Run Time

DEDRIQ run time is much larger for the full large amplitude theory than for the small amplitude theories. Thus, when $v_z^2\sigma^2$ is larger than 0.20, one can expect substantial run times. For example, the parameters used as examples here led to run times of approximately 2-3 minutes per ray when the computer was not busy.

This leads to a recommendation on how to select the optimum parameters. Note that for the example here we used only two rays. From an encircled energy standpoint, this is enough to determine the entire pattern (unless there are very large variations in grazing angle across the mirror). Thus, it is often sufficient to trace only a very few rays to see the effects of a measured or postulated set of statistical surface errors. The effects of low frequency polynomial errors can be determined separately and quickly in a ray trace using hundreds of rays. Thus, it is often only in the final stages of fabricating a system, when one must model the as-built surface errors across the entire spatial frequency range, that very long run times need be tolerated.

5.5.3 Inputs and Outputs

The input to DEDRIQ consists of a system definition GX file created by GEOSAC, all the RAY files created by either NABRAT or DRAT, the scale factor SCAL file created by SUSEQ, and a user-created file that defines the focal plane pixel array and the surface roughness parameters (SCAT file). The output consists of terminal and printer output, a focal plane pixel array file (FPSCA file), and an attenuated specular RAY file (ARAY file).

The names, types, formats and file numbers of all DEDRIQ files are summarized in Table 5.18.

Table 5.18
Files Used by DEDRIQ

Input/ Output	File Name	File Type	Format	Logical Record Length	Block Size	File Number
Input	name1	GX	FB	80	800	1
Input	name1	SCAL	FB	80	800	2
Input	name2	SCAT	FB	80	800	3
Input	name1	RAY001	FB	80	800	9
Input	name1	RAY002	FB	80	800	10
etc.[1]						
Output	name2	ARAY	FB	80	800	7
Output	name2	FPSCA	VS		800	4
Output	terminal			80		6
Output	printer			132		8

[1] The total # of input RAY files is one greater than the # of surfaces in the system.

Table 5.19 shows the format of a SCAT file. The identification line, focal plane definition parameters, and system wavelength should be self-explanatory.

Table 5.19
SCAT File Format

Header Record Group (5 Cards)	
Card 1	64-character SCAT file comments
Card 2	X_{cen}, Y_{cen}, L_x, N_x, N_y (see Figure 5.52 for definitions of these parameters) (Format 4D15.0, 2I6)
Card 3	ZLAM = wavelength. Format (E15.0)
Card 4	ACCG, ACCF, ACCR = look-up table accuracy parameters. Format (3E15.0)
Card 5	NDEFS = # of roughness definitions to follow
Data Record Group for Each Roughness Definition	
Card 1	NDTHIS = # of definitions in list (1 .LE. NDTHIS .LE. NDEFS); NMETH = user method #. Format (2I6)
Following Card(s)	See Tables 5.20, 5.21 and 5.22
Data Record Group for Each Rough Surface	
Card 1	NSURF = surface # (-1 means no more surfaces to be specified). Format (I6)
Card 2	NAREAS = # of roughness regions on surface. Format (I6)
For Each Roughness Region	
Card 1:	NDEF = roughness definition # from user's list, (AMIN, AMAX, BMIN, BMAX) = coordinate limits. Format (I12, 4E12.0)

What follows next are three accuracy parameters. The first, ACCG, is the accuracy of the look-up tables for G(v). In other words, (1 + ACCG) is the ratio between successive values of G(v) in the table. For example, if the user feels that a calculation of G(v) to an accuracy of ±5% would be sufficient (yielding a ±5% uncertainty in the final scatter intensity), then the value for ACCG would be 0.10. The second number is ACF, the accuracy of the auxiliary look-up tables that are used to refine the Taylor series approximation of the scatter profile when the grazing angle is too shallow or the wavelength too short. (See Section 5.5.2.1 for an explanation of this concept.) A reasonable value for ACCF is whatever value was specified for ACCG. The third number, ACCR, is the accuracy of the reflectivity look-up table, and needs to be included in the SCAT file only if (1) the system is an x-ray system, and (2) the values for the surface complex dielectric constant in the GI file are other than the default (*i.e.*, other than unit reflectivity regardless of grazing angle).

Otherwise, no change-in-reflectivity calculations are performed and the look-up table is not required.

The next parameter in the SCAT file is NDEFS, the number of roughness definitions to follow. These definitions form a menu from which the user can choose to define the characteristics of different regions on different surfaces. The first line of each roughness definition to follow consists of two numbers: the number of the definition in the menu (1 for the first definition, 2 for the second, etc.), and the user definition number. DEDRIQ currently allows for eleven possible user definition numbers or types. Definitions 101-109 are for specifying a surface height autocovariance function, definition 201 is for specifying a surface height power spectral density function, and definition 301 is for specifying a grating (periodic) profile. The meaning of the parameters in a roughness definition are listed for each of the above types in Tables 5.20, 5.21, and 5.22. Theoretical background of gaussian-cosine ACV models are discussed in Section 5.5.4.

Table 5.20
Roughness Definition Parameters
(Auto-covariance Function Roughness Definition)

NMETH	Autocovariance Function Definition	Parameters on (1) Card
101	$g(r) = A\,K_o(Br) + C\,e^{-Dr}$	A, B, C, D
102	$g(r) = A\,e^{-Br}/\sqrt{Br} + C\,e^{-Dr}$	A, B, C, D
103	$g(r) = A\,K_o(Br) + C\,e^{-Dr} + E\,e^{-Dr}\cos Fr$	A, B, C, D, E, F
104	$g(r) = A\,e^{-Br}/\sqrt{Br} + C\,e^{-Dr} + E\,e^{-Dr}\cos Fr$	A, B, C, D, E, F
105	$g(r) = A\,e^{-Br} + C\,e^{-Dr}$	A, B, C, D
106	$g(r) = A\,e^{-Br^2}$	A, B
107	$g(r) = A\,e^{-Br}\cos Cr + D\,e^{-Er}\cos Fr$	A, B, C, D, E, F
108	$g(r) = A\,e^{-Br}\cos Cr + D\,e^{-Er2}\cos Fr$	A, B, C, D, E, F
109	$g(r) = A\,e^{-Br2}\cos Cr + D\,e^{-Er2}\cos Fr$	A, B, C, D, E, F

Table 5.21
Roughness Definition Parameters
(Power Spectral Density Function Roughness Definition)

Card 1	NSEGS = # of segments on which to define G(v) as an inverse power function. In particular, for v inside the i^{th} segment, G(v) is given by $G(v) = A_i v^{(-B_i)}$ Format (I6)
For Each Segment	
Card 1	v_o, A, B, where, for v .GT. v_o, G(v) is given by $G(v) = A\ v^{(-B)}$. Format (3E12.4) *Note*: For v. LT. v_o (defined in the first segment), G(v) is constant, so that $G(v) = A_1\ v_{o1}^{(-1)}$. Also, it is the user's responsibility that the value of G(v) agrees to within a factor of ACCG (see Table 5.19) when calculated at the end of one segment or the beginning of the following segment.

Table 5.22
Roughness Definition Parameters (Grating Roughness Definition)
(NMETH = 301)

Card 1	A, B, C, D, ϕ, NUMAX, NVMAX. (See Figure 4.16 for definitions of the parameters A, B, C, D, and ϕ.) NUMAX and NVMAX are the maximum u- and v-lobe numbers for which the user will allow the module DERIQ to perform calculations.

The final parameters in the SCAT file specify the boundaries of the areas on the optical surfaces that are to be assigned roughness characteristics from the menu just defined. (See Section 4.8 for an explanation of how the areas are defined on the surface for either conventional or x-ray systems.) As shown in Table 5.19, the boundary specification parameters are grouped by optical surface. The first two lines in a boundary specification section define the optical surface number and the number of areas that will be defined on the surface. (If a surface is not assigned any roughness areas, then it is assumed perfectly smooth so that no scattering takes place.) Each line to follow defines one area. The parameters there are the definition number from the user menu followed by the minimum and maximum (x, y) values for conventional systems or (z, Θ) values for x-ray systems. Note: If the minimum and maximum values of any coordinate are defined equal, DEDRIQ interprets this to mean that the range of the area in the corresponding coordinate is unbounded. For example, if the minimum and maximum values were equal for both coordinates, this would mean that the entire surface was to take on the given roughness

definition. The end of the SCAT file is signified by a single line with a -1 value for the surface number.

Figure 5.48 shows a SCAT file with three roughness definitions used to analyze the x-ray system defined in the DOCXR GI file. Figure 5.49 shows the resultant printout. Figure 5.5C shows the ARAY file produced. The user can note that the format of the ARAY file is the same as that of a RAY file, except that the surface number parameter in the header is set to -1, and that the global focus information at the end of the file is deleted.

```
++ ID LINE FROM FILE 'DOCXR1 SCAT' ++
0.0  0.0  2.0  2.0  20  20
6.0E-07
0.04  0.04  0.04
3
1  101
1.0E-15  1000.0  2.0E-15  10.0
2  201
1
1.0  2.0E-15  1.5
3  301
3.0E-08  1.0  4.0E-08  2.0  20.0  3  4
1
2
1  0.0  0.0  0.0  180.0
2  0.0  205.0  0.0  180.0
2
2
1  0.0  0.0  0.0  0.0
3 -205.0  0.0  0.0  0. 0
-1
```

Figure 5.48 SCAT File for DOCXR System

```
*** OPTICAL SURFACE ANALYSIS PROGRAM (DEDRIQ ) RELEASE (06.0) VAX      PAGE  1
++ ID LINE FROM FILE 'DOCXR1 SCAT' ++                    16-07-91 09:32:51
++ID LINE FROM FILE 'DOCXR GI' (X-RAY SYSTEM)            16-07-91 09:01:54
```

FPSTAT WARNING - FOR (PSD) METHOD # 2 AT SURFACE 1, VZ**2*SIGMA**2 = 0.07
TAYLOR SERIES APPROXIMATION USED IS PROBABLY INACCURATE

SCATTER SUMMARY REPORT FOR X-RAY SYSTEM

NUMBER OF SURFACES : 2
SYSTEM WAVELENGTH : 6.00000E-07
PIXEL ARRAY CENTER X COORD : 0.00000D+00
PIXEL ARRAY CENTER Y COORD : 0.00000D+00
PIXEL ARRAY X LENGTH : 2.00000D+00
PIXEL ARRAY Y LENGTH : 2.00000D+00
NUMBER OF PIXELS IN X DIRECTION : 20
NUMBER OF PIXELS IN Y DIRECTION : 20
NUMBER OF TRACED RAYS : 50
NUMBER OF SUCCESSFUL RAYS : 50
TOTAL UNATTENUATED RAY WEIGHT : 20.47280
TOTAL STREHL-REDUCED RAY WEIGHT : 20.05950
TOTAL SCATTERED RAY WEIGHT : 2.08285E-03

ACCURACY OF G(V**2) TABLES : 0.0400
IMPLIED DYNAMIC RANGE OF TABLES : 1.5241E+14
ACCURACY OF F(VZ**2*SIG**2) TABLE : 0.0400
IMPLIED DYNAMIC RANGE OF TABLE : 5.9276E+01
IMPLIED MAX OF VZ**2 * SIG**2 : 56.9045

ROUGHNESS DEFINITION INFORMATION FOR DEFINITION # 1

USER METHOD # 101 :
ACV (R) = A * K0 (B * R) + C * EXP (- D * R)
(A, B, C, D) :
1.0000E-15 1.0000E+03 2.0000E-15 1.0000E+01
SIGMA**2 FOR THE TWO PROCESSES : 9.2565E-15 2.0000E-15
TOTAL SIGMA**2 FOR DEFINITION : 1.1256E-14
IMPLIED MAX V**2 ((RAD/DIST)**2) : 2.8661E+12
IMPLIED MAX G (V**2) : 1.2311E-16
IMPLIED MIN G (V**2) : 2.4697E-26

ROUGHNESS DEFINITION INFORMATION FOR DEFINITION # 2

USER METHOD # 201 :
G (V) DEFINED ON 1 SEGMENTS BY G (V) = A * (V ** -B)
FOR SEGMENT # 1 - (V0, A, B) : 1.0000E+00 2.0000E-15 1.5000E+00
TOTAL SIGMA**2 FOR DEFINITION : 2.0597E-12

Figure 5.49 DEDRIQ Printout for DOCXR System

```
IMPLIED MAX V**2 ((RAD/DIST)**2) :     7.3014E+18
IMPLIED MAX G (V**2) :                 2.0000E-15
IMPLIED MIN G (V**2) :                 1.3947E-29

*** OPTICAL SURFACE ANALYSIS PROGRAM (DEDRIQ ) RELEASE (06.0) VAX     PAGE  2
++ ID LINE FROM FILE 'DOCXR1 SCAT' ++                    16-07-91 09:32:51
++ID LINE FROM FILE 'DOCXR GI' (X-RAY SYSTEM)            16-07-91 09:01:54
```

ROUGHNESS DEFINITION INFORMATION FOR DEFINITION # 3

```
USER METHOD # 301
Z (X, Y) = A * COS (B * U) + C * COS (D * V),
WITH (U,V) AXES ROTATED FROM LOCAL (X,Y) BY PHI
(A, B, C, D, PHI) :
3.0000E-08  1.0000E+00  4.0000E-08  2.0000E+00      20.00
SIGMA**2 FOR THE TWO PROCESSES :      4.5000E-16  8.0000E-16
TOTAL SIGMA**2 FOR DEFINITION :       1.2500E-15
MAX ALLOWED U-LOBE # :                3
MAX ALLOWED V-LOBE # :                4
```

SURFACE INFORMATION FOR SURFACE # 1

```
 2 ROUGHNESS REGION(S) DEFINED ON SURFACE
FOR REGION #  1, USING ROUGHNESS DEFINITION #  1 - -
(ZMIN, ZMAX, THETA-MIN, THETA-MAX) :
0.0000E+00  0.0000E+00  0.0000E+00  1.8000E+02
FOR REGION #  2, USING ROUGHNESS DEFINITION #  1 - -
(ZMIN, ZMAX, THETA-MIN, THETA-MAX) :
0.0000E+00  2.0500E+02  0.0000E+00  1.8000E+02

FOR ROUGHNESS DEFINITION #  1 - -
MAXIMUM ACTUAL VALUE OF V**2 :        5.3614E+06
CALC'S (TAYLOR, NON-TAYLOR, FULL LARGE-AMPL):     10     0     0
Fig 5.39 3
FOR ROUGHNESS DEFINITION #  2 - -
MAXIMUM ACTUAL VALUE OF V**2 :        5.3706E+06
CALC'S (TAYLOR, NON-TAYLOR, FULL LARGE-AMPL):     15     0     0

(NO CALCULATIONS PERFORMED FOR DEFINITION #  3)
```

Figure 5.49 DEDRIQ Printout for DOCXR System (continued)

```
SURFACE INFORMATION FOR SURFACE #  2
-----------------------------

 2 ROUGHNESS REGION(S) DEFINED ON SURFACE
FOR REGION #  1, USING ROUGHNESS DEFINITION #  1 - -
(ZMIN, ZMAX, THETA-MIN, THETA-MAX) :
0.0000E+00  0.0000E+00  0.0000E+00  0.0000E+00
FOR REGION #  2, USING ROUGHNESS DEFINITION #  3 - -
(ZMIN, ZMAX, THETA-MIN, THETA-MAX) :
-2.0500E+02  0.0000E+00  0.0000E+00  0.0000E+00
FOR ROUGHNESS DEFINITION #  1 - -
MAXIMUM ACTUAL VALUE OF V**2 :        6.1348E+06
CALC'S (TAYLOR, NON-TAYLOR, FULL LARGE-AMPL):     20     0     0

(NO CALCULATIONS PERFORMED FOR DEFINITION #  2)

FOR ROUGHNESS DEFINITION #  3 - -
MAXIMUM ACTUAL LOBE # (U, V) :            867.2      1186.8
NO. OF GRATING CALCULATIONS :               30
```

Figure 5.49 DEDRIQ Printout for DOCXR System (continued)

```
++ ID LINE FROM FILE 'DOCXR1 SCAT' ++                    1( )7-91 09:32:51
++ID LINE FROM FILE 'DOCXR GI' (X-RAY SYSTEM)              16-07-91 09:01:54

  2  -1   5  10  2.100970E+02  3.744705E+02  -1.000000E+00 6.42000000D+03
     1       1       1       2 38520479 0.000000  0.000000  0.000000
-7.15237643774067067D-02  1.89493940613401308D-03  0.00000000000000000D+00
0.35005808953465915 0.000003 5060105020 9.99387108851927386 6637 3.084204211320
0.000000000 0.000000000 0.000000000     0.000000000 0.000000000 0.000000000
  1.538008314   -4.109536193   -0.000000014   -0.000000059
 -0.000000040    0.000000010    1.534987327   -4.112242065
     2       2       1       2 38384972 0.000000  0.000000  0.000000
-7.12195630853891259D-02  1.58336711067628351D-03  0.00000000000000000D+00
0.35153786736736084 0.00000258684313266 9.99381914624234716 6637 3.084097499041
0.000000000 0.000000000 0.000000000     0.000000000 0.000000000 0.000000000
  1.513841763   -4.110265175   -0.000000012   -0.000000048
 -0.000000033    0.000000009    1.510801168   -4.112961883
     3       3       1       2 38249339 0.000000  0.000000  0.000000

        to

    -50       0      50       0      50
 0.000000000000D+00  2.005949857488D+01
 2.004700471040D+01 -6.978540299123D-07  2.004700539886D+01 -2.870840730602D-03
-8.854208597514D-03  2.498704051387D-02 -2.292100772024D-01 -5.683449903296D-02
-8.125138436199D-03  2.142731084362D-02
```

Figure 5.50 ARAY File for DOCXR System

The printout as shown in Figure 5.49 is divided into three types of output: system

information, roughness definition information, and information about the actual scatter from each surface.

The title line of the system information section tells whether the system is conventional or x-ray. The next several parameters tell the number of surfaces, the wavelength, the focal plane pixel array defining parameters, and the numbers of traced versus successful rays. The next three parameters tell the total weight in the originally traced rays, in the scatter-attenuated rays, and in the diffusely scattered energy (total energy in the pixel array). The next parameters give ACCG (the accuracy of the G(v) look-up tables) and the implied dynamic range. The dynamic range is defined by

$$Range = (1 + ACCG)^{NTABG} \tag{5-72}$$

where NTABG is the number of elements in the look-up tables. (Note that the printout refers to $G(v^2)$ rather than G(v). This is because all the analytical forms for g(r) considered by DEDRIQ have transforms G that are functions of v^2.) The dynamic range of G is essentially the dynamic range of the scatter intensity that DEDRIQ can consider. The next parameters are the accuracy and dynamic range of the 'auxiliary look-up table' that may be used to improve the Taylor series approximation as described in Section 5.5.2.1. Since the actual meaning of this table is obscure to the general user, a third number has been added, which is the maximum of the argument of the auxiliary look-up table, $v_z^2\,\sigma^2$. The user can relate better to this number, which is the parameter used for the accuracy criterion described above for the warning message. Specifically, whereas the Taylor series approximation is abandoned for $v_z^2\,\sigma^2 > 0.01$, the printed value in Figure 5.49 of 56.905 indicates that the table can be utilized far beyond the range of reasonable accuracy and, therefore, far beyond the range of reasonable scattering energies and grazing angles.

There is one curious feature of the system information for this example: The total scattered energy is much less than the difference between the unattenuated specular ray energy and the attenuated ray energy. This is because a substantial portion of the scattered energy has been scattered beyond the focal plane. In other words, the size of the diffraction profile is not small compared to the size of the focal plane. The user must be careful, however, not to go too far in the other direction and let the size of the scatter profile become comparable to the size of a pixel. Thus, for roughness defined by an autocovariance function, a typical inverse correlation length of the autocovariance function should be larger than $(kL_{pix})/F$, where $k = 2\pi/\lambda$, L_{pix} is the width of a pixel, and F is the effective focal length of the system. For roughness defined by a power spectral density G(v), the value of v at the half-width of G(v) should be larger than $(kL_{pix})/F$. For roughness defined by a grating, the quantity $(\lambda)/D_{GRAT}$ should not be much smaller than $(kL_{pix})/F$, where D_{GRAT} is a grating spatial wavelength. (As could be gathered in the following paragraphs, this condition is violated for the grating roughness definition in the example shown. That is, many lobes fall in one pixel.)

The roughness definition information is printed for each definition in the user menu. The first few lines give the user definition method number, a short description of the method and

the defining parameters as input in the SCAT file. (Refer to Tables 5.20, 5.21 and 5.22 for a brief description of each method.) Next is shown the mean square roughness for the definition. If the definition is a sum of more than one term, then the mean square roughness due to each term is shown as well as the total. (Note: for the cases where the roughness is specified by a power spectral density or by an autocovariance function that diverges at the origin, the mean square roughness is defined in a band-limited manner as

$$\sigma^2 = \frac{1}{2\pi} \int_0^{2\pi/\lambda} v\, G(v)\, dv. \qquad (5\text{-}73)$$

This roughness corresponds to the roughness over only those spatial frequencies that can scatter radiation of wavelength λ into angles from 0° to 90°, and is thus a reasonable measure of the roughness of interest.) The final numbers are different for a statistical surface description and a periodic definition. In the statistical case they are the maximum value of the square of the spatial frequency allowed by the look-up table, and the minimum and maximum values of the power spectral density $G(v^2)$. In the periodic case they are the maximum lobe numbers that the user has allowed DEDRIQ to consider in its calculations. These limits were useful in this particular example where (as discussed below) the relationship between the radiation wavelength and the period of the grating implied a prohibitive number of lobes in the focal plane. The user is thus warned in this case that for this particular radiation wavelength the period of the grating is too long and that perhaps the periodic roughness should be modeled as a statistical process or as discrete polynomials.

The information on specific surface scatter is divided into information about each user-defined roughness area and information about the final scatter from each roughness definition. The information about the roughness areas is simply the boundaries as defined by the user in the SCAT file.

Again, the convention that equal minimum and maximum coordinate values for a region imply that the region is unbounded in the corresponding coordinate. The information about scatter from each definition consists simply of the maximum value of the square of the spatial frequency sampled for a statistical definition (or maximum lobe numbers for a periodic definition), as well as the number of calculations (i.e., number of ray-surface intersections) performed. For a statistically defined roughness, the number of calculations is shown for the Taylor approximation, the non-Taylor refinement method and large amplitude theory. The maximum v^2 or maximum lobe numbers can be compared directly with the maximum v^2 in the look-up table or the maximum user-allowed lobe number to make sure all calculations were done properly. For example, in this case, at surface #2 it is seen that the maximum sampled v^2 for definition #1 is far below the maximum look-up table value but that the maximum lobe numbers for definition #3 are 200 times higher than what the user has allowed DEDRIQ to calculate.

An example figure cannot be shown for the FPSCA file, since it is binary, or unformatted. Table 5.23 shows which parameters are output to the FPSCA file.

Table 5.23
Format of FPSCA, FPDFR and FPCOM Files

RID Record	64-character user comments from a SCAT, DIFFR, or LOOK file, with RDATE = current date and RTIME (1) = current time appended by the program. (16 * R*4, 2 * R*8)
GID Record	64-character user comments from the original GI file (in the case of an FPSCA or an FPDFR file), or from a DATA statement in the FPLOOK module (in the case of an FPCOM file), with GDATE = current date and GTIME (1) = current time appended by the program. (16 * R*4, 2 * R*8)
Data Definition Record	X_{con}, Y_{con}, L_x, L_y, N_x, N_y (see Figure 5.52 for definitions of these parameters, ZLOUT = wavelength parameter, and ITOUT = file type parameter. (6* R*8, R*4, I*4)
For Each Pixel Array Row (i.e., FOR J = 1 to N_y):	
Pixel Row Record:	Pixel row #j. (N_x * R*4)

5.5.4 Mathematical Background for ACV Models

As discussed in Section 5.5.2.1, the small amplitude theory depends on deriving a function G(v), which is related in a Fourier transform sense to the autocovariance function g(r) s follows:

$$G(v) = \iint e^{iv\tau}\, g(r) \tag{5-74}$$

or, if g(r) is symmetric,

$$G(v) = 2\pi \int dr\; r\; g(r)\; J_0(vr) \tag{5-75}$$

G(v) can be seen to be a Power Spectral Density (PSD) function in terms of the argument v, where v is in units of radians per distance. As discussed in Section 5.5.2.1, G has the unusual (for a PSD) normalization

$$\iint G(v)\; d^2v = 4\pi^2\; \sigma^2 \tag{5-76}$$

where σ^2 is the mean square roughness.

In any case, it is the function G(v) which is required for the small amplitude scatter theory, since the scatter is in fact proportional to G(v). G(v) is fairly easily derived for all of the

ACV models previously implemented. No closed form solution was derivable for the Gaussian-cosine model, however. We therefore obtained a series solution which can be evaluated on the computer. The solution is as follows:

For

$$g(v) = e^{-Br^2} \cos Cr \,,$$
$$G(v) = \frac{\pi}{B} e^{-\frac{v^2}{4B}} \sum_{m=0}^{\infty} (-1)^m \frac{m!}{(2m)!} (\frac{C^2}{B})^m L_m(\frac{v^2}{4B})] \qquad (5\text{-}77)$$

where L_m is the m^{th} Laguerre polynomial.

Table 5.24 summarizes the G(v) results for all ACV models.

Equation (5-77) is a convenient formulation, because when there is no cosine term (i.e., when C=0), the summation becomes unity, and the function G(v) takes on the familiar Gaussian form given by the term before the summation.

Table 5.24
G(v) for various g(r) (i.e., autocovariance or ACV) models

g(r)	G(v)
$K_0(Br)$	$2\pi / (B^2 + v^2)$
exp(-Dr)	$2\pi D / (D^2 + v^2)^{3/2}$
$\exp(-Br) / (Br)^{1/2}$	$\pi^{3/2} F(3/4, -1/4, 1; v^2/(v^2+B^2)) / (B^{1/2} (B^2 + v^2)^{3/4})$ (F is a hypergeometric function)
exp(-DR) cos Fr	2π Re $[(D-iF) / ((D-iF)^2 + v^2)^{3/2}]$
$\exp(-Br^2)$	$(\pi/B) \exp -(v^2/(4B))$
$\exp(-Er^2) \cos Fr$	$(\pi/E) \exp(-v^2/(4E)) \; \Sigma_{m=0} [(1-)^m (m!/(2m)!) (F^2/E)^m L_m(v^2/(4E))]$ (L_m is a Laguerre polynomial)

Research into the convergence of the series in Equation (5-77) led to a more detailed understanding of a limitation on the cosine term — not only for this Gaussian-cosine model,

but also for the already-present exponential-cosine model. The limitation on the cosine term is that its period cannot be too short compared to the correlation length of the Gaussian or exponential. If it is made too short, then the function G(v) is no longer monotonically decreasing, which is required for the OSAC analysis.

A monotonically decreasing G(v) is appealing (and, for OSAC, necessary) because it implies monotonically decreasing scatter with angle in the small amplitude limit. It makes sense intuitively that a short period cosine term would violate this requirement. This is because, as the cosine becomes more prominent within the Gaussian, G(v) must start to rise at precisely the spatial frequency of the cosine wave. In the limit of an infinitely short period cosine, G(v) becomes infinitely spiked at the cosine's spatial period.

To determine the limit on the cosine period, we analyzed G(v) and its derivative for both the Gaussian-cosine and the exponential-cosine model, and arrived at transcendental equations for the limiting period. The equations have the following approximate numerical solutions, which we have implemented in the parameter checking within the DEDRIQ program:

$$\textit{For an exponential-cosine} \qquad (e^{-BR}\cos Cr) \qquad \textit{C must be} < (0.414213\ B) \tag{5-78}$$

$$\textit{For a Gaussian-cosine} \qquad (e^{-BR^2}\cos Cr) \qquad \textit{C must be} < (1.19135\ \sqrt{B}) \tag{5-79}$$

When the conditions in Equations (5-78) and (5-79) are satisfied, then, G(v) will be monotonically decreasing. As discussed in Section 5.5, we have implemented the required parameter checking for both the Gaussian-cosine and the exponential-cosine models.

5.6 Optical Path Difference

5.6.1 Introduction

OPD provides an Optical Path Difference (OPD) map so that PSF can subsequently perform the appropriate Fourier transform to arrive at a focal plane intensity point spread function. The subroutine structure of OPD is shown in Figure 5.51.

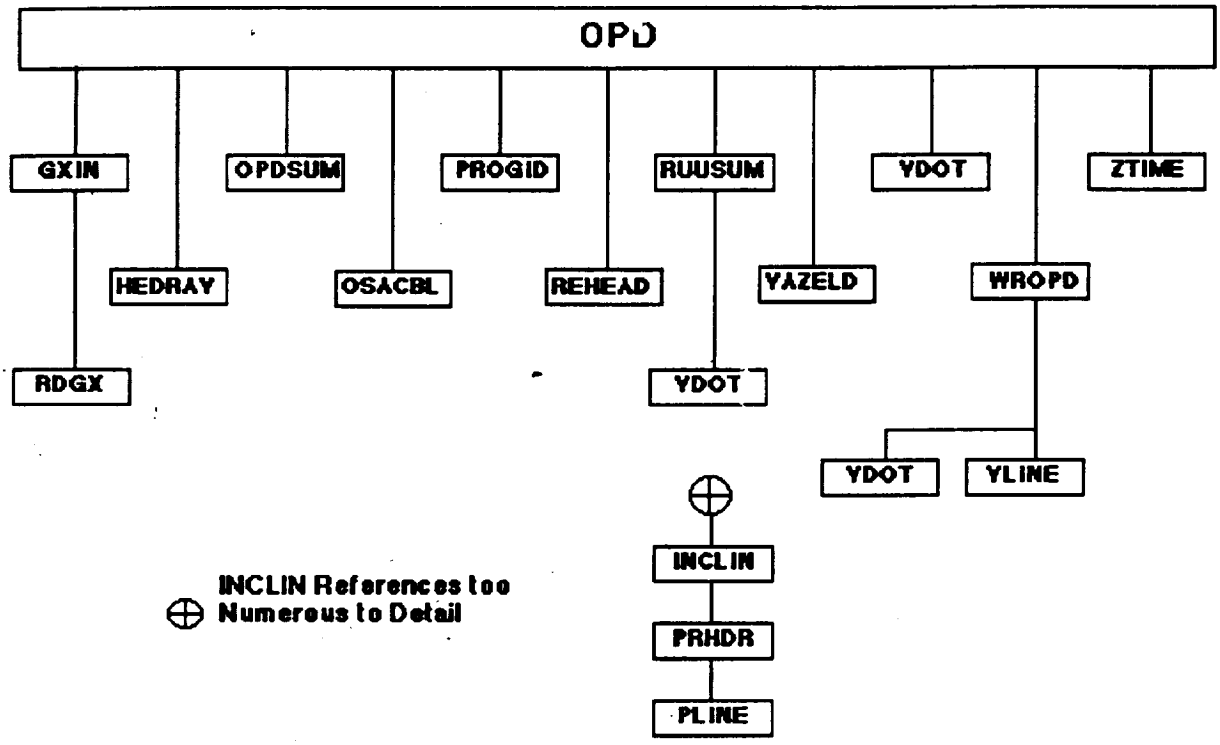

Figure 5.51 OPD External Reference Tree

5.6.2 Method

OPD uses simple geometric methods to calculate an OPD for each successfully traced ray. $|\vec{PL}_i|$ has been calculated previously by NABRAT or DRAT, and is the actual total physical path length from the (z=0) plane where ray tracing was begun.

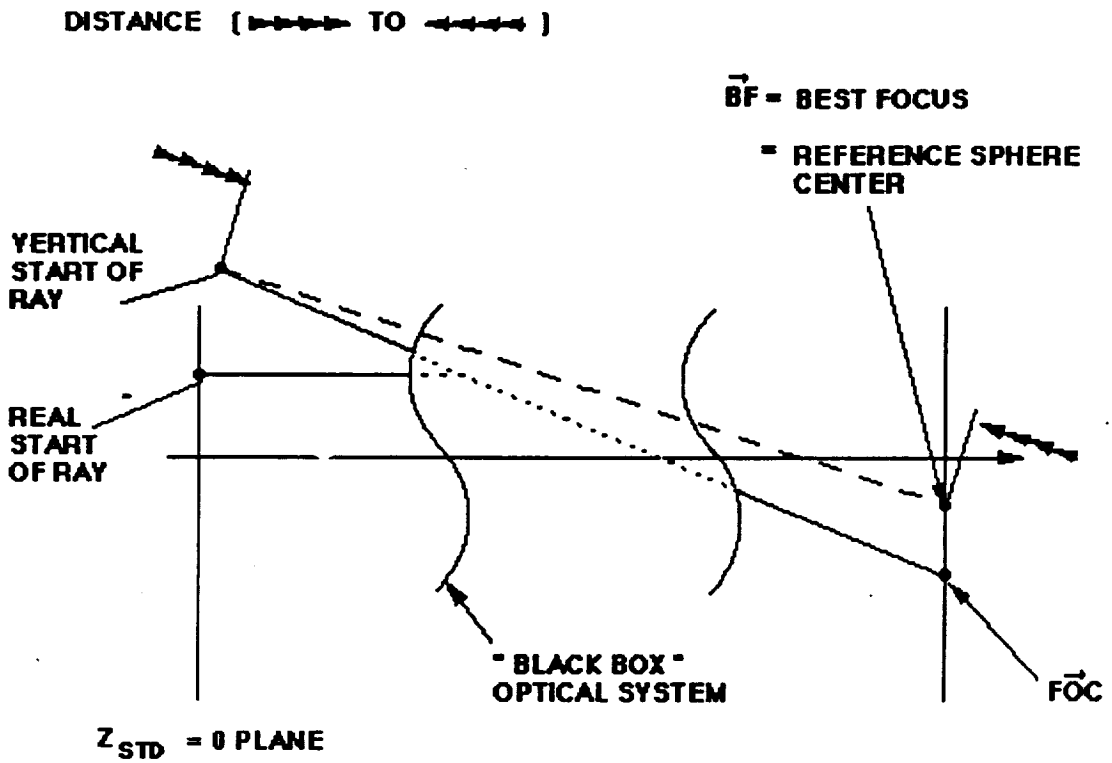

Figure 5.52 Geometry for OPD Model

The Ray is pictured as extending straight back from the focal plane for a distance of $|\vec{PL}_i|$. The starting point of this extended ray is then taken to be the origin of the ray on the reference sphere for the OPD calculations. (Note that these ' origin points' do not lie at the pupil plane defined by OPD. This is acceptable, since the actual OPD's are independent of the choice of pupil plane location. Only the actual OPD's and the system F number are relevant). The center of the reference sphere is defined to lie at the image centroid in the focal plane. (The image centroid is listed as the planar optimal focus by NABRAT or DRAT). The Optical Path Length (OPL_i) of the ray is defined simply as the distance from the origin on the reference sphere to the reference sphere center. Thus, OPL_i is seen from Figure . 52 to be defined by

$$(OPL_i)^2 = |\vec{PL}_i|^2 + |\vec{FOC}_i - \vec{BF}|^2 - 2(\vec{PL}_i) \cdot (\vec{FOC}_i - \vec{BF}) , \qquad (5\text{-}80)$$

where, as defined in Figure 5.52, $\vec{FOC}_1$ is the focal plane intercept location of the ray, and $\vec{BF}$ is the image centroid location. (The dot in the above equation is the vector dot product). Since the vector $(\vec{FOC}_1 - \vec{BF})$ is very much smaller in magnitude than the vector $\vec{PL}_1$, the term quadratic in $(\vec{FOC}_1 - \vec{BF})$ can be approximated by

$$OPL_i \approx |\vec{PL}_i| + (\vec{PL}_i)\cdot(\vec{BF} - \vec{FOC}_i) \ . \qquad (5\text{-}81)$$

The quantity OPL_i is calculated for each successful ray, and the weighted average (using the focal plane weight or intensity of the ray as the weighing factor is defined as OPL.

Then the OPD for each ray is defined as

$$OPD_i = OPL_i - \overline{OPL} \ . \qquad (5\text{-}82)$$

5.6.3 Inputs and Outputs

The inputs to OPD consist of a GX file produced by GEOSAC, a focal plane ray file produced by NABRAT, DRAT, or DEDRIQ, and a one-line user created ID file. The output of OPD consists of terminal and printer output, as well as an OPD file that contains the intensity and OPD of each ray in the pupil. The names, types, formats, and file numbers of all of OPD's files are summarized in Table 5.25.

Table 5.25 Files Used by OPD

Input/ Output	File Name	File Type	Format	Logical Record Length	Block Size	File Number
Input	name1	GX	FB	80	800	1
Input	name1	RAY001	FB	80	800	7
Input	name1 or[2] name2	RAY00k[1] ARAY	FB	80	800	3
Input	name3	ID	FB	80	800	5
Output	name1 or[3] name2	OPD OPD	FB	80	800	4
Output	terminal			80		6
Output	printer			132		8

1 "k" is one greater than the # of surfaces in the system

2 input may be either a focal plane RAY file (from NABRAT or DRAT), or an ARAY file (from DEDRIQ)

3 name convention of OPD file depends on whether a RAY or an ARAY file was used as input

Figure 5.53 shows the ID file used in analyzing the on-axis system defined in the DOCON GI file. Figure 5.54 shows the resultant printout. The first line in the printout tells whether the system is conventional or x-ray. The second line tells whether the focal plane RAY file was produced by either NABRAT or DRAT (no scattering calculated), or by DEDRIQ (scattering calculated).

```
*** OPTICAL SURFACE ANALYSIS PROGRAM (OPD    ) RELEASE (06.0) VAX      PAGE   1
+ +ID LINE FROM FILE GI(ON-AXIS CASSEGRAIN)+ + 1              16-07-91 09:55:49
+ +ID LINE FROM FILE 'DOCON GI' (ON-AXIS CASSEGRAIN)+ +       16-07-91 08:57:31
-------------------------------------------------------------------------------

                OPD CALCULATION SUMMARY REPORT
                ------------------------------

TYPE OF SYSTEM (XRAY / CONV) :      CONVENTIONAL
SOURCE OF INPUT RAY FILE :         NABRAT/DRAT
NUMBER OF SURFACES IN SYSTEM :               2
NUMBER OF TRACED RAYS :                     50
NUMBER OF SUCCESSFUL RAYS :                 38
TOTAL RAY WEIGHT :                   38.00000
X COORD OF REF SPHERE (BEST FOCUS) :  5.07128D-01
Y COORD OF REF SPHERE (BEST FOCUS) : -3.42849D+01
EFFECTIVE FOCAL LENGTH :             2.11653D+04
INNER RADIUS OF TRACED ANNULUS :     9.71000D+01
OUTER RADIUS OF TRACED ANNULUS :     5.00000D+02
RMS OPD VALUE OVER PUPIL :           8.95509D-05
```

Figure 5.53 OPD ID File for DOCON System

```
+ +ID LINE FROM FILE GI(ON-AXIS CASSEGRAIN)+ + 1              16-07-91 09:55:49
+ +ID LINE FROM FILE 'DOCON GI' (ON-AXIS CASSEGRAIN)+ +       16-07-91 08:57:31
  2   -2    5   10  9.710000E+01  6.014290E+04 -1.000000E+00 3.77526957D+03
5.071281831272D-01 -3.428489805694D+01  2.116525079186D+04
      1         1         1         2 100000000
9.709999999999996D+01  0.0000000000000000D+00  0.0000000000000000D+00
0.04987900231096049 -0.10368296895520083  9.99933807444658262   -1.238447D-04
      2         2         1         2 100000000
2.637637389786549 14D+02  0.0000000000000000D+00  0.0000000000000000D+00
0.13316497268775175 -0.10374812651056189  9.99857506929335435   -5.334027D-05
      3         3         1         2 100000000
          to
      49        4        10         2 100000000
3.5[illegible]09704471319210D+02 -2.561132918330151 68D+02  0.0000000000000000D+00
0.17749312700145251 -0.23185905199901516  9.99573596939581865    9.912468D-05
      50        5        10         2 100000000
4.045085052776434 51D+02 -2.938926320240892 10D+02  0.0000000000000000D+00
0.20346554114305063 -0.25079544881038482  9.99478381038946539    1.517836D-04
     -50       12        38         0        38
0.000000000000D+00  3.800000000000D+01
```

Figure 5.54 OPD Printout for DOCON System

The next few lines summarize some self-explanatory parameters of the previous ray trace. Next are the x- and y-coordinates of the reference sphere center. Note that these numbers duplicate the planar optimal focus information from the previous DRAT run, whose printer output was shown in Figure 5.28. The next number is the effective focal length of the system, and is defined as the weighted average value of the distance a ray would have to be traced back from the focal plane before its perpendicular distance from the optical axis were the same as that of the same ray as it originally intersected the (z=0) plane at the start of ray tracing. The next two numbers are the inner and outer radius of the annulus of traced rays, as originally specified by the user in the GI file. The final number is the weighted RMS value of the OPD value of all rays.

Figure 5.54 shows the OPD file produced in this analysis. The OPD file gives the effective focal length of the system and the reference sphere center location, as well as detailed OPD information for each ray. The format of the OPD file is given in Table 5.26.

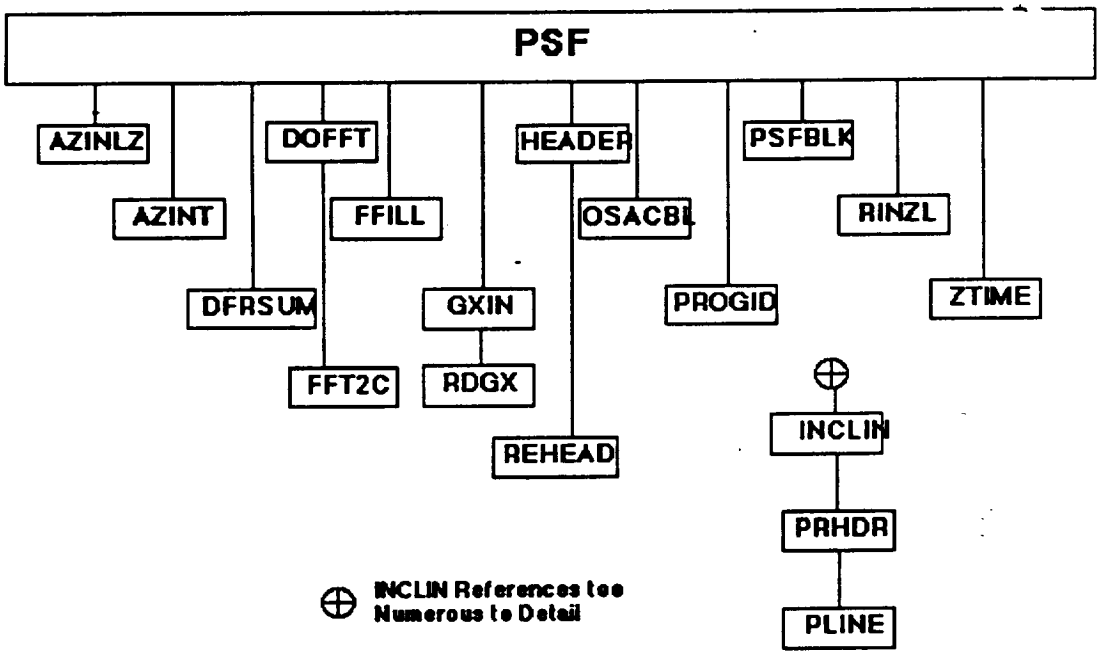

Figure 5.55 OPD File for DOCON System

Table 5.26
OPD File Format

Header Record Group (4 Cards)	
Cards 1-3	Same format as for a RAY file (see Tables 5.10(a) and 5.7(b)), except KURF = surface # = -2.
Card 4	XBF, YBF, EFLBAR = (x,y) coordinates of best focus, and system effective focal length. Format (1P3D20.12)
Data Record Group for Each Ray	
Card 1	Same format as Card 1 of focal plane RAY file Data Record Group (see Table 5.10(b))
The remaining cards are omitted whenever KODE .GT. 4, i.e., when the ray fails	
Card 2	XPU, YPU, ZPU = (x, y, z) coordinates of intersection of ray extended back from the focal plane to the pupil plane (ZPU is dummied to 0)
Card 3	XD, YD, ZD, OPD = direction cosines of the ray at the focal plane, and the optical path difference (OPD) OF THE RAY. Format (1P3F20.17, D20.6)
Trailer Record Group	
	Same format as Cards 1 and 2 of focal plane RAY file Trailer Record Group (see Table 5.10(c))

5.7 Point Spread Function

5.7.1 Introduction

The purpose of PSF is to use the ray intensity and OPD information produced by OPD to calculate a pupil function, and then to Fourier transform that pupil function in order to calculate the focal plane energy distribution, or Point Spread Function (PSF). The subroutine structure of PSF is shown in Figure 5.56.

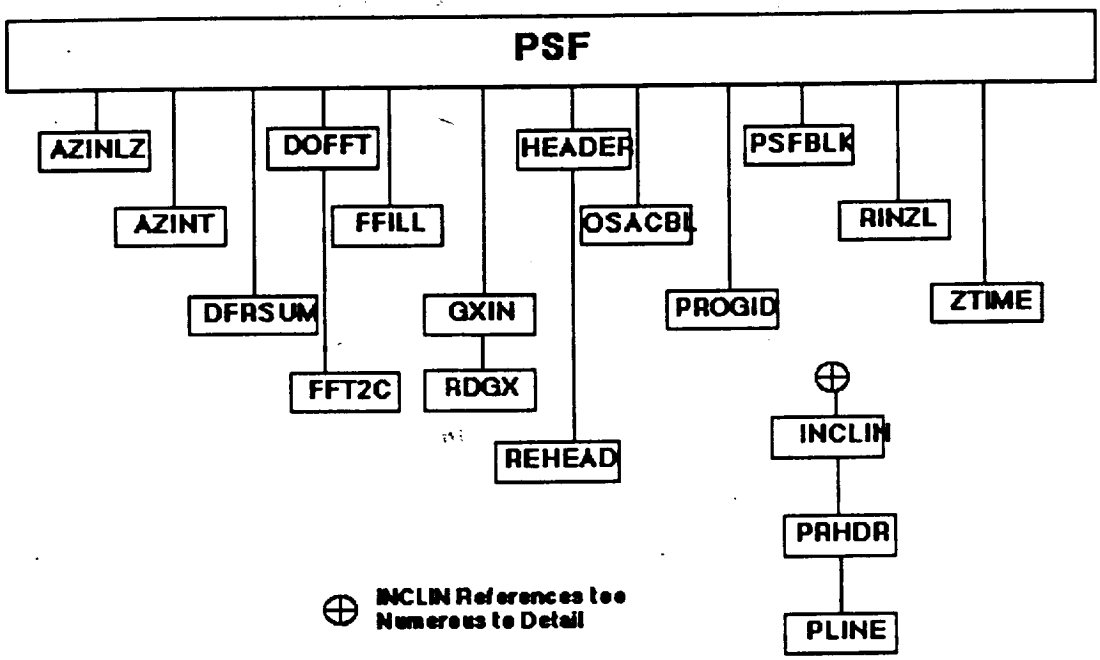

Figure 5.56 External Reference Tree for PSF

5.7.2 Method

(This subsection assumes that the reader is fairly familiar with Fourier optics and the Fast Fourier Transform (FFT).) The general theory of using a pupil function to calculate a point spread function is well known. (See, for example, Goodman's book, *Introduction to Fourier Optics*). The point spread function can basically be found as either the square of the Fourier transform of the pupil function (i.e., by using the Coherent Transfer Function), or, equivalently, as the Fourier transform of the convolution of the pupil function with itself (i.e., by using the Optical Transfer Function). The pupil function is defined by

$$PUPIL(x,y) = T(x,y)e^{ikW(x,y)}, \tag{5-83}$$

where (x,y) are the pupil plane coordinates, $k = 2\pi/\lambda$, W is the OPD at the point (x,y) and T(x,y) is the transparency of the pupil for (x,y) inside the pupil and zero for (x,y) outside the pupil. PSF calculates the point spread function using the Coherent Transfer Function

method. There is nothing noteworthy in this choice of general method. However, the numerical method used to evaluate the two-dimensional Fourier transform of the pupil function is unique. The motivation and rudiments of the technique are described below.

The pupil function of an optical system is often evaluated on a rectangular grid over the pupil. In this case, especially when the pupil has little or no central obscuration, conventional two-dimensional Fast Fourier Transform (FFT) techniques can be successfully applied to both the Coherent Transfer Function method and the Optical Transfer Function method. However, OSAC deals with systems that can be highly obscured. (For example, high energy x-ray telescopes can have an effective linear central obscuration of 98% or 99%). For such highly obscured systems, conventional FFT techniques become impractical (at least for the Coherent Transfer Function method), since the overwhelming majority of points in the grid are not contained in the clear aperture of the system thus requiring a completely unmanageable number of grid points to make accurate calculations. The Optical Transfer Function method could be a possibility, since the pupil function is convolved with itself prior to Fourier transformation. However, for highly obscured systems, the convolution is itself a very involved calculation, especially for OSAC, since OSAC of necessity evaluates the pupil function on a polar grid rather than on a rectangular grid. Also, the number of convolutions to be calculated would have to be at least as great as the number of points in the focal plane where the PSF was to be evaluated.

For the reasons outlined above, a unique numerical technique was developed for PSF. The purpose of the technique is to provide a method of efficiently evaluating the two-dimensional Fourier transform of a possible highly obscured pupil function. To introduce the technique, we write the complex field amplitude at focal plane coordinates (x,y) in terms of the pupil function PUPIL (u,v) as

$$U(x,y) \propto \iint_{PUPIL} PUPIL(u,v)\, e^{-i\frac{2\pi}{\lambda R}(xu+yv)}\, du\, dv\,, \tag{5-84}$$

where R is the effective focal length of the system. The heart of the technique lies in now changing variables in the pupil from rectangular coordinates (u,v) to polar coordinates (r,θ) so that

$$U(x,y) \propto \iint_{PUPIL} PUPIL(r,\theta)\, e^{-i\frac{2\pi}{\lambda R}(xr\cos\theta + yr\sin\theta)}\, r\, dr\, d\theta\,, \tag{5-85}$$

or

$$U(x,y) \propto \int_0^{2\pi} d\theta \left[\int_a^b dr\, r\, PUPIL\,(r,\theta)\, e^{-i\frac{2\pi}{\lambda R} r(x\cos\theta + y\sin\theta)} \right]\,, \tag{5-86}$$

where a and b are the inner and outer radii of the pupil. Using the convention that the pupil function is defined over all space and is zero outside the clear aperture, we recognize the quantity (r * PUPIL (r,θ)), where the transform variable is

$$w = \frac{1}{\lambda R} (x \cos\theta + y \sin\theta) \quad . \tag{5-87}$$

In other words,

$$U(x,y) \propto \int_0^{2\pi} d\theta \; FT_\theta (w) \quad , \tag{5-88}$$

where

$$FT_\theta (w) = \int_{-\infty}^{\infty} dr \; [r \; PUPIL (r,\theta)] \, e^{-i2\pi rw} \quad , \tag{5-89}$$

and again, w = (xcosθ + ysinθ)/(λR). The above equation for U(x,y) serves to summarize the technique used by PSF. For every radial spoke of rays in the pupil, (i.e., for each of several values of θ) PSF uses a one-dimensional FFT routine to calculate the Fourier transform of the quantity (r * PUPIL (r,θ)). Then, for each point (x,y) in the focal plane, PSF numerically integrates the integral shown above, evaluating w in terms of θ and (x,y) at an appropriate number of points in the integration. The collection of one-dimensional Fourier transform is used as two dimensional array in the variables w and θ. The integrand values are found at equal intervals in θ by using a second order polynomial interpolation (Lagrange interpolation) in w and θ. The integrand values are then weighted using Simpson's rule to arrive at a final value for the integral. This value is then scaled by the appropriate constant to give the diffracted energy incident on a pixel centered as coordinates (x,y). The constant can be determined by demanding that the total energy in the focal plane equal the total energy in the pupil, yielding the result

$$CONSTANT = \frac{(WTOT)\,(AREA_{PIXEL})}{(AREA_{PUPIL})\,\lambda^2 R^2} \quad , \tag{5-90}$$

where WTOT is the total weight of all successful rays in the pupil. Thus,

$$ENERGY(x,y) = CONSTANT \left[\int_0^{2\pi} d\Theta \; FT_\Theta (w) \right]^2 . \tag{5-91}$$

One of the special features of the implementation of this technique is the ability to change the polynomial interpolation technique mentioned above from second order in θ to first or zero'th order if only two or one radial Fourier transforms are defined consecutively. (An array is undefined if no rays were successful in the corresponding spoke of rays in the pupil).

PSF must use a non-trivial algorithm for determining the number and spacing of points in r for the Fourier transform arrays input to the FFT routine. There are two criteria for the spacing in r. First, the spacing must be close enough so that the pupil function is sampled by the FFT routine at least as often as it is defined by the configuration of rays in the radial direction. (Note that the r-spacing being determined by the program implies that the pupil function itself must be interpolated even to define an FFT array. This is done with a second order polynomial interpolation, just like the final azimuthal integration interpolation scheme. As is also the case with that scheme, the order of the interpolation polynomial depends on how many consecutive points in the radius correspond to successful rays). The second criterion for determining the r-spacing is that the spacing must be close enough so that the extent of the resulting Fourier transform array of values of (r * PUPIL (r)). Both these criteria relate to the fact that once a r-spacing is determined, the length of the array determines the resolution in w of the resulting FFT array. The first criterion is that the array must be long enough so that the resulting resolution in w is at least as fine as the pixel spacing defined by the user. The second criterion is that the array must be long enough so that the resulting resolution in w is a least as fine as four points per

$$\Delta_w = w_{AIRY} = \frac{\lambda R}{2(b-a)}, \qquad (5\text{-}92)$$

where, as before, R is the effective focal length, and b and a are the outer and inner radii of the pupil. w_{AIRY} is related to a basic diffraction-limited image size. (Note that for a=0, the radius of the Airy disc is (1.22 * w_{AIRY})). The second criterion assures that the numerical integration algorithm will be operating on a sufficiently smooth function. (Note that all elements of the input FFT array are set to zero for r outside the clear aperture. That is, the array of values of (r * PUPIL (r)) is zero filled outside the clear aperture).

5.7.3 Inputs and Outputs

The inputs to PSF consist of a GX file produced by GEOSAC, an OPD file produced by OPD, and a user-defined file that defines the focal plane pixel array and certain other parameters (DIFFR file). The output of PSF consists of terminal and printer output, as well as a focal plane pixel array file (FPDFR file). The names, types, formats, and file numbers of all PSF's files are summarized in Table 5.27.

Table 5.27 Files Used by PSF

Input/ Output	File Name	File Type	Format	Logical Record Length	Block Size	File Number
Input	name1	GX	FB	80	800	7
Input	name2[1]	OPD	FB	80	800	1
Input	name3	DUFFR	FB	80	800	3
Output	name3	FPDFR	VS		800	2
Output	terminal			80		6
Output	printer			132		8

[1] name2 should be the same as name1 if the OPD module used a RAY file, rather than an ARAY file as input

Table 5.28 shows the format of a DIFFR file. The first line is an identification line to be used in the printer headers. The second line lists the self-explanatory parameters for defining the focal plane pixel array. The third line lists the wavelength of the incoming radiation, as well as the inner and outer radii of the pupil to be considered. (Usually, these last two parameters are set to be the same as those defined in the original GI file. However, the user may wish to expand the range of r slightly for PSF in order to model the true pupil size, whereas the values in the GI file may have been contracted slightly to assure that the rays are successfully traced by NABRAT or DRAT).

Table 5.28
DIFFR File Format

Card 1	RID = 64-character user comments line. Format (16A4)
Card 2	X_{cen}, Y_{cen}, L_x, L_y, N_x, N_y (see Figure 5.52 for definitions of these parameters) Format (4D15.0, 2I6).
Card 3	ZLAM = wavelength; RA = inner radius of annular aperture; RB = outer radius. Format (3D15.0)

Figure 5.57 shows the DIFFR file used to analyze the on-axis conventional system defined in the DOCON GI file. Figure 5.58 shows the resultant printer output. The output is divided

into sections concerning system information, PSF runtime information, and diffraction image information. The system information is very much like that produced by the module OPD.

```
++ ID LINE FROM FILE 'DOCON1 DIFFR' ++
0.507  -34.285  0.1  0.1  25  25
0.6328E-03  97  500
```

Figure 5.57 DIFFR Files For DOCON System

```
** OPTICAL SURFACE ANALYSIS PROGRAM (PSF     ) RELEASE (06.0) VAX      PAGE   1
++ ID LINE FROM FILE 'DOCON1 DIFFR' ++                    16-07-91 10:46:20
++ID LINE FROM FILE 'DOCON GI' (ON-AXIS CASSEGRAIN)++     16-07-91 08:57:31
-------------------------------------------------------------------------

          POINT SPREAD FUNCTION SUMMARY REPORT
          ------------------------------------

            SYSTEM INFORMATION :
            --------------------

TYPE OF SYSTEM (XRAY / CONV) :       CONVENTIONAL
NUMBER OF SURFACES IN SYSTEM :                 2
NUMBER OF TRACED RAYS :                       50
NUMBER OF SUCCESSFUL RAYS :                   38
TOTAL RAY WEIGHT :                    38.00000
X COORD OF REF SPHERE (BEST FOCUS) :  5.07128D-01
Y COORD OF REF SPHERE (BEST FOCUS) : -3.42849D+01
EFFECTIVE FOCAL LENGTH :              2.11653D+04
INNER RADIUS OF TRACED ANNULUS :      9.71000D+01
OUTER RADIUS OF TRACED ANNULUS :      5.00000D+02
            PSF RUNTIME PARAMETERS :
            ------------------------

SYSTEM WAVELENGTH :                   6.32800E-04
INNER RADIUS OF PUPIL ANNULUS :       9.70000E+01
OUTER RADIUS OF PUPIL ANNULUS :       5.00000E+02
PIXEL ARRAY CENTER X COORD :          5.07000D-01
PIXEL ARRAY CENTER Y COORD :         -3.42850D+01
PIXEL ARRAY X LENGTH :                1.00000D-01
PIXEL ARRAY Y LENGTH :                1.00000D-01
NUMBER OF PIXELS IN X DIRECTION :             25
NUMBER OF PIXELS IN Y DIRECTION :             25
NUMBER OF FFT-IMPLIED PIXELS :                21
NUMBER OF ELEMENTS IN FFT ARRAYS :            32

            DIFFRACTION IMAGE INFORMATION :
            -------------------------------

TOTAL WEIGHT IN FOCAL PLANE :          37.74458
X COORD OF IMAGE CENTROID :          -8.00513D-05
Y COORD OF IMAGE CENTROID :           2.00016D-04
RMS X-WIDTH OF IMAGE :                1.58602D-02
RMS Y-HEIGHT OF IMAGE :               1.36434D-02
RMS IMAGE SIZE :                    2.09210D-02
```

Figure 5.58 PSF Printout for DOCON System

In fact, the user should refer to Figure 5.53 to see the similarity in format and to see that the same values for the parameters are displayed. The next section, PSF runtime parameters, should be self-explanatory after the user is familiar with the DIFFR file input. The two exceptions are the last two parameters. The first is the number of elements that PSF has determined are needed in the FFT arrays. (See Section 5.7.2 for an explanation of the method used for determining the length of the FFT arrays). The last parameter is the number of elements actually used, and is equal to the number calculated above, rounded up to the nearest power of 2. (Because of limitations on core memory size, PSF is currently limited to FFT arrays of length 512. If PSF calculates that longer arrays are called for, then a fatal error message is displayed and program execution is halted). The diffraction image information consists of six parameters. The total weight in the focal plane is the sum of the energies, or weights, in all the focal plane pixels. (A weight of unity corresponds to exactly one ray). The following x- and y-coordinates are those of the centroid of the image. (Note that this and the following parameters cannot be expected to have an accuracy greater than the dimension of a pixel). The last three parameters are the weighted RMS values of the width (x-extent), height (y-extent), and radius of the image. These parameters are defined relative to the image centroid location, and refer to the RMS value over all pixels, where the weighting factor is the energy or weight in the pixel).

Just as was the case for DEDRIQ, an example figure cannot be shown for the FPDFR file, since it is binary, or unformatted. The format is the same as the FPSCA files produced by DEDRIQ, though, except that the file type parameter is 2 instead of 1. (See Table 5.23 for the format of the FPSCA and FPDFR files). FPLOOK, described in Section 5.8, offers the method developed for looking at a focal plane pixel array file.

5.8 Focal Plane Look (FPLOOK)

FPLOOK is a short module provided for combining specular ray files and focal plane pixel array files into a single focal plane pixel array file, and for showing the user the energy contained in a user-specified set of pixels. The input consists of the file or files that are to be combined, and a user-created file (LOOK file) that specifies the form of the input and output. The output consists of terminal and printer output, as well as the combined focal plane pixel array file (FPCOM file) if requested. The names, types, formats, and file numbers of all FPLOOK files are summarized in Table 5.29 (Note that FPLOOK combines files blindly, so that it is up to the user to make sure that the combination of files has some physical significance). Figure 5.59 shows the subroutine structure of FPLOOK.

Table 5.29 Files Used by FPLOOK

Input/ Output	File Name	File Type	Format	Logical Record Length	Block Size	File Number
Input	namei[1]	RAY00j or ARAY	FB	80	800	9,10,...[1]
Input	namei[1]	FPSCA or FPDFR or FPCOM	VS		800	16,17,...[2]
Input	name1	LOOK	FB	80	800	1
Output	name1	FPCOM	VS		800	2
Output	terminal			80		6
Output	printer			132		8

[1] namei can be the name of any previously created file

[2] focal plane RAY files (from NABRAT or DRAT) or ARAY files (from DEDRIQ) are assigned ascending file numbers, starting with 9

[3] previously created pixel array files from DEDRIQ, PSF, or FPLOOK are assigned ascending file numbers, starting with 16

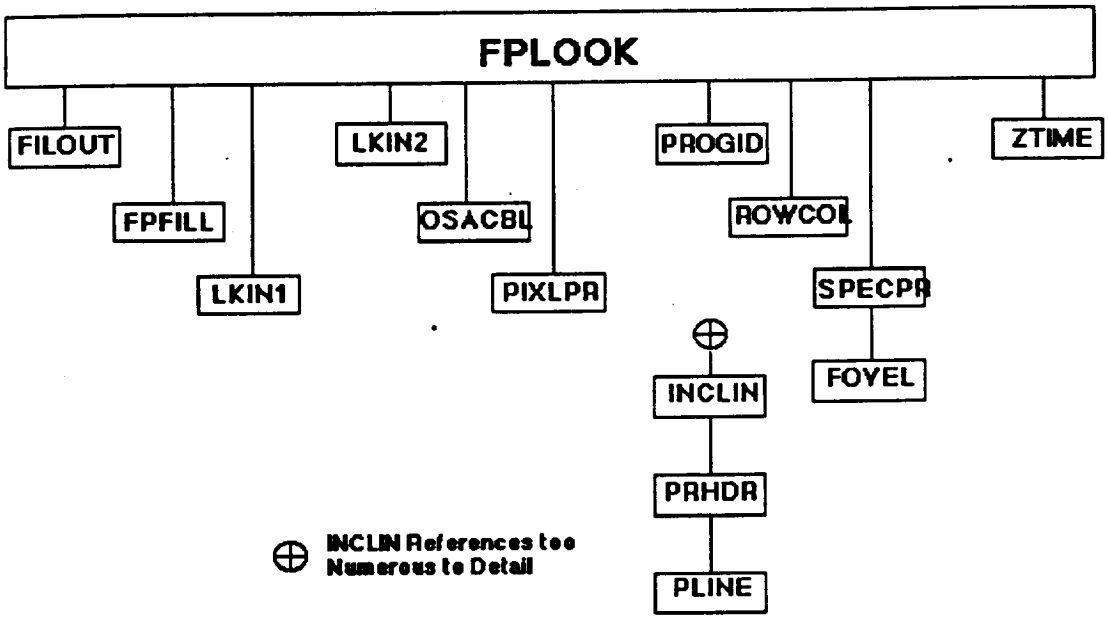

Figure 5.59 External Reference Tree for FPLOOK

Table 5.30 shows the format of a LOOK file. The first line is an identification line that is used in the printout headers and in the FPCOM file. The next line contains two integers which specify the number of specular ray (RAY or ARAY) files and the number of focal plane pixel array (FPSCA, FPDFR, or even previously produced FPCOM) files that are to be combined. The next line contains a single integer that tells whether FPLOOK is to read the remaining lines from the LOOK file, or from the terminal (file number 5). (This gives FPLOOK an interactive capability).

Table 5.30
LOOK File Format

Card 1	RID = 64-character user comments line. Format (16A4)
Card 2	NSPEC = # of specular RAY or ARAY files, NPIXL = # of FPSCA, FPDFR, or FPCOM pixel array files that are being used as input. Format (2I5)
Card 3	IMODE (0 means remaining parameters are to be read from this file, while 1 means they are to be read from the terminal instead)
Card 4	X_{cen}, Y_{cen}, L_x, L_y, N_x, N_y (see Figure 5.60 for definitions of these parameters) Format (4D15.0, 2I6)
Card 5	IPXOUT, IFLOUT = flags to determine whether or not pixel energies are to be displayed (IPXOUT), and whether or not an FPCOM pixel array file is to be created (IFLOUT). (0 means no output, 1 means output)
Card 6	(This card is included only if IPXOUT = 1) IBOT, ITOP, JBOT, JTOP = index limits for displaying pixel energies at pixel (I, J). See Figure 5.60 for the relation between pixel indices and (x, y) location

The next line contains the parameters for defining the output focal plane pixel array file. The next line contains two integers that tell FPLOOK what combination of output (pixel energy printout and/or FPCOM file) to produce. If the pixel energy printout is requested, then one final line specifies which pixels are to be displayed.

Figure 5.60 shows a LOOK file used to combine and examine the ARAY and FPSCA files generated in the DEDRIQ example detailed in Section 5.5. This LOOK file does not exercise the interactive option, and it requests both pixel information and FPCOM file output. Figure 5.61 shows the resultant printer output.

```
++ ID LINE FROM FILE 'DOCXR1 LOOK'
  1   1
  0
  0.0          0.0          2.0          2.0          20   20
  1    1
  1   20    1   20
```

Figure 5.60 LOOK File for DOCXR System

```
*** OPTICAL SURFACE ANALYSIS PROGRAM (FPLOOK ) RELEASE (06.0) VAX      PAGE  1
++ ID LINE FROM FILE 'DOCXR1 LOOK'                          16-07-91 10:57:16
+++ PERMANENT FPLOOK  IDENTIFICATION LINE +++               16-07-91 10:57:16
-------------------------------------------------------------------------------

          SUMMARY INFORMATION FOR DEDRIQ 'ARAY' FILE
          ------------------------------------------

++ ID LINE FROM FILE 'DOCXR1 SCAT' ++                       16-07-91 09:32:51
++ID LINE FROM FILE 'DOCXR GI' (X-RAY SYSTEM)               16-07-91 09:01:54

        MINIMUM                    MAXIMUM
     X             Y            X             Y
-7.15237644E-02 -3.63960281E-02  1.40953194E-02  2.46789753E-02

                    PLANAR OPTIMAL FOCUS
                    --------------------

   SUM          X           Y           Z          SPOT
  WEIGHTS     LOCATION    LOCATION    PLANE        SIZE
 2.00595D+01 -1.14336D-02 -2.83506D-03 0.00000D+00 3.04878D-02

                    GLOBAL OPTIMAL FOCUS
                    --------------------

   SUM          X           Y           Z          SPOT
  WEIGHTS     LOCATION    LOCATION    PLANE        SIZE
 2.00595D+01 -1.14805D-02 -2.97973D-03 -3.27549D-01 2.82115D-02

          SUMMARY INFORMATION FOR DEDRIQ 'FPSCA' FILE
          -------------------------------------------

++ ID LINE FROM FILE 'DOCXR1 SCAT' ++                       16-07-91 09:32:51
++ID LINE FROM FILE 'DOCXR GI' (X-RAY SYSTEM)               16-07-91 09:01:54
WAVELENGTH :                    6.00000D-07
FILE TYPE NUMBER :                    1
PIXEL ARRAY CENTER X COORD :          0.00000D+00
PIXEL ARRAY CENTER Y COORD :          0.00000D+00
PIXEL ARRAY X LENGTH :                2.00000D+00
PIXEL ARRAY Y LENGTH :                2.00000D+00
NUMBER OF PIXELS IN X DIRECTION :           20
NUMBER OF PIXELS IN Y DIRECTION             20
TOTAL ENERGY IN ARRAY :               2.08285D-03

*** OPTICAL SURFACE ANALYSIS PROGRAM (FPLOOK ) RELEASE (06.0) VAX      PAGE  2
++ ID LINE FROM FILE 'DOCXR1 LOOK'                          16-07-91 10:57:16
+++ PERMANENT FPLOOK  IDENTIFICATION LINE +++               16-07-91 10:57:16
-------------------------------------------------------------------------------
```

Figure 5.61 FPLOOK Printout for DOCXR System

```
                    RUNTIME INFORMATION
                    -------------------

 ++ ID LINE FROM FILE 'DOCXR1 LOOK'                    16-07-91 10:57:16
+++ PERMANENT FPLOOK  IDENTIFICATION LINE +++          16-07-91 10:57:16
WAVELENGTH PARAMETER :          6.00000D-07
FILE TYPE PARAMETER :            27900
  IMPLIES NRAY   =               0
        NARAY  =               1
        NFPSCA =               1
        NFPDFR =               0
PIXEL ARRAY CENTER X COORD :      0.00000D+00
PIXEL ARRAY CENTER Y COORD :      0.00000D+00
PIXEL ARRAY X LENGTH :          2.00000D+00
PIXEL ARRAY Y LENGTH :          2.00000D+00
NUMBER OF PIXELS IN X DIRECTION :          20
NUMBER OF PIXELS IN Y DIRECTION            20
TOTAL ENERGY IN ARRAY :         2.00616D+01
OUTPUT PIXEL ENERGIES (Y/N) :          YES
OUTPUT FPCOM FILE (Y/N) :             YES

                    SPECIFIC PIXEL ENERGIES
                    -----------------------

PIXEL ENERGIES IN COLUMN #'S (  1- 20)  FOR ROW # 20
1.2248E-07  1.0242E-07  9.7469E-08  1.0497E-07  1.2863E-07  2.1661E-07
1.2282E-06  6.7661E-07  1.9651E-07  1.4224E-07  1.4268E-07  1.9649E-07
6.7704E-07  1.2282E-06  2.1657E-07  1.2858E-07  1.0492E-07  9.7390E-08
1.0253E-07  1.2017E-07
PIXEL ENERGIES IN COLUMN #'S (  1- 20)  FOR ROW # 19
2.1020E-07  1.4592E-07  1.2148E-07  1.1595E-07  1.2997E-07  1.8245E-07
5.1464E-07  2.4490E-06  2.6480E-07  1.6877E-07  1.6671E-07  2.6512E-07
2.4312E-06  5.1516E-07  1.8699E-07  1.2990E-07  1.1587E-07  1.1886E-07
1.4197E-07  2.0985E-07

                ROWS 18 THRU 3 ARE NOT SHOWN

PIXEL ENERGIES IN COLUMN #'S (  1- 20)  FOR ROW #  2
2.1648E-07  1.4495E-07  1.2031E-07  1.1586E-07  1.2832E-07  1.8235E-07
4.9683E-07  2.7486E-06  2.6538E-07  1.6881E-07  1.6933E-07  2.6612E-07
2.6661E-06  4.9688E-07  1.8244E-07  1.2993E-07  1.1595E-07  1.2044E-07
1.4515E-07  2.1019E-07

PIXEL ENERGIES IN COLUMN #'S (  1- 20)  FOR ROW #  1
1.2336E-07  1.0466E-07  9.7390E-08  1.0325E-07  1.2856E-07  2.1686E-07
1.1390E-06  7.2004E-07  2.0181E-07  1.4269E-07  1.4269E-07  2.0183E-07
7.0457E-07  1.1773E-06    1661E-07  1.2861E-07  1.0331E-07  9.7469E-08
1.0264E-07  1.2138E-07
```

Figure 5.61 FPLOOK Printout for DOCXR System (continued)

First in the output is a separate list for each of the input specular ray (RAY or ARAY) files (one such file is this example). These lists begin with the two ID lines found in the RAY or ARAY

file header, produced by (NABRAT, DRAT, or DEDRIQ), and (GEOSAC). There follows next information on the minimum and maximum focal plane coordinates and on the planar and global optimal focus. These quantities are to be interpreted the same as the corresponding, equal quantities produced by NABRAT or DRAT. (See Section 5.2 and 5.3).

Following the specular ray file information lists is a separate list for each of the input pixel array (FPSCA, FPDFR, or FPCOM) files (again, one such file in this example). (Note that FPLOOK can use the output of a previous FPLOOK run for input. These lists begin with the two ID lines found in the FPSCA, FPDFR, or FPCOM header, produced by (DEDRIQ, PSF, or FPLOOK), and (GEOSAC or FPLOOK). The next parameter is the wavelength parameter. For an FPSCA or FPDFR file, this parameter is the user-specified wavelength. For an FPCOM file, it is -2 if the FPCOM file contains only specular ray file information, and -1 if the FPCOM file contains FPSCA and FPDFR files with wavelengths that disagree by more that .1%. (If the FPCOM file contains pixel files with wavelengths that do agree within 0.1%, then this parameter is the wavelength). The next parameter is the file type parameter. For an FPSCA file, this number is 1, for an FPDFR file it is 2, and for an FPCOM file it is given by

$$\text{ITYPE} = 30^* N_{RAY} = (30)^2 * N_{ARAY} + (30)^3 * N_{FPSCA} + (30)^4 * N_{FPDFR},$$

Where each N_i is the number of files of the i^{th} type contained the FPCOM file. The next six parameters define the focal plane pixel array and echo the corresponding values in the original SCAT, DIFFR, or LOOK file.

The final parameter is the total energy or ray weight in the array.

Following the pixel array file information lists is a runtime information list, which echoes the parameters in the current LOOK file by giving the same kinds of information about the combined pixel array as was detailed above for the input pixel array files.

The final list, if requested by the LOOK file, gives the energy in each pixel by column and row. Figure 5.62 shows the summary of the relation between column and row numbers, and x- and y-coordinates).

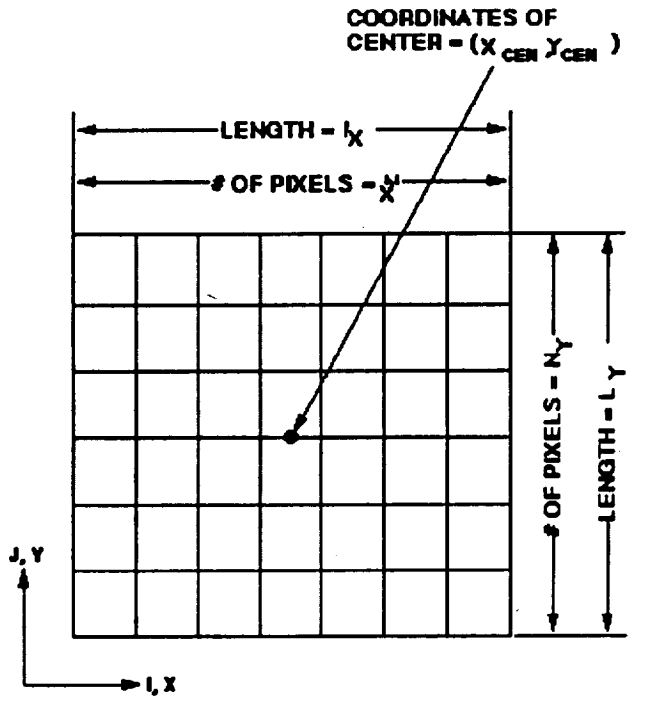

Figure 5.62 Focal Plane Pixel Array Geometry

Just as was the case for DEDRIQ and PSF, a Figure cannot be shown for the FPCOM file, since it is binary, or unformatted. The format is the same as the FPSCA or FPDFR files, though, except for the wavelength and the file type parameters described above. See Table 5.23 for the format of the FPSCA, FPDFR, and FPCOM files.

5.9 COGEN

5.9.1 Introduction

COGEN fits a set of polynomials to a set of actual mirror deformation data so that the resulting polynomial coefficients can later be used by DRAT in ray-tracing the deformed system. As detailed in Section 4.7, the polynomials are Zernike polynomials for a conventional system, and Legendre-Fourier polynomials for an X-ray system. The subroutine structure of COGEN is

shown in Figure 5.63.

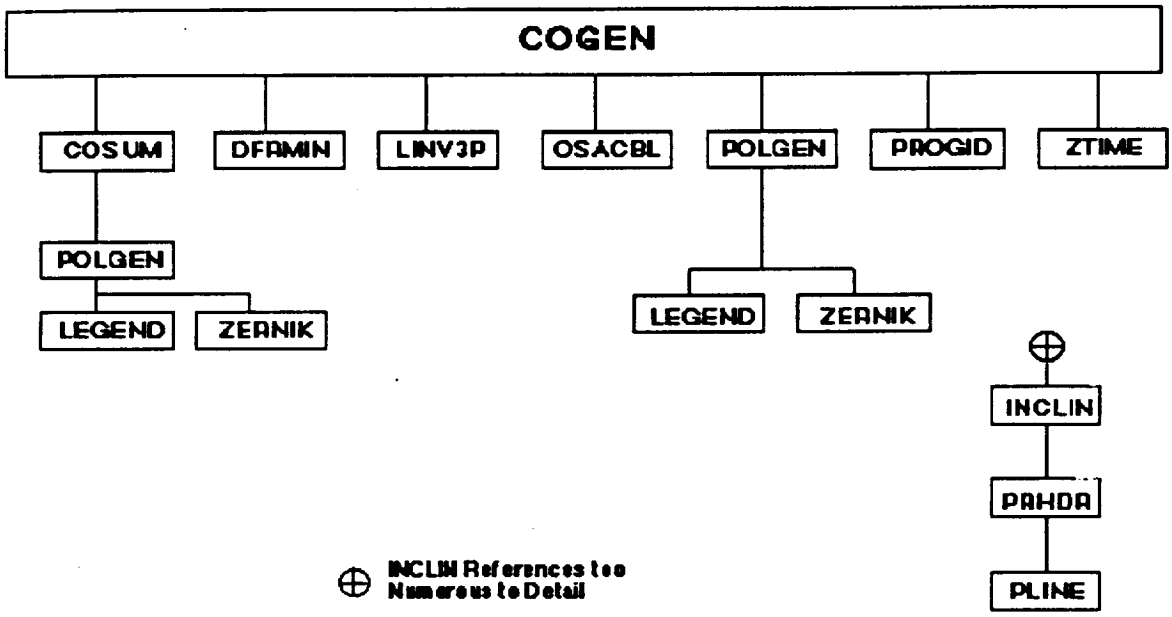

Figure 5.63 External Reference Tree for COGEN

5.9.2 Method

COGEN uses standard least-squares techniques to deduce the polynomial coefficients. In particular, if the deformation data is denoted by f_j at the j^{th} data point, and if the corresponding weighting factor for that point in the fitting is denoted by w_j, and if the i^{th} polynomial evaluated at the j^{th} data point is denoted by g_{ij}, then the quantity σ^2 that is to be minimized is given by

$$\sigma^2 = \sum_j w_j \left(f_j - \sum_i a_i g_{ij}\right)^2 \quad , \tag{5-97}$$

where $\{a_i\}$ is the set of polynomial coefficients to be calculated. At the minimum of σ^2,

$$\frac{\partial \sigma^2}{\partial a_k} = 0 \quad . \tag{5-98}$$

Therefore,

$$\sum_j w_j (2) (f_j - \sum_i a_i g_{ij}) (-g_{kj}) = 0 \tag{5-99}$$

for all k.

If the vector $\vec{c}$ is now defined as

$$(\vec{c})_m = \sum_j w_j f_j g_{mj} \quad , \tag{5-100}$$

and if the matrix $\vec{B}$ is defined as

$$(\vec{B})_{lm} = \sum_j w_j g_{ij} g_{mj} \quad , \tag{5-101}$$

and if the vector $\vec{a}$ of polynomial coefficients is defined as:

$$(\vec{a})_m = a_m \tag{5-102}$$

then the above equation for

$$\frac{\delta \sigma^2}{\delta a_k} = 0 \tag{5-103}$$

can be written in matrix form as

$$\vec{c} = \vec{B}\vec{a} \tag{5-104}$$

Note that $\vec{B}$ and $\vec{c}$ are given by the input data, the weighting factors and the form of the polynomials. Therefore, the vector $\vec{a}$ is found with the matrix equation

$$\vec{a} = (\vec{B}^{-1})\vec{a} \tag{5-105}$$

5.9.3 Inputs and Outputs

The input to COGEN consists of a user-defined file that contains the deformation data and the fitting parameters (DEFDAT file). The output of COGEN consists of terminal and printer output, as well as a DEFORM file to be used later by DRAT. The names, types, formats, and file numbers of all of COGEN's files are summarized in Table 5.32.

Table 5.31
Files Used by COGEN

Input/ Output	File Name	File Type	Format	Logical Record Length	Block Size	File Number
Input	name1	DEFDAT	FB	80	800	1
Output	name1	DEFORM	FB	80	800	2
Output	terminal			80		6
Output	printer			132		8

Table 5.33 shows the format of a DEFDAT file. The first line is an identification line to be used in the printer headers and the DEFORM file. (See Section 5.3.2 for a discussion of the DEFORM file). The next line is a single integer that tells what kind of polynomials are to be fitted. (1 = Zernike and 2 = Legendre-Fourier). The next line consists of two integers (number of data points and number of polynomials) and linear obscuration for conventional systems or three integers for x-ray systems (number of data points, number of Legendre terms, and highest order of Fourier terms). Finally, there is one line for each data point that tells the coordinates (normalized (x,y) for conventional systems or (z,θ) for X-ray systems), the deformation, and the weighting factor.

Table 5.32
DEFDAT File Format

Card 1	RID = 64-character user comments line. Format (16A4)
Card 2	ITYPE = Polynomial type indicator (1 = Zernike, 2 = Legendre-Fourier). Format (I6)
Card 3	NPTSIN, NDFI, NDFJ(x-ray systems only) NPTSIN, NDFI, OBSC (conventional systems only) NPTSIN = # of data points to follow for fitting NDFI = total number of Legendre terms for X-ray system or total number of polynomials for conventional system NDFJ = azimuthal index limit (highest degree of Fourier terms) for X-ray system, not used for conventional system Format (3I6) for X-ray system, or (2I6) for conventional system OBSC = Linear obscuration ratio for conventional systems. Format F9.6 (O.LE.OBSC.LT.1)
One Card Following for Each Data Point Specified by NPTSIN:	
	C01, C02, DF, W. (CO1, C02) = coordinates of data point on mirror surface. For an X-ray, surface (C01, C02) = z, Θ) where it assumed that z is normalized such that $-1 \leq z \leq 1$. Θ is expressed in radians. For a conventional system (C01, C02) = (x,y) where it is assumed that x and y are normalized such that $(x_2 + y_2) \leq 1$. DF = the actual deformation at this data point W = the weighting factor to be applied to this point in the least squares fit. W is often set equal to one by the user for every data point. W must be positive. Format (4F16.0)

Figure 5.64 shows a DEFDAT file used to demonstrate the use of COGEN. Figure 5.65 shows the resultant printer output, and Figure 5.66 shows the resultant DEFORM file. (Note that this is not the DEFORM file used previously in this report to demonstrate the use of DRAT).

```
+ ID LINE FOR FILE 'DEMO DEFDAT' ++
 1
 149   21  0.0
-0.999900E+00  0.000000E+00  0.506240E-05  0.100000E+01
-0.857057E+00 -0.428529E+00  0.506240E-05  0.100000E+01
-0.857057E+00 -0.285686E+00  0.189840E-05  0.100000E+01
-0.857057E+00 -0.142843E+00  0.126560E-05  0.100000E+01
-0.857057E+00  0.000000E+00  0.632800E-06  0.100000E+01
-0.857057E+00  0.142843E+00  0.126560E-05  0.100000E+01
-0.857057E+00  0.285686E+00  0.632800E-06  0.100000E+01
-0.857057E+00  0.428529E+00  0.189840E-05  0.100000E+01
                          Thru
 0.000000E+00 -0.285686E+00  0.000000E+00  0.100000E+01
 0.000000E+00 -0.142843E+00 -0.189840E-05  0.100000E+01
 0.000000E+00  0.000000E+00  0.000000E+00  0.100000E+01
 0.000000E+00  0.142843E+00 -0.949200E-06  0.100000E+01
                          Thru
 0.857057E+00 -0.428529E+00  0.442960E-05  0.100000E+01
 0.857057E+00 -0.285686E+00  0.000000E+00  0.100000E+01
 0.857057E+00 -0.142843E+00 -0.126560E-05  0.100000E+01
 0.857057E+00  0.000000E+00 -0.126560E-05  0.100000E+01
 0.857057E+00  0.142843E+00 -0.632800E-06  0.100000E+01
 0.857057E+00  0.285686E+00  0.189840E-05  0.100000E+01
 0.857057E+00  0.428529E+00  0.506240E-05  0.100000E+01
 0.999900E+00  0.000000E+00  0.506240E-05  0.100000E+01
```

Figure 5.64 DEFDAT File for COGEN Example

++ ID LINE FOR FILE 'DEMO DEFDAT' ++ 16-07-91 11:29:16

POLYNOMIAL COEFFICIENT SUMMARY

TYPE OF POLYNOMIALS: ZERNIKE
OF POLY'S, OBSCURATION: 21 0.000000
OF GOOD DATA POINTS: 149
SIGMA**2 OF ACTUAL DATA: 4.1837E-12

INDECES L	INDECES MCOS	INDECES MSIN	COEFFICIENT VALUE	SIGMA**2 OF POLY #I	SIGMA**2 OF POLY'S 1 TO I	SIGMA**2 OF DATA - POLY'S
0			1.5736E-07	2.4762E-14	2.4762E-14	4.2052E-12
1	1		2.8293E-07	8.0048E-14	1.0481E-13	4.1495E-12
1		1	-2.8390E-08	8.0599E-16	1.0562E-13	4.1492E-12
2			1.4859E-06	2.2078E-12	2.3134E-12	2.3838E-12
2	2		5.3409E-08	2.8525E-15	2.3163E-12	2.3812E-12
5		3	-2.2698E-07	5.1522E-14	3.9125E-12	1.0029E-12
5	5		-1.4171E-07	2.0080E-14	3.9326E-12	9.8552E-13
5		5	1.2146E-07	1.4753E-14	3.9473E-12	9.7275E-13

Figure 5.65 COGEN Printout

```
+ ID LINE FOR FILE 'DEMO DEFDAT' ++                          21 0.000000
  1.57360E-07  2.82927E-07 -2.83900E-08  1.48587E-06  5.34087E-08
  2.42042E-07  1.65065E-07  1.39859E-07 -5.89267E-07 -2.39419E-07
  9.12022E-07  2.11450E-08  7.85998E-08 -3.69196E-07  2.04407E-07
  1.17794E-07 -4.29752E-09  6.58739E-08 -2.26985E-07 -1.41705E-07
  1.21464E-07
```

Figure 5.66 DEFORM File from COGEN Example

The format of the DEFORM file is discussed in Section 5.3.2. The first data line of the printed output tells what type of polynomial was used for fitting. The next line tells the number of polynomials fitted, and, for X-ray systems, the number of Legendre terms and the highest order of Fourier terms. The next line tells the number of data points given by the user which were not outside the legal coordinate range. The next line tells the weighted mean square deformation as defined by the user's data. The rest of the information is given for each fitted polynomial. For polynomial number i, this information consists of the radial (for conventional systems) or Legendre (for X-ray systems) order of the polynomial; the azimuthal (cosine) index; the azimuthal (sine) index; the fitted value of the coefficient; the σ^2 value of the polynomial as discussed at the end of Section 4.7; the running sum of σ^2 as defined above for polynomials #(1

to i); and the weighted mean square value over the data points of ((deformation data) - (value found by evaluating polynomials #(1 to i)). Note that the running sum of σ^2 should approach the weighted mean square deformation as defined by the user's data, and that the number in the final column should approach zero as all of the polynomials are accounted for.

5.10 Annular Zernike Polynomials (ZERGEN)

OSAC allows the use of conventional Zernike polynomials (i.e., orthonormalized over a full unit circle) when analyzing conventional optical systems and also the use of polynomials which are orthonormalized over a unit-radius annulus with any desired inner obscuration. For simplicity, we took the approach of always specifying a linear obscuration ratio, but to allow the ratio to be zero to include conventional full circle Zernike polynomials. The annular Zernike polynomials are used in the ray tracing program DRAT, as well as in the deformation data fitting program COGEN. Also, the polynomials used in the file conversion and sensitivity analyses described in Sections 5.11 and 5.12.). In addition, the OSAC program entitled ZERGEN generates and displays the form of any set of annular Zernike polynomials (i.e., any number of polynomials from 3 to the OSAC maximum of 325, and any obscuration ratio less than one.)

The COGEN, ZERGEN, and DRAT programs all rely on the parameter OBSC (the linear obscuration ratio of the annulus over which the Zernike polynomials are orthonormalized). OBSC must be greater than or equal to zero, and less than one. The parameter OBSC is to be inserted in deformation data (DEFDAT, or DFD) files used by COGEN, deform (DEFORM, or DFR) files used by DRAT, and Zernike definition (ZDF) files used by ZERGEN. (The COGEN program, which outputs a DEFORM file for later use by DRAT, takes care of transferring the OBSC parameter from the input DEFDAT file to the output DEFORM file.) Table 5.32 defines the DEFDAT file, and Table 5.15 defines the DEFORM file.

As mentioned above, the ZERGEN program uses a Zernike definition (ZDF) file to define the number of polynomials to describe, and the obscuration ratio. Table 5.33 lists all of the input and output files used by ZERGEN. Table 5.34 defines the new Zernike definition (ZDF) file in detail. There is one final note on absolute numerical accuracy. Because there are no closed form recursion relations for annular Zernike polynomials (as there are for full circle Zernike polynomials and for Legendre polynomials), OSAC uses a whole new Gram-Schmidt approach for generating the annular polynomials.

Table 5.33
Files Used by the ZERGEN Program
(File names are those used by the OSAC.COM file on the VAX system. A file name beginning with "fn1" implies that the name is entered by the user.)

Input/Output	File Name	Formatted/Unformatted	File Number
Input	fn1.ZDF	Formatted	1
Output	(terminal)	Formatted	6
Output	ZERGEN.OUT	Formatted	8

Table 5.34
Definition of the Zernike Definition (ZDF) File
(used as input to the ZERGEN program)

Card	Item	Data Type	Format	Description
1	GID	CHAR*4(16)	16A4	User comments
2	NDF	I*4	(free format)	No. of polynomials
	OBSC	R*8	(free format)	Linear obscuration

Gram-Schmidt procedures on computers have inevitable roundoff errors which are not present for recursion relation approaches. These roundoff errors become more noticeable for polynomials far down in the sequence (in our case, polynomials with many terms). We have found that this is not a real problem for OSAC. In particular, if the user specifies even as many as approximately 250 polynomials, there is no significant error at all. This should account for all cases of real interest. However, in some of the last polynomials (those with 11 or more terms), there is an error in the definition of a few percent at most. This should be of little concern, for three reasons: (1) this many polynomials will probably never be used; (2) a few percent is not a large error in defining high order surface errors; and (3) COGEN and DRAT are consistent with each other, so that the errors fit by COGEN are precisely those used by DRAT.

For a demonstration of the ZERGEN program, Figure 5.67 shows two sample Zernike definition (ZDF) files. They both call for 37 Zernike polynomials. The first has an obscuration ratio of 0.00 (full circle polynomials), while the second has an obscuration of 0.33 (annular polynomials).

```
Z37A.ZDF  - TEST RUN FOR 37 FULL CIRCLE ZERNIKE'S
37  0.0

Z37B.ZDF  - TEST RUN FOR 37 FULL CIRCLE ZERNIKE'S FOR OBSC = .33
37  0.33
```

Figure 5.67

Sample Zernike Definition (ZDF) Fles Used to Demonstrate the ZERGEN Program. The First File is Used to Define Conventional (Full Circle) Zernike Polynomials, While the Second is Used to Define Polynomials Annularized Over an Annulus with a Linear Obscuration Ratio of .33. The ZERGEN Printed Results Are Shown in Figures 5.68 and 5.69.

Figures 5.68 and 5.69 show the ZERGEN outputs from these two input ZDF files. The outputs are fairly self-explanatory. Each polynomial is defined as an overall normalization constant, multiplied first by a power series in r (whose highest order coefficient is one), and then by a cosine or sine of a multiple of the polar angle theta.

5.11 OPD File Conversion (OPDCNV)

OSAC allows for direct least squares fitting of surface deformation data to a set of low frequency functions (Zernike polynomials or Legendre-Fourier functions). We can convert an Optical Path Difference (OPD) file to the same format as a surface deformation data (DEFDAT, or DFD) file, so that the wavefront errors can be directly fit to a set of annular Zernike polynomials. (See Section 5.10 for a discussion of the annular Zernike polynomials.)

To convert the OPD files, there is an OSAC program entitled OPDCNV, which takes an OPD file and an OPD conversion (CNV) file (and a GX file for system checks) as input, and outputs the resulting deformation data (DEFDAT, or DFD) file. Table 5.35 lists all of the input and output files used by OPDCNV. Table 5.36 defines the OPD conversion (CNV) file in detail.

DEFINITION OF 37 ZERNIKE POLYNOMIALS
ORTHONORMALIZED OVER AN ANNULAR APERTURE
RADIUS OF CENTRAL OBSCURATION = 0.0000

NUM.	NORMALIZATION FACTOR	POLYNOMIAL DEFINITION
1	1.0000000D+00	
2	2.0000000D+00	R COS(O)
3	2.0000000D+00	R SIN(O)
4	3.4641016D+00	(R^(2) + -0.500000)
5	2.4494897D+00	(R^(2)) COS(2 O)
6	2.4494897D+00	(R^(2)) SIN(2 O)
7	8.4852814D+00	(R^(3) + -0.666667 R) COS(O)
8	8.4852814D+00	(R^(3) + -0.666667 R) SIN(O)
9	2.8284271D+00	(R^(3)) COS(3 O)
10	2.8284271D+00	(R^(3)) SIN(3 O)
11	1.3416408D+01	(R^(4) + -1.000000 R^(2) + 0.166667)
12	1.2649111D+01	(R^(4) + -0.750000 R^(2)) COS(2 O)
13	1.2649111D+01	(R^(4) + -0.750000 R^(2)) SIN(2 O)
14	3.1622777D+00	(R^(4)) COS(4 O)
15	3.1622777D+00	(R^(4)) SIN(4 O)
16	3.4641016D+01	(R^(5) + -1.200000 R^(3) + 0.300000 R) COS(O)
17	3.4641016D+01	(R^(5) + -1.200000 R^(3) + 0.300000 R) SIN(O)
18	1.7320508D+01	(R^(5) + -0.800000 R^(3)) COS(3 O)
19	1.7320508D+01	(R^(5) + -0.800000 R^(3)) SIN(3 O)
20	3.4641016D+00	(R^(5)) COS(5 O)
21	3.4641016D+00	(R^(5)) SIN(5 O)
22	5.2915026D+01	(R^(6) + -1.500000 R^(4) + 0.600000 R^(2) + -0.050000)
23	5.6124861D+01	(R^(6) + -1.333333 R^(4) + 0.400000 R^(2)) COS(2 O)
24	5.6124861D+01	(R^(6) + -1.333333 R^(4) + 0.400000 R^(2)) SIN(2 O)
25	2.2449944D+01	(R^(6) + -0.833333 R^(4)) COS(4 O)
26	2.2449944D+01	(R^(6) + -0.833333 R^(4)) SIN(4 O)
27	3.7416574D+00	(R^(6)) COS(6 O)
28	3.7416574D+00	(R^(6)) SIN(6 O)
29	1.4000000D+02	(R^(7) + -1.714286 R^(5) + 0.857143 R^(3) + -0.114286 R) COS(O)
30	1.4000000D+02	(R^(7) + -1.714286 R^(5) + 0.857143 R^(3) + -0.114286 R) SIN(O)
31	8.4000000D+01	(R^(7) + -1.428571 R^(5) + 0.476190 R^(3)) COS(3 O)
32	8.4000000D+01	(R^(7) + -1.428571 R^(5) + 0.476190 R^(3)) SIN(3 O)
33	2.8000000D+01	(R^(7) + -0.857143 R^(5)) COS(5 O)
34	2.8000000D+01	(R^(7) + -0.857143 R^(5)) SIN(5 O)
35	4.0000000D+00	(R^(7)) COS(7 O)
36	4.0000000D+00	(R^(7)) SIN(7 O)
37	2.1000000D+02	(R^(8) + -2.000000 R^(6) + 1.285714 R^(4) + -0.285714 R^(2) + 0.014286)

Figure 5.68 ZERGEN Output for 37 Full Circle Zernikes

Z37B.ZDF - TEST RUN FOR 37 ZERNIKE'S FOR OBSC = .33 16-01-92 14:13:45

DEFINITION OF 37 ZERNIKE POLYNOMIALS
ORTHONORMALIZED OVER AN ANNULAR APERTURE
RADIUS OF CENTRAL OBSCURATION = 0.3300

NUM.	NORMALIZATION FACTOR	POLYNOMIAL DEFINITION
1	1.0000000D+00	
2	1.8992573D+00	R COS(O)
3	1.8992573D+00	R SIN(O)
4	3.8874443D+00	(R^(2) + -0.554450)
5	2.3137662D+00	(R^(2)) COS(2 O)
6	2.3137662D+00	(R^(2)) SIN(2 O)
7	8.3345629D+00	(R^(3) + -0.673796 R) COS(O)
8	8.3345629D+00	(R^(3) + -0.673796 R) SIN(O)
9	2.6701690D+00	(R^(3)) COS(3 O)
10	2.6701690D+00	(R^(3)) SIN(3 O)
11	1.6895979D+01	(R^(4) + -1.108900 R^(2) + 0.241243)
12	1.2033645D+01	(R^(4) + -0.750864 R^(2)) COS(2 O)
13	1.2033645D+01	(R^(4) + -0.750864 R^(2)) SIN(2 O)
14	2.9851527D+00	(R^(4)) COS(4 O)
15	2.9851527D+00	(R^(4)) SIN(4 O)
16	3.6321412D+01	(R^(5) + -1.230566 R^(3) + 0.323221 R) COS(O)
17	3.6321412D+01	(R^(5) + -1.230566 R^(3) + 0.323221 R) SIN(O)
18	1.6372202D+01	(R^(5) + -0.800100 R^(3)) COS(3 O)
19	1.6372202D+01	(R^(5) + -0.800100 R^(3)) SIN(3 O)
20	3.2700486D+00	(R^(5)) COS(5 O)
21	3.2700486D+00	(R^(5)) SIN(5 O)
22	7.4782449D+01	(R^(6) + -1.663350 R^(4) + 0.803136 R^(2) + -0.104406)
23	5.4696500D+01	(R^(6) + -1.340332 R^(4) + 0.405641 R^(2)) COS(2 O)
24	5.4696500D+01	(R^(6) + -1.340332 R^(4) + 0.405641 R^(2)) SIN(2 O)
25	2.1196833D+01	(R^(6) + -0.833345 R^(4)) COS(4 O)
26	2.1196833D+01	(R^(6) + -0.833345 R^(4)) SIN(4 O)
27	3.5320535D+00	(R^(6)) COS(6 O)
28	3.5320535D+00	(R^(6)) SIN(6 O)
29	1.6007456D+02	(R^(7) + -1.781299 R^(5) + 0.948280 R^(3) + -0.142530 R) COS(O)
30	1.6007456D+02	(R^(7) + -1.781299 R^(5) + 0.948280 R^(3) + -0.142530 R) SIN(O)
31	7.9942692D+01	(R^(7) + -1.429930 R^(5) + 0.477328 R^(3)) COS(3 O)
32	7.9942692D+01	(R^(7) + -1.429930 R^(5) + 0.477328 R^(3)) SIN(3 O)
33	2.6432307D+01	(R^(7) + -0.857144 R^(5)) COS(5 O)
34	2.6432307D+01	(R^(7) + -0.857144 R^(5)) SIN(5 O)
35	3.7759238D+00	(R^(7)) COS(7 O)
36	3.7759238D+00	(R^(7)) SIN(7 O)
37	3.3305313D+02	(R^(8) + -2.217800 R^(6) + 1.674333 R^(4) + -0.493099 R^(2) + 0.045573)

Figure 5.69 ZERGEN Output for 37 Annular Zernikes, With An Obscuration Ratio of 0.33

Table 5.35
Files Used by the OPDCNV Program
(File names are those used by the OSAC.COM file on the VAX system. An input file name beginning with "fn1," fn2," or "fn3" implies that the name is entered by the user. As shown, the OSAC.COM file is currently configured to give the output deformation data (DFD) file the same name root as the input OPD file)

Input/Output	File Name	Formatted/Unformatted	File Number
Input	fn1.OPD	Formatted	1
Input	fn2.CNV	Formatted	3
Input	fn3.GX	Formatted	7
Output	fn1.DFD	Formatted	2
Output	(terminal)	Formatted	6
Output	OPDCNV.OUT	Formatted	8

Table 5.36
Definition of the OPD Conversion (CNV) File
(used as input to the OPDCNV program)

Card	Item	Data Type	Format	Description
1	GID	CHAR*4(16)	16A4	User comments
2	NDF	I*4	(free format)	No. of polynomials
	OBSC	R*8	(free format)	Linear obscuration

Figure 5.70 shows the surface deformation (DEFORM, or DFR) file entitled ELEM1.DFR, used for the first surface. Figures 5.71 and 5.72 show the printouts from running DRAT on the ELLIP3 system, as opposed to NABRAT. Note the non-negligible, aberrated spot size in Figure 5.72. Figure 5.73 shows a printout from the OPD program. Note the non-negligible RMS Optical Path Difference (OPD).

```
ELEM1.DFR - ANNULAR ZERNIKE'S FOR ELLIP3 SURF 1                    11 0.312500
  0.00000E+00   0.00000E+00   0.00000E+00   1.00000E-05  -2.00000E-05
  3.00000E-05  -4.00000E-05   5.00000E-05  -6.00000E-05   7.00000E-05
 -8.00000E-05
```

Figure 5.70
DRF File (ELEM1.DFR) Giving the Nominal First Surface Deformations for the ELLIP3 System.

ELLIP3.GI - 2 CONFOCAL ELLIPSES, .33 OBSC, SURF 1 DEFORM 20-01-92 12:44:32

SUMMARY OF DEFORMATION COEFFICIENTS

ELEM1.DFR - ANNULAR ZERNIKE'S FOR ELLIP3 SURF 1
TOTAL NUMBER OF COEFFICIENTS = 11
LINEAR OBSCURATION RATIO = 0.312500
INDEX OF LARGEST CONTRIBUTION = 11
LARGEST CONTRIBUTION = 8.0000000E-05
ROOT SUM SQUARE = 1.4282857E-04
SUM OF THE WEIGHTED SQUARES = 2.0400000E-08

THE DEFORMATION COEFFICIENTS:

0.00000E+00 0.00000E+00 0.00000E+00 1.00000E-05 -2.00000E-05
3.00000E-05 -4.00000E-05 5.00000E-05 -6.00000E-05 7.00000E-05
-8.00000E-05

RAY SUMMARY REPORT

PREVIOUS SURFACES

STARTED		FAILED		SUCCEEDED	
NUM	WEIGHT	NUM	WEIGHT	NUM	WEIGHT
121	121.00000	0	0.00000	121	121.00000

CURRENT SURFACE (# 1)

STARTED		FAILED		SUCCEEDED	
NUM	WEIGHT	NUM	WEIGHT	NUM	WEIGHT
121	121.00000	0	0.00000	121	121.00000

Figure 5.71 DRAT Output for ELLIP3, Surface 1

ELLIP3.GI - 2 CONFOCAL ELLIPSES, .33 OBSC, SURF 1 DEFORM 20-01-92 12:44:59
ELLIP3.GI - 2 CONFOCAL ELLIPSES, .33 OBSC, SURF 1 DEFORM 20-01-92 12:44:32

RAY SUMMARY REPORT

PREVIOUS SURFACES

STARTED		FAILED		SUCCEEDED	
NUM	WEIGHT	NUM	WEIGHT	NUM	WEIGHT
121	121.00000	0	0.00000	121	121.00000

CURRENT SURFACE (# 2)

STARTED		FAILED		SUCCEEDED	
NUM	WEIGHT	NUM	WEIGHT	NUM	WEIGHT
121	121.00000	0	0.00000	121	121.00000

FOCAL PLANE HITS: GFOC - 7.5197880300000D+01 ZOFF = 0.000000D+00

MINIMUM		MAXIMUM	
X	Y	X	Y
6.47781676E+00	1.47493962E+01	6.53381318E+00	1.47904351E+01

PLANAR OPTIMAL FOCUS

SUM WEIGHTS	X LOCATION	Y LOCATION	Z SPOT PLANE	SIZE
1.21000D+02	6.51260D+00	1.47678D+01	0.00000D+00	1.19327D-02

GLOBAL OPTIMAL FOCUS

SUM WEIGHTS	X LOCATION	Y LOCATION	Z SPOT PLANE	SIZE
1.21000D+02	6.51384D+00	1.47696D+01	-2.95609D-02	1.11504D-02

Figure 5.72 DRAT Output for ELLIP3, Surface 2

```
*** OPTICAL SURFACE ANALYSIS PROGRAM (OPD    ) RELEASE (06.0) VAX     PAGE  1
ELLIP3.GI - 2 CONFOCAL ELLIPSES, .33 OBSC, SURF 1 DEFORM 2   20-01-92 12:46:05
ELLIP3.GI - 2 CONFOCAL ELLIPSES, .33 OBSC, SURF 1 DEFORM     20-01-92 12:44:32
```

OPD CALCULATION SUMMARY REPORT

TYPE OF SYSTEM (XRAY / CONV) :	CONVENTIONAL
SOURCE OF INPUT RAY FILE :	NABRAT/DRAT
NUMBER OF SURFACES IN SYSTEM :	2
NUMBER OF TRACED RAYS :	121
NUMBER OF SUCCESSFUL RAYS :	121
TOTAL RAY WEIGHT :	121.00000
X COORD OF REF SPHERE (BEST FOCUS) :	6.51260D+00
Y COORD OF REF SPHERE (BEST FOCUS) :	1.47678D+01
EFFECTIVE FOCAL LENGTH :	1.12412D+02
INNER RADIUS OF TRACED ANNULUS :	4.95100D+00
OUTER RADIUS OF TRACED ANNULUS :	1.49990D+01
RMS OPD VALUE OVER PUPIL :	3.65792D-04

Figure 5.73 OPD Output for ELLIP3

Figure 5.74 shows the OPD conversion (CNV) file entitled ELLIP3A.CNV, used to tell the new OPDCNV program to convert the OPD file into a format suitable for fitting by COGEN.

```
ELLIP3A.CNV - 11-ZERNIKE DEMO OF OPDCNV
 11 4.95 15.00
```

Figure 5.74 CNV File (ELLIP3A.CNV) for ELLIP3 System

Note that 11 Zernike polynomials have been requested. The polynomials are defined over an annulus which slightly overfills the pupil defined in the original geometry information (GI) file (see Figure 5.15). Note that the ratio of the inner to outer radius of the annulus is (4.95/15.00)=0.33. This obscuration ratio will be used later in Section 5.12 for sensitivity analysis demonstrations.

Figure 5.75 shows the output from the OPDCNV program. This output is fairly self-explanatory, and mostly echoes the parameters defined in the OPD conversion (CNV) input file. Note that OPDCNV also produces a deformation data (DEFDAT, or DFD) file for fitting by COGEN.

```
*** OPTICAL SURFACE ANALYSIS PROGRAM (OPDCNV ) RELEASE (06.0) VAX      PAGE   1
ELLIP3.GI - 2 CONFOCAL ELLIPSES, .33 0BSC, DURF 1 DEFORM 2    20-01-92 12:46:05
ELLIP3.GI - 2 CONFOCAL ELLIPSES, .33 0BSC, DURF 1 DEFORM      20-01-92 12:44:32
-------------------------------------------------------------------------------

HEADER TEXT FROM CNV FILE INPUT:
   ELLIP3A.CNV - 11-ZERNIKE DEMO OF OPDCNV

NUMBER OF RAYS CONVERTED:       121
NUMBER OF ZERNIKE POLYNOMIALS:  11

RADIUS OF INNER PUPIL OBSCURATION:  4.9500000000D+00
OUTER RADIUS OF PUPIL:              1.5000000000D+01
X-COORDINATE OF PUPIL CENTER:       9.6510050330D+00
Y-COORDINATE OF PUPIL CENTER:       1.9476640440D+01
```

Figure 5.75 OPDCNV Output for ELLIP3

Figure 5.76 shows the results of running COGEN on this file. Note the non-negligible coefficients, resulting from the deformed first surface. In fact, the reader can verify that the wavefront coefficients are roughly twice the surface coefficients defined in Figure 5.70 as would be expected. The small differences are attributable to the tilt, focus, astigmatism, and coma caused by the limited accuracy used in defining the tilts and decenters in this non-symmetric system.

POLYNOMIAL COEFFICIENT SUMMARY

TYPE OF POLYNOMIALS: ZERNIKE
OF POLY'S, OBSCURATION: 11 0.330000
OF GOOD DATA POINTS: 121
SIGMA**2 OF ACTUAL DATA: 1.3380E-07

INDECES L MCOS MSIN	COEFFICIENT VALUE	SIGMA**2 OF POLY #I	SIGMA**2 OF POLY'S 1 TO I	SIGMA**2 OF DATA-POLY'S
0	3.2272E-05	1.0415E-09	1.0415E-09	1.3485E-07
1 1	1.3639E-04	1.8602E-08	1.9644E-08	1.1835E-07
1 1	-1.8704E-04	3.4984E-08	5.4627E-08	8.7177E-08
2	3.6651E-05	1.3433E-09	5.5970E-08	8.55 CE-08
2 2	-3.8098E-05	1.4514E-09	5.7422E-08	8.405 7E-08
2 2	5.8027E-05	3.3672E-09	6.0789E-08	8.0572E-08
3 1	-7.3864E-05	5.4559E-09	6.6245E-08	7.4327E-08
3 1	9.7628E-05	9.5313E-09	7.5776E-08	6.3417E-08
3 3	-1.1380E-04	1.2950E-08	8.8726E-08	4.9456E-08
3 3	1.3296E-04	1.7679E-08	1.0641E-07	3.0396E-08
4	-1.4464E-04	2.0921E-08	1.2733E-07	4.7761E-12

Figure 5.76
COGEN Output for ELLIP3. This Output Shows the Wavefront Coefficients for the Nominal System before any Constructional Changes have been applied.

There is one final note on file names. Although Table 5.35 lists the file naming conventions for OPDCNV, there is a possible pitfall to stress. In OSAC, there are files which have identical formats, but which serve different purposes. Specifically, the wavefront deformation data (DEFDAT, or DFD) files resulting from the OPD file conversions are identical to the surface deformation files from before. This is because both kinds of files serve as input to COGEN. However, the user should be aware that the deformation data files can apply either to wavefronts or to surfaces, and should choose file names appropriately. The same caution applies to the corresponding deform (DEFORM, or DFR) files output by COGEN.

5.12 Wavefront Tolerancing (WFSNS1, WFSNS2, and OPDGEN)

OSAC has a capability to analyze the sensitivities of wavefront errors to various constructional changes within the optical system. Furthermore, OSAC can also use the derived sensitivities to calculate the wavefront from a specific set of constructional changes, without having to perform a new ray trace. This gives OSAC tolerancing capabilities which utilize the annular Zernike polynomial and OPD file conversion enhancements (see Sections 5.10 and 5.11). In addition, there are three OSAC programs, entitled

(1) WFSNS1;
(2) WFSNS2; and
(3) OPDGEN.

(Note: These programs assume that the user has already characterized the nominal optical system using the GEOSAC, DRAT (or NABRAT), OPD, OPDCNV, and COGEN programs, which give complete system characterization including wavefront Zernike decomposition.)

WFSNS1 starts with an existing, nominal OSAC optical system, and generates the OSAC input files for similar systems with the required constructional changes. After other OSAC programs have been run for these changed optical systems, WFSNS2 collects the output files and generates a file which defines the appropriate wavefront sensitivities. Finally, OPDGEN uses the sensitivity file and a set of user specified constructional changes, and generates the resulting Optical Path Difference (OPD) file. The user may then fit this file to a set of Zernike polynomials, calculate the point spread function, or perform various other OSAC analysis functions on it. Section 5.12 covers the WFSNS1, WFSNS2, and OPDGEN programs in more detail.

On the VAX system, the OSAC programs are all accessed and run through a Digital Control Language (DCL) file entitled OSAC.COM. It allows the user to define file names interactively, so that the OSAC programs can be run quickly and easily. The OSAC.COM file and other COM files enable the WFSNS1, WFSNS2, and OPDGEN programs can be run easily. After typing "OSAC" to activate the OSAC.COM file, the user is prompted for a program to run. The options for wavefront sensitivity calculations are WFSENS and OPDGEN. If the user selects WFSENS, WFSNS1 is first run to generate the OSAC input files; various other OSAC programs are run to analyze the changed optical systems; and WFSNS2 is run to generate the sensitivity file. If the user selects OPDGEN, OPDGEN is run to generate an OPD file for a specific set of constructional changes. Sections 5.12.4 and 5.12.5 describe in more detail the WFSENS and OPDGEN options in running OSAC via the OSAC.COM file.

5.12.1 WFSNS1 Program Description

WFSNS1 is the first of the three wavefront sensitivity modules to be run. WFSNS1 starts with an existing, nominal OSAC optical system, and generates the OSAC input files for similar systems with the required constructional changes.

The nominal optical system is defined by the geometry information (GI) file, and optionally by deformation (DEFORM, or DFR) files containing polynomial coefficients for the optical surfaces. WFSNS1 also uses a change definition (CDF) file supplied by the user, which defines the constructional changes to be considered. WFSNS1 produces a set of output GI files (and DFR files if appropriate) incorporating the constructional changes, and an OPD conversion (CNV) file for later wavefront fitting to annular Zernike polynomials. (See Section 5.10 for a discussion of the annular Zernike polynomials, and Section 5.11. for a discussion of the wavefront fitting capability.) Figure 5.77 shows this file interaction for WFSNS1, and additionally shows the entire program and data flow for WFSNS1, WFSNS2, and OPDGEN.

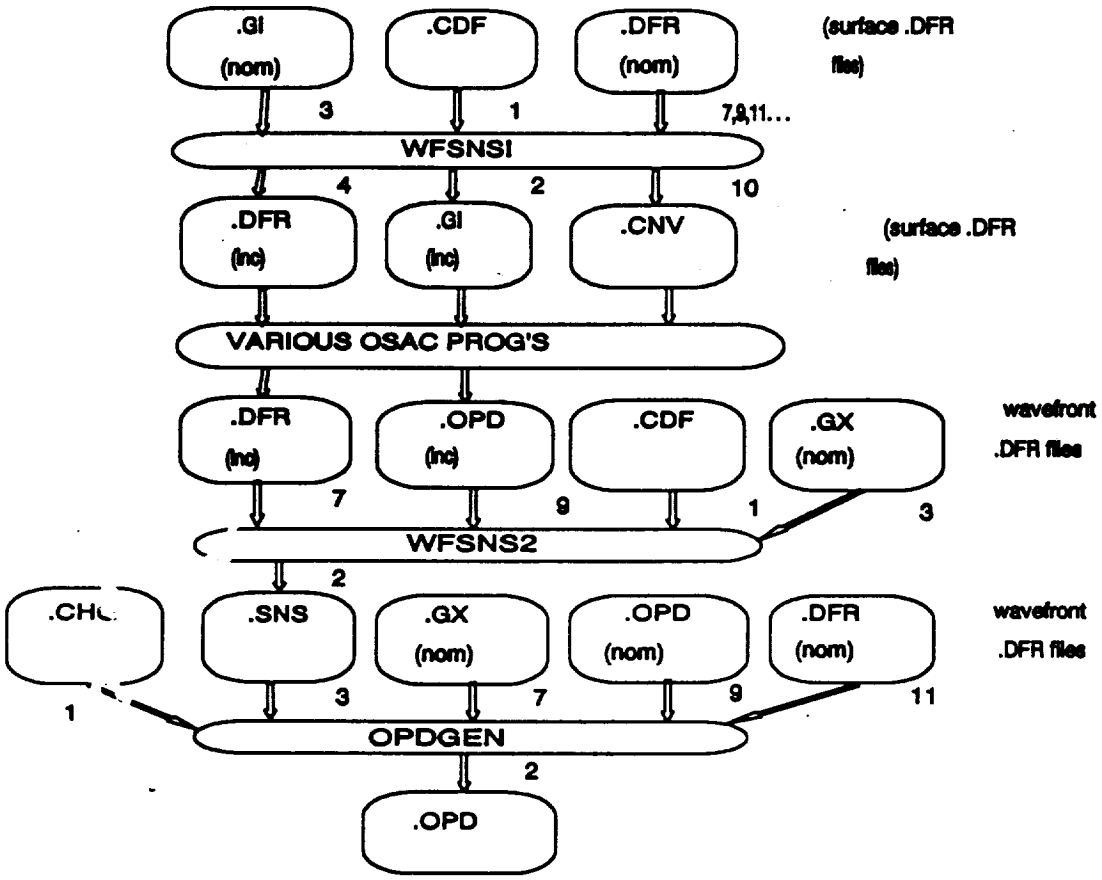

Figure 5.77

Data and Program Flow for the WFSNS21, WFSNS2, and OPDGEN Programs. The Numbers to the Right of the Arrows Denote the FORTRAN File Numbers. "Nom" means a File for the Nominal Optical System, and "inc" means a File for one of the Systems with an Incremented Constructional Change Parameter.

Figure 5.77 will be frequently referred to in Sections 5.12.1 through 5.12.5. Table 5.37 lists all of the input and output files used by WFSNS1. Table 5.38 defines the new change definition (CDF) file in detail.

Table 5.37
Files Used by the WFSNS1 Program
(File names are those used by the OSAC.COM file on the VAX system. An input file name beginning with "fn1," "fn2," ... implies that the name is entered by the user. Figure 5.77 shows the data and program flow for the programs WFSNS1, WFSNS2, and OPDGEN in more detail)

Input/Output	File Name	Formatted/Unformatted	File Number
Input	fn1.GI	Formatted	3
Input	fn2.CDF	Formatted	1
Input	fn3,4,...DFR	Formatted	7,9,11,...
Output	GI -- Note 1	Formatted	2
Output	DFR -- Note 2	Formatted	4
Output	WFSNS1.CNV	Formatted	10
Output	(terminal)	Formatted	6
Output	WFSNS1.OUT	Formatted	8

Note 1: The GI files are named as follows:
GI file name = "WFPnnn.GI"
and "WFMnnn.GI"
where nnn is a three-digit number which tells the number of the constructional change, with the first change being designated 001, etc. The "P" ("WFPnnn.GI") corresponds to the nominal file Plus the constructional change, and the "M" ("WFMnnn.GI") corresponds to the nominal file Minus the constructional change.

Note 2: The (surface) DFR files are named as follows
DFR file name = "WFPnnn.Xmm"
and "WFMnnn.Xmm"
where nnn is as above, and mm is a two digit number which tells the surface number, with the first surface being designated 01, etc. The "P" and "M" are as above.

Table 5.38
Definition of the Change Definition (CDF) File
(used as input to the WFSNS1 and WFSNS2 programs)

Card	Item	Data Type	Format	Description
1	RID	CHAR*4(16)	16A4	User comments
2	NDF	I*4	(free format)	No. of polynomials
	ROBSC	R*8	(free format)	Inner radius of pupil obscuration
	RPUPIL	R*8	(free format)	Outer radius of pupil
3	NCH	I*4	(free format)	Number of constructional changes
4,5,...	ICHS	I*4	(free format)	Code number for the next constructional change (see Section 5.12)
	CHGS	R*8	(free format)	Numerical incremental value for the next constructional change (see Section 5.12)

Note: It is assumed that there is one card for each constructional change, starting with card 4, containing the values of ICHS (the code number) and CHGS (the numerical incremental value). See Section V for descriptions of the code number and the numerical incremental value.

As summarized in Table 5.38, the change definition (CDF) file uses a simple coding system for defining the constructional changes. The code corresponds very closely to the code used to define parameters initially in the geometry information (GI) file. (See Table 5.1 - 5.8 in this report for a complete description of the GI file). In the GI file, each parameter is defined by two numbers — ITY, and ITN. ITY is zero for a system parameter, and is the surface number for a surface parameter. ITN is the parameter number as defined in the GI file definition tables. The code for defining a parameter in the CDF file is simply to multiply ITY by 100, and add ITN. Thus, for example, the code for system parameter 7 would be 7, and the code for surface 2 parameter 9 would be 209. The code also allows the user to specify a polynomial coefficient in a surface deformation (DEFORM, or DFR) file. In that case, the user multiplies the surface number by 100, adds the polynomial coefficient number, and finally makes the resulting code negative. Thus, for example, the code for surface 3 coefficient 4 would be -304.

As shown in Table 5.38, for each constructional change, the user specifies both the code, and a numerical value by which to change the coded parameter. It is the user's responsibility to choose a value that is (1) large enough to make a wavefront change that is significant when compared to the ever present computer roundoff accuracy, and (2) small enough so that the resulting wavefront change is reasonably linear in the constructional change. In practice, this usually means simply that the user should choose a value which is in the range of physical values that might occur. In Section 5.12.2, we discuss in more detail the subjects of linear wavefront changes and constructional change values.

For a demonstration of the WFSNS1 program, Figure 5.78 shows a change definition (CDF) file prepared for the ELLIP3 system which has been used throughout this report. Three constructional changes are defined: (1) x-decenter of surface 1; (2) elevation misalignment of surface 1; and (3) change in Zernike polynomial coefficient number 5 for surface 1.

```
ELEM1.CDF - ELEMENT 1 RIGID & NON RIGID SENSITIVITIES
 11 4.95 15.00
 3
 101 7.D-02
 108 2.D-01
-105 3.D-04
```

Figure 5.78 CDF File (ELEM1.CDF) for ELLIP3 system

```
*** OPTICAL SURFACE ANALYSIS PROGRAM (WFSNS1  ) RELEASE (06.0) VAX      PAGE   1
ELEM1.CDF - ELEMENT 1 RIGID & NON RIGID SENSITIVITIES          20-01-92 13:26:24
ELLIP3.GI - 2 CONFOCAL ELLIPSES, .33 OBSC, SURF 1 DEFORM
------------------------------------------------------------------------------

 NUMBER OF ZERNIKE POLYNOMIALS:  11
 PUPIL OUTER RADIUS:              1.500000D+01
 LINEAR OBSCURATION RATIO:        0.330000

 NUMBER OF CONSTRUCTIONAL CHANGES:  3
 CHANGE  SURF #   PARAM #   INCRMNTL    --  PARAMETER VALUES  --
 NUMBER  (0: SYS) (-: POLY) CHANGE      BEFORE CHANGE   AFTER CHANGE
   1       1        1      7.0000D-02  1.00000000D+01  1.00700000D+01
   2       1        8      2.0000D-01  3.00000000D+00  3.20000000D+00
   3       1       -5      3.0000D-04 -2.00000000D-05  2.80000000D-04
```

Figure 5.79 WFSNS1 output for ELLIP3 system

Figure 5.79 shows a printout from the WFSNS1 program for this input. The printout is fairly self explanatory. It first shows the number and type of polynomials selected for the sensitivity analysis. Then it shows the desired constructional changes, and their effects on the nominal parameter values. WFSNS1 actually creates two sets of output files -- one set with the changes added, and a second set with the changes subtracted. As discussed in Section 5.12.2, this allows

WFSNS2 to calculate the linear wavefront sensitivities more reliably in the presence of small quadratic sensitivities.

WFSNS1 takes care of naming and creating the various GI and surface DFR output files. These files, and the later corresponding output files from running other OSAC programs, will remain on the system after WFSNS1, WFSNS2, and OPDGEN are finished. The user should therefore be aware of them so that disk cleanup procedures can be performed if appropriate.

The GI files are named as follows:

GI file name = "WFPnnn.GI"
and "WFMnnn.GI"

where nnn is a three digit number which tells the number of the constructional change, with the first change being designated 001, etc. The "P" ("WFPnnn.GI") corresponds to the nominal file Plus the constructional change, and the "M" ("WFMnnn.GI") corresponds to the nominal file Minus the constructional change.

The DFR files are named as follows:

DFR file name = "WFPnnn.Xmm"
and "WFMnnn.Xmm"

where nnn is as above, and mm is a two digit number which tells the surface number, with the first surface being designated 01, etc. The "P" and "M" are as above.

5.12.2 WFSNS2 Program Description

WFSNS2 is the second of the three wavefront sensitivity modules to be run. After other OSAC programs have been run for these changed optical systems, WFSNS2 collects the output files and generates a file which defines the appropriate wavefront sensitivities.

WFSNS2 uses as an input the Optical Path Difference (OPD) and wavefront deformation (DEFORM, or DFR) files produced by various OSAC programs (GEOSAC, DRAT, OPD, OPDCNV, and COGEN) after WFSNS1 is run. It also uses the GX file (GEOSAC output) from the nominal optical system, and the change definition (CDF) file originally used as input for WFSNS1. WFSNS2 generates a sensitivity (SNS) file which defines the linear sensitivity of the specified wavefront Zernike coefficients to the specified constructional changes. Figure 5.77 shows this file interaction for WFSNS2, and additionally shows the entire program and data flow for WFSNS1, WFSNS2, and OPDGEN. Table 5.39 lists all of the input and output files used by WFSNS2. Table 5.40 defines the new sensitivity (SNS) file in detail.

Table 5.39
Files Used by the WFSNS2 Program

(File names are those used by the OSAC.COM file on the VAX system. An input file name beginning with "fn1" or "fn2" implies that the name is entered by the user. As shown, the OSAC.COM file is configured to give the output sensitivity (SNS) file the same name root as the input CDF file. Figure 5.77 shows the data and program flow for the programs WFSNS1, WFSNS2, and OPDGEN in more detail.)

Input/Output	File Name	Formatted/Unformatted	File Number
Input	fn1.GX	Formatted	3
Input	fn2.CDF	Formatted	1
Input	OPD — Note 1	Formatted	9
Input	DFR — Note 2	Formatted	7
Output	fn2.SNS	Formatted	2
Output	(terminal)	Formatted	6
Output	WFSNS2.OUT	Formatted	8

Note 1: The OPD files are named as follows:
OPD file name = "WFPnnn.OPD"
and "WFMnnn.OPD"
where nnn is a three-digit number which tells the number of the constructional change, with the first change being designated 001, etc. The "P" ("WFPnnn.GI") corresponds to the nominal file Plus the constructional change, and the "M" ("WFMnnn.GI") corresponds to the nominal file Minus the constructional change.

Note 2: The (wavefront) DFR files are named as follows:
DFR file name = "WFPnnn.DFR"
and "WFMnnn.DFR"
where nnn, "P", and "M" are as above.

Table 5.40
Definition of the Sensitivity (SNS) File
(used as output from the WFSNS2 program and input to the OPDGEN program)

Card	Item	Data Type	Format	Description
1	RID	CHAR*4(16)	16A4	User comments
2	NDF	I*4	I6	No. of polynomials
	ROBSC	R*8	IPD25.17	Inner radius of pupil obscuration
	RPUPIL	R*8	IPD25.17	Outer radius of pupil
3	NCH	I*4	I6	Number of constructional changes
4,5,...	(ICHS (ICH), ICH=1,NCH)	I*4	I2I6	Code numbers for all the constructional changes (only as many cards as required are used)
...	(SNSMAT (IDF,1),IDF= 1,NDF)	R*8	1P5D15.7	Sensitivities of the IDF'th Zernike polynomial coeff to 1st constructional change (only as many cards as required are used)
... (SNSMAT card(s) above, for constructional changes 2,3,4,...)				
...	(XBFSNS (ICH), ICH=1,NCH)	R*8	1P5D15.7	X-centroid shift sensitivities for all of the constructional changes (only as many cards as required are used)
...	(YBFSNS (ICH),ICH=1, NCH)	R*8	1P5D15.7	Y-centroid shift sensitivities for all of the constructional changes (only as many cards as required are used)

For a demonstration of the WFSNS2 program, Figure 5.80 shows a printout from WFSNS2 which continues the WFSNS1 run documented in Section 5.12.1. (The running of the intervening OSAC programs, GEOSAC, DRAT, OPD, OPDCNV, and COGEN, as discussed in Section 5.4.). Figure 5.81 shows the corresponding sensitivity (SNS) file produced. The

printout in Figure 5.80 first shows basic information on the selected Zernike polynomials and construction changes. Then it shows some summary information for each change, including (1) the numerical incremental value chosen by the user in the change definition (CDF) file; (2) the RMS wavefront error (defined by Zernike polynomials above tilt) induced by a unit constructional change; and (3) the image centroid shifts induced by a unit constructional change. Finally, the printout shows the desired sensitivity information in detail. (The following paragraphs define the sensitivity values mathematically.) Note that the relative numerical sensitivity values make intuitive sense. In particular, changes 1 and 2 (surface 1 decenter and tilt) primarily affect focus, astigmatism, and coma (coefficients 4-8), while change 3 (surface 1 polynomial coefficient number 5) primarily affects wavefront polynomial coefficient number 5 (and by the expected ratio of 2:1). (The reason that decenter and tilt affect focus and astigmatism instead of just coma is that the system is slightly non-symmetric, or off-axis).

The calculations performed by WFSNS2 are relatively straightforward. In particular, if a constructional change dC is first added and then subtracted from the system, and if the corresponding wavefront coefficients are WP and WM respectively, then it can be shown that the sensitivity is

$$S=(dW/dC)=(WP-WM)/(2dC) \qquad (5\text{-}106)$$

where S = the linear rate of change of wavefront coefficient W with constructional change C

dC = incremental constructional change

WP = wavefront coefficient for the case when dC is added to the nominal system

WM = wavefront coefficient for the case when dC is subtracted from the nominal system

S is the desired linear sensitivity, regardless of the nominal wavefront coefficient value, and regardless of any quadratic wavefront change that may have occurred due to the constructional change. Thus, we see that the user is actually free to choose a change value so large that quadratic wavefront changes become significant, as long as the cubic changes are insignificant. This gives the user more flexibility in choosing the numerical values for the constructional changes.

WFSNS2 does make one additional type of calculation, in addition to the wavefront coefficient sensitivity analysis just described: it calculates the sensitivity of centroid position to the constructional changes. This is useful because the OPDCHG program, in predicting the wavefront for a particular set of constructional changes, combines all of the incremental centroid position shifts with all of the nominal and incremental wavefront tilt coefficients to arrive at a conglomerate centroid position. Consequently the tilt in the final predicted wavefront can be and is set to zero, which is useful for subsequent diffraction analyses using the PSF program.

The required relationship between an annular Zernike tilt coefficient (coefficient number 2 or

3) and equivalent centroid position shift is as follows:

$$Shift = \frac{Tiltcoeff\ (2EFL)}{(1+OBSC^2)^{1/2} R_{pupil}} \qquad (5\text{-}107)$$

where Shift = focal plane centroid position shift (x or y)

Tilt coeff = annular Zernike polynomial tilt coefficient (coefficient number 2 or 3) for the entrance pupil wavefront

EFL = effective focal length

OBSC = entrance pupil linear obscuration ratio

R_{pupil} = entrance pupil outer radius

Finally, before describing the OPDGEN program, it is useful to summarize why the sensitivity analysis is kept to a linear analysis -- why, in other words, quadratic and higher order wavefront changes are not considered. The reason is simply the nature of a sensitivity analysis. The very assumption that the response of a system to a set of inputs can be defined in terms of the responses to the individual inputs implicitly uses linearity. This is because, in general, the cross-talk for a pair of inputs (i.e., the part of the response which differs from the sum of the responses to the individual responses) is of the same order as the quadratic part of each individual response. Therefore, it is inconsistent to calculate a total response as a sum of individual responses, while at the same time considering anything beyond linear responses.

```
*** OPTICAL SURFACE ANALYSIS PROGRAM (WFSNS2  ) RELEASE (06.0) VAX      PAGE  1
ELEM1.CDF - ELEMENT 1 RIGID & NON RIGID SENSITIVITIES          20-01-92 13:30:27
ELLIP3.GI - 2 CONFOCAL ELLIPSES, .33 OBSC, SURF 1 DEFORM       20-01-92 12:44:32
-------------------------------------------------------------------------------

 NUMBER OF ZERNIKE POLYNOMIALS:  11
 PUPIL OUTER RADIUS:            1.500000D+01
 LINEAR OBSCURATION RATIO:      0.330000

 NUMBER OF CONSTRUCTIONAL CHANGES:  3
                                  * SENSITIVITIES TO UNIT CHANGES *
 CHANGE  SURF #   PARAM #   INCRMNTL    RMS WVFRNT   CENTROID SENSITIVITY
 NUMBER  (0: SYS) (-: POLY) CHANGE      SNS (NP>3)   DELTA-X     DELTA-Y
   1       1        1      7.0000D-02  2.7577D-04  1.2288D+00  4.3503D-04
   2       1        8      2.0000D-01  9.8968D-04 -1.1391D-03 -2.8629D+00
   3       1       -5      3.0000D-04  1.9326D+00 -3.4383D-02  4.8380D-02

 DETAILED ZERNIKE COEFFICIENT SENSITIVITIES TO CHANGE NO.  1:
  2.2285714D-07 -3.8835714D-04  3.4000000D-06  1.3208643D-04  1.1283643D-04
  5.3862143D-05  2.0727429D-04 -1.2700000D-06  3.3571429D-07 -1.3285714D-06
 -9.0000000D-07

 DETAILED ZERNIKE COEFFICIENT SENSITIVITIES TO CHANGE NO.  2:
 -7.8875000D-07 -1.3015000D-05  6.6370825D-04 -8.7584500D-04  2.4454200D-04
 -1.6071150D-04  3.5497500D-06 -3.5594300D-04 -3.2000000D-06 -3.4000000D-07
  2.8525000D-06

 DETAILED ZERNIKE COEFFICIENT SENSITIVITIES TO CHANGE NO.  3:
  1.8333333D-06  3.8666667D-04  4.3500000D-04  9.9383333D-04  1.9326250D+00
  3.5246667D-03 -7.2400000D-04  2.3468333D-03 -3.8783333D-03 -7.6933333D-03
 -6.6666667D-06
```

Figure 5.80 WFSNS2 output for ELLIP3

```
ELEM1.CDF - ELEMENT 1 RIGID & NON RIGID SENSITIVITIES
   11  4.94999999999999996D+00  1.50000000000000000D+01
    3
  101   108  -105
 2.2285714D-07 -3.8835714D-04  3.4000000D-06  1.3208643D-04  1.1283643D-04
 5.3862143D-05  2.0727429D-04 -1.2700000D-06  3.3571429D-07 -1.3285714D-06
-9.0000000D-07
-7.8875000D-07 -1.3015000D-05  6.6370825D-04 -8.7584500D-04  2.4454200D-04
-1.6071150D-04  3.5497500D-06 -3.5594300D-04 -3.2000000D-06 -3.4000000D-07
 2.8525000D-06
 1.8333333D-06  3.8666667D-04  4.3500000D-04  9.9383333D-04  1.9326250D+00
 3.5246667D-03 -7.2400000D-04  2.3468333D-03 -3.8783333D-03 -7.6933333D-03
-6.6666667D-06
 1.2288195D+00 -1.1390503D-03 -3.4382515D-02
 4.3502950D-04 -2.8628740D+00  4.8380183D-02
```

Figure 5.81 SNS File (ELEM1.SNS) for ELLIP3 System

5.12.3 OPDGEN Program Description

OPDGEN is the last of the three wavefront sensitivity modules to be run. OPDGEN uses the sensitivity (SNS) file and a set of user specified constructional changes, and generates the resulting Optical Path Difference (OPD) file.

OPDGEN uses as input the sensitivity (SNS) file generated by WFSNS2; the geometry information (GI), Optical Path Difference (OPD), and wavefront deformation (DEFORM, or DFR) files for the nominal optical system; and a change (CHG) file supplied by the user to define the particular set of constructional changes. OPDGEN generates an OPD file which incorporates the OPD's of the nominal system, as well as the linear wavefront changes induced by all of the specified constructional changes. Figure 5.77 shows this file interaction for OPDGEN, and additionally shows the entire program and data flow for WFSNS1, WFSNS2, and OPDGEN. Table 5.41 lists all of the input and output files used by OPDGEN. Table 5.42

Table 5.41
Files used by the OPDGEN program
(File Names are those used by the OSAC.COM file on the VAX system. An input file name begining with "fn1", "fn2", ... implies that the name is entered by user. As shown, the OSAC.COM file is currently configured to give the output Optical Path Difference (OPD) file the same name root as the input CHG file. Figure 5.77 shows the data and program flow for the programs WFSNS1, WFSNS2, and OPDGEN in more detail.)

Input/Output	File Name	Formatted/Unformatted	File Number
Input	fn1.GX	Formatted	7
Input	fn2.OPD	Formatted	9
Input	fn3.DFR	Formatted	11
Input	fn4.SNS	Formatted	3
Input	fn5.CHG	Formatted	1
Output	fn5.OPD	Formatted	2
Output	(Terminal)	Formatted	6
Output	OPDGEN.OUT	Formatted	8

Table 5.42
Definition of the Change (CHG) File
(used as input to the OPDGEN program)

Card	Item	Data Type	Format	Description
1	RID	CHAR*4(16)	16A4	User comments
2,3,...	(CHGS (ICH), ICH=1,NCH)	R*8	(free format)	Desired amounts for all of the constructional changes (only as many cards as required are used)

For a demonstration of the new OPDGEN program, Figure 5.82 shows a change (CHG) file entitled ELEM1.CHG. This file simply defines three numerical values for the changes which were originally defined in the change definition (CDF) file. Figure 5.83 shows the corresponding printout from OPDGEN, which continues the WFSNS1-WFSNS2 run documented in Sections 5.12.1 and 5.12.2. The printout first shows basic information on the selected constructional changes. Then it shows the conglomerate image centroid positions described in Section 5.12.2. (These positions define the best diffraction focus, in that there is no tilt in the wavefront for these positions.) Next it shows basic information on the selected Zernike polynomials. Finally, it shows three pieces of information for each Zernike polynomial, and for the wavefront as a whole. The three pieces of information are (1) the coefficient (or RMS wavefront without piston and tilt) value before any constructional changes; (2) the incremental change implied by the sum of all the constructional changes; and (3) the resulting conglomerate coefficient (or RMS wavefront without piston and tilt) value. Note that the changes for the first three Zernike coefficients are set to the negatives of the nominal coefficients. This is so that the resulting conglomerate wavefront will have no tilt (or piston) in it, as previously discussed. For all other coefficients, and for the RMS wavefront as a whole, the values are for the true sum of the constructional changes.

To complete the demonstration, Figure 5.84 shows the COGEN printout which results from running OPDCNV (to convert the OPD file for fitting by COGEN) and then COGEN on the OPD data resulting from this OPDGEN run.

```
ELLIP3A.CHG - 3 PARTICULAR ELEMENT 1 CHANGES
8.D-02 -3.D-01  4.D-04
```

Figure 5.82 CHG File (ELLIP3A.CHG) for ELLIP3 System

ELLIP3A.CHG - 3 PARTICULAR ELEMENT 1 CHANGES 20-01-92 14:00:35
ELLIP3.GI - 2 CONFOCAL ELLIPSES, .33 OBSC, DURF 1 DEFORM 20-01-92 12:44:32

ID TEXT FROM THE SENSITIVITY FILE:
ELEM1.CDF - ELEMENT 1 RIGID & NON RIGID SENSITIVITIES

NUMBER OF CONSTRUCTIONAL CHANGES: 3

CHANGE #	SURF. # (0: SYS)	PARAM # (-: POLY #)	CHANGE
1	1	1	8.0000D-02
2	1	8	-3.0000D-01
3	1	-5	4.0000D-04

BEST FOCUS X-COORDINATE AFTER CHANGES: 6.612794D+00
BEST FOCUS Y-COORDINATE AFTER CHANGES: 1.562118D+01

NUMBER OF ZERNIKE POLYNOMIALS: 11
PUPIL OUTER RADIUS: 1.500000D+01
LINEAR OBSCURATION RATIO: 0.330000

-----RMS WAVEFRONT VALUES-----

POLY #	NOMINAL (NO CHANGES)	CHANGES ONLY	TOTAL COMPOSITE
1	3.227210D-05	-3.227210D-05	0.000000D+00
2	1.363890D-04	-1.363890D-05	0.000000D+00
3	-1.870390D-04	1.870390D-04	0.000000D+00
4	3.665110D-05	2.737179D-04	3.103690D-04
5	-3.8097880D-05	7.087143D-04	6.706165D-04
6	5.802730D-05	5.393229D-05	1.119596D-04
7	-7.386370D-05	1.522742D-05	-5.863628D-05
8	9.762830D-05	1.076200D-04	2.052483D-04
9	-1.137970D-04	-5.644762D-07	-1.143615D-04
10	1.329640D-04	-3.081619D-06	1.298824D-04
11	-1.446420D-04	-9.304167D-07	-1.455724D-04
TOTAL RMS:	2.952570D-04	7.914390D-04	8.422353D-04

Figure 5.83 OPDGEN Output for ELLIP3

POLYNOMIAL COEFFICIENT SUMMARY

TYPE OF POLYNOMIALS: ZERNIKE
OF POLY'S, OBSCURATION: 11 0.330000
OF GOOD DATA POINTS: 121
SIGMA**2 OF ACTUAL DATA: 7.0936E-07

INDECES L	MCOS	MSIN	COEFFICIENT VALUE	SIGMA**2 OF POLY #I	SIGMA**2 OF POLY'S 1 TO I	SIGMA**2 OF DATA - POLY'S
0			9.3247E-12	8.6949E-23	8.6949E-23	7.0936E-07
1	1		4.1756E-10	1.7436E-19	1.7444E-19	7.0936E-07
1		1	8.0873E-11	6.5404E-21	1.8099E-19	7.0936E-07
2			3.1037E-04	9.6329E-08	9.6329E-08	5.9377E-07
2	2		6.7062E-04	4.4973E-07	5.4606E-07	1.2821E-07
2		2	1.1196E-04	1.2535E-08	5.5859E-07	1.1523E-07
3	1		-5.8636E-05	3.4382E-09	5.6203E-07	1.1129E-07
3		1	2.0525E-04	4.2127E-08	6.0416E-07	6.3075E-08
3	3		-1.1436E-04	1.3078E-08	6.1723E-07	4.8975E-08
3		3	1.2988E-04	1.6869E-08	6.3410E-07	3.0788E-08
4			-1.4557E-04	2.1191E-08	6.5529E-07	4.7762E-12

Figure 5.84
COGEN Output Following OPDGEN and OPDCNV. This Listing Characterizes the OPDGEN Performance Prediction, without utilizing any new Ray Tracing.

Figure 5.85 shows a similar result, but for the case where the entire ray trace was performed from scratch, using the constructional changes specified in Figure 5.78.

POLYNOMIAL COEFFICIENT SUMMARY

TYPE OF POLYNOMIALS: ZERNIKE
OF POLY'S 1 1
0.330000
OF GOOD DATA POINTS: 121
SIGMA**2 OF ACTUAL DATA: 8.5829E-07

INDECES L	MCOS	MSIN	COEFFICIENT VALUE	SIGMA**2 OF POLY # I	SIGMA**2 OF POLY'S 1 TO I	SIGMA**2 OF DATA-POLY'S
0			3.2524E-05	1.0578E-09	1.0578E-09	8.59343-07
1	1		1.0896E-04	1.1872E-08	1.2930E-08	8.4881E-07
1		1	-3.8678E-04	1.4960E-07	1.6253E-07	7.1581E-07
2			2.8921E-04	8.3644E-08	2.4617E-07	6.1543E-07
2	2		6.8657E-04	4.71383-07	7.1756E-07	1.2745E-07
2		2	1.0803E-04	1.1669E-08	7.2923E-07	1.1537E-07
3	1		-5.86463-05	3.4394E-09	7.3267E-07	1.1144E-07
3		1	2.0557E-04	4.2258E-08	7.7492E-07	6.3068E-08
3	3		-1.1442E-04	1.3091E-08	7.8802E-07	4.8955E-08
3		3	1.2981E-04	1.6850E-08	8.0487E-07	3.0789E-08
4			-1.4557E-04	2.1192E-08	8.2606E-07	4.6745E-12

Figure 5.85 COGEN Output for ELLIP3
This Listing Characterizes the Performance Prediction made if you did not use the OSAC Program. Note the Close Similarity to Figure 5.84.

Note the close similarity between the wavefront Zernike coefficients in Figure 5.84 (which required no additional ray tracing at all), and those in Figure 5.85. The slight discrepancies in the focus and astigmatism coefficients show that the linear sensitivity range is perhaps being very slightly exceeded. This is not surprising, since the system is very nearly symmetric, in which case there would be no linear sensitivity of focus and astigmatism to the selected changes.

5.12.4 WFSENS Option in Running OSAC.COM

As discussed at the beginning of Section 5.12, the proms WFSNS1, WFSNS2, and OPDGEN can be run easily and interactively by using the OSAC.COM file on the VAX.

If the WFSENS option is selected, OSAC.COM prompts the user for the names of the nominal geometry information (GI) file, any nominal surface deformation (DEFORM, or DFR) files, and a change definition (CDF) file. OSAC.COM then runs the WFSNS1 program, producing a set of changed GI and DFR files (to define changed optical systems), and an OPD conversion (CNV) file. Then, OSAC.COM loops (without operator intervention) over the following set of OSAC programs for each changed optical system:

(1) GEOSAC
(2) DRAT
(3) OPD
(4) OPDCNV
(5) COGEN

OSAC.COM uses DRAT to do the ray tracing, even if there are no surface deformations, in which case the user may have originally used NABRAT to trace the nominal system.

The result is a set of Optical Path Difference (OPD) files and wavefront deformation (DEFORM, or DFR) files. Finally, OSAC.COM uses these files, along with the GEOSAC output (GX file) for the nominal system, and the original change definition (CDF) file, to run the WFSNS2 program. The final result of running WFSNS2 is a sensitivity (SNS) file which can be used as input to run the OPDGEN program (see Sections 5.12.3 and 5.12.5). This data and program flow is shown in Figure 5.77. As with the rest of the OSAC.COM options, the WFSENS option allows the user to look at or print any file when the programs have finished running.

5.12.5 OPDGEN Option in Running OSAC.COM

If the OPDGEN option is selected while running OSAC with the OSAC.COM file, OSAC.COM prompts the user for the names of the GEOSAC output (GX file) for the nominal system, the nominal Optical Path Difference (OPD) file, the nominal wavefront deformation (DEFORM, or DFR) file, the sensitivity (SNS) file, and a change (CHG) file. OSAC.COM then runs the OPDGEN program, producing an OPD file which characterizes the changed system. This data and program flow is shown in Figure 5.77. As with the rest of the OSAC.COM options, the OPDGEN option allows the user to look at or print any file.

APPENDIX A - INSTALLING OSAC ON A VAX/VMS SYSTEM

OSAC Installation procedure

The following procedure is used to install the OSAC program on a DEC VAX computer running the VMS operating system. A TK50 tape cartridge or a 9-track, 1600 bpi tape is normally used as the medium. VMS BACKUP is used to load the program onto tape.

1) Define the logical symbol DISK$OSAC

```
$DEFINE DISK$OSAC device:[directory]
```

where: 'device' refers to an available disk drive such as DUA0;
'directory' refers to the directory into which the top level OSAC files are written, such as [OSAC] or [USERNAME];

If this directory does not exist, it must be created.

NOTE: if [000000] IS USED AS THE DIRECTORY NAME, WRITE ACCESS TO THAT DIRECTORY IS REQUIRED BY THE USER.

2) Change to directory DISK$OSAC:

```
$SET DEF DISK$OSAC
```

3) Physically mount the tape onto the appropriate drive.

4) Mount the tape as a foreign tape (for use by BACKUP):

```
$MOUNT/FOR device:
```

(e.g. MUA0: for a TK50 cartridge or MSA0: for a 9 track tape on a MicroVAX II)

5) Select the first saveset off the tape (MAKEOSAC.BCK). This saveset contains two command procedures used to load the program (including source, executable modules, command procedures, and testcases).

```
$BACKUP/LOG device:MAKEOSAC.BCK *.*
```

6) Execute the command procedure MAKEOSAC.COM (if VMS Version 4 is being used, then it is the command procedure MAKEOSACV4.COM which is actually used.

```
$@MAKEOSAC
```

7) Under the directory established via symbol DISK$OSAC, the following subdirectories will be created ("n" refers to the OSAC version; currently n = 7):

[.OSAC.Vn] - contains the command procedures which run OSAC
[.OSAC.Vn.EXEC] - contains the executable modules
[.OSAC.Vn.SOURCE] - contains the source code, compiling, and linking command procedures.
[.OSAC.TESTCASES] - contains sample input & output files
[.OSAC.UTILITY] - contains a set of GSFC-developed programs used in the analysis of OSAC-created files (such as contours, encircled energy, etc., an editor useful in the creating/editing of OSAC input files is included).

The following files will be created in DISK$OSAC:

a) OSAC.COM - main procedure for running OSAC
b) MAKEOSAC.COM - procedure used to load OSAC from tape (VMS 5)
c) MAKEOSACV4.com - same as MAKEOSAC.COM but runs under VMS 4.x
d) INSTALL.DOC - this document
e) OSACSYMBOLS.COM - defines OSAC-related symbols needed to run the program (used by the command procedures)

8) Define a symbol for executing OSAC.COM:

$OSAC :== @DISK$OSAC:OSAC.COM

9) Disk space requirements

Total space required by the program <4000 blocks including the source. Each user, however, can require many 1000's of blocks if they need many rays and have many surfaces in their system under analysis: about 250 blocks are needed for each ray file (D0x, R0x, DFP, etc.).

10) CPU Usage

Most OSAC modules run interactively in a very short period of time (seconds). The exception is DEDRIQ, which in a extended scattered light analysis (such as an XRAY of EUV instrument) take several hours of CPU time (on a MicroVAX II).

11) Memory requirements

OSAC modules generally required 1-2 Mbytes each.

APPENDIX B - RUNNING OSAC ON A VAX/VMS SYSTEM

The OSAC program has been installed and made operational on a DEC VAX computer system running the VAX/VMS 5.3 operating system. The program (which is a set of many individual programs) is executed by a series of command procedures.

REQUIRED HARDWARE

A DEC VT100 terminal (or emulator) is required to run OSAC. A printer is useful for printing the OSAC-generated output files.

STARTING THE PROGRAM

Upon installation of the program (see your system manager), a symbol named OSAC should have been created; this symbol executes the main OSAC command procedure (DISK$OSAC:OSAC.COM) which provides a menu-oriented screen from which the user may select and execute the desired OSAC module. The user should enter the following command (as shown in general form):

$OSAC :== @DISK$OSAC:OSAC
$OSAC module project

The "module" and "project" parameters are optional. The "module" input selects the desired OSAC routine (GEOSAC, DRAT, etc.); if absent, the menu of all programs is presented to the user (see Appendix A). The "project" parameter is used to select the default filename from which the user selects the input files for the program. For example,

$OSAC GEOSAC PROJECTX

or just **$OSAC**

will select the GEOSAC module and use PROJECTX.? files as default input files (PROJECTX.GI would be used for GEOSAC input in this case). If the "project" value is not entered, then all appropriate files are presented to the user for selection as an input file.

If no parameters are entered, the user is prompted for a project name; the default response to this is no project (i.e. <CR>).

From the main menu, other utility programs can also be chosen or the user can enter any valid VAX/VMS command.

The user is reminded that the command procedures do NOT check to see if the OSAC modules have been run in an appropriate sequence.

QUITTING

If a CONTROL-Y key sequence is entered by the user, the command procedure will exit back to VMS. Selecting "X" from the main menu will also cause the procedure to exit. If a CONTROL-Y sequence is entered at any time during the execution of a module, the execution is stopped and the main menu presented again.

PROGRAM INPUT/OUTPUT

Program input from the terminal generally consists of selecting the appropriate program to execute, the input files required for program execution, and determining if an output file should be viewed. All actual OSAC commands MUST be in an input file prior to execution of a module. These files can be created via any standard editor (such as EDT), or selecting the EDITOR program from the set of Utility programs.

All OSAC output goes to a XXX.OUT file, where XXX represents the name of the executed module (e.g. GEOSAC.OUT). These files are standard ASCII files.

Because the programs are executed from DCL command procedures, the normal VMS command recall features (up arrow, etc.) can be used.

INDIVUAL PROGRAM SCREENS

Appendix E lists the program screens for each OSAC module. All required files are either prompted for or obtained from the default associated with the name of the project entered.

UTILITY PROGRAMS

Several utility programs have been developed at NASA/GSFC which aid in the analysis of OSAC output. The programs provide such analysis as encircled energy, contour plots (for a line printer), and 3d plots of the point spread function generated by the FPLOOK module. Users should feel free to modify these programs as required. There is included a screen-editor for creating/editing all files which need to be created by the user (e.g. a GI file). See Appendix C for a more detailed description of these programs.

APPENDIX C - OSAC UTILITIES

Included with OSAC are several NASA-developed utility programs which analyze OSAC output. These programs perform the following functions:

1) Contour mapping of the energy distribution on the focal plane
2) Encircled Energy distribution at the focal plane
3) Plotting of COGEN fit vs. actual data points
4) 3-D plot of point spread function
5) On-line editor for input data files (such as GI, SCT, etc.)

Each of these routines is described in more detail below.

GRAPHICS

The graphics routines used by the utility program are part of the GRAFKIT™ software package; this package was chosen for reasons of device independence and portability. This package is similar to the public domain plotting package NCAR. The routines were written in such a manner,however, that the actual calls to plotting routines can be replaced in a straight forward manner with any package the user desires. The routines which actually do the plotting using the software package are PSFPLOT and DEFORM; CONTOUR assumes a lineprinter type of output.

The following is the screen presented when the UTILITIES option is selected from the main OSAC menu:

O S A C U T I L I T I E S

1. CONTOUR - Contour plotting of focal plane files from FPLOOK.
2. GETRAD - Find focal plane energy distribution.
3. DEFORM - Plot surface deformation approximated by COGEN.
4. PSFPLOT - 3-D plot of focal plane file
5. EDITOR - Create/Edit GI, SCT, or LOOK files
X. EXIT - Return to Main Menu

ENTER NUMBER [1-5], [C,G,D,P,E], or X:

CONTOUR

This subroutine plots the focal plane energy contours in a lineprinter mode, using alphabetic characters to represent increasing intensity.

PSFPLOT Version 1.1

PSFPLOT provides a 3-d plot of the point spread function on the detector. The energy distribution is created by FPLOOK program and stored in an FPCOM (*.FCM) file. The peak height of the plot can be set by the user to show the maximum energy in the distribution or the total energy sum in the array. A plot title, as well as the name of the FPLOOK output binary file, is entered by the user. The date and time of the plot are printed on the plot.

PSFPLOT was modified to allow both lower case and Greek characters in the plot's title. To enter Greek characters in the title put a back quote before each letter while entering the title. To get the correct Greek letter use the table from the GRAFkit Reference Manual. In order to get a character from the PGU (Principal Greek Upper) or PGL (Principal Greek Lower) columns input the corresponding letter from the PRU (Principal Roman Upper) or PRL columns in the table. For example, to plot a lower case miu enter '**l** or an upper case omega enter '**X**. Or in order to enter a title of "α = 10 μ" enter "'**a** = 10 '**l**". This might be a little confusing but it has to do with the order of the Greek alphabet compared to the Latin alphabet.

Version 1.1 will also output the number of pixels and the size of the array being plotted.

GETRAD

GETRAD calculates the energy distribution of an OSAC FPCOM file (*.FCM) as produced by FPLOOK. This involves the calculation of the radial encircled energy. The output can be either the amount of encircled energy in a given spot size or the distribution.

USER INPUTS

The user is prompted for the following information:

1) ENTER PERCENTAGE OF ENERGY
?
Enter a value >0 and ≤ 100; for example, entering 80 will have GETRAD calculate the spot size which contains 80% of the energy.

2) DO YOU WANT :
1: THE CENTER AS PEAK VALUE
2: TO INPUT THE CENTER COORDINATES
3: THE CENTER AS MINIMUM OF ENERGY DIFFERENCES

ENTER 1, 2, OR 3

If option 1 is chosen, the program will scan the array row by row for the pixel with the highest energy value. If there is more than one pixel with a peak value, the first one in the scan will be considered the center.

For option 2, the user is prompted for the row and column number of the pixel to be used as the center of the distribution.

For option 3, perform the following computation for each row I and column J:

NORTH = sum of energy values in rows 1,2,3,...I-1
SOUTH = sum of energy values in rows $I+1,I+2,\ldots,N_r$
WEST = sum of energy values in columns 1,2,3,...,J-1
EAST = sum of energy values in rows $J+1,J+2,\ldots,N_c$

$$DIFFERENCES(I,J) = \left|\,|NORTH-SOUTH| - |WEST-EAST|\,\right|$$

The center of energy will be defined as MIN (DIFFERENCES(I,J)) for all rows and columns of the array.

3) THE CENTER IS IN ROW #M, COLUMN #N

DO YOU WANT PERCENTAGE OF

1. TOTAL SYSTEM ENERGY
OR 2. TOTAL PIXEL ENERGY

ENTER 1 OR 2:

Depending on the dimensions of the pixel array, defined in the LOOK file, some of the energy might be falling outside the array; in this case the user can input the energy of the focal plane. The user is prompted for this energy:

TOTAL ENERGY =

4) The program will calculate the encircled energy and display the following output:

THE TOTAL ENERGY = m
THE RADIUS IN PIXEL UNITS IS n AND
THE PERCENTAGE OF ENERGY = p

The user is then prompted for plotted and tabular output:

DO YOU WANT TO PLOT? (Y/N)
and
DO YOU WANT A TABLE OF ENERGIES? (Y/N)

The plot is percentage energy vs. radius (in pixels).

The table will be printed to both the screen and a file, with radius increments of 1 pixel. The radii will be additionally converted to arc seconds via the system focal length information provided by the user:

WHAT IS THE FOCAL LENGTH ?

This must be in the same units as the pixels used in the detector array.

DEFORM

The DEFORM program plots the results of a COGEN fit to a set of (X,Y,Z) data points used to describe an optical surface. For normal incidence optics, Zernike coefficients are used to describe the surface in OSAC; the DEFORM program will plot a curve based upon these Zernike coefficients, then overlay markers on this plot which represent the actual data points used in the analysis. In this fashion, the user can determine if the fit is acceptable. The plot is a two-dimensional one, meaning that is done for a "slice" through the surface; this slice can be taken through either the X or Y direction.

The required input to DEFORM is the following:

1) A COGEN-generated DFR file.
2) User input as to the direction of the slice (X or Y) and the relative location of the slice ($-1 \leq$ value ≤ 1)
3) Whether or not the user plots markers at the actual data points (yes or no).

Colors, line types, etc. are fixed by the graphics program.

EDITOR

The EDITOR utility allows the user to enter any of the required OSAC user-created files, including the GI, SCT, and LOOK files. Simplified online help is available during this process, selected by choosing the HELP option when displayed on the screen.

NOTE: This option uses the VMS-supplied SMG routines.

APPENDIX D - MAIN MENU OSAC SCREEN

O S A C V E R 6

1. GEOSAC - Geometric calculations for subsequent ray tracing.
2. NABRAT - Non-aberrated ray tracing.
3. COGEN - Polynomial coefficient generation.
4. DRAT - Deformed surface ray tracing of a single element.
5. SUSEQ - Scattered ray analysis.
6. DEDRIQ - Analysis of effects of high spatial frequency deformation.
7. OPD - Diffraction analysis : Optical path difference mapping.
8. PSF - Diffraction analysis : Calculate point spread function.
9. FPLOOK - Combine files into one pixel array file.
10. ZERGEN - Generate and display annular or full Zernike polynomials.
11. OPDCNV - Convert OPD files to serve as COGEN input.
12. WFSENS - Wavefront OPD sensitivites to constructional changes.
13. OPDGEN - OPD result for a specific set of constructional changes.
U. UTILITY - Use a utility program (for plotting, radialenergy, etc.)
V. VAX - Enter any legal VAX command
X. EXIT

ENTER A NUMBER BETWEEN 1 AND 16:

APPENDIX E1 - GEOSAC INPUT SCREEN

```
O S A C  V E R  7

      GEOSAC : GEOMETRIC CALCULATIONS FOR SUBSEQUENT RAY TRACING

ENTER NAME OF THE GI FILE :

      GI FILES
%DIRECT-W-NOFILES, no files found
```

APPENDIX E2 - NABRAT INPUT SCREEN

O S A C V E R 7

NABRAT : NON-ABERRATED RAY TRACING

ENTER NAME OF THE GX FILE :

GX FILES
%DIRECT-W-NOFILES, no files found

APPENDIX E3 - COGEN INPUT SCREEN

```
                    O S A C   V E R   7

COGEN : POLYNOMIAL COEFFICIENT GENERATION

ENTER NAME OF THE DEFDAT FILE :

        DEFORMATION DATA FILES (DEFDAT)
%DIRECT-W-NOFILES, no files found
```

APPENDIX E4 - DRAT INPUT SCREEN

```
O S A C  V E R  7

DRAT : DEFORMED SURFACE RAY TRACING OF ONE ELEMENT

ENTER NAME OF THE GX FILE :

      GX FILES
%DIRECT-W-NOFILES, no files found
```

APPENDIX E5 - SUSEQ INPUT SCREEN

```
O S A C  V E R  7

SUSEQ : SCATTERED RAY ANALYSIS

ENTER NAME OF THE GX FILE :
```

APPENDIX E6 - DEDRIQ INPUT SCREEN

```
O S A C  V E R  7


DEDRIQ : CALCULATE DIFFUSE SCATTER FROM ROUGH SURFACES

ENTER NAME OF THE GX FILE :

GX FILES
%DIRECT-W-NOFILES, no files found
```

APPENDIX E7 - OPD INPUT SCREEN

```
O S A C   V E R   7

OPD : DIFFRACTION ANALYSIS - OPTICAL PATH DIFFERENCE MAPPING

ENTER NAME OF THE GX FILE :

        GX FILES
%DIRECT-W-NOFILES, no files found
```

APPENDIX E8 - PSF INPUT SCREEN

O S A C V E R 7

PSF : DIFFRACTION ANALYSIS - CALCULATE POINT SPREAD FUNCTION

ENTER NAME OF THE GX FILE :

GX FILES
%DIRECT-W-NOFILES, no files found

APPENDIX E9 - FPLOOK INPUT SCREEN

```
                    O S A C   V E R   7

FPLOOK : COMBINE FILES INTO ONE PIXEL ARRAY FILE

ENTER NUMBER OF SPECULAR RAY FILES TO BE INPUT :

        SPECULAR RAY FILES (RAY OR ARAY)
%DIRECT-W-NOFILES, no files found
```

APPENDIX E10 - UTILITY PROGRAM INPUT SCREEN

OSAC UTILITIES

1. CONTOUR - Contour plotting of focal plane files from FPLOOK.
2. GETRAD - Find focal plane energy distribution.
3. DEFORM - Plot surface deformation approximated by COGEN.
4. PSFPLOT - 3-D plot of focal plane file
5. EDITOR - Create/Edit GI, SCT, or LOOK files

X. EXIT - Return to Main Menu

ENTER NUMBER [1-5], [C,G,D,P,E], or X: